# Proceedings of the Fourth International Symposium on Analytical Methods In Philately

THE INSTITUTE OF ANALYTICAL PHILATELY, INC.

# Proceedings of the Fourth International Symposium on Analytical Methods in Philately

**13–14 November 2020**
*Smithsonian National Postal Museum*
*Washington, D.C.*

*Edited by*
*Thomas Lera and John H. Barwis*

## Abstract

Lera, T. and Barwis, J. H. *Proceedings of the Fourth International Symposium on Analytical Methods in Philately.* x + 104 pages, 114 figures, 8 tables, 2020. This publication contains papers presented at the Fourth International Symposium on Analytical Methods in Philately, hosted by The Smithsonian National Postal Museum, Washington D.C. 2020. The eleven papers describe a wide range of techniques for stamp identification and expertizing. Several describe the use of visible, infrared, and ultraviolet light to discriminate among printings of the same design. Others report nondestructive analyses of ink chemistry to document how inks were modified over time. Together the papers illustrate philatelic applications of a wide range of equipment, including desk-top scanners, Video Spectral Comparator (VSC), X-ray fluorescence (XRF), scanning electron microscope (SEM), X-ray diffraction (XRD), Fourier-transform infrared fluorescence (FTIR), and ultraviolet fluorescence.



Published by The Institute for Analytical Philately, Inc.
PMB 31
1668 Merriman Road
Akron, OH 44313





Design and Layout by Kenneth Trettin

Printed by Wilcox Printing & Publishing, Inc., 102 S. Main St., PO Box 167, Madrid, IA 50156





ISBN: 978-0-578-67273-1
Library of Congress Control Number: 2020906136

# Contents

# Welcome Letter

March 17, 2020

It is my great pleasure to present the Proceedings of the Fourth International Symposium on Analytical Methods in Philately. The symposium is being held at the Smithsonian National Postal Museum, home to one of the world's largest philatelic collections, from 13–14 November 2020.

This gathering builds on the work of the first three symposia, held respectively in Washington DC in 2012 at the Smithsonian National Postal Museum (NPM), in Chicago in 2015 prior to CHICAGOPEX, and in London in 2017 at the Royal Philatelic Society London. The Institute of Analytical Philately (IAP) solicited papers for all three symposia. The Institute was formed in 2010 as a nonprofit corporation dedicated to deepening our understanding of stamps and covers using scientific technology and the open publication of experimental results. The technical and financial support IAP provides can be tailored to the needs of philatelists with no scientific background, as well as those with advanced degrees in science or engineering.

Accordingly, and in conjunction with the Smithsonian Institution's mission to increase and diffuse knowledge and that of NPM to study and present postal history and philately, this publication aims to introduce the field of analytical philately to a general audience and to promote conversation among those philatelists using forensic tools and methods to learn more. We thank the Institute of Analytical Philately for publishing these papers and making them freely available on its website, and Susan Smith, the Winton M. Blount Research Chair at NPM, for her work organizing the gathering.

We look forward to welcoming you to the museum.

Elliot Gruber
Director, National Postal Museum

# Preface

The Institute for Analytical Philately Inc. (IAP) was formed in 2010 as a philanthropic, nonprofit corporation dedicated to encouraging and supporting technical research on philatelic materials, and publication of experimental results. IAP support can be tailored to the needs of any philatelist, from those with no scientific background to those with advanced degrees in mathematics, science or engineering.

IAP grants are intended to help fund travel, lodging, and laboratory use. Researchers may conduct their research anywhere they choose. Additional funding may be available through cost sharing with alliance members, who can also provide advice on previous work, or in conceiving and planning a research project. Current alliance members include the Smithsonian National Postal Museum, The U.S. Philatelic Classics Society, The Confederate Stamp Alliance, the Vincent G. Greene Philatelic Research Foundation, and the Philatelic Foundation. Detailed information on grants can be found on the IAP website: WWW.ANALYTICALPHILATELY.ORG.

This book contains papers presented at the Fourth International Symposium on Analytical Methods in Philately, held at the Smithsonian National Postal Museum in Washington DC on November 13-14, 2020. Readers will find insights into technical research methods used across a broad spectrum of philatelic interests. Some of the methods described here involve approaches previously never attempted.

The success of the symposium was due in large part to Susan Smith, NPM Winton M. Blount Research Chair, and James Allen, IAP Director, as well as the speakers and attendees. We also thank the philatelic and scientific individuals who completed multiple peer reviews of these papers.

If you enjoy these papers and the symposium, please continue to support the Institute for Analytical Philately, National Postal Museum and the next symposia.

John H, Barwis, RDP, FRPSL
Institute for Analytical Philately, President

Thomas Lera, FRPSL
Institute for Analytical Philately, Director

# Use of X-Ray Diffraction and Infrared Absorption Spectroscopy for the Study of Paper and Ink in Postage Stamps

*Harry G. Brittain**

## Introduction

In its simplest definition, the forensic analysis of a stamp consists of using appropriate analytical technology to identify (1) the various components in the ink used to print the stamp, and (2) any components in the paper itself (besides cellulose) on which the stamp was printed. One could very well consider this approach as being akin to performing an autopsy on a given stamp, with the aim of obtaining philatelic history by integrating its ink and paper composition with known trends deduced from a larger study. The study in question ultimately requires that one chemically identify the components in order to develop a profile of the stamp under analysis. The acquisition of this information falls entirely within the sciences of analytical chemistry and technology.

However, as interesting as chemical analysis of the ink and paper components might be, the philatelist requires more. When the results of the forensic analysis are complete, and one fully understands the composition of the stamp under study, the next logical step is to use the analytical conclusions as an entry into the historical background of the stamp. Sometimes this latter process might require consultation with compilations of collections in libraries that catalog historical documentation.

There is another way to elucidate the history of a stamp, and that is to let the analyzed subjects speak for themselves. Over the past ten years or so, the author has developed analytical schemes such that when one has access to an extensive series of stamps, the determination of their ink and paper compositions coupled with some means to assign an approximate date to the stamps has facilitated the correlation of the analytical results into a narrative having philatelic interest.

One scheme is highly suited for the study of stamps printed by the United States Bureau of Engraving and Printing (i.e., the BEP). Beginning in 1894, when the BEP took over the printing of United States postage stamps, each plate was sequentially numbered. Fortunately for the forensic philatelist, the time periods that defined the usage of each plate have been chronicled. As long as one is analyzing stamps that bear plate numbers, an approximate date when that stamp was printed can be estimated using the B.I.A. Plate Number Checklist (Cleland, 1990). Then, to chronicle the forensic history of a particular stamp, one would acquire information regarding the ink and paper composition of a series of plate-numbered stamps, and correlate that information with the plate chronology of the B.I.A. listing to develop the compositional story of a particular issue over time. This type of analysis has been used in studies of a large number of B.E.P. stamps (Brittain, 2019), and the utility of this approach will be further illustrated in this paper.

An alternative scheme to develop compositional history would be to analyze the ink and paper composition of stamps on covers that have been postmarked with a recognizable date and year. This approach works best for the most common stamps, where the assumption would be such stamps would be used nearly as quickly as they were printed, and thus one could assume that the postmark data would be an indicator of the approximate printing time of the stamp. One would then obtain covers having sequential dates and use the ink and paper compositions of the stamps to develop the historical chronology of that issue. Thus far, this second analytical scheme has not been thoroughly explored, but will be discussed in another paper to be presented at this symposium.

*Center for Philatelic Forensics, 10 Charles Road, Milford, NJ 08848

## X-Ray Diffraction: Forensic Technique for the Study of Paper

X-ray diffraction (XRD) is a methodology that is highly suited for the study of crystalline substances in analyzed samples, and one that has been shown to be highly useful in the elucidation of components contained in the paper on which a stamp is printed. The basis for XRD analysis is based in the fact that the three-dimensional pattern of atoms or molecules in a crystalline solid allows it to act as a diffraction grating to light having wavelengths of the same order of magnitude as the spacings between planes of atoms or molecules in the crystal. Electromagnetic radiation having the proper range of wavelengths for such studies is commonly known as X-rays, and the methodology itself has been discussed at length in many references (Klug and Alexander, 1974, and Brittain, 2003)..

Stamps, of course, are not crystals, but their ink or underlying paper can contain crystalline components capable of diffracting X-rays. In powder XRD, a randomly oriented sample is prepared in a flat plane so as to expose all the planes of a sample and is then irradiated with monochromatic X-ray radiation. Typically, the angles at which diffraction occurs are determined by slowly rotating the sample and using a scintillation counter to measure the intensity of diffracted X-rays with respect to the angle of the incident beam. One therefore obtains a series of peaks detected at characteristic scattering angles, and this is known as the XRD pattern. XRD patterns are ordinarily displayed where the ordinate is the intensity of scattering (in units of either counts-per-second or in percentage units), and the abscissa is the angle (in units of degrees 2-theta) at which those intensities were detected.

The value of XRD analysis is since every crystalline compound is defined by a unique structure, each must necessarily yield a unique and characteristic XRD pattern. The XRD pattern of a substance can be taken as a "fingerprint", which is then used for qualitative identification of the crystalline components in the sample. Typically, one develops a reference library of XRD patterns of reference materials and uses the known patterns to identify the components in an unknown sample.

***Figure 1.*** Interior view of the X-ray diffractometer, illustrating the goniometer and the mounting relationship of a studied stamp with the X-ray source (extreme left of the figure) and the detector (the cylindrical object at the right side of the figure).

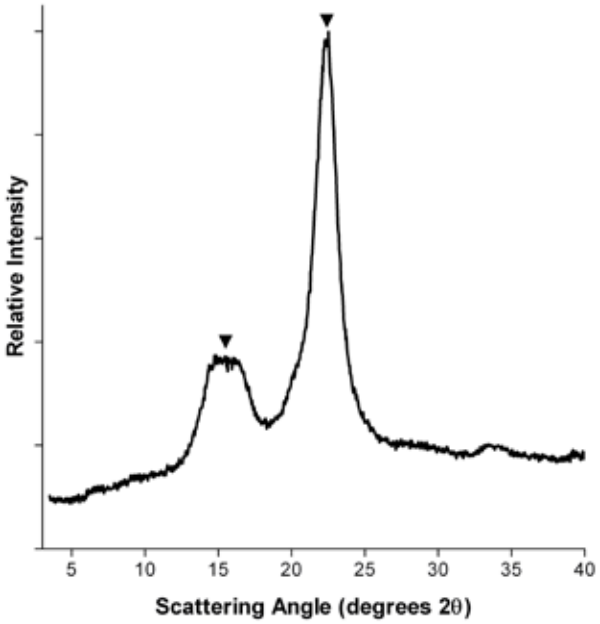


***Figure 2.*** XRPD pattern of microcrystalline cellulose, with the diagnostic peaks marked by the inverted triangles.

Since a stamp would necessarily present a flat face to an X-ray beam, it follows the technology commonly used to study the XRD of powdered solids can be used to study the crystalline materials present in a stamp. Simply put, one measures the XRD pattern of a stamp by situating it so its surface is in the same plane that would have been used for a powdered sample. A typical experimental configuration used by the author to obtain the XRD pattern of a stamp is shown in Figure 1.

As it would happen, the cellulose in stamp printing paper is present in a microcrystalline form. As illustrated in Figure 2, the primary feature in the XRD pattern of a stamp will often be associated with the cellulosic component.

XRD peaks attributable to the cellulose in a stamp are ordinarily observed as a broad peak centered around 15.5 degrees 2θ, and a more intense peak at an angle of 22.4 degrees 2θ.

To illustrate how a forensic philatelist would use XRD to identify a component in the stamp's paper, consider the example of printing paper used by the BEP at the time when it assumed responsibility for the printing of postage stamps in 1894. Such paper has been shown to contain kaolin (also known as China Clay), and Figure 3 shows a typical XRD pattern from paper of this time frame (obtained from the unprinted margin of a Scott* 279B plate strip).


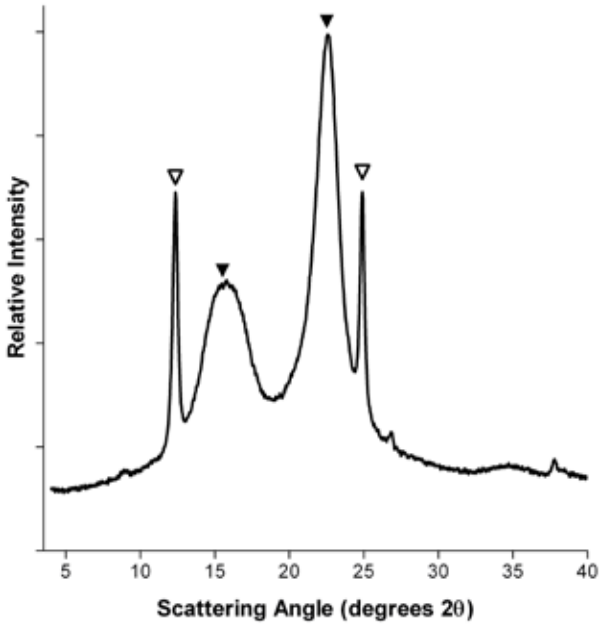


***Figure 3.*** (Above and right) XRPD pattern of the paper used to print Scott #279B. The cellulose peaks are marked by the dark triangles, the kaolin peaks the open triangles.

The presence of kaolin in the paper is evident by the additional peaks (open triangles) observed at scattering angles of 12.25 and 24.8 degrees 2θ, the identification of which was made by superimposing the XRD pattern of the kaolin reference with that of the stamp paper.

It must be pointed out that when the printing ink of a given stamp contains pigments that are strongly crystalline in nature, scattering peaks from the ink components can often be observed in the XRD pattern of that stamp. This possibility is shown in Figure 4 for Scott #219D, the lake variety of the 2¢ Washington stamp of the 1890 series printed by the American Bank Note Company. In the figure, the XRD peaks associated with cellulose and kaolin are clearly visible, but one can immediately see a large number of additional peaks are evident.

Note also the cellulose feature around 15 degrees 2θ has actually split into two recognizable components, located at 14.7 and 16.2 degrees 2θ. This disruption of the cellulose microcrystalline structure demonstrates the existence of strong chemical bonding between the underlying paper and the superimposed printing ink.



## Infrared Absorption Spectroscopy: Forensic Technique for the Study of Ink

Clearly, XRD analysis is a technique of choice for studying the crystalline components in stamp printing paper and can even provide information on printing inks when those inks contain crystalline mineral pigments. However, many pigments used as ink colorants or modifiers are not crystalline in nature, and thus their presence

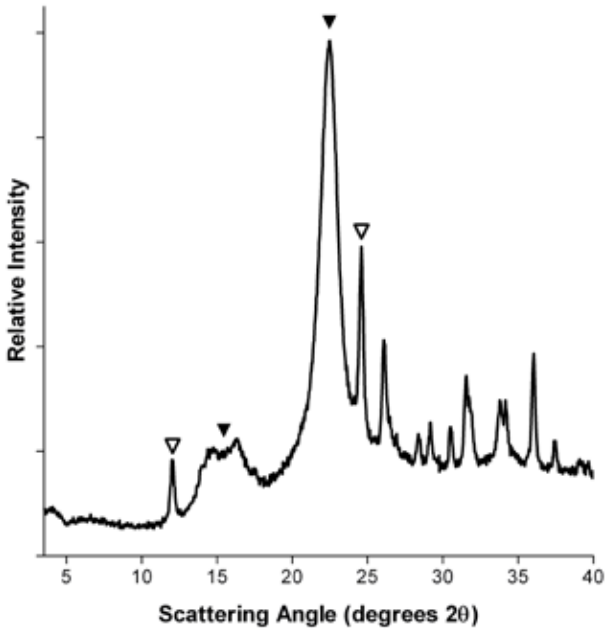


***Figure 4.*** (Left and below) XRPD pattern characteristic of Scott #219D stamps containing kaolin and additional peaks attributed to crystalline pigments in the printing ink. The cellulose and kaolin peaks are marked as in Figure 2.

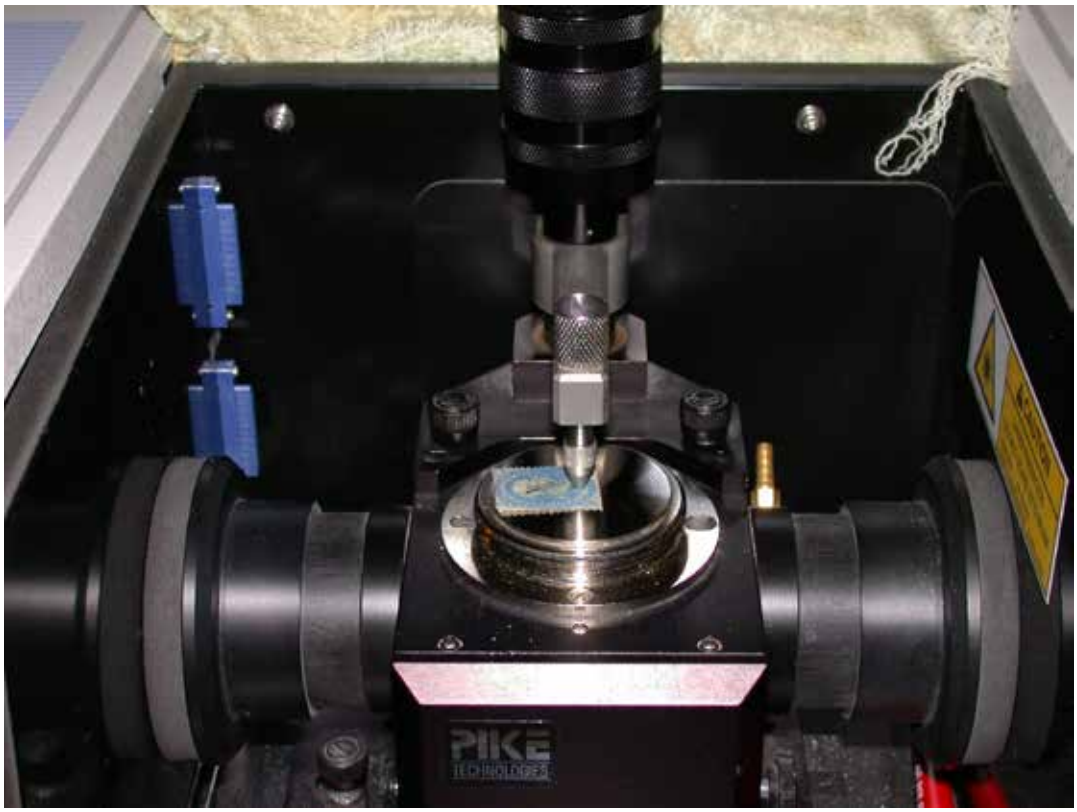


***Figure 5.*** View of the attenuated total reflectance sampling accessory used to obtain FTIR spectra of the portion of stamp surface directly under the pressure clamp. The stamp has actually been mounted upside down in order to demonstrate the small spot size studied in each measurement (i.e., immediately below the anvil).

cannot be detected by XRD. Such analysis requires a technique which uses physical properties inherent to a pigment molecule that can be detected regardless of the crystalline state of the compound. This analysis requirement is met through the use of infrared absorption (IR) spectroscopy, as the observable results of an IR analysis are derived from the intramolecular motions that are inherent to the compounds used in printing inks.

The patterns of intramolecular motion existing in molecules are characterized by repetitious oscillations of atoms about the center of gravity of the molecule, and these correlated motions are termed the vibrational modes of the molecule (Brittain, 2006). Energies associated with the lowest energy vibrational modes of a chemical compound will lie within the range of 400 to 4000 wavenumbers (also known as $cm^{-1}$), and therefore transitions among these modes fall into a region of the electromagnetic spectrum denoted as the mid-infrared region. Infrared absorption spectroscopy is a highly useful technique for the physical characterization of solids, and its utility has been demonstrated in a wide variety of applications (Bugay and Brittain, 2006). For a variety of experimental reasons, the acquisition of high-quality infrared absorption spectra appropriate for the characterization of substances is now almost universally performed using Fourier Transform technology. As a result, the technique is referred to as FTIR spectroscopy.

The principles underlying the absorption of infrared energy by molecules can be understood using a simple example. Consider a bent molecule consisting of three atoms, such as water ($H_2O$), which would be capable of undergoing a variety of bending and stretching motions. For example, a symmetric mode of water would be the simultaneous motions of the end hydrogen atoms and the central oxygen atom in a symmetric stretching of the bonds. Also possible is an asymmetric stretching vibration arising from compression of one bond and a stretching of the other bond, as well as a bending vibration consisting of an opening and closing of the bond angle.

However, in order for these molecular motions to be initiated, the water molecule must absorb infrared energy, and that energy must exactly match the energy required to effect a change in the pattern of molecular motion. Since every molecule possesses only a finite number of molecular vibrational modes, a molecule can only absorb a finite number of discrete infrared energies. Each of these will correspond to the energy of a particular vibrational mode of the molecule, and the sum total of infrared absorptions is termed its absorption spectrum.

One of the outcomes of spectroscopic theory is the energy of a particular vibrational mode is primarily determined by two factors. One factor is the strength of the intermolecular bonds involved in the vibration, the other is the mass of the atoms involved. Consequently, the vibrational energy of every molecular group will fall within a fairly narrow defined range, and correlation tables that relate molecular properties and absorption energies are well developed (Socrates, 2001). Infrared spectra is often divided into two regions: one being termed the "fingerprint" region (400-2300 $cm^{-1}$) where groups of similar atomic masses undergo absorption, the other being termed the "high-frequency" region (2500-4000 $cm^{-1}$) where hydrogen is one of the atoms undergoing absorption.

While the energy associated with a particular molecular vibrational mode can be roughly understood, the exact

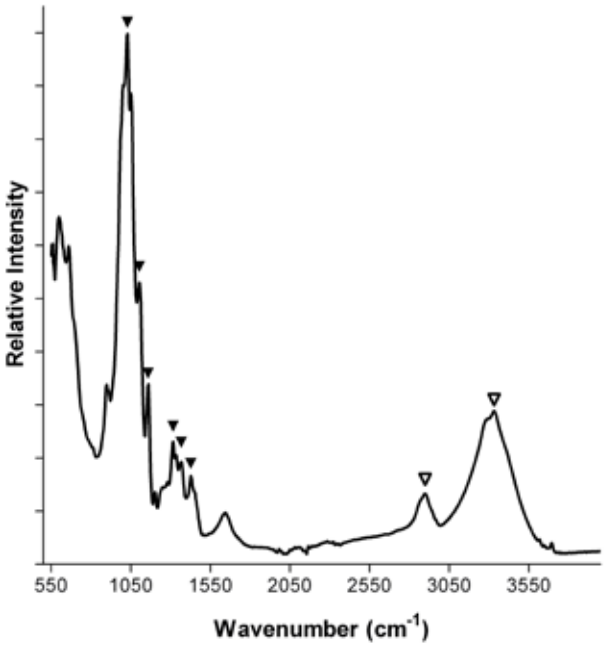


***Figure 6.*** FTIR spectrum of microcrystalline cellulose. The cellulose peaks in the fingerprint region are marked by the dark triangles, while the cellulose peaks in the high-frequency region marked by the open triangles.

value of that energy will be strongly influenced by the rest of the molecule whose motions couple into the vibrational mode of interest. As a result, every molecule will have its own characteristic and defining absorption spectrum, and this enables one to use infrared absorption spectroscopy for identity testing. The conduct of an infrared identification study proceeds much in the same manner as does an XRD investigation. The FTIR spectra of appropriate reference materials are obtained, and these are compared to the spectrum of the unknown sample. When an equivalence in peak energy between reference and sample is obtained, one can be assured that the peak in the sample can be attributed to that of the compound constituting the reference.

Probably the most useful sampling method for FTIR spectroscopy is attenuated total reflectance (ATR), where infrared radiation is passed through a crystal at an angle causing the light to undergo total internal reflection. At each reflection, the radiation penetrates a small distance beyond the crystal surface so that the internally reflected energy will be attenuated at those frequencies corresponding to changes in molecular vibrational states of whatever is held in physical contact with the crystal. The advantage of the ATR technique is it requires effectively no sample preparation, since one simply clamps the analyte onto the surface of the crystal with moderate pressure to ensure a sufficient degree of optical contact. The internal reflectance process does not permit the infrared beam to pass very deeply into the sample, and so the ATR sampling method permits one to effectively study only the outermost layers of a sample. A typical experimental configuration used by the author to obtain the FTIR spectrum of a stamp is shown in Figure 5.

Given that postage stamps are printed on paper, and that paper consists largely of processed cellulose, it is appropriate to first consider the FTIR spectrum of cellulose itself. Figure 6 shows the FTIR spectrum obtained from a sample of microcrystalline cellulose, where the fingerprint region peaks are marked at 1028, 1103, 1159, 1315, 1367, and 1427 wavenumbers, and the broad bands in the high-frequency region are observed at 2900 and 3330 wavenumbers.

The ability of FTIR spectroscopy to elucidate the components in the printing ink of a stamp is illustrated in Figure 7. Here, where the FTIR spectrum obtained in the fingerprint region of a Scott-264 plate numbered strip is superimposed with the spectrum obtained from the unprinted region of this stamp. In addition to the background peaks associated with cellulose, the FTIR spectrum also contains

***Figure 7.*** (Below and right) FTIR spectrum obtained within the blue inked region of a Scott #264 stamp. Marked peaks are due to the presence of cellulose (◊), calcium sulfate (▼), calcium carbonate (▽), and Prussian blue (*)


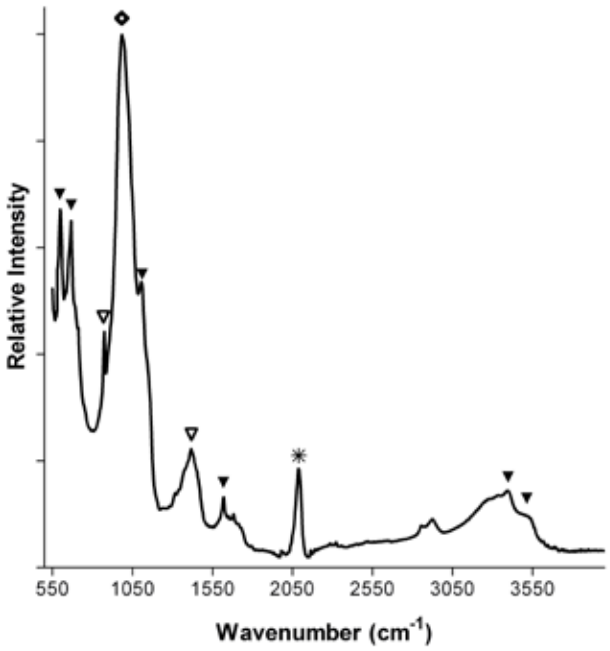

peaks attributable to calcium sulfate, calcium carbonate, and Prussian blue. Prussian blue is the primary pigment of the blue color of the stamp image, while the calcium carbonate and calcium sulfate are whitening agents formulated into the stamp to achieve the desired degree of blue coloration.

## Summary

The preceding brief tutorial amply demonstrates the forensic techniques associated with X-ray diffraction and infrared absorption spectroscopy provide the ability to profile the chemical components contained in both the printing ink and the paper on which that ink has been impressed. However, the ability to obtain data is only the first step toward creating this type of profile. Since the observed XRD and FTIR peaks do not come with assignments, the investigator must also have a comprehensive database of known patterns and spectra that can be used to deduce the origins of the peaks noted in the data derived from the stamps in question. The essential aspect of the analysis is rooted in the interpretation of the experimental data, and this part of the study requires both experience and background obtained by a prior study of reference materials. If that underlying support is available, then the acquisition of XRD and FTIR forensic data can yield extremely important information.

The generation of the information database also serves as the foundation for studies of unusual stamps, such as those who exhibit non-standard colors. Identifying the components in the "normal" stamps enables one to study an "anomaly" to determine whether that stamp is actually anomalous, and what makes it anomalous. For example, in a recent work, the existence of an authentic color variation among Scott #416 stamps has been experimentally demonstrated (Brittain and Lowther, 2019). While the typical method of stamp authentication mostly involves visual evaluation, the forensic evidence obtained using instrumental methods would be inarguable.

## References

Brittain,H.G. 2003. X-ray Diffraction of Pharmaceutical Materials, in *Profiles of Drug Substances, Excipients, and Related Methodology*, Volume 30, Chapter 7, H.G. Brittain, ed., Elsevier Academic Press, Amsterdam, pp. 273–319.

———. 2006. Molecular Motion and Vibrational Spectroscopy, in *Spectroscopy of Pharmaceutical Solids*, Chapter 7, H.G. Brittain, ed., Taylor and Francis, New York, pp. 205–233.

———. 2019. Kaolin Content in the Paper Used by the Bureau of Engraving and Printing to Produce 1¢ and 2¢ Stamps between 1894 and 1908, *United States Specialist*, 90(2): 61–71.

Brittain, H.G. and K.G. Lowther 2019. FTIR Spectroscopy Used to Analyze Brown-Yellow Washington-Franklins; Unlisted Postally-Used Examples of Scott 416a Are Thereby Documented, *United States Specialist*, 90(11): 519–523.

Bugay, D.E. and H.G. Brittain. 2006. Infrared Absorption Spectroscopy, in *Spectroscopy of Pharmaceutical Solids*, Chapter 8, H.G. Brittain, ed., Taylor and Francis, New York, pp. 235–269.

Cleland, W. Wallace. 1990. *B.I.A. Plate Number Checklist, Plates 1-20,000,* Bureau Issues Association, Belleville, IL.

Klug, H. P. and L. E. Alexander. 1974. *X-Ray Diffraction Procedures for Polycrystalline and Amorphous Materials*, 2nd edition, Wiley-Interscience, New York.

Socrates, G. 2001. *Infrared and Raman Characteristic Group Frequencies*, John Wiley & Sons, Chichester.

# Evolution of the Ink and Paper Composition in the Stamps of the 1893 Columbian Issues

*Harry G. Brittain**

## Introduction

As discussed in my previous presentation (Brittain, 2020), the forensic analysis of a stamp entails the use of appropriate analytical technology to identify the various components in printing inks and the paper on which the stamp was printed. In that preceding paper, the two schemes outlined allowed a forensic scientist to correlate the ink and paper compositions of a particular issue in order to develop a historical narrative of the stamps involved based on the forensic results. One of the schemes required the analysis of plate-numbered stamps and a correlation of their approximate printing dates (accessible in the volumes of the *B.I.A. Plate Number Checklist* (Cleland, 1990; Larson and Johnson, 1990)) with the results of forensic studies in order to observe differences in ink and paper composition over time.

The alternative scheme disclosed in the earlier paper to develop compositional history involved the analysis of stamps remaining on covers postmarked with a recognizable date and year. The assumption was the most common stamps would be used as they were printed, enabling one to use the postmark date as a means to deduce its approximate printing time of the stamp. Assuming one could acquire covers where the stamps were cancelled in a sequential manner to generate the timeline, knowledge of the ink and paper composition of each stamp would allow one development of the historical chronology of that issue.

The utility of correlating the forensic results obtained from stamps on dated covers to develop a historical picture was illustrated by summarizing forensic work conducted on the 2¢ stamps (Scott #231) printed by American Bank Note Company as part of the Columbian Exposition series.

## 1. January 1893 to June 1893

The first sheets of the Scott #231 were printed by the American Bank Note Company in November of 1892. Over time, colors variously described as violet, deep violet, and gray violet have been found (Brookman, 1967). The official color listed in the *Scott Catalogue* is brown-violet, with January 1, 1895, as the earliest documented date of use (Scott, 2015). The image on the stamp was derived from a painting by John Vanderlyn, entitled "The Landing of Columbus".

The first dated cover characterized was dated January 9, 1893 and is shown in Figure 1. Figure 2a contains the full XRPD pattern obtained for the stamp on the cover, and figure 2b contains the fingerprint region of its FTIR spectrum.

Beside cellulose, the only contributing substance in the XRPD pattern of the January 9 stamp is due to the presence of barium sulfate (i.e., barite), and peaks attributable to this substance were also found in the FTIR spectrum. Given the high degree of crystallinity associated with this substance, it is not surprising barite peaks were noted in


***Figure 1.*** Scott #231 cover, dated January 9, 1893.

*Center for Philatelic Forensics, 10 Charles Road, Milford, NJ 08848

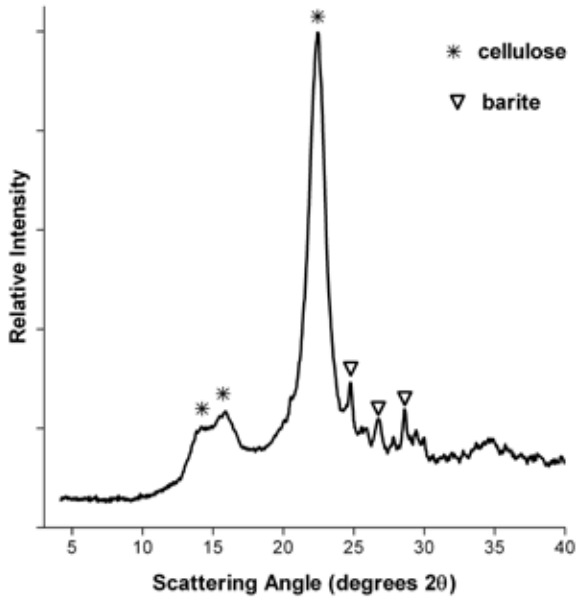


***Figure 2a.*** XRPD pattern of the stamp on the Scott #231 cover, dated January 9, 1893.

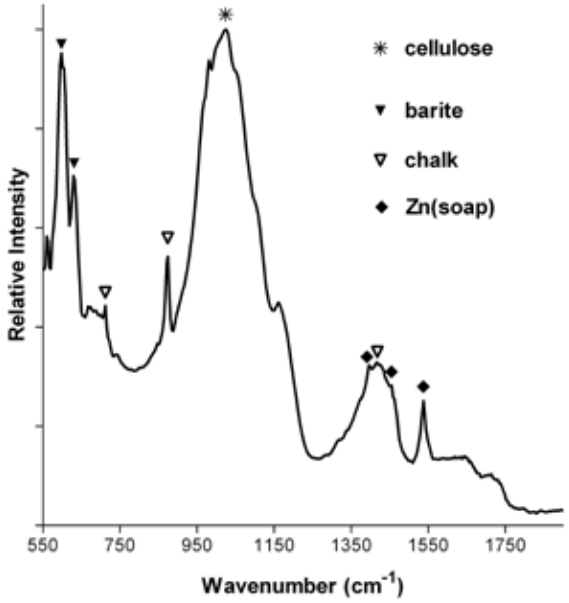


***Figure 2b.*** FTIR spectrum (fingerprint region) of the stamp on the Scott #231 cover, dated January 9, 1893.

the XRPD pattern of this stamp, even though it would have only been present in the printing ink. The FTIR spectrum also contained peaks characteristic of a zinc-soap complex, undoubtedly formed from the surfactants that were used to facilitate mixing of the ink components.

Perhaps the most interesting detail regarding the FTIR spectrum is there were no strong peaks from substances that would have been the coloring pigments in the ink. Nevertheless, such pigments must be present in the ink in order for the stamp to acquire its purple color. Figure 3a contains a superimposition of the fingerprint region the FTIR spectrum of the January 9 stamp with the corresponding FTIR spectrum of the printing paper. Figure 3b contains an expanded view of the differential FTIR spectrum obtained after the spectrum of the paper was digitally subtracted from the spectrum of the stamp.

Through comparison to known reference standards, the peak at 874 wavenumbers (marked by the symbol ¯ in

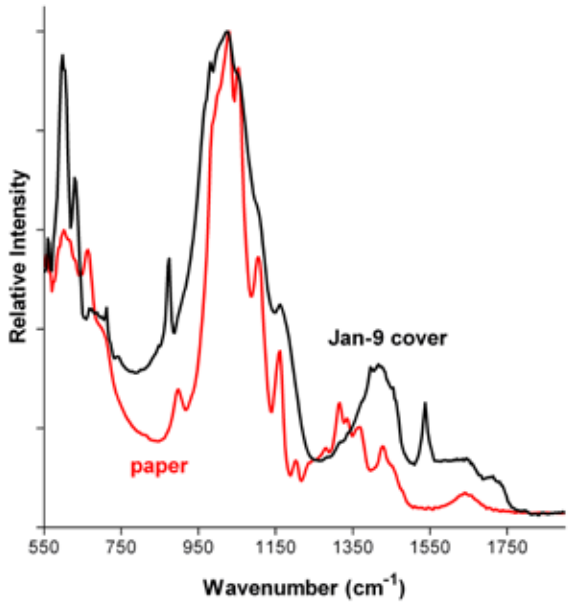


***Figure 3a.*** Black trace: FTIR spectrum (fingerprint region) of the stamp on the Scott #231 January 9 cover, dated, 1893. Red trace: FTIR spectrum (fingerprint region) of the unprinted margin of the January 9 stamp.

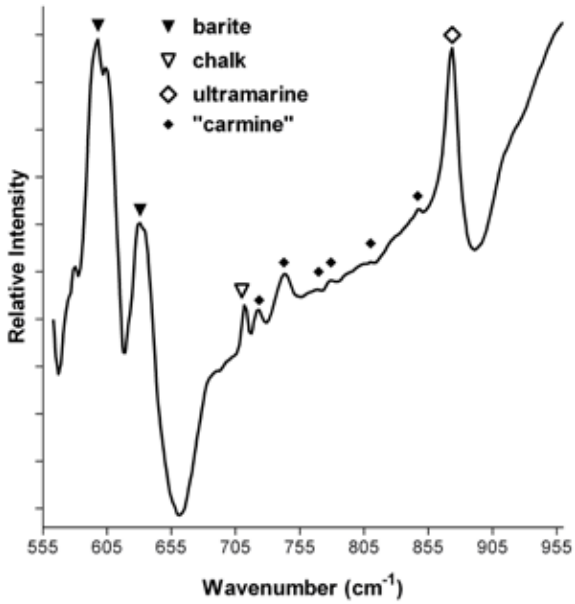


***Figure 3b.*** FTIR spectrum (fingerprint region) obtained by the differential subtraction of the spectrum of the printing paper from the spectrum of the Scott #231 stamp on the January 9 cover.


***Figure 4.*** (Left) Scott #231 cover, dated July 7, 1893.

***Figure 5a.*** (Below, left) XRPD pattern of the stamp on the Scott #231 cover, dated July 7, 1893.
***Figure 5b.*** (Below, right) FTIR spectrum (fingerprint region) of the stamp on the Scott #231 cover, dated July 7, 1893.

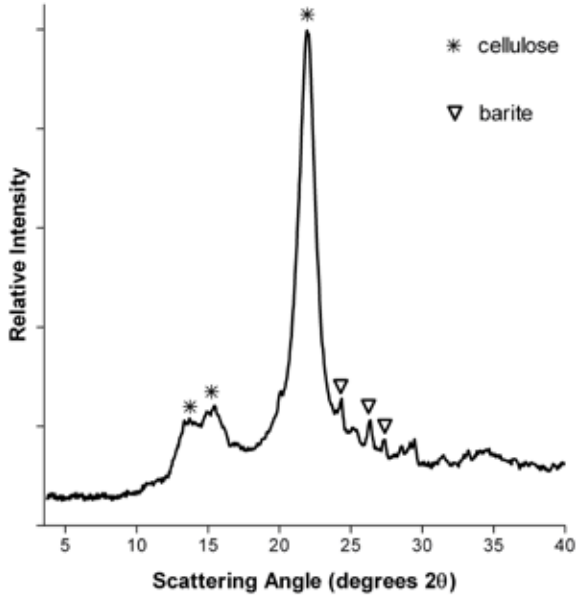


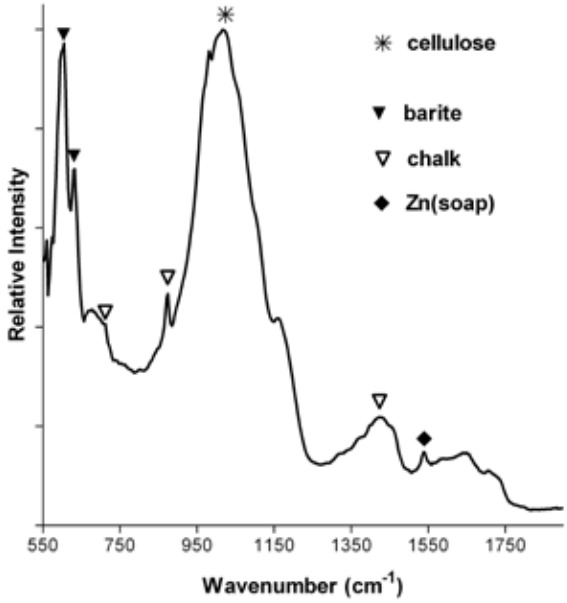


Figure 3b) was determined to be due to the presence of the blue pigment ultramarine in the printing ink. Similarly, by comparison to a synthesized sample of the aluminum salt of carminic acid, a series of weak peaks within the region spanning 723-810 wavenumbers (marked in Figure 3b by the symbol t) was attributed to the presence of carmine in the printing ink.

It is therefore concluded the purple color of the Scott #231 stamps was achieved by the formulation of the pigments ultramarine and carmine, with the resulting color being softened using chalk and barite as whitening agents. The same XRPD pattern and FTIR spectra shown in Figures 2 and 3 was observed for Scott #231 stamps on 1893 covers dated February 27, March 8, April 22, May 8, and June 29.

## 2. July 1893 to October 1893

1893 covers bearing the Scott #231 stamp, postmarked July 7 (see Figure 4), August 26, September 25, October 7, and November 1 were found to exhibit roughly the same XRPD pattern as shown in Figure 2a for the January - June 1893 covers (see Figure 5a). However, as shown in Figure 5b, the FTIR spectra obtained for the stamps on these covers was found to contain significantly less of the zinc(soap) component.

The stamps on the covers within the July to October 1893 time period are all characterized by a significant reduction in intensity associated with the Zn(soap) peak relative to that shown in Figure 2b for the stamp on the January 9 cover. The other Zn(soap) peaks of Figure 2b are too weak to be detected in the spectrum of the stamp on the July 7 cover. The consistency observed among the FTIR spectra of stamps within this time period indicates the existence of a small, but definite change in the ink composition.

## 3. November 1893 to February 1894

In the latter half of 1893, the forensic analysis demonstrated that further changes had been made by American to both the ink and the paper. These changes were evident in stamps used on 1893 covers postmarked on November 26 (see Figure 6) and December 16, as well on 1894 stamps on covers postmarked January 22 and February 14. As evident in the FTIR spectrum of Figure 7a, no peaks attributable to the Zinc(soap) complex were detected.

Perhaps the most distinguishing feature of Scott #231 stamps in the November 1893 to February 1894 time period

***Figure 6.*** (Right) Scott #231 cover, dated November 26, 1893.

***Figure 7a.*** (Below, left) XRPD pattern of the stamp on the Scott #231 cover, dated November 26, 1893.
***Figure 7b.*** (Below, right) FTIR spectrum (fingerprint region) of the stamp on the Scott #231 cover, dated November 26, 1893.

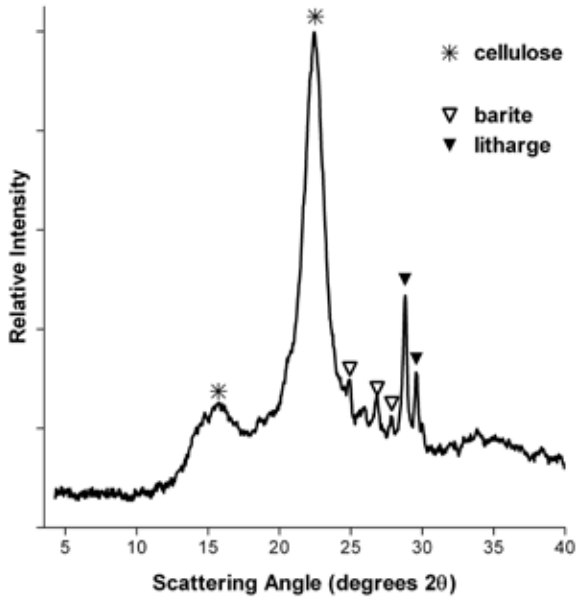


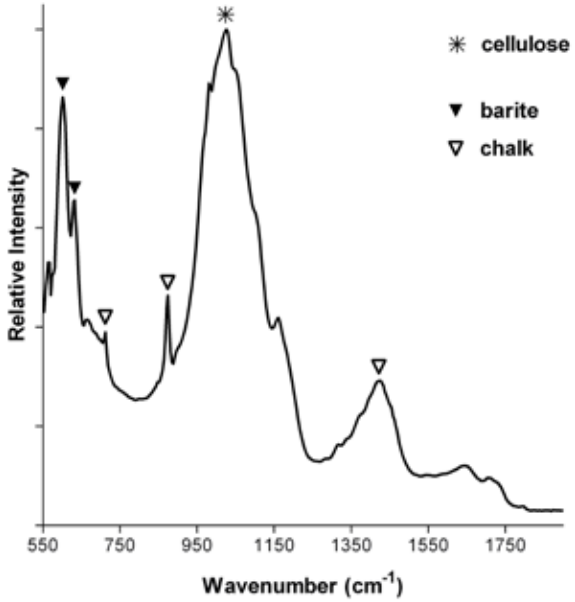


is the sharp doublet of peaks observed at angles of 28.8 and 29.6 degrees 2θ. The XRPD patterns of a large number of potential substances were obtained for identification purposes, but, in the end, a nearly identical peak match was obtained for litharge, a complex lead oxide substance. Litharge (also known as massicot) can be obtained in colors ranging from pale yellow to red, depending on the amount of iron oxide present in the material. Litharge is not detectable in an FTIR spectrum if the sample contains calcium carbonate (i.e., chalk) since both of their main absorption bands are observed at nearly the same wavenumber.

It is worth noting I have observed use of litharge-containing paper in nearly all of the stamps that were printed by the American Bank Note Company during the latter months of 1893 and throughout much of 1894, so the use of this particular printing paper is not restricted to the 2-cent Columbian issues.

## 4. March 1894 to December 1894

Around March 1894, American elected to change the composition of its printing paper, while effectively using the same ink composition as that of the preceding time period. The stamps studied for this time period were postmarked during 1894, and dated March 4 (see Figure 8), April 19, May 21, June 24, July 3, August 27, September 8, and December 6.

Comparison of the FTIR spectra obtained for the Scott #231 stamps on the covers of the March 1894 to December 1894, with the stamps on the covers of the November 1893 to February 1894, reveals the spectra were very nearly equivalent to each other. This finding supports the conclusion that the composition of the printing ink used during this time period was a consistent and unchanging formulation.

On the other hand, the XRPD patterns of the stamps on the covers from the March 1894 to December 1894 time period are quite different from those of the preceding time period. The doublet of peaks at 28.8 and 29.6 degrees 2θ are no longer present in the diffraction patterns, indicating a change in the nature of the printing paper used. In addition, the XRPD patterns of stamps within this time period were found to contain peaks attributable to kaolin (i.e., China clay). It is interesting to note the diffraction patterns of both litharge and kaolin contain peaks around 29.5 degrees 2θ, but that is merely a coincidence of one compara-

***Figure 8.*** (Left) Scott #231 cover, dated March 4, 1894.

***Figure 9a.*** (Below, left) XRPD pattern of the stamp on the Scott #231 cover, dated March 4, 1894.
***Figure 9b.*** (Below, right) FTIR spectrum (fingerprint region) of the stamp on the Scott #231 cover, dated March 4, 1894.

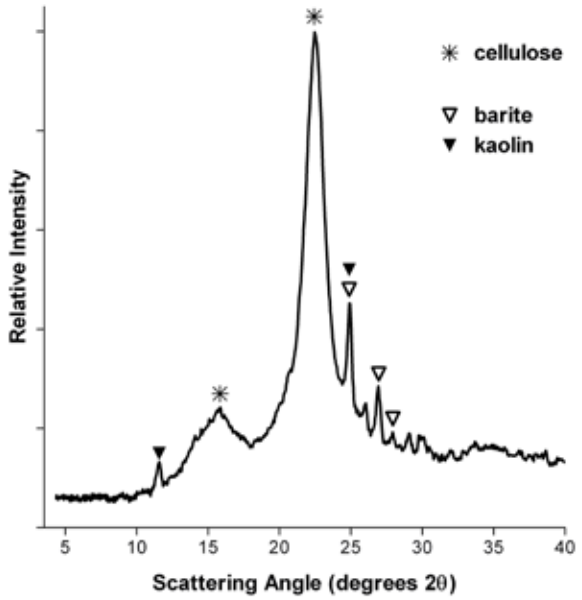


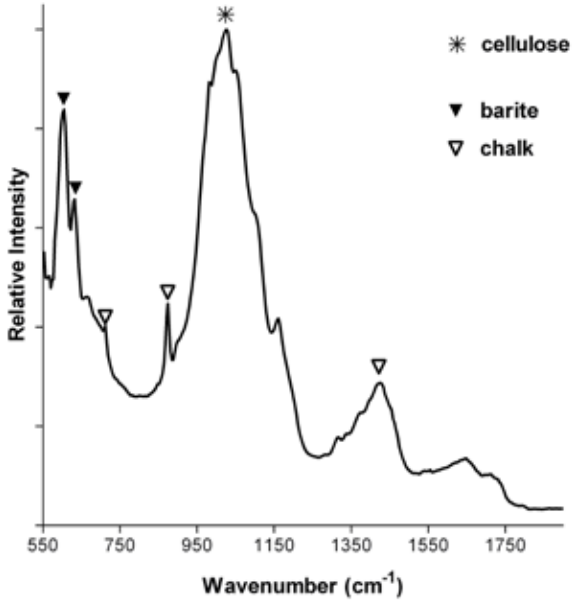


ble molecular plane in the microcrystalline particles of the two compounds.

## Conclusions

By obtaining X-ray diffraction patterns and infrared spectra for stamps postmarked during 1893 and 1894, it was possible to determine that the American Bank Note Company printed four different types of Scott #231 stamps. Furthermore, the effective dates of usage for these different stamp types was roughly determined by conducting the analyses only on stamps existing on postmarked covers.

The assumption underlying this approach is, since the 2-cent stamps would have been used to pay the basic postage rate, they would have been used nearly as fast as they were produced. The time intervals identified in this work for the four types of Scott #231 stamps should not be taken as being rigorously accurate, since there would have been a lag time between the time when the stamps were actually printed and when they were actually used. Nevertheless, the forensic characterization of stamps on postmarked covers can be an extremely useful tool for tracking the evolution of ink and paper in a series of postage stamps.

## References

Brittain, H. G. 2020. Use of X-Ray Diffraction and Infrared Absorption Spectroscopy for the Study of Paper and Ink in Postage Stamps. In: *Proceeding of the Fourth International Symposium on Analytical Methods in Philately.* Washington, DC, p. xx.

Brookman, L. G. 1967. *The United States Postage Stamps of the 19th Century, seijulaakso@gmail.com Volume III.* New York: H. L. Lindquist Publications, pp. 56–58.

Cleland, W. Wallace. 1990. *B.I.A. Plate Number Checklist, Plates 1–20,000.* Belleville, IL: Bureau Issues Association.

Larson, J. L. and K. D. Johnson. 1990. *B.I.A. Plate Number Checklist, Plates 20,000–41303.* Belleville, IL: Bureau Issues Association.

Scott Publishing Company. 2015. *Scott Specialized Catalogue of United States Stamps and Covers, 94th edition.* Sidney, Ohio: Amos Media Co., p. 42.

# Handheld Macro-XRF scanning: Development of Collimators for Sub-mm Resolution

*Aaron N. Shugar**

## Abstract

Handheld XRF spectrometers were modified by creating new collimators to reduce the beam size. These systems can be mounted onto scanning gantries and used to perform MA-XRF mapping of smaller artifacts. The scanning can have valuable benefits for the study of philatelic materials with more than one pigmentation color. Examples are provided, demonstrating the resolution attainable and potential information that can be collected from the resulting data.

## Introduction

The use of X-ray Fluorescence (XRF) to identify pigmentation used on stamps has gained popularity in the last few years (i.e. Sánchez and Valentinuzzi 2006; Castro et al. 2008; Badovinac et al. 2010; Allen et al. 2013; Lera et al. 2013). The ability to quickly identify elemental composition (higher than Na on the period table) has aided in authentication studies and helped develop a database of elemental signatures covering temporal and geographical space. The traditional use of XRF as a macro spot scan, typically based on the irradiation spot size of the XRF system (from ~1mm– ~ 8mm depending on the system), can be limiting as the entire spectral response from the surface of that area is collected at once.

Although this method has been successful at identifying changes in pigmentation, it is difficult at best to clearly determine the relationship of those pigments to one another. Scanning across the surface at higher resolution allows further differentiation between the specific pigments used, as well as how those pigments were laid down and relate to one another.

Macro area X-ray fluorescence scanning (MA-XRF) has become a staple for the technical study of works of art, in particular paintings (i.e. Dik et al. 2008; Mosca et al 2016; Ravaud et al. 2016; Alberti et al. 2017; Sawerwyns et al. 2018). With the advancement and miniaturization of instrumentation, lab-based systems have been developed allowing for macro area scanning of artifacts. These systems were developed in house by many laboratories integrating both motorized sources and detectors, as well as motorized easels with isolated stable sources and detectors. Semi-portable systems offer the ability to image at a spot resolution as low as 90μm using polycarpellary collimation (i.e. Bruker Jetstream Alfeld et al. 2013). As such, these scanning systems are relatively expensive and prohibitive for smaller labs or museums to obtain.

A potentially viable alternative to these systems is to use handheld XRF spectrometers to perform MA-XRF scanning. Although most were not designed to be used for this purpose (Bruker Elio is an exception as it was designed for limited area scanning), the potential for them to be further developed for MA-scanning is a viable alternative. (Shugar 2019). The limiting factors in using handheld spectrometers, however, are the beam spot size and speed of collection.

Currently, the smallest beam size offered by manufacturers of handheld XRF systems is 1 mm (i.e. Bruker Elio). Bruker's handheld XRF (Tracer 5i/g) comes with manually interchangeable collimators with an expected spot size at the face of the instrument of either 3 or 8 mm. Custom collimators can be made, to reduce the spot size for the Tracer systems, but are are truly 'masks' that decreases photon output. This results in decreased photon interaction with the sample, and a reduced overall detector signal, creating poorer quality spectra, limiting the ability to collect quality data. New systems overcome this to some extent as they use

*Andrew W. Mellon Professor of Conservation Science; Art Conservation Department, Buffalo State College

higher wattage tubes (4 watt) and larger area detectors (up to 40mm$^2$ on the Tracer 5i/g), allowing for a higher total flux at the source and increased detection capability.

Handheld XRF systems can now be mounted to X Y gantries allowing for larger area scanning of works of art. If needed, these scans can be "stitched together" to create larger elemental maps (Pocobene et al. 2020).

Although successful scanning can be performed at 1mm, when looking at smaller artifacts, such as stamps, that resolution is not satisfactory. The development of small beam collimators with increased photon output has allowed for collimators with bore diameters as low as 0.47mm diameter. Altering the bore hole shape results in improved signal per pixel at a sub-millimeter resolution, revealing more detail than previously allowed using handheld XRF instruments (Shugar 2019).

## Methodology

A Bruker Tracer 5i/5g collimator was modified to decrease the beam diameter by replacing the existing collimators with newly fabricated ones. The original aluminum collimators (3mm and 8mm spot sizes at the instrument face—2mm and 4.5mm bore size respectively) are held in a brass casing. The central aluminum collimator was removed and newly manufactured ones, with variable bore hole sizes, were inserted. As stated above, these collimators are 'masks' restricting photon intensity. The straight bore hole was modified by cutting a cone angle into the collimator at 45 degrees, with a 2mm straight bore at the tip to eliminate photon bleeding from the head of the collimator. The 45-degree bore was made to take advantage of the diffraction angle of brass, which theoretically would add photon intensity in the collimator resulting in increased photon interaction with the sample *(ibid)*. Since stamps are rather small, a smaller beam size is important to ensure accurate elemental map production. Thus, the most effective bore size for MA-XRF mapping of philately was determined to be around 0.5mm.

***Figure 1.*** DeWitt MSS-150E scanning stage with the Bruker Tracer 5i attached.


***Figure 2.*** (Left) French .25 F Gallic Rooster stamp designed by Albert Decaris, initially printed in 1962—measures ~ 20x26mm. (Right) 3¢ Oleander Bermuda Colonial stamp from the 1970 Island Flowers issue—measures ~ 30x45mm.

The XRF was coupled to a DeWitt MSS-150E scanning stage (Figure 1), to allow for step sizes down to 0.1mm in both the X and Y axis. Proprietary software outputs data either as individual Bruker PDZ files, or as Bruker Artax project files. This project file contains all the individual spectra which can be investigated individually or combined to assess the larger dataset. The data can then be deconvoluted and converted to an excel data-cube file which subsequently can be converted to elemental maps in Golden Software's Surfer software or any preferred mapping software. The specific instrument setting is variable for each set of scans and will be provided when discussing those scans.

Presented here are two stamps scanned to assess the viability of using handheld XRF for micro-area scanning (Figure 2). The first is a 0.25F French Gallic Rooster stamp designed by Albert Decaris, and initially printed in 1962. The second is a 3¢ Oleander stamp from the 1970 Bermuda Colonial Island Flowers issue.

## Results

### *French .25 F Gallic Rooster stamp:*

To investigate the potential difference in resolution based on step size, scanning was done with a 0.47 mm bore collimator at different scanning rates. Step rates were based on a 0.4mm (X) x 0.5 mm (Y) at 0.4 mm/sec movement. This was compared to over-scanning at a rate of 0.2mm (X) x 0.3mm (Y) at 0.2mm/sec. Both scans were taken at 35kV and 110 uA with no filter. The French 0.25 Franc Gallic Rooster stamp measures approximately 20mm x 25mm.

In Figure 3, both scans are displayed side by side for each scan resolution. It is clear the over-scanning at 0.2x0.3mm can resolve more detail in the stamp. The resolution allows for clearer delineation of features and the use of pigmentation on the stamp. The drawback being limited to a collection rate of one second per pixel (1sec/pixel) means the time requirement is rather high. For the

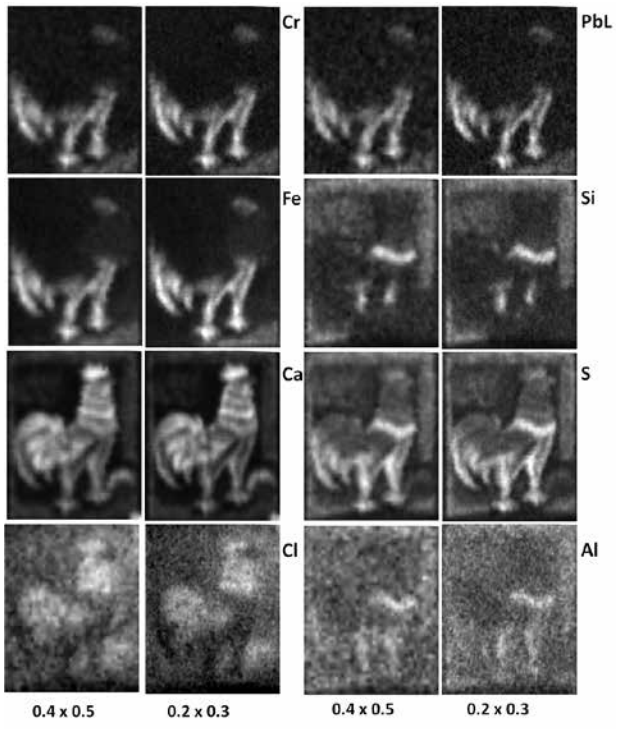


***Figure 3.*** Comparison of two scanning speeds, showing the difference in resolution.

0.4x0.5mm, the scan time is approximately 0.9 hours vs the scan time for the 0.2x0.3mm which is 2.6 hours. The decision on what resolution is required may be dependent on the detail of the individual stamp itself. Nonetheless, the improved quality is clear, and more detail can be resolved.

Since the data extraction provides an excel datacube with peak intensities associated with all the elements present, additional statistical analysis can be performed. Correlation tables can indicate which elements have a positive or negative relationship with one another (Figure 4).

In this case, for example, there is a strong positive correlation between Fe, Cr, Pb, and S. This suggests one pigment contains all these compounds, or multiple elements were blended or overlaid on one another to create the visible hue. The specific pigment or pigments used would need to be confirmed using additional analytical techniques (i.e. FITR Multispectral imaging, Raman Spectroscopy—see Vollmeier 2000; Badovinac et al 2010; Brittain 2016 Pinto and Melo 2018 for examples of alternative analytical techniques).

Although these correlation tables are very useful, they can be misleading, because some elements might be located in several pigments. Thus, their associations may not be as recognizable when at lower concentrations. Looking at elemental scatter plots can help reveal those potential issues.

When looking at the scatterplot of Si and S two datasets are visible. A positive correlation can be seen between Si and S as well as an isolated increase in S devoid of Si. This confirms the visual assessment seen in the maps with S associated with both Si rich areas and the areas associated with Fe, Pb, and Cr.

A spectral assessment can also be made from the data. By taking an accumulated spectrum from all spectra collected (8552 individual spectra), a comparison can be made from the spectral response similar to one gotten if a larger

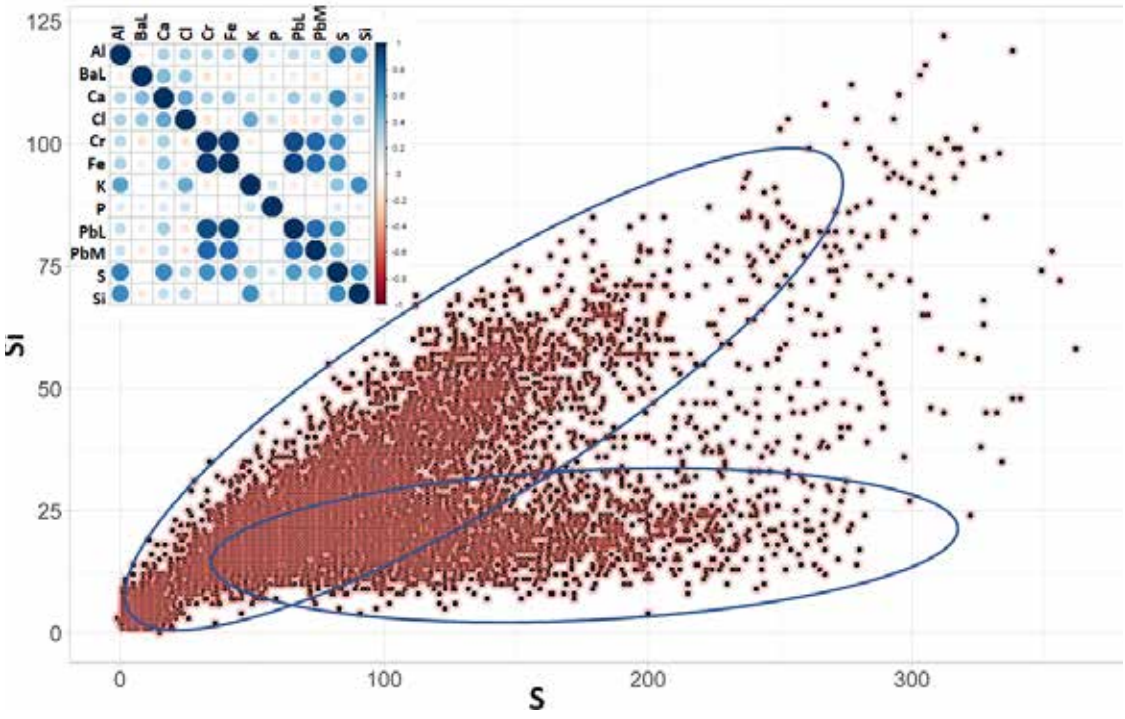


***Figure 4.*** Scatterplot of SiK and SK lines showing a positive correlation between the two elements as well as an isolated increase in S devoid of Si. This suggests the two elements are both present in the same locations on the stamp as well as a second pigment that contains S and not Si. The inset shows the correlation table for all elements identified.

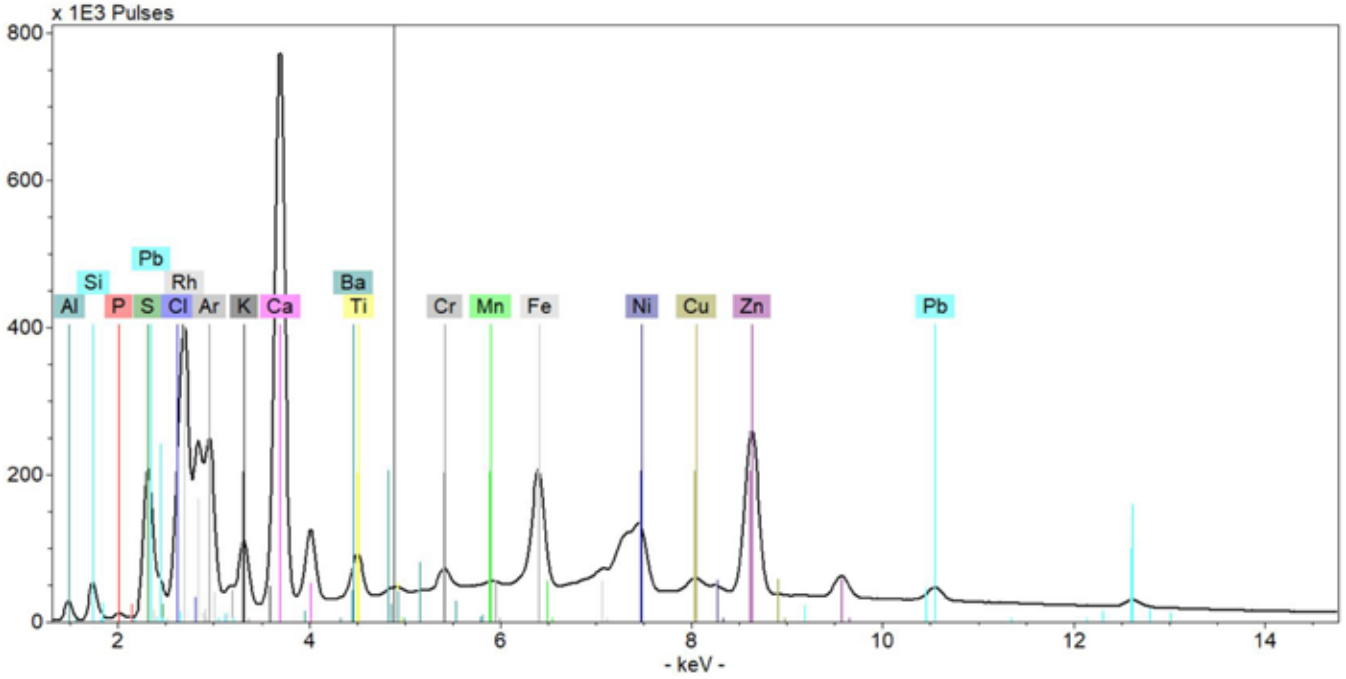


***Figure 5.*** Accumulates spectrum from 8552 spectra collected from the area MA-XRF scan showing all elements associated with the pigmentation and the paper. Extracting which elements are associated with which pigment is difficult from this general macro scan.

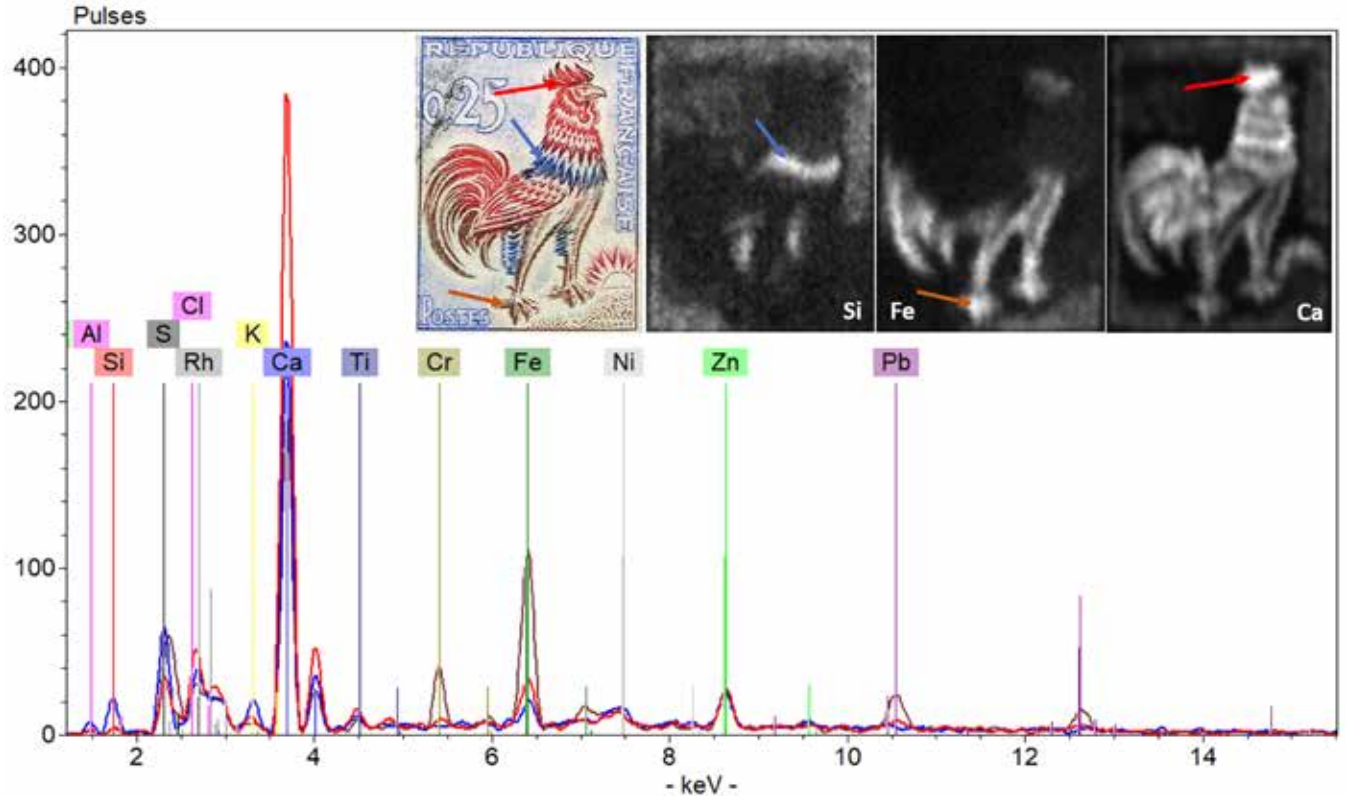


***Figure 6.*** Spectra from individual pixels of high concentration regions from Si, Fe, and Ca respectively. Each location shows the correlative elements from the pigmented regions of blue, brown, and red.

collimator XRF, that collects the elemental composition over a macro area of the stamp, was used. All the elements are present, but it is not possible to extract those related to specific pigments or dyes (Figure 5).

From the scanned data, specific pixel information can be extracted to better investigate the elements associated with pigmentation. In this case, the extracted spectra from one pixel for blue, brown and red pigmentation from the

stamp. The specific location for each spectrum is indicated on the associated elemental map that shows higher concentrations of pigmentation (Figure 6).

Although determining a specific pigment based on XRF analysis alone is not recommended, the elemental data obtained can be used to confirm the use of other analytical techniques. The data shows clear differences between the spectra. The blue pigment shows higher association with Si, Al, K and S, which might suggest the use of French ultramarine ($Na_8–10Al_6Si_6O_{24}S_{2–4}$). The brown pigment shows higher concentrations of Pb, Cr, S, and Fe, which may be the result of blending lead chromate ($PbCrO_4$), or lead (II) chromate ($PbCrO_4 \cdot Pb(OH)_2$) with and iron-based pigment (ochre or Prussian blue). The red pigment shows higher concentrations of Ca and Cl, which could indicate an organic dye or lake pigment with a calcite bulking agent.

### *1970 3¢ Oleander Bermuda Colonial stamp*

A 0.47mm collimator with no filter was used for this scan at 20kV 142uA, and a pixel size of 0.3mm (X) x 0.4mm (Y) at 0.3m/sec. The stamp measures approximately 30mm x 45mm. A total of 21344 spectra were collected over this scan, the resulting elemental maps their relationships to one another. The pigment color can be seen in Figure 7.

The correlation data shows a limited relationship between Fe and S but when plotted there are clearly two data sets associated with these two elements (Figure 8). One is a positive relationship, the other is Fe rich with no S, which explains the limited correlative value.

Exploring the relation further, a pixel spectrum was taken from areas associated exclusively with Fe, and another from a positive correlation point (Figure 9). Both spectra show the differences between the two regions containing Fe. The first spectrum is associated with areas of blue, has relatively low Fe concentration, but not much else associated with the pigment. This is most likely a Prussian blue pigment which tends to have low Fe concentrations and can be hard to identify by XRF alone. The second spectrum is associated with a region consisting of a toned green pigment in the plant leaves. Both the elemental maps and the correlation data from this area suggest higher levels of Cr, S, and Pb. The green leaves are likely a chrome yellow - lead (II) chromate ($PbCrO_4$) toned green by blending Prussian blue. The red and pink are likely organic dyes with some minor association with Al and Si (see Figure 7).

## Conclusions

MA-XRF mapping has become a staple in the analysis of art. The instrumentation used is often cost prohibitive, however, using handheld XRF for mapping is now possible. Using a custom collimator, a Bruker Tracer 5i/g can be modified to have a sub millimeter spot size. By coupling the XRF with a DeWitt MSS-150E scanning bed, MA-XRF elemental mapping can be performed. Taking advantage of the smaller spot size in conjunction with over-scanning pixel collection, it is possible to collect data at resolutions as low as 0.25mm. The resulting datacube can be mined to extract more information about pigmentation used on stamps or other small artifacts.

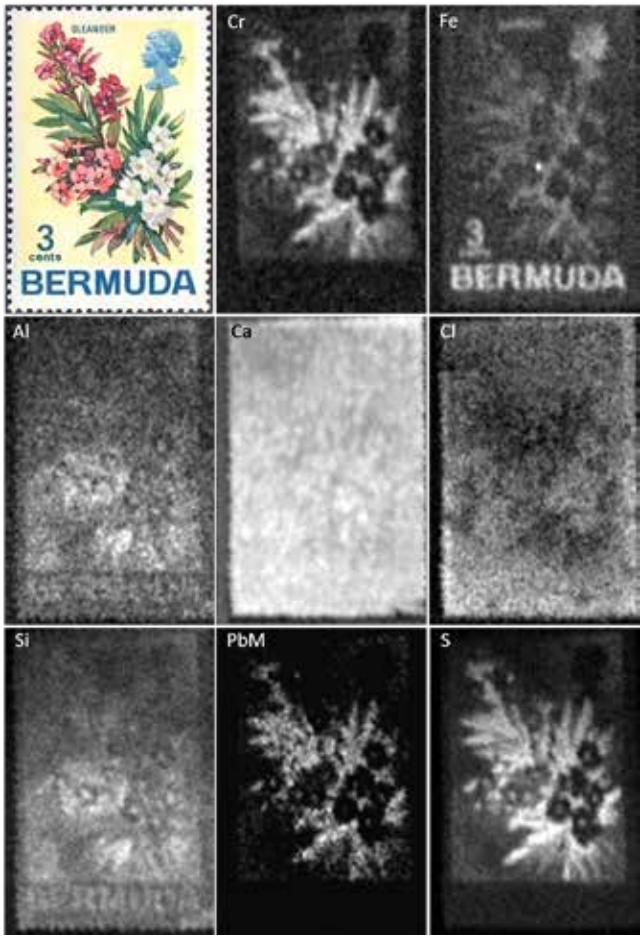


***Figure 7.*** MA-XRF map of the 3¢ Oleander Bermuda Colonial stamp from the 1970 Island Flowers issue. The range of elements associated with each color can clearly be seen.

Although definitive pigment identification is not possible by XRF alone, the data can provide key information and determination when used in conjunction with other analytical techniques (i.e. Raman, Spectroscopy, multi/hyperspectral imaging, FITR). The value of this technique may best be recognized when investigating stamps colored by several pigments.

## Acknowledgements

I would like to thank Lee Drake for providing the software to do more detailed analysis of the spectral data (Drake 2018), Bruker Kaiser for his support and sharing his ideas. Funding for this research comes from the Andrew W. Mellon Foundation.

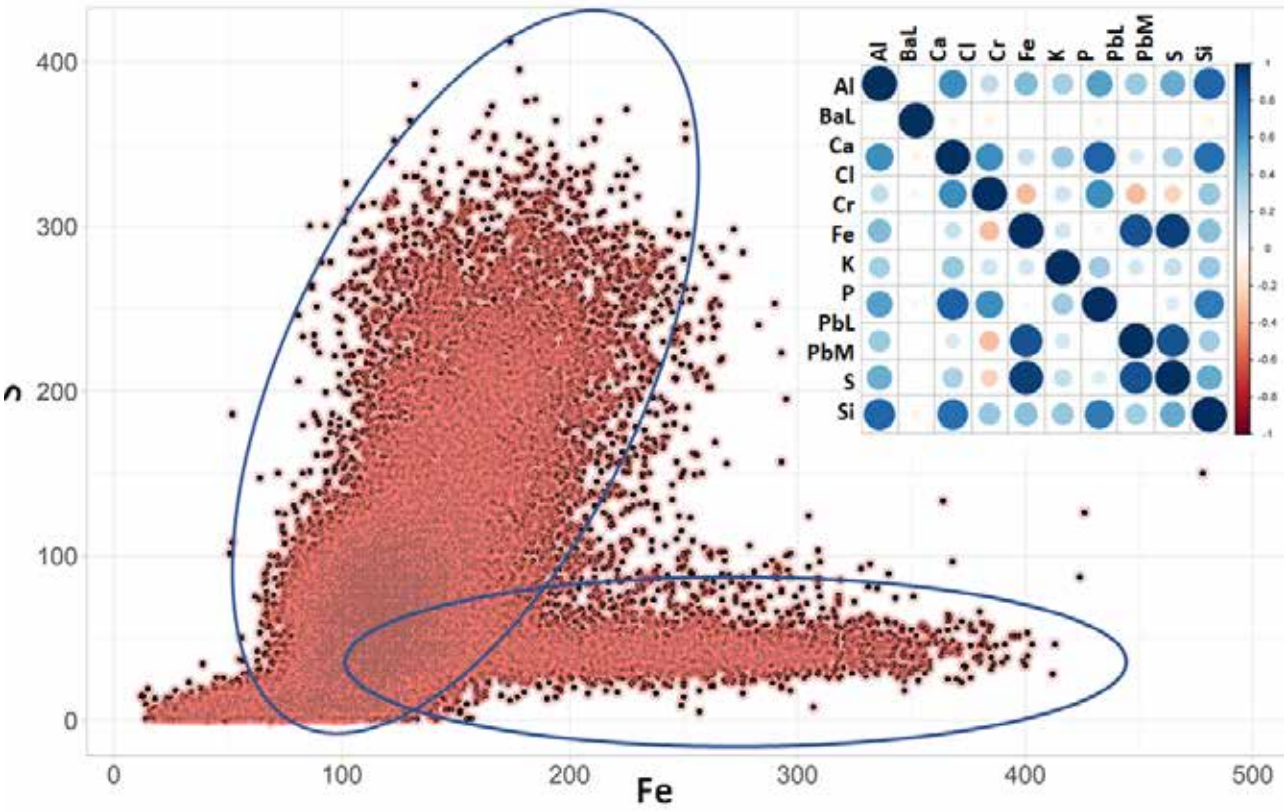


***Figure 8.*** Scatterplot of FeK and SK lines showing a positive correlation between the two elements as well as an isolated increase in Fe devoid of S. This suggests both elements are present in the same locations on the stamp, as well as a second pigment containing Fe and not S. The inset shows the correlation table for all elements identified.

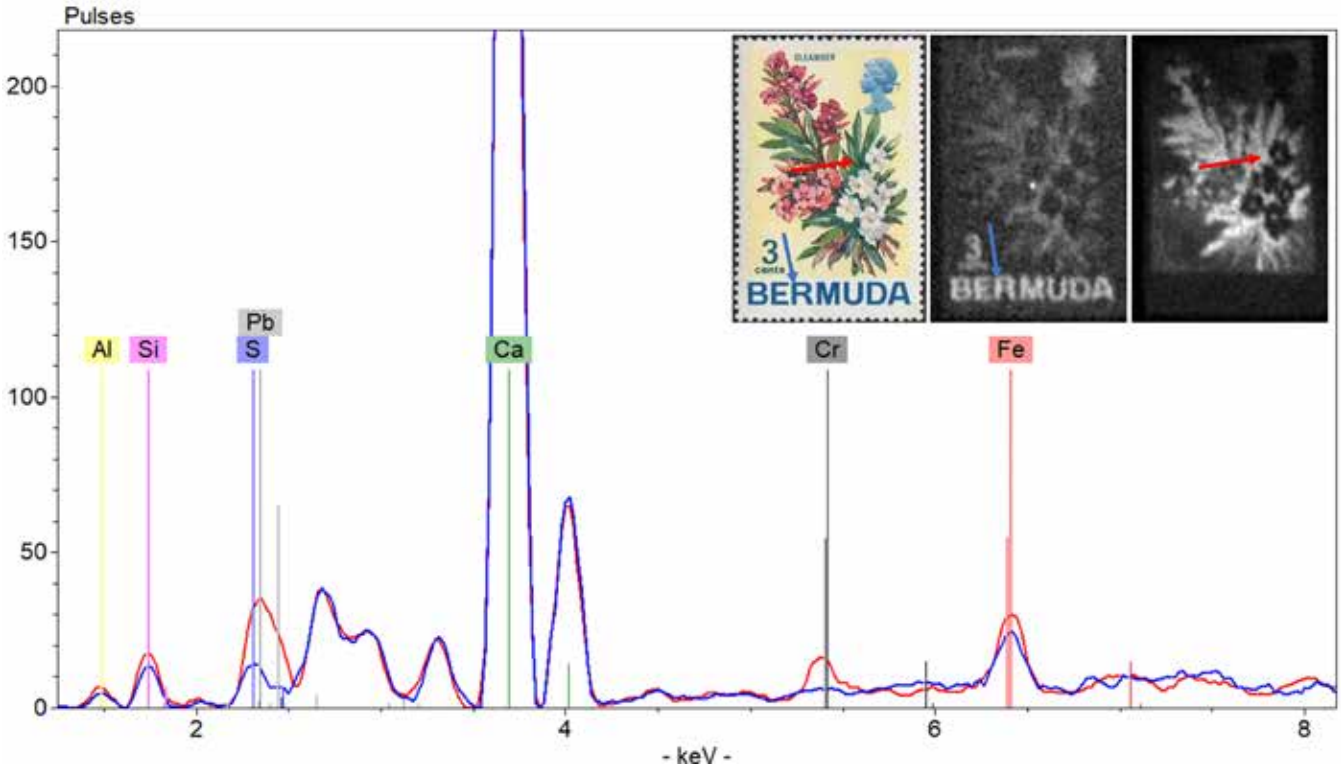


***Figure 9.*** Spectra from individual pixels from two regions with higher concentrations of Fe. The first spectrum (Blue Line) shows a relatively low concentration of Fe (typical for Prussian blue), while the second spectrum (Red Line) shows associated higher concentrations of Cr and Pb. The location of the extracted pigment spectrum is marked respectively.

## References


Alberti, R., T. Frizzi, L. Bombelli, M. Gironda, N. Aresi, F. Rosi, C. Miliani, G. Tranquilli, F. Talarico, and L. Cartechini. 2017. CRONO: A Fast and Reconfigurable Macro X-ray Fluorescence Scanner for In-situ Investigations of Polychrome Surfaces. *X-Ray Spectrometry* 46 (5): 297–302.

Alfeld, M., J. Vaz Pedroso, M. van Eikema Hommes, G. Van der Snickt, Gwen Tauber, Jorik Blaas, Michael Haschke, Klaus Erler, Joris Dik, and Koen Janssens. A mobile instrument for in situ scanning macro-XRF investigation of historical paintings. *Journal of Analytical Atomic Spectrometry* 28, no. 5 (2013): 760-767.

Allen, James A., and Thomas M. Lera. 2013. The US 1851 3¢ Stamp: Color, Chemistry, and Changes. In: Lera, T., J. H. Barwis, and D. L. Herendeen, editors. *Proceedings of the First International Symposium on Analytical Methods in Philately.* Washington, DC: Smithsonian Institution Scholarly Press, pp 71–82.

Brittain, Harry G. 2016. Attenuated Total Reflection Fourier Transform Infrared (ATR FT-IR) Spectroscopy as a Forensic Method to Determine the Composition of Inks Used to Print the United States One-Cent Blue Benjamin Franklin Postage Stamps of the 19th Century. *Applied Spectroscopy* 70 (1): 128–36. https://doi.org/10.1177/0003702815615343.

Castro, Kepa, Benito Ábalos, Irantzu Martínez-Arkarazo, Nestor Etxebarria, and Juan Manuel Madariaga. 2008. Scientific Examination of Classic Spanish Stamps with Colour Error, a Non-Invasive Micro-Raman and Micro-XRF Approach: The King Alfonso XIII (1889–1901 'Pelón') 15 Cents Definitive Issue. *Journal of Cultural Heritage* 9 (2): 189–95. https://doi.org/10.1016/j.culher.2008.02.001.

Dik, J., K. Janssens, G. Van Der Snickt, L. van der Loeff, K. Rickers, & M. Cotte, *Analytical Chemistry* 80(16), (2008), 6436–6442

Drake, B.L. 2018. Sheetcrunch GitHub. https://github.com/leedrake5/sheetCrunch.

Gill, Thomas E. 2013. Analysis of Postage Stamps by Proton-Induced X-Ray Emission Spectrometry. In: Lera, T., J. H. Barwis, and D. L. Herendeen, editors. *Proceedings of the First International Symposium on Analytical Methods in Philately.* Washington, DC: Smithsonian Institution Scholarly Press, pp 83–90,

Gianfranco Pocobene, Jess Chloros, Aaron Shugar, Bruce Kaiser, Richard Newman and Courtney Books. 2020. Titian's Rape of Europa: Artist's Pigments and Changes Revealed through Macro-XRF Mapping (Part I). Conference Presentation at the AIC Annual Meeting in Salt Lake City.

Herendeen, David L. 2013. Documenting Science in Philatelic Literature: A New Perspective. In: Lera, T., J. H. Barwis, and D. L. Herendeen, editors. *Proceedings of the First International Symposium on Analytical Methods in Philately.* Washington, DC: Smithsonian Institution Scholarly Press, pp . 35–46

Jelovica Badovinac, I., N. Orlić, C. Lofrumento, J. Dobrinić, and M. Orlić. 2010. Spectral Analysis of Postage Stamps and Banknotes from the Region of Rijeka in Croatia. *Nuclear Instruments and Methods in Physics Research*, A 619 (1–3): 487–90. https://doi.org/10.1016/j.nima.2009.10.174.

Lera, Thomas, Jennifer Giacci and Nicole Little. 2013. A Scientific Analysis of the First Issue of Chile, 1853-1862, London Printing. In: Lera, T., J. H. Barwis, and D. L. Herendeen, editors. *Proceedings of the First International Symposium on Analytical Methods in Philately.* Washington, DC: Smithsonian Institution Scholarly Press, pp. 19–34.

Mosca, Sara, Tommaso Frizzi, M. Pontone, Roberto Alberti, Luca Bombelli, Valentina Capogrosso, A. Nevin, Gianluca Valentini, and Daniela Comelli. 2016. Identification of Pigments in Different Layers of Illuminated Manuscripts by X-Ray Fluorescence Mapping and Raman Spectroscopy. *Microchemical Journal* 124: 775–84.

Oliaiy, P., D. Agha-Aligol, F. Shokouhi, and M. Lamehi-Rachti. 2009. Analysis of Iranian Postage Stamps Belonging to the Qajar Dynasty (18th–20th Century's) by Micro-PIXE. *X-Ray Spectrometry: An International Journal* 38 (6): 479–86.

Paolo Vollmeier. 2000. New Methods to Identify Forgeries in Philately. In: *Photonics East '99,* 1999, Boston, MA, United States. Vol. 3851. https://doi.org/10.1117/12.379869.

Pinto, Catarina, and Melo J. Sérgio Seixas de. 2018. The Molecules of Color in Portuguese Postage Stamps (1857–1909). *Pure and Applied Chemistry 90 (3):* 435–445. https://doi.org/10.1515/pac-2017-0701.

Ravaud, E., L. Pichon, E. Laval, V. Gonzalez, M. Eveno, and T. Calligaro. 2016. Development of a Versatile XRF Scanner for the Elemental Imaging of Paintworks. *Applied Physics* A 122 (1): 17.

Sánchez, Héctor Jorge, and María Cecilia Valentinuzzi. 2006. Authentication of Postal Pieces by Spatially Resolved X-ray Fluorescence Analysis. *X-Ray Spectrometry* 35 (6): 379–82. https://doi.org/10.1002/xrs.924.

Saverwyns, Steven, Christina Currie, and Eduardo Lamas-Delgado. 2018. Macro X-Ray Fluorescence Scanning (MA-XRF) as Tool in the Authentication of Paintings. *Microchemical Journal* 137: 139–47.

Sherali, Ms. n.d. Nondestructive Authenticity of Postage Stamp: New Approach In: Questioned Document Examination.

Shugar, Aaron. 2019. Advancing Handheld Macro-XRF Scanning: Development of Collimators for Sub-um Resolution. Poster, *Technart* 2019 Bruges, May 2019.

Shugar, Aaron N., and Jennifer L. Mass. 2012. *Handheld XRF for Art and Archaeology. Vol. 3.* Leuven University Press.

Vollmeier, Paolo. 2000. New Methods to Identify Forgeries in Philately. In: *Scientific Detection of Fakery in Art II,* 3851:61–65. International Society for Optics and Photonics. https://doi.org/10.1117/12.379869.

# Examination and Analysis of the Inks used to Print the 1851 3-cent Stamp Using a Scanning Electron Microscope

*Daniel W. Brinkley, III*

## Abstract

An environmental scanning electron microscope (SEM), with an attached energy dispersive X-ray spectrometer (EDS), was used to characterize the ink in several different shades of the 1851 3-cent stamp. No sample preparation or alteration of the stamps was required to perform the examinations. Atomic number contrast images were combined with the EDS analysis results to identify possible chemical compounds for individual particles used in the inks. Since this is a microanalysis technique, there were limitations with characterizing these inks because of their inhomogeneity at the magnifications required to image and analyze them. The obtained results were in general agreement with those reported by Allen and Lera (2013), and it should be recognized the XRF bulk analysis of the inks provide the more accurate analysis of the compositions of the inks

## Introduction

The first scanning electron microscopes (SEMs) were limited to the examination of electrically conductive materials because an accelerated beam of electrons was being focused on a specimen in a relatively high vacuum, with microamps of current being passed through it. These instruments are used in many industries for quality control, failure analysis, and materials characterization.

A schematic of an SEM and illustrations of some electron beam interactions with specimens are shown in Figure 1 (Goldstein *et. al,* 1992). The SEM allows one to examine samples at high magnification (up to 300,000 times) while simultaneously collecting radiation (X-rays, visible light, secondary electrons, backscattered electrons, etc.) emitted by the interaction of the electron beam with the sample. Nonconductive specimens accumulate a negative charge and deflect the primary beam from the feature to be examined or cause that feature (particle) to be displaced. To permit the examination of nonconductive specimens, conductive coatings of gold or carbon were applied to the specimen to allow it to be imaged in a high vacuum mode. However, these coatings interfered with the elemental analysis of specimens using attached X-ray spectrometers.

In the late 1980s, the first commercial environmental scanning electron microscope (ESEM) was demonstrat-

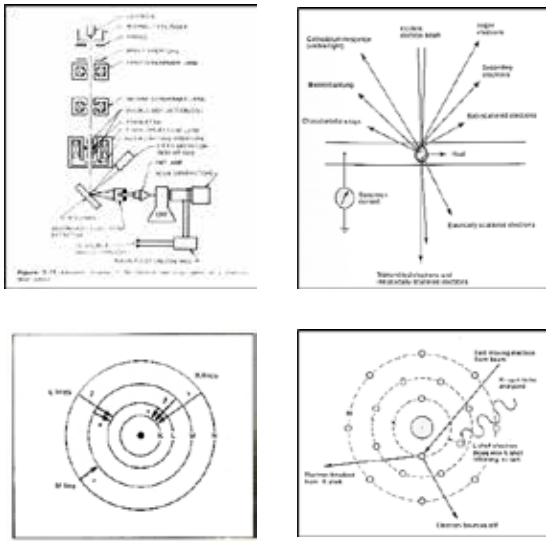

***Figure 1.*** Simple illustrations of a scanning electron microscope schematic (top left), primary electron beam interactions with a specimen (top right), a simplified model of electron shells in an atom (bottom left), and a simplified model for X-ray generation using an accelerated electron beam. [The top left illustration is from *Scanning Electron Microscopy and X-ray Microanalysis,"2nd Edition,* by J. I. Goldstein, *et.al.*, Plenum Press, 1992.]

ed by the ElectroScan Corporation. Now, with lapse of patents, nearly all manufacturers offer an ESEM. The ESEM allows the examination and analysis of nonconductive specimens, without having to coat the specimen, by increasing the pressure in the specimen chamber while keeping the electron gun at high vacuum.

## Background

The color range of these stamps summarized in Table I was first noted by Chase in 1928 (Chase, 1942). While the first six months of the originally specified "brick red" stamps were described by Dr. Chase as various shades of orange brown, the colors/shades changed significantly during its production. Dr. Chase also postulated on the pigments used to create the inks.

**Table I**

**Chase Colors**

| Year | Colors | Postulated Pigments |
|---|---|---|
| 1851 | Orange brown | Probably 80% Venetian red, 20% vermilion |
| 1852 | Brownish-carmine, dull rose claret | Venetian red |
| 1853 | Pale dull red, dull rose red | Venetian red & vermilion |
| 1854 | Dull rose red | ? |
| 1855 | Dull rose red, dull orange red | Poor quality Venetian red & vermilion |
| 1856 | Dull yellowish rose red, brownish-carmine | Better grade of Venetian red & vermilion |
| 1857 | Dull rose claret, brownish-claret, plum, yellowish brown, pale rose brown | ? |

*Notes: venetian red – iron oxide ($Fe_2O_3$); vermilion – mercuric sulfide (HgS)*

In the 1975 reprint of Dr. Chase's book, these colors were expanded from about 20 to 34 different colors/shades by other students of this stamp. In the most recent article on colors, the basic number of colors increased to 38, after some shades were added and others dropped. Amonette and Hulme (2005) summarize their studies with the statement "it must be understood that there is no fine dividing line between the various colors as they merge gradually with one another with in-between shades, and only typical color samples should be used to illustrate the various colors."

A more recent, groundbreaking paper by Allen and Lera (2013) provided the results of X-ray fluorescence (XRF) analyses of plated stamps and color measurements using a colorimeter—analytical instruments to make objective measurements on selected stamps. The XRF results showed the inks consisted of mixtures of a variety of compounds based on the measured elemental concentrations of lead, iron, calcium, sulfur, and barium depending upon the shade.

These analyses showed there were no mercury compounds (vermilion—mercuric sulfide) in any of the pigments analyzed in their studies, contrary to Chase's postulation. These results are summarized in Table II. Their color analyses of the stamp inks placed the examined stamps in the "brown or orange" region of the red-blue-green color spectrum.

It should be noted, the XRF instrument provides an elemental analysis of material being analyzed but does not identify chemical compounds. The compounds used in the inks are postulated based on the authors' research into the natural and synthetic compounds used for printing in the mid-1800's. Later work by Allen (courtesy of work performed at the Smithsonian) confirmed conclusively, via X-ray diffraction analysis, the primary compounds represented by these elements were lead oxide (red lead, "minium"), calcium carbonate, and iron oxide (hematite).

The primary conclusions of Allen/Lera were:

1. iron compounds are the primary pigment for the 1851 orange brown stamps and red lead oxide is a secondary pigment
2. several extenders/possible tinting agents such as $BaSO_4$ and $CaCO_3$ seem to have been used in the first 24 months of production
3. no vermilion (mercuric sulfide) was detected in the ink pigments of stamps from the first 24 months of production

**TABLE II**

**Summary of Allen & Lera XRF Results**

| Sample | Description | Ca | Fe | Pb | S | Others |
|---|---|---|---|---|---|---|
| A | 59L1e yellowish OB[1] | 54,000 | 96,000 | 99,000 | 4,400 | 0 Hg |
| B | 7R1e yellowish OB[2] | 170,000 | 360,000 | 332,000 | 6,500 | 0 Hg |
| C | 92R1i OB | 50,000 | 101,000 | 80,000 | 4,500 | 0 Hg |
| D | 91R2e OB | 88,000 | 310,000 | 152,000 | 6,500 | 0 Hg; 8,000 Ba |
| E | Exp. OB 8 Oct 1851 | 260,000 | 0 | 650,000 | 12,000 | 0 Hg |
| F | Exp. OB | 114,000 | 0 | 462,000 | 9,200 | 0 Hg |
| G | Exp. OB | 110,000 | 0 | 420,000 | 12,000 | 0 Hg; 5,000 Ba |
| H | Mid-1852 OB | 90,000 | 4,000 | 150,000 | 8,500 | 0 Hg |
| J | 4R3 1852 Br.Car. | 138,000 | <10,000 | 353,000 | 6,600 | 0 Hg |
| K | 1852 Claret | 127,000 | 0 | 397,000 | 7,700 | 0 Hg |
| L | Early Dull Red | 190,000 | 0 | 300,000 | 10,000 | 0 Hg; 15,000 Cr |

*Notes: [(1)] yellowish orange brown, earliest color, [(2)] first two weeks of production 1851, Ca—calcium, Fe—iron, Pb—lead, S—sulfur, Hg—mercury, Ba—barium, Cr—chromium, OB—orange brown, Br.Car.—brownish-carmine, Exp. OB—experimental orange brown*

4. there was a move away from the iron oxide-based system towards a lead-based system around mid-September 1851
5. the experimental orange brown colors represent a major pigment transition rather than the appearance of an odd color
6. the primary brownish-carmine pigments of the early period were likely red lead with no iron present.

## Analysis Methods

The stamps were examined using a Hitachi S-3600N scanning electron microscope (SEM); the elemental analyses were performed using a Bruker XFlash 6/60 energy dispersive X-ray spectrometer (EDS) attached to the SEM. The Hitachi SEM can operate with a partial vacuum in the main chamber (i.e., environmental mode), which reduces the charging effect of electrically non-conductive specimens, such as paper. In a partial vacuum, this instrument only allows the use of a solid-state backscattered electron (BSe-) detector for imaging.

The backscattered electron (BSe-) detector uses atomic number contrast for image formation. The higher the average atomic number of a feature, the brighter the image appears. For example, lead appears brighter than iron, and iron appears brighter than carbon. The BSe- image quickly provides information on whether a sample is heterogeneous or homogeneous, and if heterogeneous, the image shows the spatial distribution of the various constituents.

The EDS system provides an elemental analysis and can detect beryllium through uranium on the Periodic Table of the Elements when present in concentrations between one tenth to a few weight percent, depending upon the element. The SEM/EDS analysis technique is often described as a microanalysis technique because features as small as a cubic micron ($10^{-3}$ millimeters) can be analyzed. However, it must be recognized the excitation volume is larger than the beam diameter due to secondary excitation (fluorescence effects) and other specimen interactions.

This analytical technique identifies the elements present but does not identify the compound. The SEM/EDS system will not detect X-rays from hydrogen, helium, or lithium. Significant concentrations of beryllium, boron, carbon, nitrogen, and oxygen have to be present for their detection.

With any of the techniques that use X-rays for characterization, there can be overlaps for the elements in question that require interpretation. For example, the sulfur Kα peak (2.309 keV), the molybdenum Lα peak (2.292 keV), and the lead Mα peak (2.342 keV) all have energy values that overlap within the best resolution of any commercially available EDS system.

## Stamps Examined

Four stamps presented in this paper were selected based primarily on what was available to the author, and because they represented different colors/shades. These four stamps are shown in Figure 2.


*Pale Yellowish Orange Brown First Printing* *1851 Orange Brown*

*1852 Brownish Carmine* *1854 Orange Red*

***Figure 2.*** The four stamps examined for this study.

### *Scott 10A Pale Yellowish Orange Brown, First Printing*

Two areas on 92R1E were initially examined. The first location was the lower left corner, away from the cancellation as shown in Figures 3 through 6. Opposite the optical images of the stamp, the backscattered electron images are lighter where the ink is located because the ink consists material of a higher atomic number than the cellulosic paper fibers. Figure 3 shows this difference where the "T" (paper with no ink) is lighter in the optical image and darker in the backscattered electron (BSe-) image.

At higher magnifications (Figures 4 through 6), the ink is shown to be a mixture of higher atomic number particles within a lower atomic number matrix. Based on the analysis of X-rays generated from an area smaller than one square millimeter, the ink (and possibly the underlying paper) shows the presence of carbon, lead, oxygen, calcium, iron, silicon, and aluminum.

The electron beam can be placed on a single feature (versus scanning an area), in this case a particle having an

**Table III**

**Stamps Examined in this Study**

| Type | Position | Color/Shade |
|---|---|---|
| Scott 10A | 92R1E | Pale Yellowish Orange Brown |
| Scott10A | 97R1E | 1851 Orange Brown with a Magenta Cancellation |
| Scott 11A | 50L2L | 1852 Brownish Carmine |
| Scott 11 | 56R4 | Orange Red |

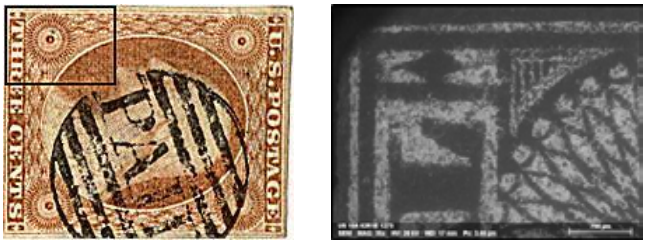

BSe Image 35 X

***Figure 3.*** An image of the stamp rotated 90 degrees and a backscattered electron image of the lower left corner of the stamp (marked with a box in the upper image). Note the inked areas appear to be dark in the optical image and light in the backscattered electron image (BSe-) due to the ink pigments consisting of higher average atomic number materials compared to the paper. This location was selected because it was away from the cancellation.

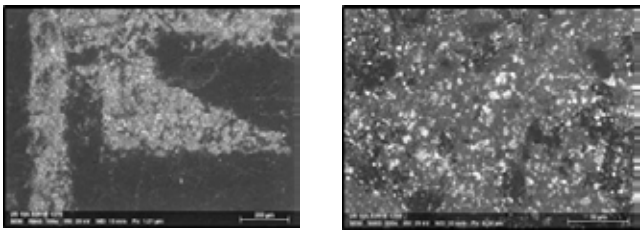

BSe Image 100 X BSe Image 500 X

***Figure 4.*** Higher magnification backscattered electron images of the lower left corner of the stamp shown in Figure 3. The approximate location of the right image is is the center of the left image. Note this inked area consists of a mixture of different materials as indicated by the relative brightness of the particles. Brighter particles have a higher average atomic number compared to the darker particles.

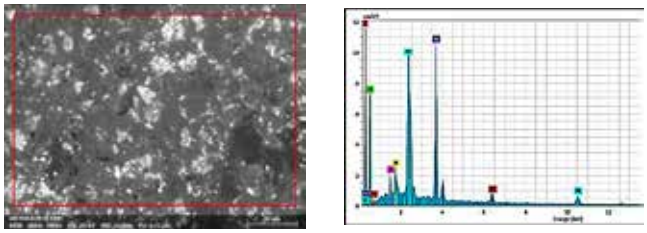

BSe Image 1000 X EDS Spectrum

***Figure 5.*** *A higher magnification backscattered electron image of images shown in Figures 3 and 4, and an energy dispersive X-ray spectrum (EDS) for the area inside the box. Note this inked area consists of a mixture of lead, calcium, carbon, oxygen, iron, silicon, and aluminum.*

approximate diameter of 5 microns (0.005-millimeters) and X-rays can be collected and analyzed. As shown in Figure 6, the higher atomic number particulate was a lead-rich compound. The lower atomic number phase showed higher concentrations of calcium and oxygen, compared to the overall area suggesting this phase was most likely calcium carbonate or a related compound.

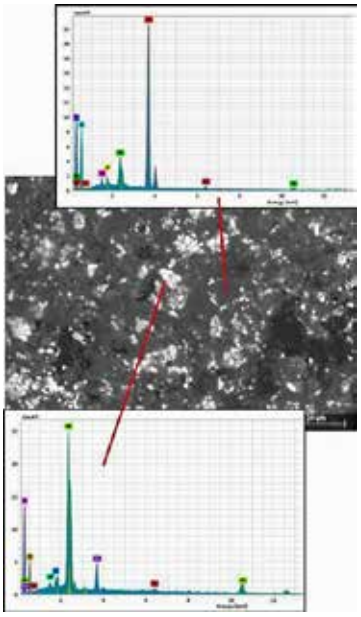

***Figure 6.*** The same BSe- image shown in Figure 5 and energy dispersive X-ray spectra (EDS) for the bright, higher atomic number particle marked with a red line and the medium gray phase marked with a second red line. Note the particle consists predominantly of lead with lesser amounts of carbon, calcium, oxygen, iron, silicon, and aluminum, and the medium gray phase consist primarily of calcium, oxygen, and carbon with lesser amounts of lead, iron, silicon, and aluminum. These results suggest the particle is a lead compound, possibly lead oxide (Pb3O4—Paris Red).

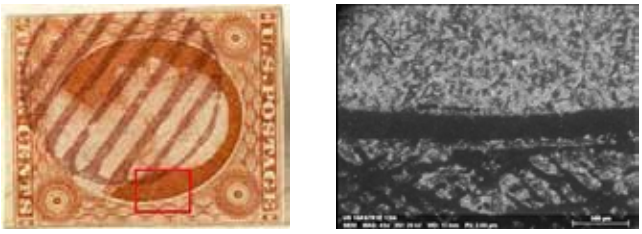

BSe Image 45 X

***Figure 7.*** An image of the top right stamp in Figure 1 rotated 90 degrees, and a backscattered electron image of the center right oval of the stamp (marked with the lower red box in the upper image). Note the inked areas of the stamp appear to be dark in the optical image and light in the backscattered electron image (BSe-) due to the pigments used in the ink consisting of higher average atomic number materials compared to the paper. This location was selected because it was away from the cancellation.

### *Scott 10A Orange Brown with a Magenta Cancellation*

One area on 97R1E was examined at the center right of the stamp away from the magenta cancellation and is shown

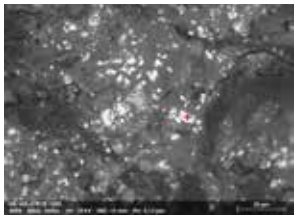

*BSe Image 1000 X*

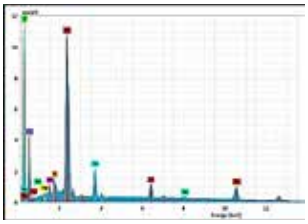

*EDS Spectrum*

***Figure 8.*** The same BSe- image shown in Figure 7 and an energy dispersive X-ray spectrum (EDS) for the bright, higher atomic number particle marked with a red crosshair. Note this particle consists predominantly of lead with lesser amounts of carbon, calcium, oxygen, iron, silicon, aluminum, copper, and magnesium. These results suggest the particle is a lead compound, possibly lead carbonate ([PbCO3]2·Pb[OH]2 – white), lead oxide (Pb3O4 – Paris Red, PbO – yellow to yellowish red), or a mixture of all of these.

at higher magnification in Figures 7 through 9. Again, the inked areas appeared brighter than the paper only areas, and the ink consisted of a mixture of different materials. An EDS spectrum of the ink at 1000 times magnification showed it to consist of carbon, lead, oxygen, calcium, iron, silicon, aluminum, barium, and copper. As a general observation, the higher atomic number particulate present in the 97R1E ink appeared to be smaller compared to that present in 92R1E. EDS analysis of the higher atomic number particulate showed this material was a lead-rich compound. This ink also showed a higher concentration of iron compared to 92R1E.

The same area was examined at higher magnification as shown in Figure 9. In addition to the brighter, lead-rich phase, three additional phases were identified: (1) a barium-sulfur-oxygen-rich phase [e.g., barium sulfate, $BaSO_4$], (2) a lead-rich phase with chromium present [e.g., lead chromate, $PbCrO_4$—Cologne yellow or $Pb_2(CrO_4)O$ – Persian red], and (3) a lower atomic number aluminum-silicon-oxygen-rich phase [e.g., mineral based filler such as clay].

### *Scott 11A 1852 Brownish Carmine*

One area on 50L2L was examined in more detail. This location was within the right center of the oval surrounding Washington's bust as shown in Figures 10 through 12. Again, the inked areas appear brighter than the paper only areas, and the ink consisted of a mixture of different materials. An EDS spectrum of the ink at 1000 times magnification showed it to consist of lead, carbon, calcium, oxygen, aluminum, silicon, copper, and magnesium. As a general observation, the higher atomic number particulate present in the 50L2L ink appeared similar to those present in 92R1E and 97R1E.

The same area was examined at higher magnification as shown in Figures 11 and 12. EDS analysis of the higher atomic number particulate showed was a lead-rich compound. EDS analysis of the lower atomic number phase

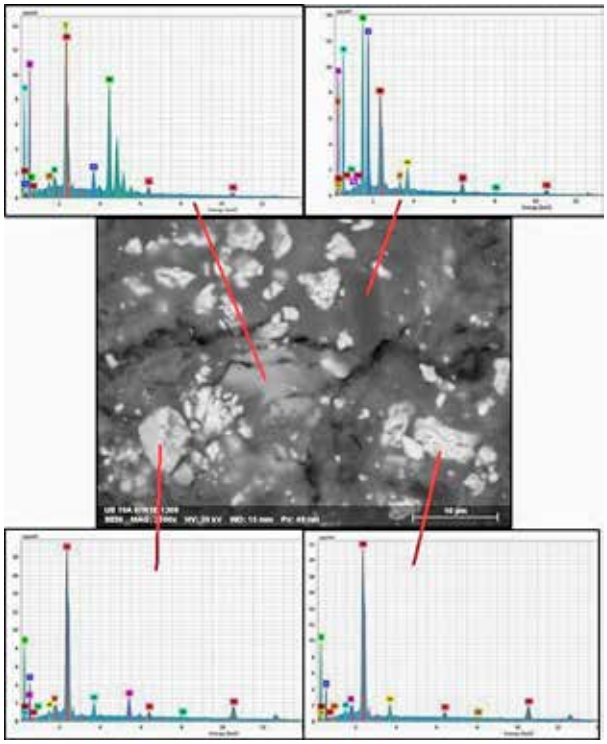

***Figure 9.*** A higher magnification image of the center area of Figure 8 and energy dispersive X-ray spectra (EDS) for the four different gray level phases with red lines matching each spectrum to each phase. The top left spectrum shows a barium-sulfur-rich phase, probably barium sulfate (BaSO4—white), the top right an aluminum-silicon-oxygen-rich phase (mineral filler). The bottom left spectrum shows a lead-chromium-rich phase (e.g., lead chromate), the bottom right a lead-rich phase (lead oxide?).

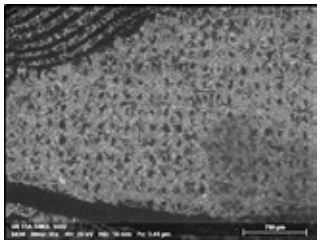

*BSe Image 35 X*

***Figure 10.*** Scott 11A, Position 50L2L 1852 brownish carmine shade, used, manuscript and faded red cds, genuine, thinned (APS Certificate 193404, 9/24/2010). The position of the right image is shown by the blue box on the left image.

showed this material to have a higher concentration of calcium, carbon, and oxygen suggesting it could be a calcium carbonate compound. Unlike 97R1E, there did not appear to be multiple higher atomic number chemical compounds present.

### *Scott 11 Orange Red*

The fourth stamp examined was a Scott 11, Position 56R4 with an orange red shade as shown in Figures

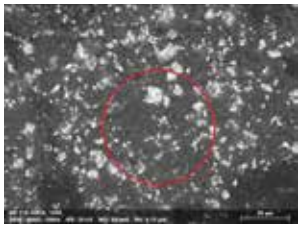

*BSe Image 1000 X*

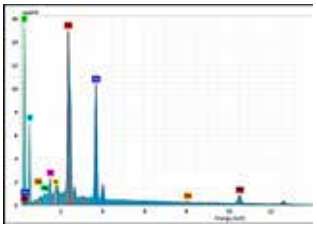

*EDS Spectrum*

***Figure 11.*** A higher magnification image of the area at the lower center of the right image of Figure 10 and an EDS spectrum of the area within the red circle.

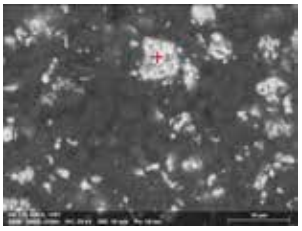

*BSe Image 2500 X*

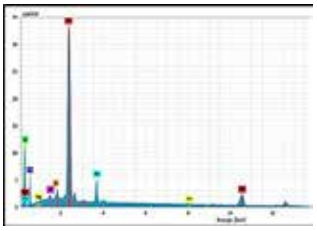

*EDS Spectrum*

***Figure 12.*** A higher magnification image of the area shown in Figure 11 and an EDS spectrum of the particle marked with the red crosshair.

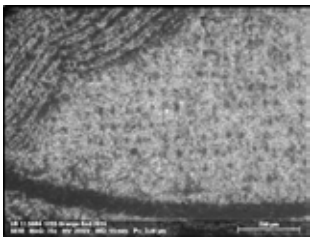

*BSe Image 35 X*

***Figure 13.*** Scott 11, Position 56R4, 1855 orange red. The position of the right image is shown by the blue box on the left image.

13 through 15. This location was the center right behind Washington's neck inside the oval (Figure 13). This area was away from the cancellation. The inked areas consists of a mixture of different materials and appeared brighter than the paper only areas.

An EDS spectrum of the ink at 1000 times magnification (Figure 14) shows the ink to consist of lead, carbon, oxygen, calcium, aluminum, chromium, silicon, and copper. At least three different types of materials were used in this orange red ink: (1) a calcium-carbon-oxygen-rich phase [e.g., calcium carbonate] that appeared to be a binder for the other particulate, (2) a lead-rich phase that appeared as smaller, brighter particles [<1 to 5 microns], and (3) a lead-chromium-rich phase that appeared as larger particles [5 to 10 microns] having a slightly lower brightness compared to the smaller particles [Figures 14 and 15].

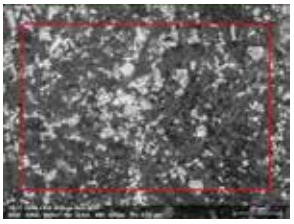

*BSe Image 1000X*

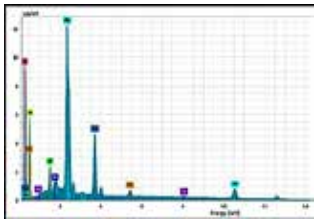

*EDS Spectru*

***Figure 14.*** A higher magnification image of the right image of Figure 13 (yellow box) and an EDS spectrum of the area within the red box. Note this material inside the red box consists of a mixture of lead, carbon, oxygen, calcium, aluminum, chromium, silicon, and copper.

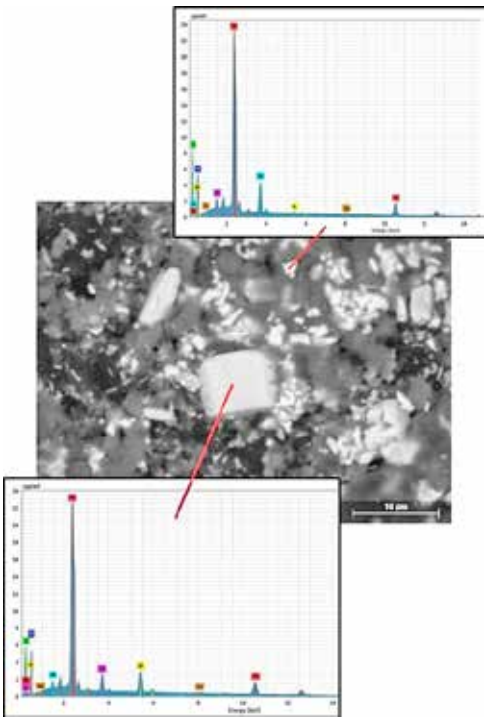

***Figure 15.*** A higher magnification image of a different area and EDS spectra of the two particles with red lines matching the spectra to the particles. Note that the larger particle has a higher concentration of lead and chromium compared to smaller particle that is mostly lead. The large particle is probably a lead chromate-based pigment.

## Discussion

Allen and Lera (2013) showed the inks used for the Scott 10/10A stamps consisted of a mixture of iron compounds, lead compounds, and calcium compounds with barium compounds present in some stamps. They concluded the composition of the experimental orange brown inks (and later inks) represented a significant change with the elimination of the iron compounds. My results obtained from the examination of a smaller number of Scott 10/10A and 11/11A stamps using the SEM/EDS analytical technique agree with the Allen and Lera results.

**Table IV**

## Comparison of "Raw Counts" Data Reported by Allen/Lera to the EDS Data

| Description | Ca | Fe | Pb | S | Cr | Ba | Al | O |
|---|---|---|---|---|---|---|---|---|
| **Allen and Lera XRF Data (from Table 2)** | | | | | | | | |
| 59L1e yellowish OB | 54,000 | 96,000 | 99,000 | 4,400 | … | … | … | … |
| 7R1e yellowish OB | 170,000 | 360,000 | 332,000 | 6,500 | … | … | … | … |
| 92R1i OB | 50,000 | 101,000 | 80,000 | 4,500 | … | … | … | … |
| 91R2e OB | 88,000 | 310,000 | 152,000 | 6,500 | … | 8000 | … | … |
| Exp. OB 8 Oct 1851 | 260,000 | 0 | 650,000 | 12,000 | … | … | … | … |
| Exp. OB | 114,000 | 0 | 462,000 | 9,200 | … | … | … | … |
| Exp. OB | 110,000 | 0 | 420,000 | 12,000 | … | 5000 | … | … |
| Mid-1852 OB | 90,000 | 4,000 | 150,000 | 8,500 | … | … | … | … |
| 4R3 1852 Br.Carmine | 138,000 | <10,000 | 353,000 | 6,600 | … | … | … | … |
| 1852 Claret | 127,000 | 0 | 397,000 | 7,700 | … | … | … | … |
| Early Dull Red | 190,000 | 0 | 300,000 | 10,000 | 15,000 | … | … | … |
| **SEM/EDS Data** | | | | | | | | |
| 92R1e yellowish OB | 23303 | 1675 | 2117 | … | … | … | 1521 | 8345 |
| 97R1e OB | 33482 | 17863 | 14003 | … | Detected | 2815 | 5289 | 33464 |
| 97R1e, Ba-rich ph. | 11190 | 5781 | 4854 | 59959 | … | 122444 | 2803 | 40379 |
| 97R1e, Pb/Cr-rich | 14445 | 7281 | 31050 | … | 22845 | … | 2555 | 18441 |
| 50R1L Br.Carmine | 87211 | … | 21332 | … | … | … | 10110 | 43168 |
| 50L2L Br. Carmine | 124207 | … | 21264 | … | … | … | 10999 | 43748 |
| 18R2L Br. Carmine | 62135 | … | 12773 | … | … | … | 3551 | 20042 |
| 56R4 orange red | 52222 | … | 20218 | … | Detected | … | 13382 | 35334 |
| 56R4 Pb/Cr-rich | 25073 | … | 43667 | … | 37751 | … | 6500 | 28568 |
| 56R4 Pb-rich | 38368 | … | 40246 | … | 3659 | … | 10345 | 26065 |
| 56R4 Ca-rich | 209277 | … | 9862 | … | 2895 | … | 8765 | 33915 |
| 22R1L rose red | 63929 | … | 14398 | … | 2628 | 5016 | 5558 | 31480 |
| 27L1L Exp OB | 74645 | … | 25275 | … | … | 7258 | 8639 | 59081 |
| 25R1i reddish OB | 51943 | 37632 | 12249 | … | … | … | 10746 | 50367 |
| Orange cancellation | 4858 | … | 26084 | … | 26264 | … | 2200 | 16177 |
| Red cancellation | 8678 | … | 2980 | 105838 | *Hg - 52022* | | … | 8727 |

The XRF technique involves irradiating an area with a relatively large diameter beam compared to the SEM/EDS technique that sweeps a small diameter beam over an area, with X-rays being generated at each location. The resultant spectrum is the summation of these individual location results. As a rule of thumb, the SEM/EDS technique performs best on flat, polished homogeneous samples.

Since this examination showed the inks used on the stamps are obviously nonhomogeneous, caution must be used in the selection of areas to be analyzed with the SEM/EDS technique. The lower magnification backscattered electron images were used to provide an indication of the relative composition of different areas of the stamps and used to assist with the selection of areas to be analyzed. However, it must be recognized that this selection process can introduce a potential bias in the analysis which could influence the results. This is a limitation with the SEM/EDS technique, and, on this basis, the XRF would provide

more accurate results for a "bulk" analysis of a non-homogeneous sample compared to the SEM/EDS system.

Allen and Lera reported "raw counts" for each element analyzed in their paper. With both the XRF and the SEM/EDS techniques, the concentration was generally proportional to the area under the elemental X-ray peak. Experimentally determined correction factors were applied to the "raw counts" to obtain semi-quantitative results. As shown in Table IV, the "raw counts" obtained by the EDS system (using the smaller Pb-Lα peak versus the larger Pb-Mα peak) showed similar results to those reported by Allen and Lera.

It should be noted, there are multiple lead peaks showing in the EDS spectra with X-rays generated by the M-shell (tallest/largest peak at about 2.3 keV), and X-rays generated by the L-shell (smaller peaks at 10.5 and 12.6 keV). The EDS quantitation software automatically selected the L-shell peak (presumably due to the substantial overlaps of the M-shell peak and lack of any secondary filters) to determine the approximate concentration (based on the area under this peak, which was substantially smaller than the M-shell peak). If one accepts the results from the EDS quantitation software, the lead concentration is about five times higher than that for iron (using the Pb-Lα peak and the Fe-Kα peak). However, the SEM/EDS analysis results confirmed iron compounds were not used in any significant concentration on the 1852 brownish carmine stamps examined, or any of the later shades that were examined other than in cancellations.

Another difference between the two analytical techniques was the XRF system will not detect elements below sodium on the Periodic Table (without a gas purge) whereas the EDS system did detect some of the lower atomic number elements (e.g., carbon, nitrogen, and oxygen). This detection of lighter elements provided additional information on the composition of the inks, but it further complicated the quantification of the results. Comparisons of the "raw counts" did permit a more "apples to apples" comparison of the XRF and EDS results, but this was probably an oversimplification.

The spatial resolution of the SEM/EDS system provided more information on the ink composition because of the ability to isolate the electron beam on individual particles used in the pigment. The backscattered electron images also provided an indication of the composition of the different inks by showing the number, size, and distribution of different chemical compounds in the inks.

These results showed the presence of multiple compounds in the ink used to print the stamps. Although there was obvious excitation of the materials surrounding some of the individual particles, the analysis results identified (1) a lead compound showing the presence of chromium [e.g., lead chromate], (2) a lead-rich compound without chromium [e.g., red lead oxide], (3) an iron-oxygen-rich compound [iron oxide, hematite, $Fe_2O_3$], (4) a barium-sulfur-oxygen-rich phase [e.g., barium sulfate], and (5) probable mineral fillers such as calcium carbonate, clays, or diatomaceous earth.

Mercury-sulfur-rich particles were identified to be present in both a black and a magenta cancellation ink of the Scott 10/10A stamps (not presented in this paper), and the red cancellation on the Scott 11A stamp. It is worth noting, mercuric sulfide is identified in the Merck Index occurring both as a black form and a red form (Vermilion). Older editions of the Merck Index state the Vermilion form of mercuric sulfide would blacken on exposure to light, suggesting it could be unstable. No mercury-sulfur-rich phases were identified to be present in any of the orange brown stamp inks, which agreed with the Allen and Lera results.

It is not apparent why there was such a variation in the color of the inks used to print the 1851 3¢ stamps over their service life. One could speculate the printers were never satisfied with any of their formulations or they had "quality issues" with their pigment/ink suppliers. Allen/Lera indicated "the inks for the banknotes were compounded 'in house' most of the time." This was probably the case for the 1851 3¢ stamp inks as well. Another possible explanation is the variation of color for the same compound (Table V). However, one could reason visual color (and the stability of these colors) would be the main factor in the selection of the various pigments used in these inks.

Allen/Lera (2013) showed a significant change in the ink composition was made starting in September 1851, with the experimental orange brown stamps for some unknown reason. Another observation made during this examination was the relative size and distribution of the higher atomic-number particles in the inks. The size and distribution, in addition to the composition of the ink pigments could affect the resultant colors. The pigment size/distribution observations could also be related to the quality or degree of preparation of the pigments (i.e., inconsistent grinding, etc.).

Based on limited data, there were compositional differences between the colors/shades examined in this study. For instance, the orange brown shade examined (97R1E) showed the presence of barium and chromium compared to the yellowish orange brown stamp (92R1E). Both the orange red shade (56R4) and the bright rose red shade (22R1L) showed the presence of chromium, but only the bright rose red showed the presence of barium. These limited data suggest a possible relationship between the composition of the inks and their colors, but this would require additional study to confirm or reject. There was an observed correlation between the relative particle sizes and morphologies for the lead-rich and lead-chromium-rich particles.

## Conclusions

1. The development of the environmental scanning electron microscope (ESEMs) allowed for the routine examination and analysis of electrically non-conductive materials such as papers, inks, and minerals without having to apply electrically conductive coatings to the specimens, thus per-

**Table V**

## Selected Data from the Merck Index

| Compound | Colors | Uses |
|---|---|---|
| Barium carbonate ($BaCO_3$) | White | In ceramic, paints, and enamels |
| Barium chromate ($BaCrO_4$) | Yellow | In yellow paint, coloring ceramics, glasses |
| Barium manganate ($BaMnO_4$) | Green | Pigment in fresco painting |
| Barium oxide (BaO) | White | |
| Barium sulfate ($BaSO_4$) | White | Photographic paper, artificial ivory, filler for rubber, watercolor pigment for colored paper |
| Calcium carbonate ($CaCO_3$) | White | Paris or English white |
| Calcium sulfate ($CaSO_4 \cdot 2H_2O$) | White | As a white pigment |
| Chromium oxide ($Cr_2O_3$) | Light to dark green | Pigment, abrasive |
| Diatomaceous Earth (Infusorial Earth) | White to light gray to pale buff | Clarifying agent, filler for paper, paints |
| Ferric hydroxide [$Fe(OH)_3$] | Brown | pigment |
| Ferrous sulfate | Pale bluish-green | Inks, dyes, pigments |
| Iron oxide (hematite - $Fe_2O_3$) | ***Brown, red, brownish red*** | Pigment, abrasive |
| Iron oxide (magnetite – $Fe_3O_4$) | Black | |
| Lead carbonate [$(PbCO_3)_2 \cdot Pb(OH)_2$] | White | Pigment in oil paints |
| Lead Chromate (PbCrO4) | Yellow to orange yellow | Pigment in oil and watercolors, Chrome, Paris, Leipzig, Cologne yellow |
| Lead Chromate ($PbCrO_4 \cdot PbO$) | Red, Persian red | pigment |
| Lead dioxide ($PbO_2$) | Brown | |
| Lead monoxide (PbO) | Yellow | Glazing pottery, pigment for rubber |
| Lead Oxide ($Pb_3O_4$) | Red | Paris or Saturn red |
| Lead sesquioxide ($Pb_2O_3$) | Reddish-yellow | |
| Lead Sulfide (PbS) | Black | Glazing earthenware |
| Mercuric oxide (HgO) | ***Red, yellow to orange-yellow*** | Paints |
| Mercuric sulfide (HgS) | Black, red | The red form is generally referred to as vermilion |

*See Merck, 1952 and Merck 1969.*

manently altering them. This capability was essential for the study.

2. Imaging of the stamps using a backscattered electron detector provided an image whose grey levels were a function of the average atomic number of the various particles. These images showed the stamp ink consisted of a complex mixture of different compounds based on the average atomic number of the different particles/phases.
3. Spatial resolution of the SEM/EDS technique permitted the analysis of individual particles, which allowed a better identification of different compounds used for the pigments, extenders, or fillers in the inks.
4. Results of these examinations showed the SEM/EDS analytical technique provides more detail on individual particles in the various inks used to print the Scott 10/10A and 11/11A stamps. In general, the results obtained from the examination of a limited number of expertized and plated stamps agreed with the XRF data obtained by Allen and Lera.
5. Some of the later inks (orange red and rose red colors) used a mixture of coarser lead-chromium-rich (lead chromate) particles with finer lead-rich (lead oxide or other lead compounds) particles. As discussed by Allen/Lera, a barium-sulfur-rich compound was identified to have been used in some of the inks to alter their color/shade (e.g., orange red versus rose red). On this basis, some of the variations in colors/shades appeared to be related to the elemental composition, size, and distribution of the ink constituents.
6. The "measured" concentrations of iron compounds in the orange brown stamps using the

SEM/EDS technique did not agree with the XRF results obtained by Allen/Lera. This illustrates one limitation of the SEM/EDS technique versus an instrument designed for the chemical analysis of non-homogeneous samples such as an XRF. The SEM/EDS technique is a "microanalysis" method and the relative homogeneity, and subsequent selection of the sample being analyzed, can greatly influence the compositional results. The XRF results should be considered the more accurate of the two analytical instruments for the general composition of the inks and correlations to colors.

## Future Work

Area fraction measurements of backscattered electron images versus shades might show measurable differences between the concentrations of the various pigment particles—additional software is available that permits image analysis functions of the SEM images (i.e., area fraction measurements of the different atomic number phases).

Analysis of stamps using FTIR (Fourier Transform Infrared analysis) instruments—FTIR analyses using a microscope attachment could be used to identify the types of bonds associated with organic and inorganic compounds. It would be interesting to see what information could be obtained from these analyses.

X-ray diffraction has been used for nearly a century to identify the crystal structure of various chemical compounds and is routinely used for compound identification. X-ray diffraction analyses done on this study show the inks used to print the 1851 3¢ stamps are a mixture of inorganic pigments and organic vehicles (e.g., linseed oil). This combination of materials could significantly weaken the diffracted signal obtained from the stamp inks. Also, the beam is more energetic than those used by the SEM/EDS technique and could damage the stamps.

## References

Allen, James A. and Thomas Lera. 2013. The U.S. 1851 3¢ Stamp: Color, Chemistry, and Changes. In: Lera, T., J. H. Barwis, and D. L. Herendeen, editors. *Proceedings of the First International Symposium on Analytical Methods in Philately.* Washington, DC: Smithsonian Institution Scholarly Press, pp. 71–81.

Chase, Carroll. 1942. *The 3¢ Stamp of the United States 1851–1857 Issue.* Springfield, Mass.: Tatham Stamp and Coin Company. Reprinted by Lawrence, Mass.: Quarterman Publications, Inc., 1975, pp. 36, 154–158.

Goldstein, J. I., Newbury, D. E., *et.al.* 1992. *Scanning Electron Microscopy and X-ray Microanalysis, Second edition.* New York City: Plenum Press.

Hulme, W. Wilson and Wilbur F. Amonette. 2005. Color Study of the 3¢ Stamp of the United States 1851–57 Issue: An Update. *U.S. Philatelic Classics Society Chronicle*; 57 (2): 103–109.

Merck & Co., Inc. 1952. *The Merck Index of Chemicals and Drugs, 6th Edition.* Rahway, NJ.

———. 1969. *The Merck Index, 8th Edition.* Rahway, NJ.

Scott Publishing Company. 2019. *Scott Specialized Catalogue of United States Stamps and Covers.* Sidney, Ohio: Amos Media Co.

# Single Pixel Colorimetry and Optical Densitometry in Philately

*Robert Hisey*

## Abstract

This study is to determine if single pixel colorimetry is of use to determine the hue of the ink used to print the 1917 Finnish 10p red stamp. The case showed that the various shades listed in the literature were all printed with the same color ink. Also, optical densitometry (OD) of the sample stamps gave a reading related to the amount of ink picked up by the stamp, which correlated with the deepness of the color. OD of the paper affects the appearance of the stamp. These readings characterize the color and shade of the examples.

## HSB Color Model

The color model used is so-called HSB as measured by Photoshop® and other applications:

H for Hue. The scale is a circle of 360 degrees, with pure red at the top at H=0 or 360. Clockwise at 120 degrees is green and at 240 degrees is blue.

S for Saturation. Fully saturated (100%) is a very DEEP color, low saturation, a pastel.

B for Brightness. On a scale of 0-100% or 0-255, a low number is a very DARK color, with a lot of black, while a high number indicates a bright color.

The common RGB model is strictly for machines and is inappropriate for this study.

## Problems When Determining Ink Hues

Most colored inks look very dark when undiluted, some almost black, as seen in the ink drawdown. However, some colors, like red and yellow in Figure 1, do not look especially dark. Inks provide color when spread out on paper as part of the printing process, allowing us to determine their hues. To make accurate ink hue measurements, one must consider at least two issues.

One problem in determining ink hue is eliminating the effect of paper color. To correct for paper color, one should use a "single pixel" sample of the ink to determine ink hue. One can separately sample the paper color and consider its effect on the ink hue measurement.

Single pixel colorimetry takes advantage of the uneven deposition of ink on the paper due to film splitting in the inking rollers (Figure 2). With darkish colors, it is possible

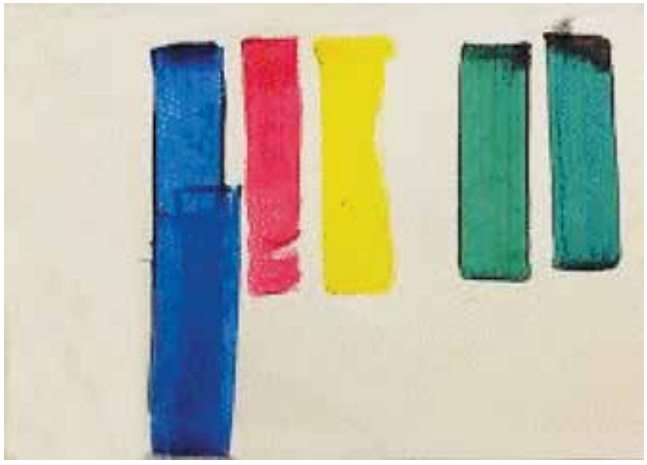

***Figure 1.*** Images of various inks drawdown.

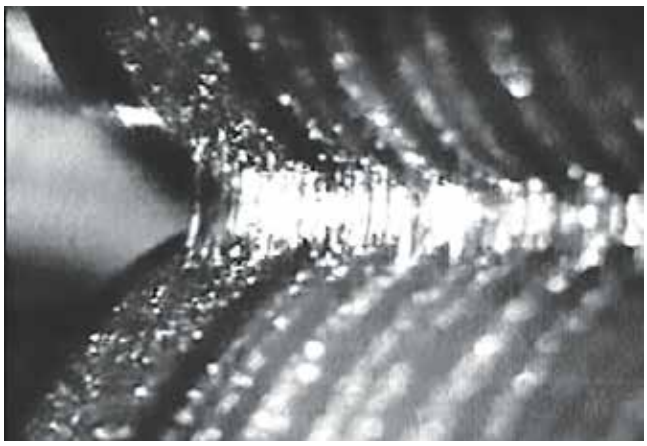

***Figure 2.*** Ink film stretched or split between two rollers.

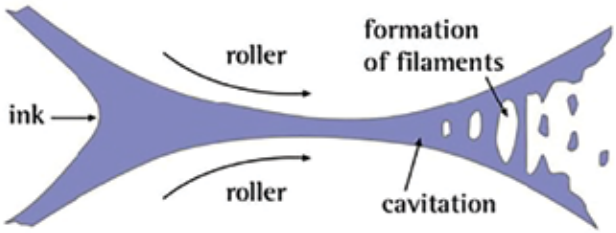


***Figure 3.*** Diagram of how ink film splits.

to find pixels in a scan that have heavy enough ink to obscure the paper influence, giving a true ink hue measurement.

One can see the filaments of ink stretching until breaking, causing spots of heavier ink, as seen in Figure 3.

Typo, gravure and engraved prints all show this to some degree (Figures 4, 5, and 6).

The single pixel sample size also permits us to more accurately determine ink hues.

## Determining Ink Hue

The procedure to determine ink hue was:

1. The stamp was scanned and cropped down to the chosen darkest area. A Brother All-In-One MFC-J6530DW office scanner was used scanning in 24 bit color at 1200 dpi. Note that office scanners give sharp images, while photograph scanners give soft, slightly blurry images.
2. The cropped image was enlarged 10-fold in Photoshop®, which should leave the pixels unblurred.
3. Look for darkest/deepest pixels. The darkest pixels were then measured by the eyedropper set to "point" sample size, i.e., one pixel. Measured at least five points to get the deepest color which was closest to the actual ink color.
4. The HSB panel of Photoshop® was used to read the results.

As noted *supra,* a single pixel sample size results in the most accurate measurement of ink hue. Choosing the darkest color and using a single pixel are the best means to overcome the effects of paper and gum color and mottling that results from ink splitting.

## Optical Density

The concept and term "optical density" originated with black and white photography. It is a measure of blackness based on how the eye responds, which is logarithmic, as opposed to reflectance, which appears to be more linear (Figure 7).

OD is now in common use in printing to control the amount of each color of ink applied, measured with densitometers. However, all densitometer measurements are from a separate solid in the margin, the common "stoplights" or "color strips." They are not useful on the printed work itself, as they only give a relative value.

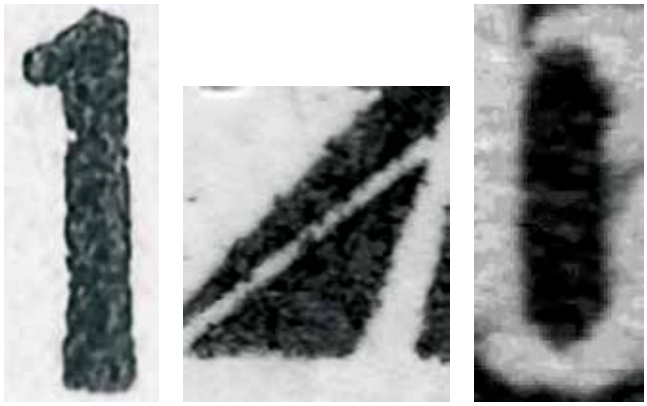

***Figure 4.*** (Left) A 1200 dpi scan of a "1" from the margin of a typo stamp. Meant to be solid, but shows the mottle arising from the film splitting.

***Figure 5.*** (Center) 1200 dpi scan of a gravure 'solid.'

***Figure 6.*** (Right) 1200 dpi scan of an engraved 'solid.'

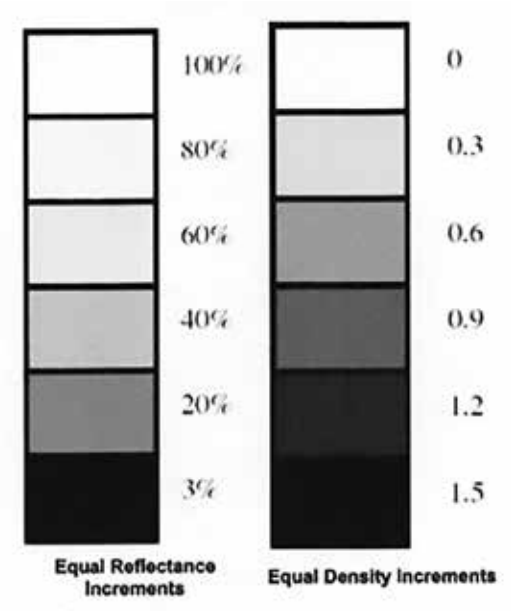


***Figure 7.*** Comparison of equal reflectance increments on left with OD increments on right. OD shows much more contrast in the middle range of darkness.

Now: Optical Density (OD) = $\text{Log}_{10}(I_o/I_r)$ (Beer's Law)
where $I_r$ = reflected light and $I_o$ = illuminating light

OD goes from white to black as the number increases on a logarithmic scale from 0.02 to 3.05. The eye cannot distinguish whiter than OD=0.02, nor blacker than OD=3.0, but in practice the middle range is useful.

"B" in the HSB system is the reverse of OD. B goes from 0=black to 255=white and is linear. So (255-B)/255 is Blackness as a fraction. Ergo,

$$OD=\log 255/(255-B)=\log 255-\log(255-B)=2.406-\log(255-B)$$

The problem is determining the mean B of all the pixels of an area such as a stamp or portion thereof. Recently,

***Figure 8.*** (Left) Stouffer OD calibration card (Product R2110).

however, the National Institutes of Health developed a program, called ImageJ, that can do just this. Its original purpose was to determine transmissivity of turbid solutions, but it can also be applied to reflectivity, B. The program, available free online for OS X, Windows, and Linux, has many applications. In our case, it can average the B of all the pixels in a given area, such as a stamp.

All scanners may not have the exact same sensitivity to B, so a calibration is needed against a standard. Stouffer Industries, Inc. (HTTP://WWW.STOUFFER.NET/PRODUCTLIST.HTM) supplies, at a modest cost, a calibrated 21 step OD card (Figure 8) of which only the middle range is of interest.

Rearranging the formula for a given step value of OD and a directly measured B:

$$\log(255\text{-}B)=2.406\text{-}OD$$

Using the Brother scanner, the direct relationship between B and OD is shown in Figure 9.

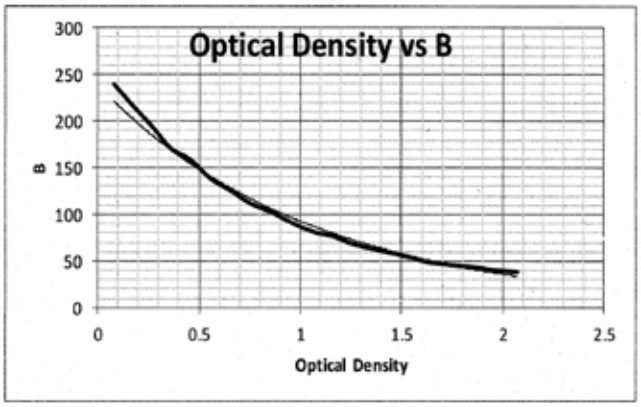


***Figure 9.*** For a Brother scanner, calibrated OD vs measured B.

## Procedure for Measuring B of a Stamp (and then OD)

1. Open ImageJ (NIH program) to reveal this toolbox (Figure 10).

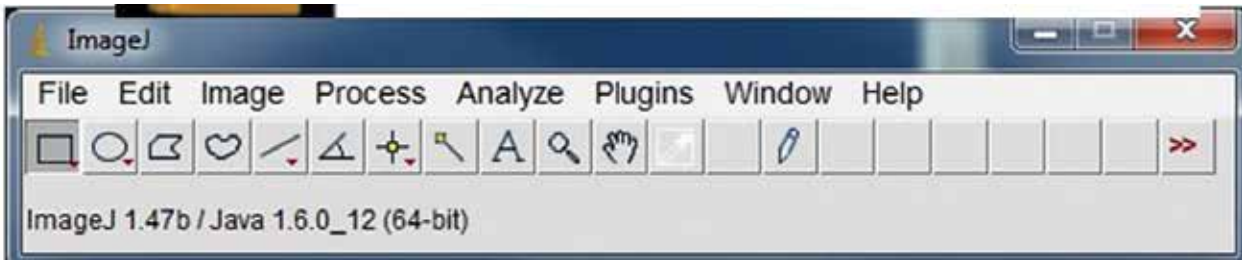


***Figure 10.*** ImageJ panel.

2. Click on "FILE" to pull up a scanned TIFF image of the stamp from your computer at 300 dpi (Figure 11).


***Figure 11.*** 10p Red of Finland 1917-1918.

3. Outline the stamp just within perforations.
4. Click "ANALYZE"
5. Click "MEASURE"
6. A box appears with a set of numbers, one for each sampling (Figure 12).
7. Find the Column of the Means and record those numbers.
8. Interpolate on chart OD vs B (Figure 9.) to find OD of the defined area.
9. Repeat for an unprinted area to get the OD of the paper.

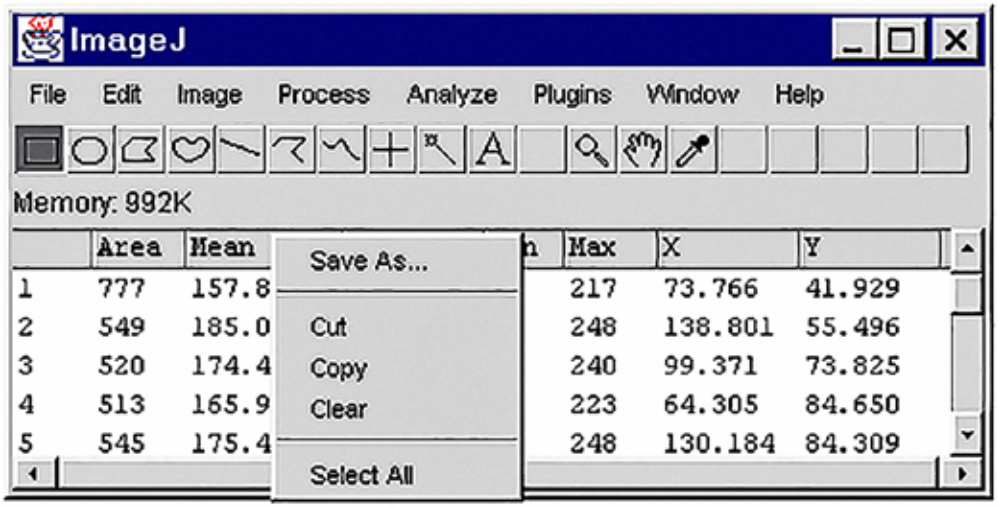


***Figure 12.*** Shows five different measurements of "mean" in the 3rd column.

## Study of 10p Red of Finland 1917–1918

The 10p red of Finland (Figure 11) was chosen for this study. It has six printings in a rather short period, and each printing can be identified by its printing number and date. *The Handbook of Finnish Stamps* (Hangon Kirjapaino Oy, 1986) gives color descriptions and "darkness" of each printing (PO=Print Order). Each stamp was from a control block, giving the printing number and date, so identification is absolute.

## Single Pixel Hue determination

The mean hue is 0.62 and standard deviation 0.33. The closeness of the hues and the short time period indicate the same ink was used. The mean is just slightly on the yellow side of pure red, H=0. The Finns did not make their own ink but purchased it, probably from Germany, thus assuring close quality control of the ink. This indicates the actual color is probably close to pure red, but some of the measurements picked up a bit of the yellow paper.

**Table I**

**Hue Measurements of the Six Printings of the 10p Red with the Handbook Data**

| Sample # | PO # | Color, Handbook | Darkness Handbook | Printing dates | Plates | Paper | Gum | Ink Hue | Ink Hue Mean |
|---|---|---|---|---|---|---|---|---|---|
| 1 | 2 | Red, bluish | 5-Apr | 5-7/10/17 | I/II | Yellowish | Yellowish | 0,1,0,359,359 | 0.5 |
| 2 | 10 | Red, bluish | 6-Mar | 21-12/17-25/2/1918 | I/II | Yellowish | Yellowish | 359,2,0,3, 1 | 1 |
| 2 | 10 | Dark red, bluish | 7-Jun | 21-12/17-25/2/1918 | I/II | Yellowish | Yellowish | 1,0,0, 359,1 | 0.8 |
| 3 | 19 | Red, bluish | 6-Mar | 20.8-3.9.1918 | I/II | Yellowish | Yellowish | 0,1,1, 0,0 | 0.4 |
| 4 | 21 | Red, bluish | 5-Mar | 4-12.9.18 | I/II | Yellowish | Yellowish | 0,0,1, 0,0 | 0.2 |
| 5 | 29 | Red | 5-Mar | 8.2-18.3.19 | III/IV | Yellowish | Yellowish | 1, 1, 1, 2, 2 | 1.2 |
| 5 | 29 | Dark red | 7-May | 8.2-18.3.19 | III/IV | Whitish, dense, transparent | Pale gum | 1,1,2, 0,1 | 1 |
| 5 | 29 | Bright Red | 7-Mar | 8.2-18.3.19 | III/IV | Whitish, dense, transparent | Pale gum | 0,0,0, 1,0 | 0.2 |
| 6 | 36a | Red | 6-Apr | 29.8-22.9.19 | I/II | Whitish, dense, transparent | Pale gum | 0,1,1, 1,0 | 0.6 |
| 6 | 36b | | | | | | | 1,1,2, 0,1 | 1 |
| 6 | 36c | | | | | | | 2,1,0, 0,2 | 1 |

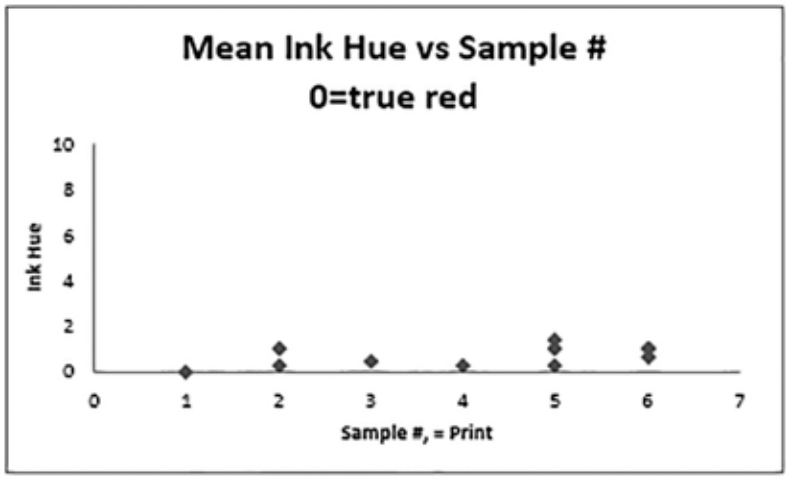


***Figure 13.*** Mean Ink Hue vs Sample Number.

There is no known way to absolutely prove the inks are identical, but in this case, one can conclude that the same ink was used for all these printings. At the very least, all the inks were the same hue (Figure 13).

The three circles below demonstrate how little difference to the eye there is between Hue=0 and H=2, and even Hue=5 (Figure 14).

## Optical Illusion

This leads to the question of why the Handbook calls for a bluish tinge in the first issues. These issues are reported to have a yellowish tinged paper/glue and the others do not. But a red print and a yellow paper do not equal blue.

The explanation is the same illusion that makes snow look white when wearing yellow goggles. The brain interprets the lightest color as white. In this case, the stamp is usually viewed against a black background. The eye perceives the yellowish paper as being white, and so subtracts a bit of yellow from other colors, making the red less yellow or a bit bluish. This bluish cast would disappear against a white background, or with the gum washed off.

Measurements show printings 1, 2, 3, and 4 all have an OD of 40. Printing 5 is higher. Printing 6 is lower.

The best condition for the illusion is strong yellowish paper and light (or thin) red ink.

Printing 5 has a yellowish cast with an OD of 45 but has the heaviest ink coverage. Printing 6 has the lightest color paper and middling to heavy ink. Printings 1 through 4 have middling paper color, yellowish gum and the lightest inking.

For the "clear red" or "bright red" reported in Printing 5, the best conditions would be the whitest papers and the lightest inking, conditions not found in the stamps examined. The "dark red" in Printing 5 shows clearly it has the highest ink OD and the highest stamp OD.

## References

Hangon Kirjapaino Oy. 1986. *Handbook of Finnish Stamp V.*, Philatelic Federation of Finland, ISBN951-95522-0-0).

NIH program, HTTPS://IMAGEJ.NIH.GOV/IJ/DOWNLOAD.HTML accessed February 20, 2020. [This program uses Java and is available in OS X, Windows, and Linux versions as free downloads.]

Stouffer OD calibration card (Product R2110). HTTP://WWW.STOUFFER.NET/SPECIALTYGUIDES.HTM accessed February 20, 2020.

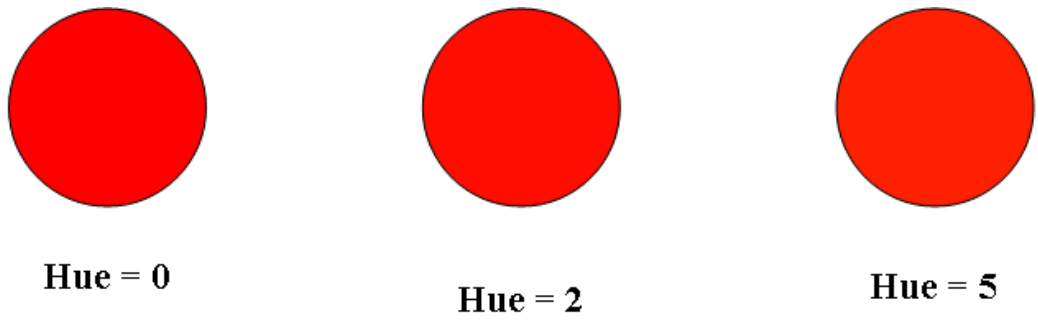


***Figure 14.*** Three Hues (0, 2, 5) at same Saturation and Darkness.

# Microscopic Structure of Stamp Paper Surfaces and Fibers

*Lin Yangchen*

## ABSTRACT

Stamps are 99% paper, but relatively little is known about the surface of stamp paper. Using an array of "remote sensing" techniques, including Nomarski interference contrast, laser scanning confocal and scanning electron microscopy, I characterized the microscopic structure of different types of papers printed with a single stamp design, the coconut definitive of Malaya. Paper structure, a function of both the fiber network and the coating, may influence print quality in unexpected ways.

## INTRODUCTION

Paper is one of the variables that give rise to varieties in stamp issues, alongside others like shade and perforation. For most philatelic purposes, it is usually not too difficult to distinguish catalogued paper varieties by feel and through a magnifying glass.

But this is far from the whole story of stamp papers, which can get much more complicated and fascinating. Why? Because paper is a composite material, made up of different types of plant fibers often mixed with other substances. The paper's physical and chemical properties vary widely depending on the composition of its many constituents.

A fair amount of biological, chemical and physical analysis of stamp papers has been done. Lin (2019) and Barwis (2013) identified paper fibers used in specific stamp issues, while Glazer (1997, 2004) detailed papermaking processes and analyzed the chemical composition of paper coatings. Researchers have also precisely measured physical properties such as thickness, stiffness, opacity and permeability (Barwis, 2013; McKee, 2015).

Very little, however, is known about the microscopic surface topography of stamp papers, which depends on the network of fibers and on the coating, if present. Surface topography can affect inks and print quality.

Being a single design printed on about 10 types of paper from the 1930s to 1950s, the Malaya coconut definitives of De La Rue (Figure 1) are an interesting case study of how paper surfaces can vary. I must quickly add that only four main paper types were used for the actual stamp issues. The rest were used for other material such as essays and aerogrammes. These are not normally recognized as paper types, but more attention should be paid to them because they give us fascinating and valuable insights on paper texture and print quality.

### *Paper Types*

The four main papers, chalky, striated, rough, and substitute, listed in specialized catalogues such as Murray Payne (2015) and Tan (1999) need little introduction. Chalky paper was De La Rue's predominant stock until World War II, when striated and rough-surfaced papers took over.

When the war ended, "substitute" paper appeared briefly, which means different things to different people, and is called various names by different catalogs. Malaya was reportedly one of the very few colonies to have stamps printed on this paper (Lowe, 1951). I used the principle of anomaly detection to define this paper – simply, its characteristics are distinct from the other three as will be shown later.

Chalky paper made a comeback soon after the war. Post-war chalky paper was analyzed separately from pre-war chalky paper to determine whether they were different. Besides the four main paper types, I also examined papers used for essays, aerogrammes, postal stationery cards and plate proofs (see Figure 1 and Table I).

Other papers used for the coconut definitives were the glazed card for die proofs and uncoated paper for some test prints (located in the Crown Agents, Philatelic and Security Printing Archive at the British Library). These are not covered in this study.

Paper surfaces and fibers were examined using various microscopical techniques. Pitting in paper coatings was also examined in detail. De La Rue's chalky and substitute papers both have pits in the coating, contrary to the common assumption that only chalky paper has pits. I encoun-


***Figure 1.*** (Above) Malaya coconut definitive paper types. See Table I for key to codenames.

tered two separate incidents of misidentification of substitute paper as chalky paper in BMA Malaya stamps, involving different philatelists, because pits were present. One particularly interesting example investigated was the BMA 50 cents, recorded on two distinct varieties of substitute paper, one sparsely pitted, the other heavily pitted (Pollard, 2012).

Coatings were also analyzed chemically, as both chemical and physical factors play a role in determining print quality. Glazer (1997, 2004) found considerable variation in the chemical constituents of British colonial stamp coatings during the King George VI period, but did not discuss how this variation might translate to differences in print quality.

## METHODS

***Profilometry.*** Three-dimensional surface profiles were taken from the samples in Figure 1. There were two samples of each of the four main paper types (refer to Table 1). Reasonably clean mint examples were used, so disturbance to the paper was likely to have been minimal.

The stamps were placed under a Keyence VHX microscope and kept flat on the microscope stage with glass slides to prevent curling, exposing just the area of interest. The target area on each stamp was the large uninked area beside the foot of one of the coconut palms.

The surface of the stamp was perpendicularly lit, and a photomicrograph was obtained from the reflected light. The microscope takes many micrographs while moving vertically through different focal planes 0.1μm apart. On

**Table I**

**Code names (ID) and descriptions of paper samples for profilometry.**

| ID | Paper | Description |
|---|---|---|
| Ae | aerogramme | Singapore 25¢ (1951) |
| Ch1 | chalky pre–war | Straits Settlements KGVI 2¢ green |
| Ch2 | chalky pre–war | Straits Settlements KGV 40¢ |
| Ch3 | chalky post–war | Penang QEII 4¢ |
| Ch4 | chalky post–war | Penang QEII 10¢ |
| Es | essay | printed by the local Survey Department 1933–1934 (Norris 1985) |
| Pc | postcard | BMA MALAYA 4¢ postal stationery card (1945) |
| Pw1 | printer's waste | printer's waste (plate proof) (Stanway 2009) on buff paper |
| Pw2 | printer's waste | printer's waste (plate proof) on greenish–grey paper |
| Ro1 | rough | Straits Settlements KGVI 3¢ |
| Ro2 | rough | Straits Settlements KGVI 15¢ |
| St1 | striated | Straits Settlements KGVI 2¢ orange single |
| St2 | striated | Straits Settlements KGVI 2¢ orange block |
| Su1 | substitute | BMA MALAYA overprinted $1 |
| Su2 | substitute | BMA MALAYA overprinted $5 purple and orange |

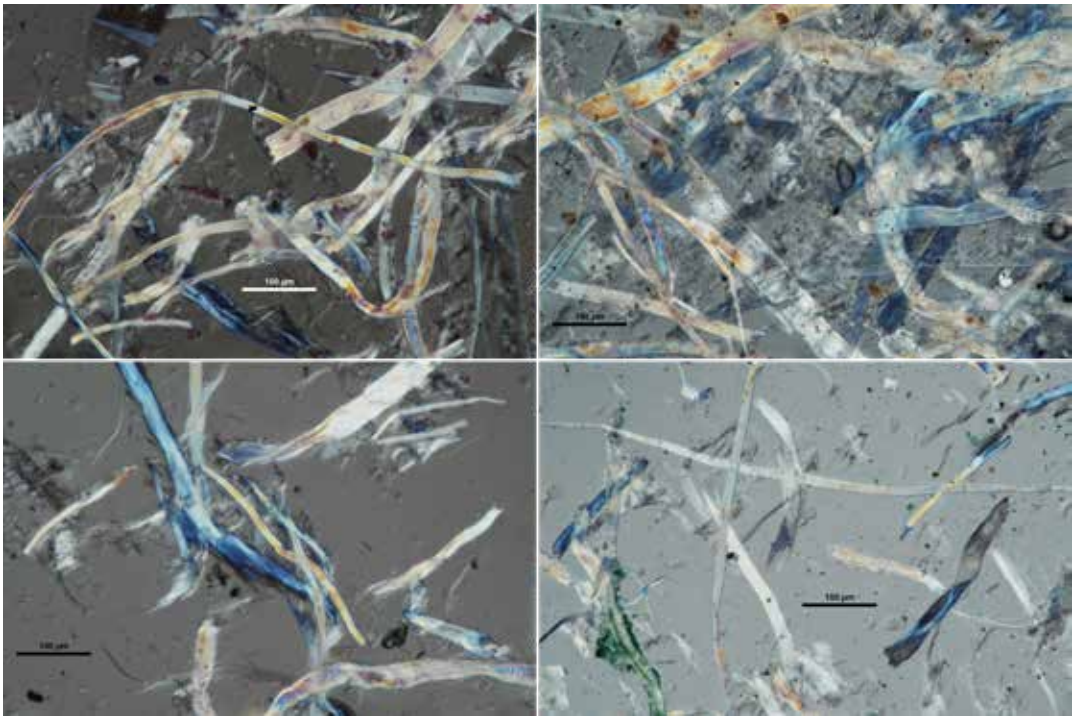

***Figure 2.*** Fibers extracted from the four main paper types, observed using Nomarski interference contrast microscopy. Clockwise from upper left: chalky, striated, rough and substitute papers. Fiber density is not comparable across images as the extraction process was not quantitatively standardized.

each focal plane, only certain parts of the stamp are in focus. The microscope's software estimated the height of a given point on the stamp by finding the focal plane where the point showed maximal contrast in the image, which indicated the point was in focus.

***Light microscopy.*** The four main paper types, chalky, striated, rough, and substitute, were also observed under transmitted light using a Nikon Ni-E microscope on a fresh batch of stamps. This shows some internal structure as well as surface texture. Photomicrographs were taken with a Nikon DS-Ri2 35-mm-format full-frame digital microscope camera.

***Fiber analysis.*** Paper fibers were also extracted from these papers for microscopy (Lin, 2019), using methods simplified from those of Barwis (2013). Fibers were separated by boiling and agitation only, as chemicals were not available. Stains were not available, so Nomarski interference contrast was used to examine the fibers. The stains used to differentiate fiber types are also very short-lived and require immediate observation; I did not have suitable facilities for this.

***Laser scanning confocal microscopy*** was used to examine the three-dimensional structure of pits on the surface of chalky paper. This can resolve more detail than a normal optical microscope as a laser scans the surface of the specimen while a pinhole cuts off out-of-focus light. The stamps were examined unstained under a Nikon Ti2-E microscope with Nikon A1+ confocal module in reflectance mode.

***Scanning electron microscopy*** (SEM) was used to compare the surface topography of chalky and substitute papers. Although it gave only two-dimensional information, it had a much higher resolution with great depth of field, which showed surface topography much more clearly than an optical microscope. Stamps were mounted uncoated in a JEOL JSM-6010LA InTouchScope™. The chamber was evacuated to high vacuum mode for optimal imaging. A low accelerating voltage of 3kV and a small aperture were used to minimize charging artifacts. Images were produced by secondary electron emission. Stamps pose difficulties in being non-conductive and difficult to coat with conductive material (Donaldson, 2009), but I managed to obtain useful images.

***Energy-dispersive X-ray spectroscopy*** was done to compare the chemical makeup of the coatings of chalky and substitute paper. Electron bombardment in the SEM stimulated the emission of X-rays from the atoms in the stamp. Elements were identified by their unique X-ray energy spectra.

## RESULTS

### *Fiber analysis*

No major qualitative differences were seen in the fiber compositions of the four main paper types (Figure 2). This suggests coatings are largely responsible for differences between papers.

Bast fibers were found in all four main paper types. These have a high content of crystalline cellulose, which is birefringent and showed up with Newtonian interference colors under Nomarski interference contrast (Figure 3). The fibers are most likely flax, as hemp is brown and was not used for stamps. The fiber had characteristic nodes at irregular intervals.

Softwood is also present, as evident from the characteristic bordered pits in some of the fibers (Figure 4). The pits allow fluid to flow from cell to cell. Different species of softwood have different pit patterns; this is probably from

***Figure 3.*** Bast fiber from chalky paper under Nomarski interference contrast.

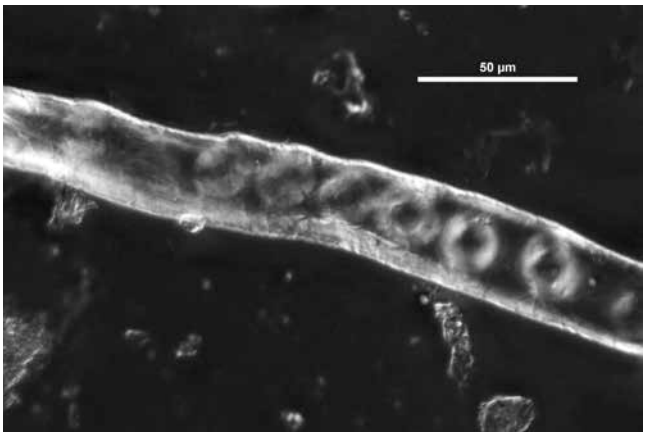


***Figure 4.*** A softwood tracheid (water-conducting vessel) from substitute paper, with characteristic pits revealed by Nomarski interference contrast.

Norway spruce. The species has strong and flexible fibers particularly suitable for printing and writing (Tullis Russell, 1950).

A single instance of a hardwood xylem vessel element (Figure 5) was observed among fibers extracted from chalky paper. With its characteristic fine oblique pitting this was probably Scandinavian birch (see Parham & Gray, 1982; Safdari et al., 2011); while eucalyptus has a similar pattern (see Foelkel, 2007) it was not used at that time. This

***Figure 6.*** Contour maps of paper surfaces generated from the focus stacking of images from the Keyence microscope (see Table I for key to codenames). The actual area covered by the field of view in each panel is about 0.1mm$^2$. This magnification was chosen as a reasonable compromise between capturing a large-enough area while recording fine-enough detail to encompass multi-scale topographical features. Although attempts were made to keep the stamp flat during observation, there appeared to be slight tilting or warping in some specimens. The color gradient is mapped onto the entire range of recorded elevations within each panel; colors should not be compared across panels.

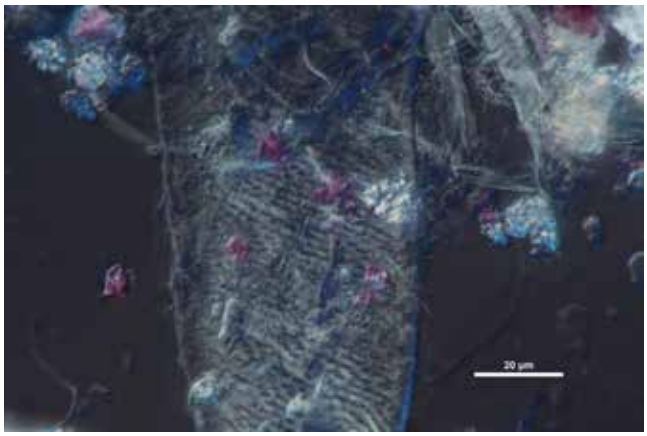

***Figure 5.*** Hardwood xylem vessel element seen in a fiber sample from chalky paper, probably Scandinavian birch (*Betula* sp.).

birch vessel was probably a contaminant, as hardwoods were not then in widespread use (Robert Hisey, personal communication).

### *Surface topography*

Contour models from the Keyence microscope (Figure 6) show qualitative differences between papers. Raw height data was also extracted from five roughly evenly spaced horizontal transects across each of the contour models and plotted in Figure 7. Raw data can be downloaded from https://github.com/linyangchen/paper-surface-topography. The data was analyzed and visualized using the R Language for Statistical Computing.

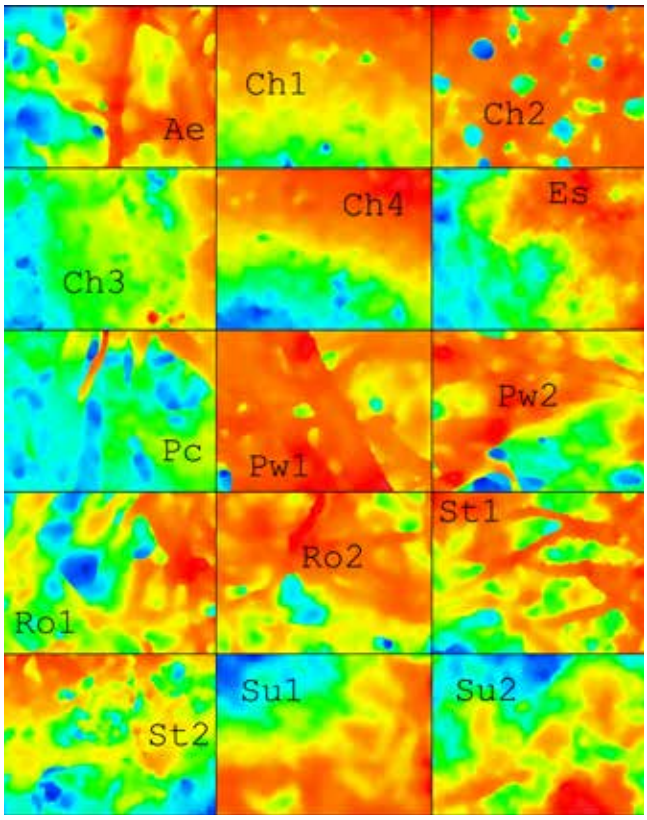

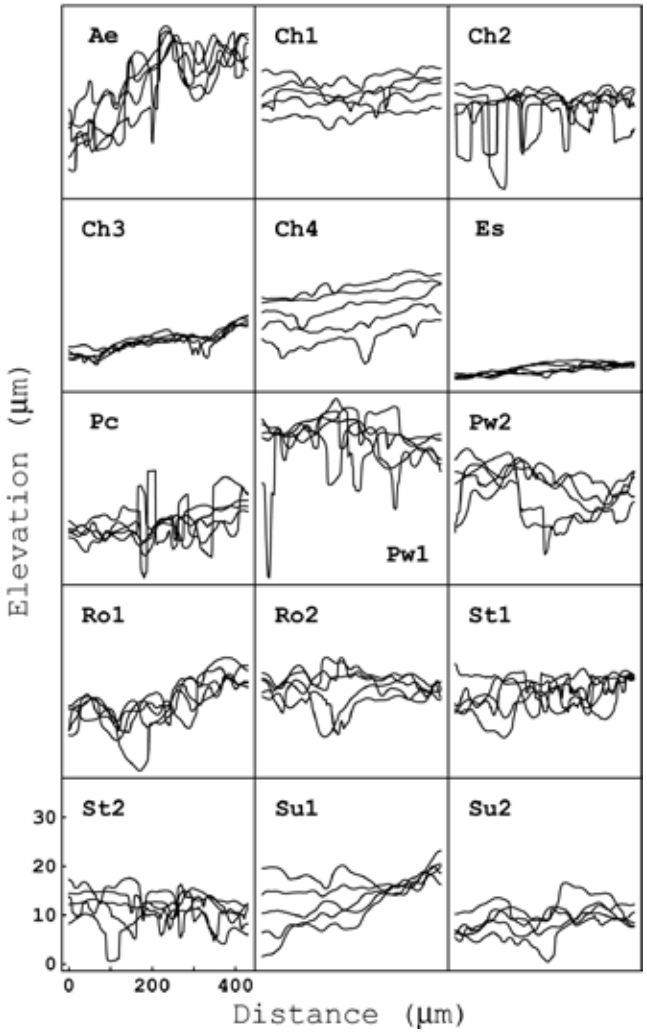


***Figure 7.*** Five cross-sections of the surface of each stamp, with 1600 data points along each line. The wide spacing of profiles in a few of the panels, especially Ch4 and Su1, are due to the paper not being perfectly horizontal under the microscope.

Aerogramme paper is the roughest, its profiles resembling mountain ranges (Figure 7). Aerogrammes were meant to be as thin and light as practical, so it is not unreasonable to suppose the coating was omitted for that reason.

Striated paper, rough paper, printer's waste and postal stationery card are all on the rough side, but less so than aerogramme paper. The roughness is generally due to lack of a coating and exposure of the fiber network.

The coating of chalky paper makes it less rough, but it can be deeply pitted as in Ch2 (Figure. 6, 7). Pitting could have been influenced by factors such as viscosity, agitation, heating or even chemical reactions that generated bubbles.

Substitute paper turns out to be quite smooth, more so than chalky paper. This goes against the general expectation that the superior print quality of chalky paper is conferred by a smooth coating. I will say more on this later.

Of all the papers, the essay paper is the smoothest. The print quality of the essays is very crisp, but should not be compared with the issued stamps, as they were lithographed, while the stamps were letter pressed.

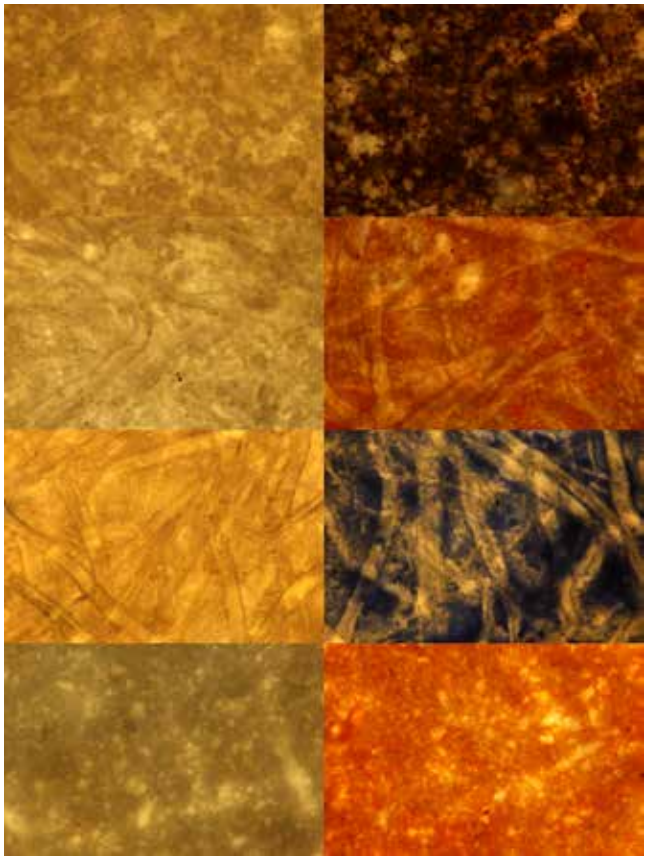

***Figure 8.*** The four main paper types under transmitted light, showing both unprinted and printed areas. Rows from top to bottom are chalky, striated, rough and substitute papers. Each panel shows a field of view of about 0.45mm along the diagonal.

Light micrographs (Figure 8) corroborate the profilometry results and reveal additional features. Chalky and substitute papers have much thicker coatings than striated paper, while rough paper appears to have no appreciable coating, but does have a similar fiber network to striated paper. The ink does not seem to adhere well to the fibers, tending to accumulate in the interfiber space.

Given the variability of paper surfaces, it is not surprising philatelists have observed many different print characteristics on different papers and even on a given paper in the coconut definitives. But the paper surface is only one of several factors that interact with one another to give the final print quality. Other factors include ink consistency, printing pressure, and chemical reactions between the ink and the coating to name a few.

From the perspective of security printing, the finished product should be consistent. Instead, the economic and political upheavals from the 1930s to the 1950s forced De La Rue and the Crown Agents into detours they could not avoid.

In-depth knowledge of the characteristics of the different paper types could also enable one to determine, with greater confidence, whether a stamp has been tampered with. For example, I was examining a copy of what was supposed to be post-war chalky paper, but it did not look as

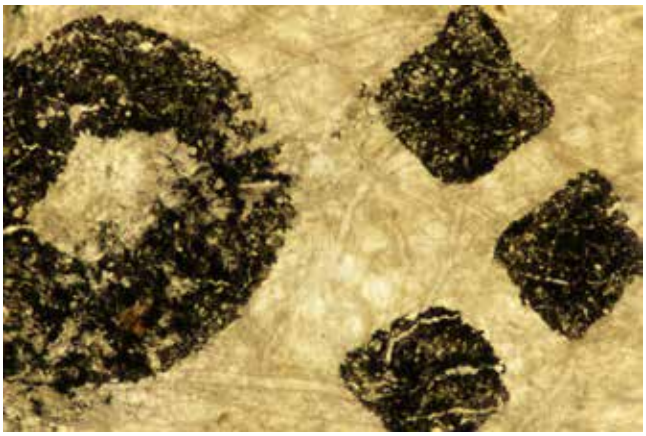

***Figure 9.*** Micrograph of the surface of a Perlis 1-cent showing the fiber network. This is supposed to be post-war chalky paper.

it should—it seemed to have no coating (Figure 9). To the naked eye, the stamp looked unnaturally white, both front and reverse. This stamp seemed to have been artificially cleaned to make it more saleable or presentable. Microscopic observation supports this assessment as it suggests the coating was lost during the cleaning process.

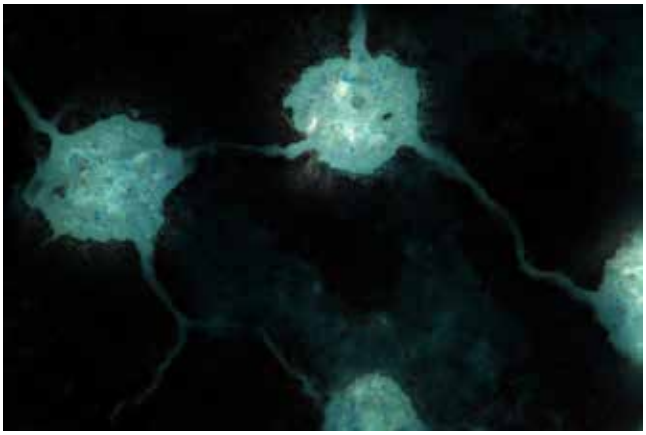

***Figure 10.*** Pre-war blue chalky paper of the Straits Settlements KGVI $1 under transmitted light. Field of view about 450$\mu$m along the diagonal.

### *Surface pitting*

Figure 10 shows large pits on the surface of pre-war colored chalky paper. The translucent rim indicates there may be a significant overhang. This is not surprising as the pits are thought to have been created by bubbles. They can be up to at least 50µm wide and deep, as measured by confocal microscopy (Figure 11). This confocal 3D model did not capture overhangs because the vertical scanning laser cannot see under them.

The cracks reached about 30µm in depth (Figure 11), but this could be an underestimate because the opposing faces in the deeper parts of the cracks may have been touching or too close together to be resolved by the microscope. These particular cracks propagated from pit to pit; the forces at work were probably similar to those that separate stamps along perforations. As the cracks are crooked, it is more likely that the cracking here occurred when the coating was drying during manufacture, rather than from subsequent bending of the paper. It is of course possible additional cracking could have occurred through bending.

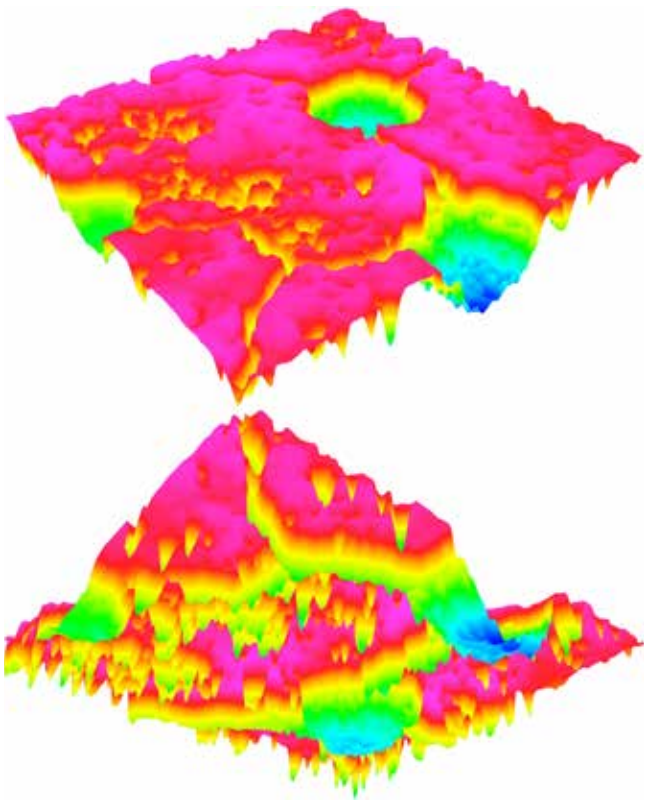

***Figure 11.*** 3D model (views from above and underneath) generated from confocal laser scan of the same pits as in Fig. 10. Field of view about 250$\mu$m on each side.

Next, I did a largely qualitative comparison between chalky and substitute papers regarding pit size and how closely pits were spaced to one another. I examined six examples each of pre-war and post-war chalky paper and six of substitute paper under the light microscope. In addition, I examined two BMA 50-cent stamps, one on pitted substitute paper, the other unpitted. I examined used stamps as mint copies were not available in sufficient quantity.

I measured randomly selected pits, in high resolution, with a ruler to determine their actual diameters, using a scale bar embedded in a test image taken at the same magnification. This worked better than digital thresholding, which was inconsistent in accurately capturing pit edges even within individual samples. This was due to the watermark, which caused the brightness range of unpitted parts of the paper to overlap with the brightness range of the pits. Furthermore, some large fibers let light through which got picked up by thresholding.

Pre-war chalky paper varies widely in pit spacing (Figure 12); there are stamps with abundant pitting and those with very little. The pits tend to be relatively large, with estimated diameters mostly from 36µm to 64µm, although smaller pits are sometimes present. In contrast, post-war

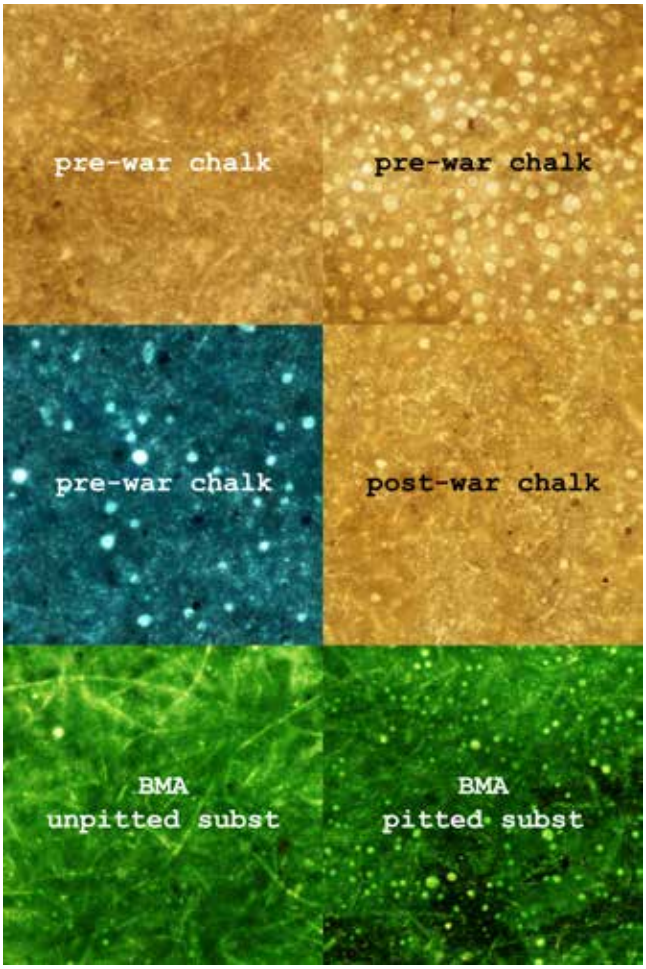


***Figure 12.*** Varieties of chalky and substitute papers under transmitted bright-field microscopy. Each square panel shows an area on the stamp measuring about 1.2mm on each side.

chalky paper tends to have smaller and more sparsely spaced pits (Figure 12), mostly between 14 to 29μm in diameter, occasionally up to 43μm. Otherwise pre-war and post-war papers are similar, being pockmarked by "pinholes" much smaller than the pits (Figures 12, 13).

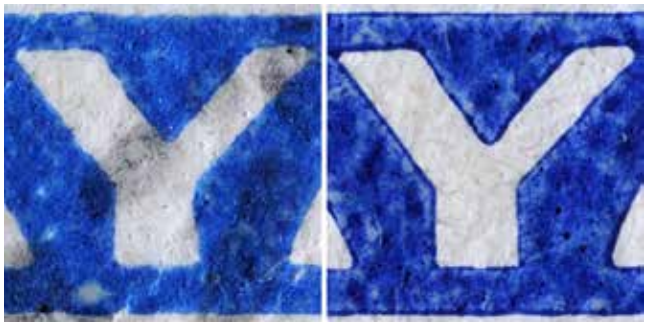

***Figure 14.*** Visual differences in surface roughness and print characteristics between chalky paper (left) and substitute paper (right). These can be discerned under a strong magnifying glass.

The pits on substitute paper are similar in size to those on post-war chalky paper. But unlike the latter, there is noticeably less "pinhole" pitting. The surface of substitute paper also appears more fibrous under a loupe. The heavily pitted form of substitute paper (Figures 12, 13) occurs occasionally on other BMA denominations also; I have seen it on a 15-cent stamp.

As these observations show, one may find pits on substitute paper and none on chalky paper. Pitting therefore does not seem to be a reliable indicator of paper type.

There are actually more reliable, albeit less obvious, characteristics that can be used to distinguish between chalky and substitute paper. One is the microscopic roughness of chalky paper mentioned earlier, although this is difficult to see without a microscope. Another is the puddling of ink at the edges of the printed areas on substitute paper that can be seen under a magnifying glass or even with the naked eye (Figure 14). I have found this to be quite a reliable identifier of substitute paper. Although ink tends to accumulate along the edges in letterpress printing in general, it is especially pronounced on substitute paper. It turns out chalky and substitute papers are coated with quite different substances.

### *Chemistry of paper coatings*

X-ray spectroscopy shows both pre-war and post-war chalky papers of the coconut definitives have a mainly calcium carbonate or chalk coating (Figure 15). Meanwhile substitute paper, whether pitted or unpitted, has a mostly kaolin coating (Figure 15).

The roughness of the chalk coating indicates that ground rock chalk was used rather than the more expensive precipitated calcium

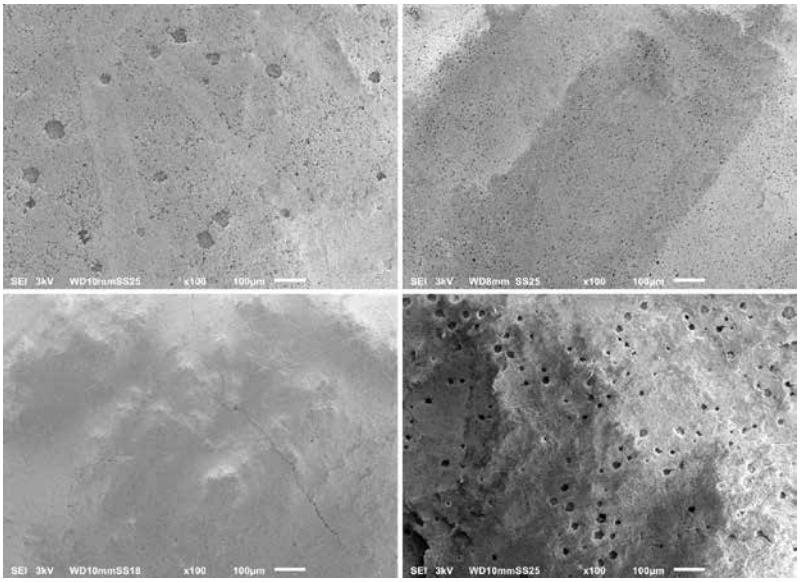

***Figure 13.*** Scanning electron micrographs (100×) of (clockwise from upper left) pre-war chalky, post-war chalky, pitted substitute and unpitted substitute papers.

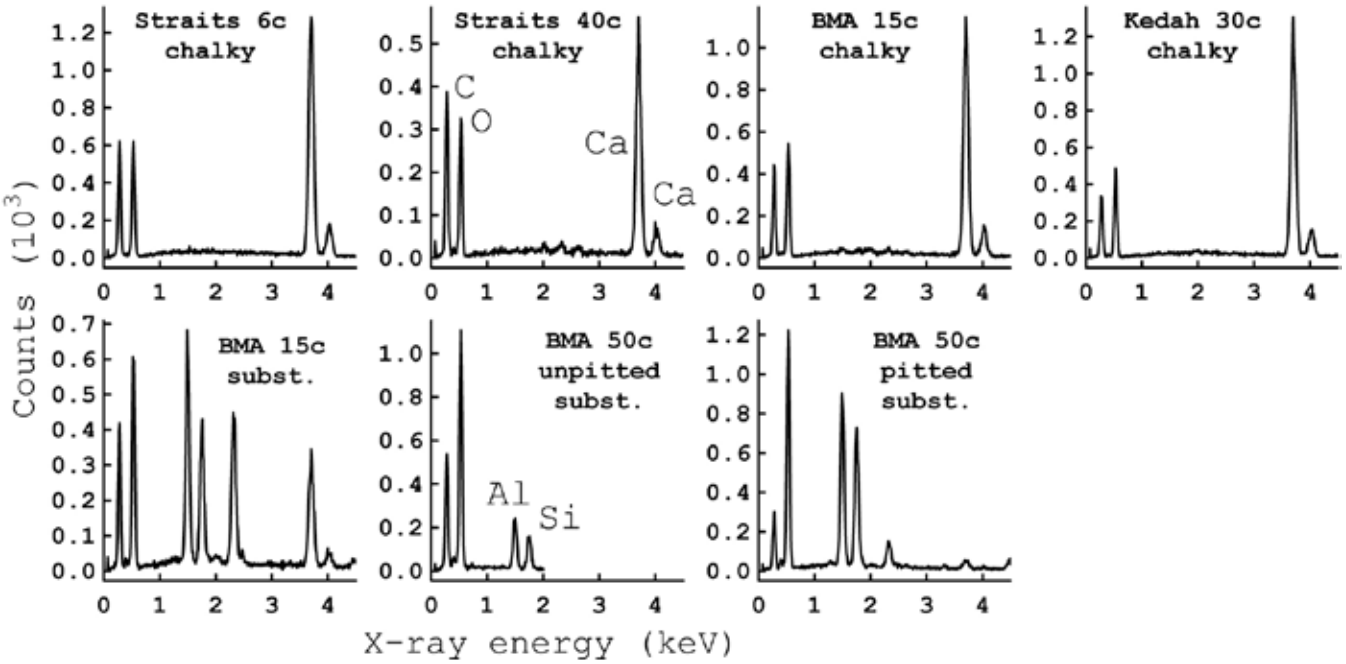


***Figure 15.*** X-ray energy spectra of the surface of chalky and substitute papers. A few other examples of chalky paper returned similar spectra (not shown). Raw spectral data can be downloaded at https://github.com/linyangchen/edx

carbonate. The microscopic bumps and pores helped it absorb ink evenly.

In contrast, kaolin was a fine powder that gave substitute paper its smooth surface. English kaolin in particular was of very high purity (Robert Hisey, personal communication). There were few microscopic irregularities on the coating to trap the ink, so it pooled. I have seen extreme cases where the finer lines in the stamp design are smudged together, which seemed to occur only on substitute paper.

Although chalk was plentiful in the British Isles, such as in the White Cliffs of Dover, it required casein salts as a binder (Glazer, 1997), and casein was in short supply during the war (United States Tariff Commission, 1945). The main constituents of paper coatings in wartime were therefore kaolin and aluminum oxide (Glazer, 1997). Besides the coconut definitives, many other colonial stamps printed during and shortly after the war were found with kaolin coatings (see Glazer, 2004). Chalk would make a comeback in 1948 (Glazer 2004).

## CONCLUSION

For philatelists, it is often enough just to identify catalogued paper types. Still, for accurate identification, it may be necessary to examine several characteristics, rather than just single traits, such as the presence or absence of pits, as explained in this study.

Hopefully the physical and chemical differences identified in this study will spur further research and ultimately advance the art of detection of alterations and forgeries. The Perlis stamp described in this study is a case in point.

But even if the purpose is nothing more than to appreciate the hidden physical and chemical beauty of stamps and the potential historical insights they bring (such as the use of kaolin during the war), one could argue it is worthwhile. That's simply because philately is a hobby and is about the joy of exploration and discovery for its own end.

## Acknowledgements

I am grateful to David Beech, John Barwis, Robert Hisey, Rein Bakhuizen van den Brink, Julian Tan, Edmond Soh, Ernest Cheah, Benedict Sim, Clement Khaw, Wulf Hofbauer and Li Zhen and Peter Cockburn for discussions and expert assistance, and to Keyence Singapore, Nikon Imaging Centre (Singapore Bioimaging Consortium) and Science Centre Singapore for providing the facilities that made this research possible.

## References

Barwis, J. H. 2013. Paper characteristics of U.S. 3¢ stamps, 1870–1881. In: Lera, T., J. H. Barwis, and D. L. Herendeen, editors. *Proceedings of the First International Symposium on Analytical Methods in Philately.* Washington, DC: Smithsonian Institution Scholarly Press, pp. 5–18.

Donaldson, L. A. 2009. Analysis of fibers using microscopy. In *Handbook of Textile Fiber Structure Volume 1: Fundamentals and Manufactured Polymer Fibers* eds. Eichhorn, S., Hearle, J. W. S., Jaffe, M. & Kikutani, T. pp. 121–153. Elsevier.

Foelkel, C. 2007. *Vessel Elements and Eucalyptus Pulps.* Associaçao Brasileira Técnica de Celulose e Papel.

Glazer, M. D. 1997. WWII paper coatings on some King George VI large Nyasa-type stamps. *GEOSIX* 181:3–10.

———. 2004. The papers used to print the King George VI colonial stamps. *GEOSIX* 213:1–10.

Lin, Y. 2019. Paper fiber analysis of the small heads issues. *The Malayan Philatelist* 60:40–46.

Lowe, R. 1951. *The Encyclopedia of British Empire Postage Stamps Volume III: the Empire in Asia*. Robson Lowe, London.

McKee, A. 2015. Paper and color varieties of the People's Republic of China "workers and soldiers" definitive set of 1955–1961. In *Proceedings of the Second International Symposium on Analytical Methods in Philately* eds. Barwis, J. H. & Lera, T. pp. 9–19. The Institute for Analytical Philately, Ohio, USA.

Murray Payne 2015. *Commonwealth King George VI Catalogue* 20th ed. Murray Payne, Somerset, United Kingdom.

Norris, A. 1985. *Malaya: The Survey Department Essays of 1933–34*. Malaya Study Group.

Parham, R. A. & Gray, R. L. 1982. *The Practical Identification of Wood Pulp Fibers*. TAPPI Press.

Pollard, D. 2012. Malaya BMA 50 cents. *The Malayan Philatelist* 53:17–18.

Safdari, V., Sigarody, M. R. N. & Ahmed, M. 2011. Identification of fibers of woody and non-woody plant species in pulp and papers. *Pakistan Journal of Botany* 43(4):2127–2133.

Stanway, L. C. 2009. *Malaysia and the Federation of Malaya: Their Stamps and Postal Stationery Volume 1*. Malaya Study Group.

Tan, S. 1999. *Standard Catalogue of Malaysia–Singapore–Brunei Stamps & Postal Stationery* 24th ed. International Stamp & Coin, Kuala Lumpur.

Tullis Russell & Co. Ltd. 1950. *Papermaking Fibers*. Tullis Russell & Co. Ltd., Scotland.

United States Tariff Commission 1945. *Post-War Imports and Domestic Production of Major Commodities: a Report of the United States Tariff Commission in Response to Senate Resolution No. 341 (78th Congress)*.

# The Computer Analysis of Die Cut Separations of U.S. Stamps

*Robert V. Mustacich*

## Abstract

This paper describes a method for fully characterizing the profile of the serpentine die cut edges of self-adhesive stamps. Prior to this work, only gauge measurements and visual observations have been used to describe them. The method presented analyzes each peak and valley of the serpentine shapes to capture the variability in a die cut and provides averaged results such as the familiar gauge measurement. By fitting the arcs of circles to the separate peaks and valleys, the die cuts are characterized by radii and the locations of their circle centers, in addition to height and gauge. The measurement precision of these features from scanned images is several microns, and the standard deviation of gauge measurement is ± 0.001 gauge unit.

For the U.S. stamps analyzed, the trends of these different features by year and producer suggest the emergence of preferred designs. Beyond providing a generalized forensic capability, the method demonstrates the ability to detail anomalies in die cuts, along with the ability to fingerprint die cuts based on the existence of irregularities. Using this process, collectors can characterize and make precise comparisons with reference stamps if the authenticity of a die cut stamp is in question.

## Introduction

The commercial production of U.S. postage stamps began to transition to self-adhesive stamps in the late 20th century. The separation of stamps correspondingly transitioned from perforation to die cutting, which offered speed and convenience. Using die mats lead to better integration with printing and production equipment.

The die mats are very thin, they can be manufactured by different methods, and they are attached to cylinders (Nazar, 2013). Like the early stamp perforation process, designs for die cuts went through a period of experimentation and evolution toward designs which resulted in ease of separation, durability, and ease of manufacture.

The production of die cut stamps in the U.S. involved a variety of contractors with an eventual phase-out of government production. Over the time period studied, 1995 to 2016, there is also a reduction in the number of contractors producing die-cut stamps. This study characterizes and compares die cutting features done by the government and the different contractors.

The feature characterization methods and results in this paper provide a foundation for forensic assessment of die cut stamps. Proliferation of die cutting machinery for the commercial production of labels and stickers has greatly spread the same technology used to produce modern stamps (Wista, 2019). However, because of the micron precision of the image analysis methods, the ability of a counterfeiter to match genuine die cuts should be very difficult. Nonetheless, it is likely counterfeits of die cut, self-adhesive stamps will continue to grow (Snee, 2017). The ability to more fully characterize die cuts as presented in this paper may become important as the printing techniques of the counterfeiters improve.

A brief comment on terminology. We philatelists are accustomed to referring most often to "perforations," "perforation gauge" and similar terms. The standard practice with die cut stamps is to similarly describe them by gauge, referring to the number of peaks or valleys in a 20 mm length of edge.

## Measurement Method

Die cut separations are generally "serpentine," having the appearance of a continuous wave. While it is straightforward to estimate the gauge of a die cut stamp's edge using a standard perforation gauge, the small gauge differences between some can be more challenging to measure. Further, the use of a perforation gauge does not characterize the particular shape of a die cut edge.

While many die cut edges appear approximately sinusoidal, the shapes range from very rounded to more trian-

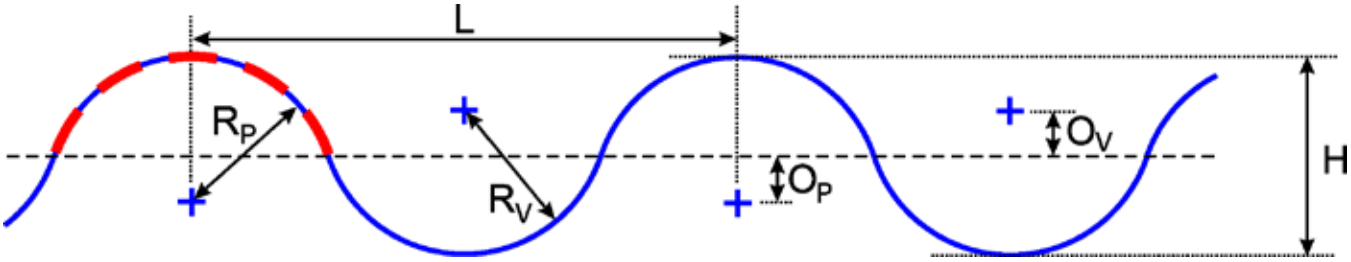


***Figure 1.*** Illustration of a die cut analyzed as a separate series of circular arcs. The serpentine shape (in blue) has a peak-to-peak length (L), which, divided into 20mm, is the gauge. The average height (H), the radii ($R_P$ and $R_V$) of the separate arcs fit to the peaks and valleys, the offsets ($O_P$ and $O_V$) from the dashed center line of the circular arc centers ("+" marks) provide a characterization of the shape of the die cut. The first arc fit to the left-most peak is illustrated with a dashed red arc. Using a scanned image of a die cut, the analysis requires less than 1 second of computer time. This example shows the familiar case in which the peak and valley radii are nearly equal.

gular. A sine wave, a standard trigonometric shape, can be mathematically fit to any regular periodic shape, but this procedure does not provide any description of the shape, other than perhaps a statistical measure of how well the sine wave fits the image of the edge.

For this reason, I have developed a description for die cut edges in which separate circular arcs are mathematically fit to the individual peaks and valleys without being constrained to match the gauge. This essentially "floats" the location of each peak and valley for a comprehensive analysis that captures any variations in the die cuts.

The result provides a full description of the shape of the die cut edge in addition to measurement of gauge and height. For example, die cut edges having more triangular shapes whose smaller arcs show more pointed peaks and valleys yield a different description than more rounded arcs. In addition, this approach also accommodates variation in shape, and, by capturing irregularities, it creates the possibility of fingerprinting die cut edges. For simplicity in the remainder of this article, I will refer to a die cut edge simply as a "die cut."

Figure 1 illustrates a die cut consisting of semicircular arcs. A centerline runs through the middle of the die cut dividing the edge into these peaks and valleys. The "+" marks indicate centers of circles having arcs that provide the best fit to the respective peaks and valleys. The centers of these arcs may lie above or below the horizontal center line depending on the shape of the die cut. The dashed red line illustrates the circular arc fit to the first peak on the left. Each arc fit has its own radius measure, labeled in Figure 1 as $R_P$ and $R_V$, for the first peak and valley on the left.

For the first peak in Figure 1, its maximum distance from the horizontal axis is the radius minus the offset of the center of the fitted arc, $R_P - O_P$. If the offset is to the same side of the centerline as the peak, the maximum peak height will instead be $R_P + O_P$. The sum of the average of the upper and lower maximum distances provides the average height (H). For the situation of the relatively shallow serpentine shape shown in Figure 1, the offsets are subtractive and give a reduced value of the height. Because of the symmetry generally observed in die cut serpentines, the peak and trough offsets are similar in size and opposite in direction, one being below and the other above the centerline.

Analogous to the usual depictions of wave forms in physics, H would be the wave height, the wavelength (L) is the peak-to-peak (or trough-to-trough) distance as called out in Figure 1. The gauge (G) commonly used by stamp collectors is equal to 20/L where L is expressed in millimeters.

I previously published an example of the analysis of a die cut using circular arc fitting (Mustacich, 2016). The computer methods for fitting circular arcs to image data are identical to the methods I used previously to analyze perforations (Mustacich, 2014).

My overall method was to scan the stamp image in positive monochrome film mode at 2400 dpi to a TIFF image file using a Canon 9000F flatbed scanner. I affixed die cut stamps to a clear polypropylene sheet cut from an Avery Heavy Duty sheet protector. The stamps were placed face down directly on the platen (polypropylene sheet side up) with small weights on them to ensure flatness on the platen. The edge shapes were extracted from the images using the same computer programming methods published previously in my analyses of perforations (Mustacich, 2014). Because it is impractical to align stamps on the scanner to be perfectly horizontal at high resolution, the analysis software fit a line through the data for the entire edge, then used the slope of this line to rotate the image to horizontal, to remove any tilt from the image.

The next task was to locate the approximate peaks and valleys in the image, which I accomplished by smoothing each point of the edge shape by averaging with the surrounding 50 data points. This smoothed shape accurately followed the general undulations of the shape. This average is shown in green in the analysis examples described later in this article. This smoothed curve provided a relatively noise-free shape for easily estimating the locations of the peaks and valleys. These estimated peak and valley positions were used to launch the same computer-based searches for the best circular arc fits to the local data as described previously (Mustacich, 2014). The fitted arcs are shown in analysis examples as red circles truncated at the centerline.

Three examples in Figure 2 of greatly differing die cuts demonstrate the robustness of this approach. The image

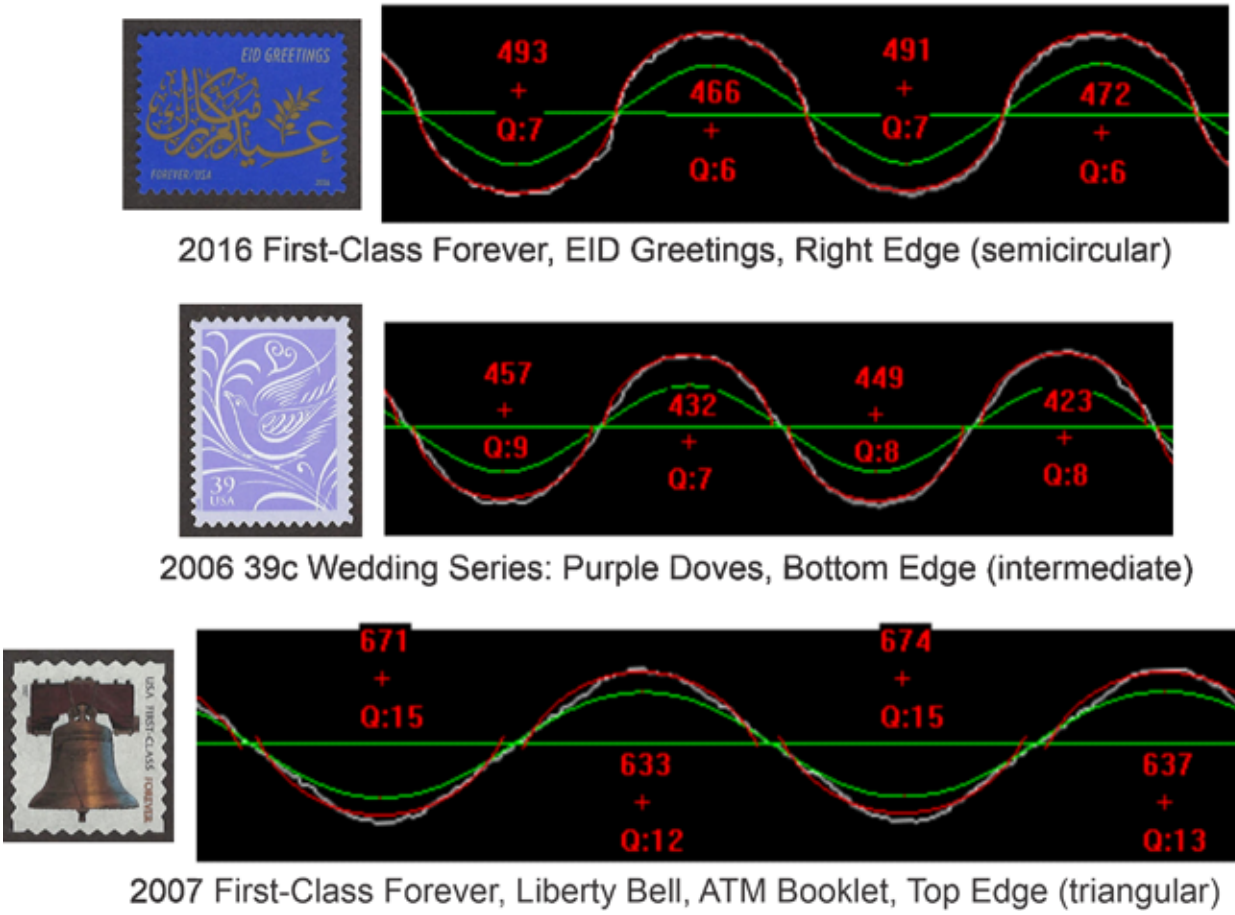


***Figure 2.*** Three die cut analyses showing the large differences in shape of the die cut. Most die cuts are like the top two examples—intermediate between a semicircular and a more sinusoidal shape, with the circular arcs fit closely to the data. The bottom example is atypical and represents a more extreme situation, but the circular arcs nonetheless provide a good approximate description of the shape and height of the die cut.

data is in white, the arc fits in red. The centerline and the peak/valley estimating curve are both in green. The red '+' marks are the circle centers of the fitted arcs. The number above the center mark is the arc radius in microns, and the quality of fit value (Q) is a statistical measure of the error of the arc fit to the data (Mustacich, 2014). Good fits of arcs to the data give smaller statistical errors resulting in lower values of Q.

The upper die cut example has a profile with nearly semicircular arc fits in which the arcs of the peaks nearly meet the arcs for the valleys. The second die cut example in Figure 2 is more sinusoidal in shape, and the narrower shapes have circular arc fits that do not quite meet each other at the centerline. The Q values for this case are slightly larger. The increased deviation from a circular shape is likely responsible for this small increase in error.

The bottom example is an extreme case of a relatively triangular die cut with rounded peaks and valleys. This type of serpentine cut has been referred to as a "wide teeth" variety (Blanks, 2010). There is a modest increase in the error of fit (a Q of 12-15), but the circular arcs fit much better than one might expect. The arcs remain centered above the peaks and valleys, and this results in precise gauge measurements. There is a small underestimation of H by 7% for this extreme case. Overall, the circular arc fits are quite close to the image data, even in this extreme example. Instead of forcing the entire edge to fit to a sine or other periodic wave formulation, this method has the flexibility to capture the variations in shape as well as asymmetry and local differences.

For this study I made a survey of die cuts by selecting about 20 different issues per year from 1995 through 2016 (see Appendix), seeking to obtain a wide selection of the different producers of die cuts over this period. All stamps were mint, carefully peeled from their backing, and applied to a transparent sheet for scanning as described above. All the die cut edges on each stamp provided a set of more than 1,280 different images of die cuts for this study. Stamps are occasionally referenced with Scott catalogue numbers to specify which variety of a stamp was used for study.

Information regarding the producers of die cuts was largely obtained from the *Scott Specialized Catalogue of United States Stamps and Covers* (Scott, 2017), *Linn's Yearbooks of U.S. Stamps* (Linn's, 1995–2016), and other published literature. For stamp production contracted out by the Bureau of Engraving and Printing, I associated the die

cutting with the single contractor typically cited, unless there was information the die cutting was done by a subcontractor. For example, Bank Corporation of America subcontracted the production of the 1999 33-cent Berries to Guilford Gravure, with die cutting done using a George Schmidt rotary die cutter (Smithsonian, 2019). These stamps are accordingly identified as a product of Guilford Gravure rather than a product of Bank Corporation of America.

Because of ownership changes among contractors, sometimes the new parent company is referenced in the literature, and sometimes the more familiar, wholly owned subsidiary is still referenced. An example is the acquisition of Bank Corporation of America by Sennett Security Products in 2004, then Sennett Security Products by CCL Industries, Inc. in 2015. Throughout all of this, Bank Corporation of America is still cited as a stamp producer. I tried to be consistent with the citations from familiar sources, and only specify subcontractors for die cutting where it was clearly called out in reference materials. These are the die cutting contractors (and their subcontractors) to the Bureau of Engraving and Printing in this study: Avery Dennison, Bank Corporation of America, CCL Industries, Ashton Potter, American Packaging Corporation, Guilford Gravure, and Stamp Venturers.

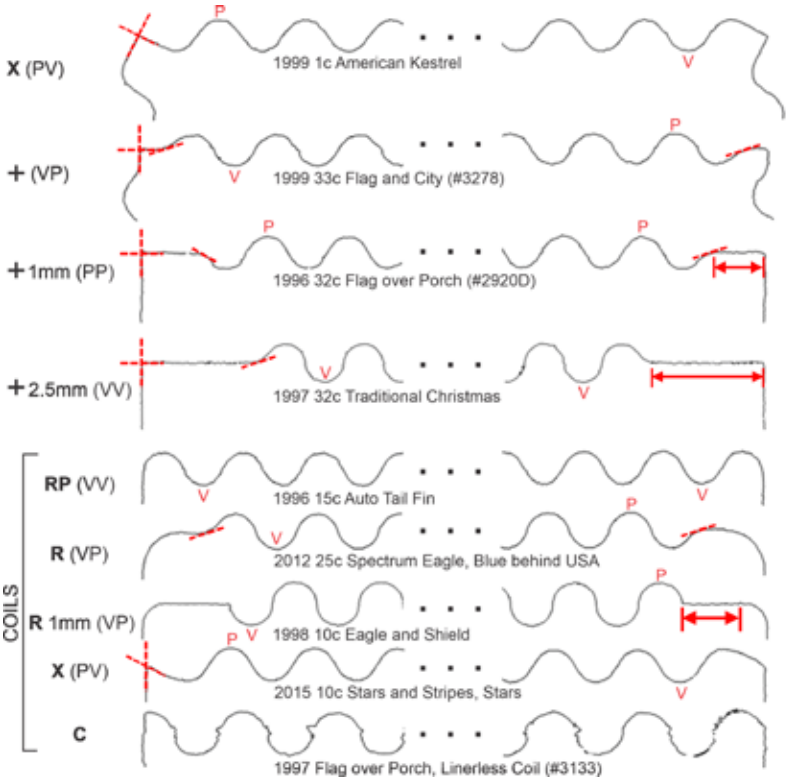


***Figure 3.*** Varieties of die cuts encountered in this study. The shapes of the stamp corners differ in style, and my nomenclature is adapted from various references in the literature. Corner intersections of the die cuts are basically "square" which I have denoted as +, tilted which I have denoted X (the most common variety), rounded as in the case of many coil stamps, or simply an intersection with a straight cut C.

I grouped the stamps into three categories for measurement purposes, which differ in how the horizontal and vertical die cuts intersect at the corners, and where the fully formed peaks and valleys begin and end. In the most common variety (about 69% of the die cuts in this study), the die cuts depart slightly from their otherwise regular shapes near the stamp corners to intersect each other at approximately right angles, but with a tilt. Because of this tilt, I have termed these the "X" group, but it has also been termed "wavy die cut" (Blanks, 2005a). Opposite edges of a stamp are complimentary shapes. The X corner matches a peak with a valley, so these patterns repeat around the stamp in a clockwise manner.

A similar grouping, I have termed the "+" group, does not have the tilt of the X group at its corners. This type of corner has also been termed "squared" (Blanks, 2005b). The horizontal and vertical die cuts meet at right angles at the corners, but there are variations in the length of the flattened portion of the die cut at the corners. This group is well represented, but less numerous in my survey than the X group.

A remaining small group is coil stamps, distinguished by straight edges on two opposite sides with a variety of die cuts on the other pair of sides. The die cuts meet the corners of these coil stamps in a variety of ways.

Some of styles encountered in this survey are shown in Figure 3. Typical corners for the X group are shown by the top example of Figure 3, the 1999 1-cent American Kestrel. The Figure 3 die cut profiles have been labeled based on the stamp edges starting and ending with either peaks (P) or valleys (V) (Nazar, 2019).

Thus, starting with a peak from the upper corner and ending with a valley would be termed "PV." Figure 3 highlights the starting and ending peaks and valleys I accepted for analysis. This may differ in some cases with the choices made for descriptive nomenclature for the stamps because I wish to exclude peaks or valleys near corners that are rounded into, and merge with, the straighter cutting at the stamp corners. Excluding such peaks or valleys from the analysis makes the statistical comparisons and average values of the mostly identical appearing peaks and valleys in a die cut more meaningful. I have added dashed tangent lines to indicate locations where peak or valley shapes are compromised to merge with the corner profile.

The next three images in Figure 3 are variations of the + type, where approximate horizontal lengths are indicated after the "+" in millimeters. The profiles are die cuts from the 1999 33-cent Flag and City (Scott #3278), the 1996 32-cent Flag over Porch (Scott #2920D), and the 1997 32-cent Traditional Christmas. Approximately 20% of the die cuts in this study are the + type.

The remaining five examples in Figure 3 are coils from top to bottom: rounded peak (RP); rounded (R); rounded with an approximately 1mm horizontal length adjacent to

the rounded corner (R1); an approximately linear intersection at an acute angle to the straight edge of the coil (an "X" variety (X) of a coil stamp). The bottom example is a linear cut (C) which intersects the serpentine die cuts.

The die cuts for the above described coils are from the 1996 15-cent Auto Tail Fin, the 2012 25-cent Spectrum Eagle (Blue behind USA), the 1998 10-cent Eagle and Shield, the 2015 10-cent Stars and Stripes, and the 1997 Flag over Porch linerless coil (Scott #3133), respectively.

What I refer to as rounded (R) types have also been termed "rounded shoulder" (Blanks, 2005c). Various + types of coil stamps are also included in the study, and their corners are the same as those illustrated for non-coil stamps in the upper part of Figure 3.

The coil stamps account for the remaining 11% of the die cuts in this study. The C variety in Figure 3 exhibits small paper remnants from gaps in the die cut, sometimes called "bridges." Such bridges are prominent in very early, hand-rouletted stamps as they helped prevent the sheets of unbacked paper from falling apart (Linder & Dromberg, 1983).

## Results

Most of the die cuts in this study have a slightly sinusoidal shape. This is demonstrated in Figure 4 which shows of plot of arc radius versus gauge for the 1,280 die cuts characterized in this study. A theoretical profile consisting of uniform, 180° semicircular arcs which adjoin perfectly at the centerline will have a length (L) equal to four times the radius (4·R). Substituting this into the gauge equation G=20/L gives the relationship R =20/(4·G) for this shape.

Figure 4 shows this as a dashed line in the plot. Most of the data in Figure 4 is close to this line, but with a slightly smaller radius consistent with a more sinusoidal shape as in the second example in Figure 2. There is a fair amount of data revealing larger than semicircular radii (data above the dashed line), a consequence of smaller heights that are best described with larger radius arcs having large offsets of the arc centers from the centerline. This point is developed further in the discussion of Figure 11.

This study found a small systematic deviation in the measured average radius when comparing peaks and valleys. This is easily demonstrated measuring the features of the shared edges on a pair of stamps after separating them. When comparing the peaks of one die cut with the matching valleys of the other die cut, the peaks are typically smaller by about 0.01mm in measured radius. The width of the cut made to separate the stamps appears to be ≤1 pixel (about 0.02mm of resolution) when scanning pairs of stamps at 1200 dpi. This width in producing the die cut separation will increase the radius of the valley and decrease the radius of the matching peak by a small amount. While small optical artifacts could result in some shadowing or similar imperfections in image scanning, the expected effect of the cut width could well account for this small systematic deviation.

Because there are some cases in which the peak and valley radii of a die cut edge differ much more than this small amount, I report the upper and lower radii and their statistics separately. There are cases in which the die cuts have differing peaks and valley shapes, and even varying sizes, as presented in later examples in this paper.

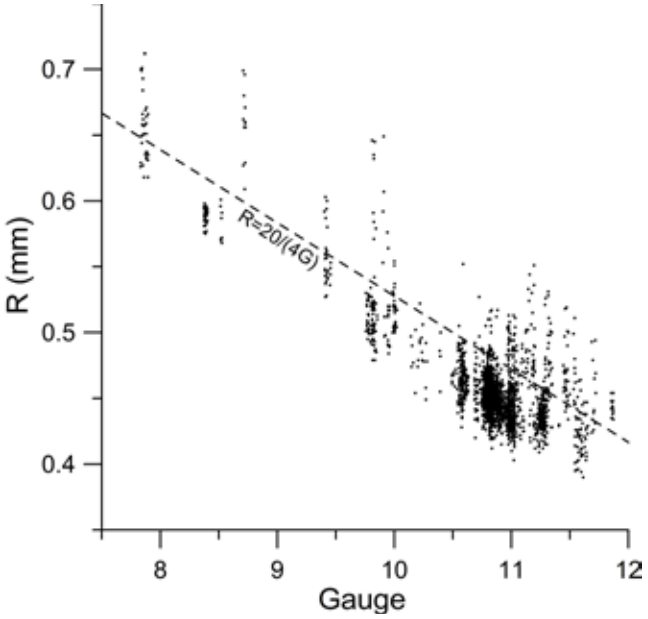


***Figure 4.*** A plot of average arc radius vs. gauge for 1,280 die cuts analyzed in this study. The dashed line R=20/(4·Gauge) shows the theoretical relationship for a die cut consisting of semicircles perfectly fit to the gauge. Most are approximately of this shape, but with smaller radii as in the second and third examples in Figure 2.

If comparing statistics from opposite sides of the stamp, keep in mind the complementarity of the stamp edges and the image rotation, since the peaks of one side are the die cut valleys on the other, especially if there are significant asymmetries. Two early die cut stamps, Scott #3031 and #3031a, were noted in the scanned images to have approximately 0.05mm of extra material attached to the teeth of the roulettes after separation of the stamps. This resulted in 0.05mm larger peak radii than the complimentary valley radii on the adjacent stamps. Most stamp edges in the study had sharp die cuts free of debris with complimentary peak and valley sizes between adjacent stamps.

The variation of die cut parameters in comparing stamps taken from the same sheet is shown for some example issues in Table I. Nonadjacent stamps were taken from the same sheet for three issues, identified by Scott numbering. Using nonadjacent stamps avoids the inclusion of any edges that are direct complements of other edges. The total number of horizontal and vertical edges measured for each issue is listed in the table, along with the average results. The standard deviations are included with the measurements, in the final row of Table I, is an estimate of the standard deviations of the measurement method. This was obtained by taking a single die cut and performing 15 different scans of the die cut, repositioning the stamp on the platen between scans. I have termed these results the "mea-

| Scott Number | Edges Measured | Sides | Gauge | Peak Radius (mm) | Valley Radius (mm) | Peak Offset (mm) | Valley Offset (mm) | Peak-to-Valley Height (mm) |
|---|---|---|---|---|---|---|---|---|
| 3049a | 17 | Hz | 11.270±0.009 | 0.426±0.006 | 0.434±0.006 | -0.073±0.008 | 0.082±0.008 | 0.704±0.004 |
| | 13 | Vert | 11.602±0.013 | 0.413±0.005 | 0.421±0.005 | -0.059±0.008 | 0.067±0.007 | 0.708±0.003 |
| 3050a | 20 | Hz | 11.220±0.007 | 0.429±0.007 | 0.435±0.007 | -0.082±0.013 | 0.088±0.012 | 0.694±0.017 |
| | 10 | Vert | 11.221±0.005 | 0.432±0.009 | 0.437±0.008 | -0.088±0.013 | 0.091±0.012 | 0.689±0.012 |
| 3052d | 13 | Hz | 11.600±0.012 | 0.421±0.006 | 0.416±0.006 | -0.071±0.008 | 0.065±0.010 | 0.700±0.005 |
| | 17 | Vert | 11.278±0.007 | 0.426±0.005 | 0.436±0.005 | -0.078±0.007 | 0.088±0.007 | 0.695±0.003 |
| Measurement Variation | 15 | All | ±0.001 | ±0.005 | ±0.003 | ±0.008 | ±0.005 | ±0.002 |

***Table I.*** Standard deviations of measured features of die cuts. The measurement variation demonstrates a high precision with standard deviations of the features in the micron range. The multiple die cuts taken from the sheets exhibit slightly more variation, still a high degree of uniformity.

surement variation" in the final row of the table.

The measurement variation in the final row of Table 1 is smaller than the otherwise small variation observed between stamps originating from the same sheet. This indicates there are some differences in the die cutting, likely the result of slight variations in the die mats.

The average standard deviation of the gauge in these examples is approximately 0.01 gauge unit, one tenth of the 0.1 gauge unit resolution typically obtained with better quality visual gauges. The error in the process itself is only about 0.001 gauge unit, the result of mathematical curve fitting to get high precision peak positions along the die cut.

The average radii of the arc fits to the peaks were generally smaller than for the valleys. This accords with the expected effect of the cut width. The average difference is on the order of 0.01mm, consistent with general observations of the difference between the peak and valley sizes for die mats, presuming the die mats have been designed to have equal peak and valley sizes.

The offsets, the positions of the circle centers of the arcs, typically mirror each other because of the symmetry of most die cuts, the sign indicates the direction from the centerline. While there was some variation in the radii and offsets of the arc fits to the die cuts, the combination of offsets and radii provided measures of the height with similar standard deviations. Overall, the data for these examples shows that the die cuts are quite uniform, and the small measurement variation indicated that they could be measured with a high degree of precision.

While most die cuts exhibit uniformity of gauge and symmetry of shape, there are some exceptions. Two examples of irregular die cuts encountered in this study are shown in Figure 5. The vertical die cuts of the 2006 24-cent Common Buckeye, right edge shown horizontally in the

***Figure 5.*** Two examples of anomalous die cut edges. The 24c Common Buckeye stamp of 2006 has one slightly wider peak in the middle of the right side of the die cut. Including this anomaly increases the gauge measurement compared to measuring on either side of it. The Music Icons, Jimi Hendrix stamp of 2014 has an unusual asymmetric peak shape near the top of the stamp as shown for the peak nearest the top edge on the left.

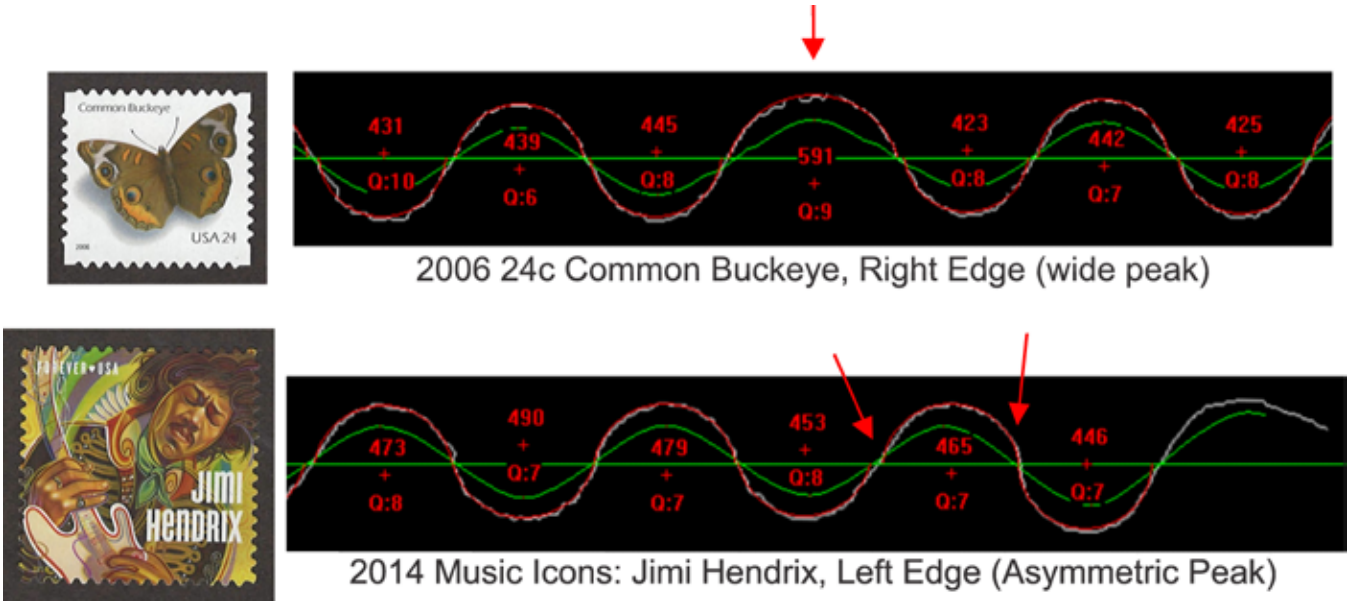

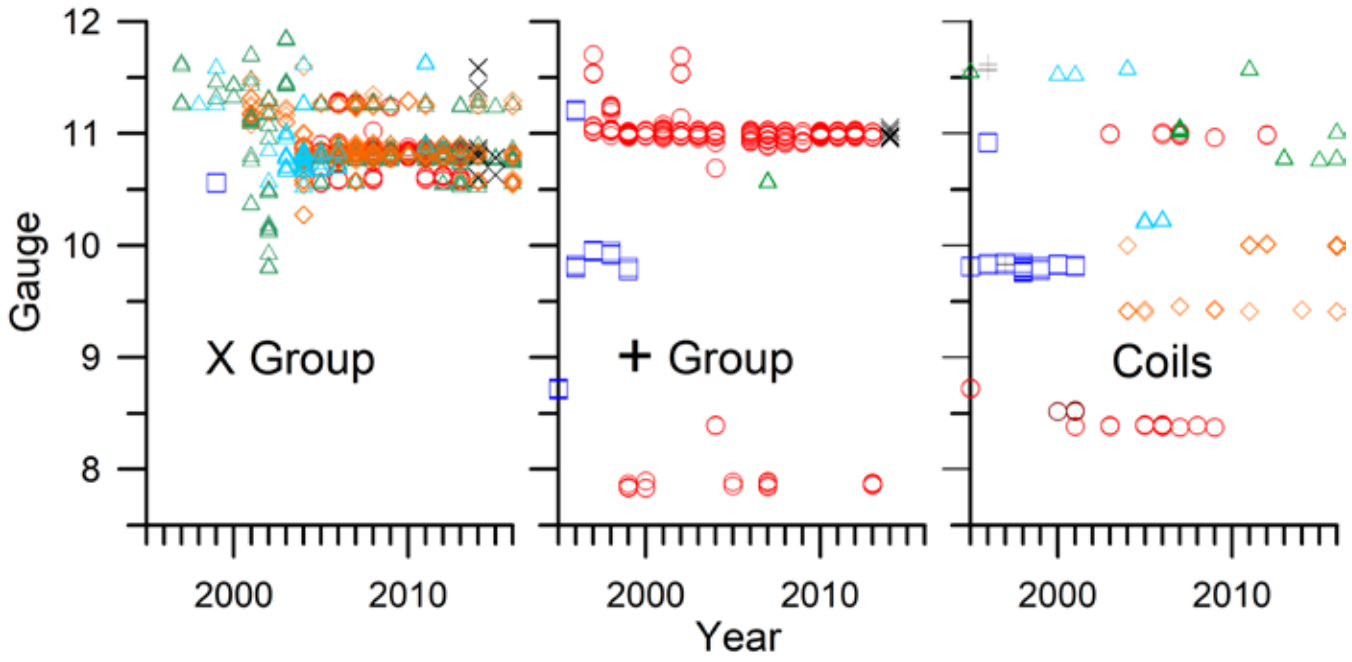


***Figure 6.*** The gauges of die cuts by type, year and producer. It appears that producers generally continue to keep using their specific die cut profiles. There is also a relative narrowing of gauge selections in the later years. Data key: □ Bureau of Engraving & Printing; ○ Avery Dennison; Δ Bank Corp. of America; X CCL Industries; ◊ Ashton Potter; △ American Packaging Corp; + Stamp Venturers; o Guilford Gravure.

upper example, has a large gauge deviation at the midpoint of the stamp edge. A single radius of approximately 0.14mm greater size occurs at this location. The die cut on either side of this inhomogeneity has uniform shape with a gauge of 11.0, but inclusion of this wider peak in the middle of the die cut creates a step in the otherwise uniform peak spacing. This large step has the effect of lengthening the edge when counting the number of peaks in a 20mm length to determine gauge. Consequently, the gauge fit to the entire edge gives a lower value of 10.7. The *Scott Specialized Catalogue* listing for this stamp cites a gauge of 11, a value obtained only by measuring on one side or the other of the anomalous center feature of the edge. This stamp was produced in 2006 by Avery Dennison.

The lower example in Figure 5 shows the left edge die cut from 2014 Music Icons: the Jimi Hendrix stamp, turned horizontally, exhibits an irregular shape near the corner. There are three smaller radii (453, 465 and 446) with a large tilt present in the second of the three. This is most apparent in the angles the die cut makes with the centerline. The opposite side of the stamp has the complement to this irregular shape. Bank Corporation of America is reported to have produced this stamp in 2014.

I cannot conclude whether either of these anomalies are intentional security measures to allow better detection of potential counterfeits, or if they are design compromises in the die cutting mats.

### *Gauge*

Gauge is the only parameter commonly used to describe die cuts. The precision reported in the *Scott Specialized Catalogue* (Scott, 2017) is often in fractions of a gauge unit—one-quarter, or even tenths of a unit, and other times to the nearest unit (but probably when closer to the unit than the nearest fractional value). For the 1,280 die cuts studied, gauge measurements were typically within 0.2 gauge units of the stated value in the catalogue, with a standard deviation of 0.1 gauge unit. A few discrepancies surfaced, such as the 2011 EID Greetings forever stamp produced by Avery Dennison, and the 2015 Purple Heart 49-cent stamp produced by Bank Corporation of America for Sennett Security Products. The catalog lists gauge values of 11.25 and 11 for these two issues compared to my gauge measurements of 10.8 x 10.9 and 11.25 x 10.8, respectively.

Figure 6 shows plots of the gauges found for the three generic stamp types from 1995 to 2016, with the data points coded for each stamp producer. For all three types, there appears to be greater gauge variety in the early years of production. Most producers have engaged in repeated use of the same gauges, as evidenced by the horizontal repeats in the plots.

A conspicuous exception is the X variety stamps produced by Bank Corp of America in 2001–2002. After 2004, most of the X variety stamps are of three approximate gauges: 10.5, 10.8, and 11.25. Less gauge variation is observed in the + varieties. This is also typical of coil stamps, and these are similarly limited to just a few gauges in the later years. Besides converging toward die cutting designs optimal for durability and separability, this may also be the result of a reduced number of contractors producing stamps, especially since they appear to reuse tooling or design processes.

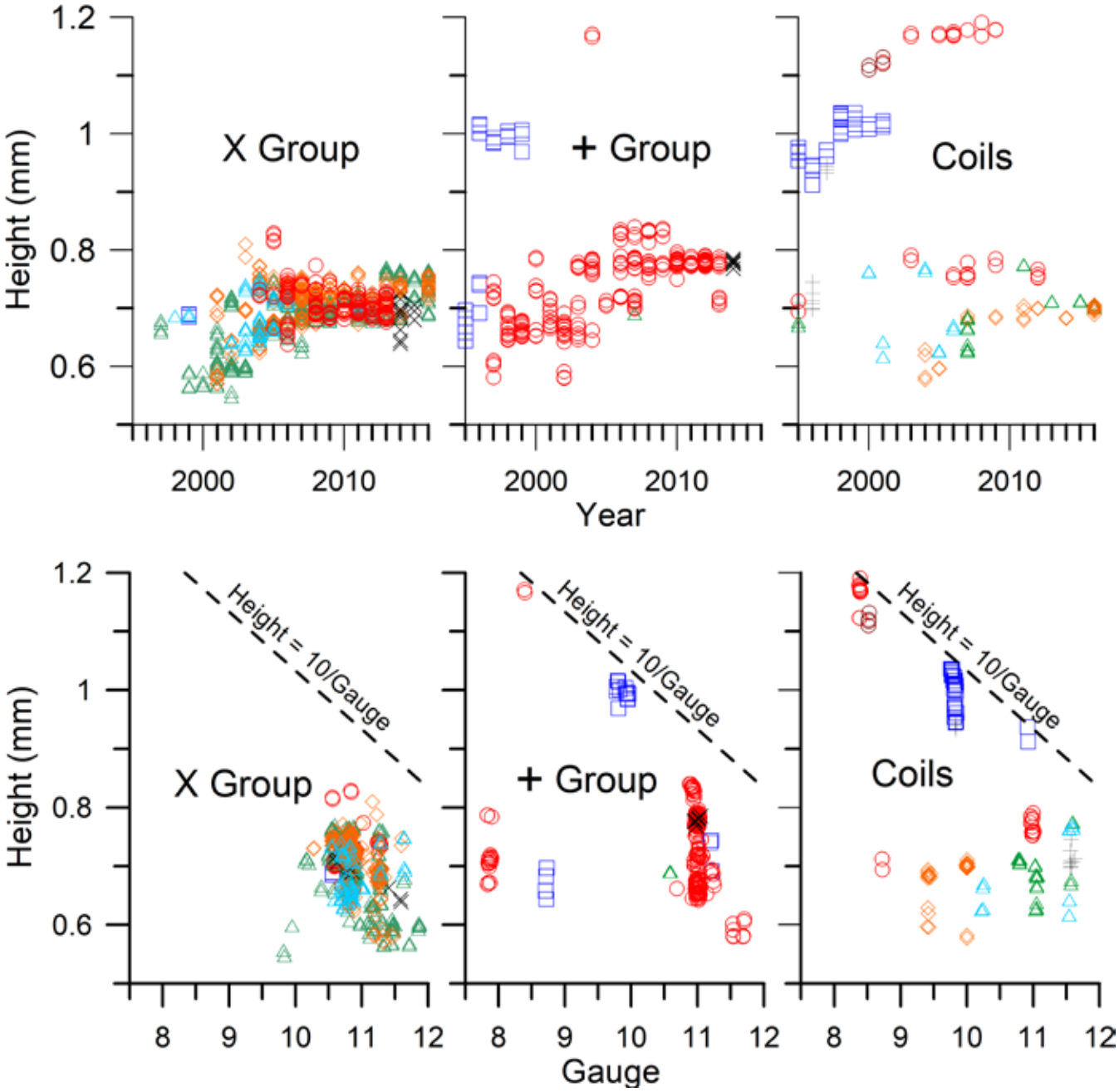


***Figure 7.*** (Top) The die cut height by type, year and producer. Like the gauge, there is a relative narrowing of height values in later years, the result of several factors. Data key: □ Bureau of Engraving & Printing; o Avery Dennison; Δ Bank Corp. of America; X CCL Industries; ◊ Ashton Potter; Δ American Packaging Corp; + Stamp Venturers; o Guilford Gravure.

***Figure 8.*** (Bottom) Plots of height vs. gauge for the types of die cuts. The dashed lines show the value for the theoretical case of die cuts consisting of semicircles (Height = 10/Gauge). While a few die cuts have a nearly semicircular shape, most have smaller height values. Data key: □ Bureau of Engraving & Printing; o Avery Dennison; Δ Bank Corp. of America; X CCL Industries; ◊ Ashton Potter; Δ American Packaging Corp; + Stamp Venturers; o Guilford Gravure.

### *Height*

The range of die cut heights for the three groups of stamps also narrows over time as shown in Figure 7.

Again, there appears to be some narrowing by producers of the choices for heights, such as Avery Dennison's production of the + group stamps to heights of 0.69mm and 0.75mm in 2013. The X group shows a wider range in height prior to 2006. Reduced variety because of fewer producers is evident in the plot of coil heights. Further variations may be revealed with additional sampling.

For a serpentine shape consisting of identical 180° semicircles meeting at the centerline with no offset of the circle centers, the height is equal to twice the radius. Since the radius will be 20/(4·Gauge) in mm for this situation,

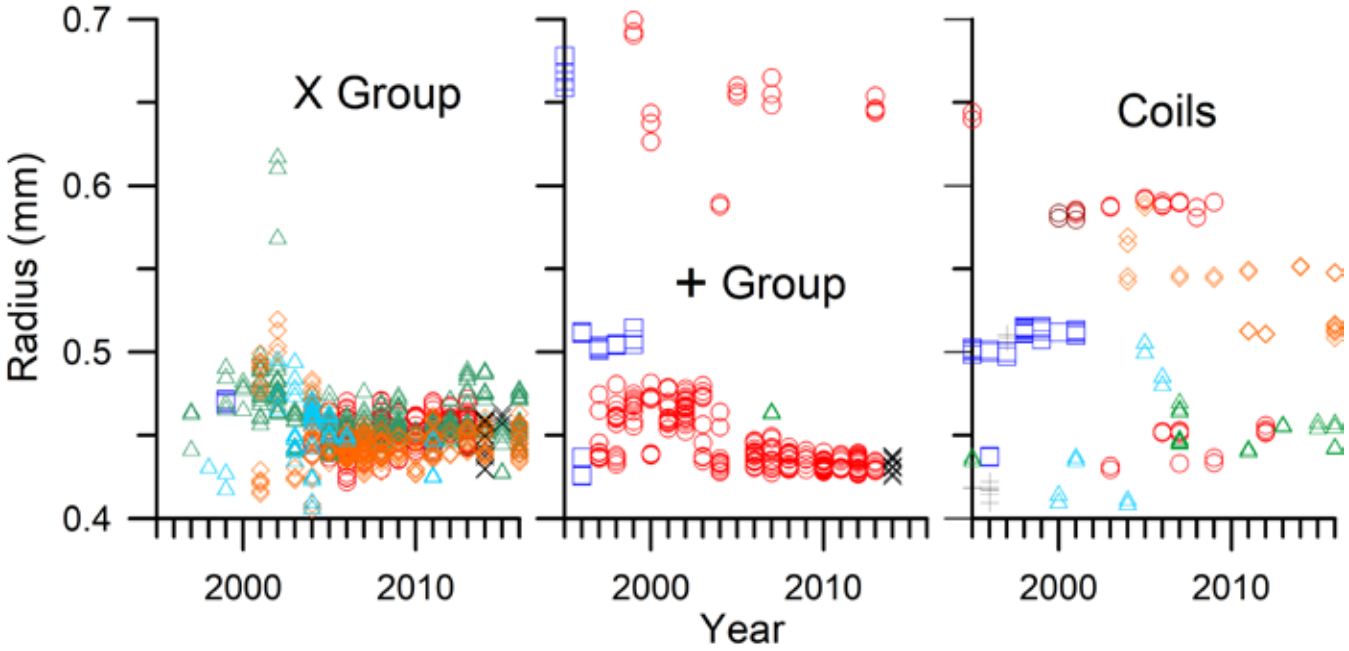


***Figure 9.*** The average radii of peaks and valleys in die cuts by type, year and producer. While there may be some narrowing of design choices, the narrowing in later years may be partly accounted for by the reduced number of producers. Data key: □ Bureau of Engraving & Printing; ○ Avery Dennison; △ Bank Corp. of America; X CCL Industries; ◊ Ashton Potter; △ American Packaging Corp; + Stamp Venturers; ○ Guilford Gravure.

the height will be 10/Gauge in mm. This represents an idealized maximum height based on the idea that yet greater heights with increasing radius would result in interlocking perforations for a constant gauge value.

Height vs. gauge is plotted in Figure 8 for the three die cut types, and this idealized height for a semi-circular serpentine appears to provide an upper limit for the values of the die-cut heights for different gauge values. Some data lies near this boundary and represents die cuts with nearly semicircular peaks and valleys. Many of the stamps produced by BEP are close to the plot of Height = 10/Gauge in Figure 8.

### *Radius*

The trends observed in this survey for the radii fit to the peaks and valleys of die cuts are presented in Figure 9. Similar to the trends for gauge and height, the die cuts have radii that effectively have settled in on a few values over time, especially as the number of producers declined in recent years. The X group after 2005 has values approximately 0.45mm, while the + group has similar values in addition to a few of approximately 0.65mm. The coil group radii in this survey, after 2010, are largely of three approximate values produced by three printers: 0.45mm (Avery Dennison and Bank Corp. of America), 0.52mm (Ashton Potter), and 0.55mm (Ashton Potter).

Because the limiting profile, consisting of adjoining semicircles matching the gauge, has the relationship of the height equal to twice the radius, it is interesting to examine plots of the height vs. radius for the three groups of die cuts. These plots are shown in Figure 10. In this figure the limiting Height = 2·Radius bounds are shown as dashed lines. The data near them is very similar to the data near the same bounds presented in Figure 8.

The verticality of data clusters away from the boundary lines in Figure 8 is mostly replaced with downward sloping trends (illustrated with lines drawn in the data) in Figure 10. The dense vertical cluster for the X group, at about 10.8 gauge in Figure 8, is now a more diagonal cluster in Figure 10 as suggested by the line drawn through the cluster. This is more easily observed in the + group die cuts of gauge 11 produced by Avery Dennison in comparing the vertical cluster in Figure 8 with the more diagonal spread of this cluster in Figure 10. While the coil data is sparser, some similar differences can be found for some of the data in comparing Figures 8 and 10.

The sloping height vs. radius trends in Figure 10 can be explained by a trade-off of height with radius while maintaining a constant gauge. A plot of the height vs. radius in the X group data having a gauge in the range of 10.72-10.78 is presented in Figure 11, along with some example plots of die cut analyses of points selected from the nearly linear spread of the data. This is illustrated in the upper right where arcs from three circles overlap to create a single peak for the same peak width (constant gauge) on the green line representing the centerline of a die cut. This relationship likely explains some of the linear relationships suggested in Figure 10.

### *Fingerprinting*

Two types of fingerprinting of die cut edges are clearly possible based on these research results. One is a generic fingerprint based on overall characterization using the average edge features, the other is a full characterization of

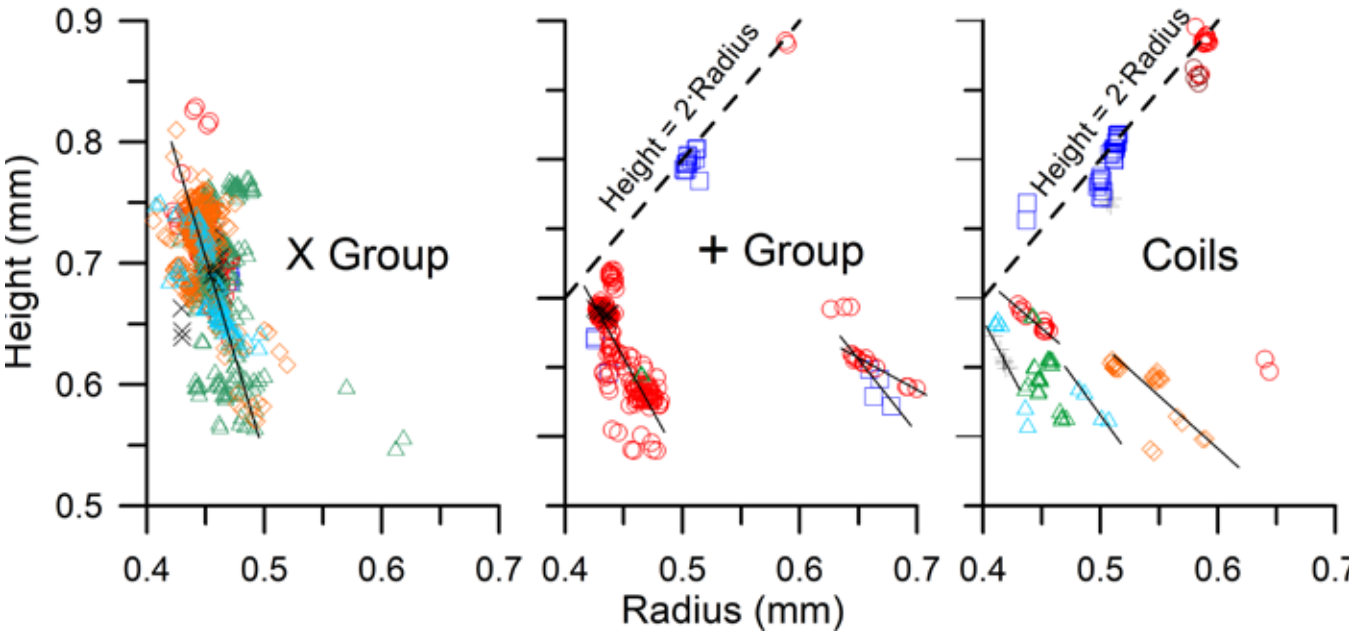


***Figure 10.*** Plots of height vs. radius for die cut types. A profile consisting of joined semicircles is represented by the dashed lines (Height = 2·Radius), and a few die cuts have this shape. Lines are sketched through different groups of the same producer to suggest possible underlying relationships. Most stamps have heights that are less than the values required for a semicircular profile. Data key: □ BEP; ○ Avery Dennison; Δ Bank Corp. of America; X CCL Industries; ◊ Ashton Potter; △ American Packaging Corp; + Stamp Venturers; ○ Guilford Gravure.

the sequence of the specific peaks and valleys along the edge. Because of the high precision in the software-based measurement of these features, either approach could be used for testing the relatedness and grouping of stamps.

The clustering of data that is observed in Figures 6 through 11 suggests stamps can be subjected to overall characterization to see their average features are in reasonable alignment with previously measured parameters such as gauge, average height, and the average radii of peaks and valleys.

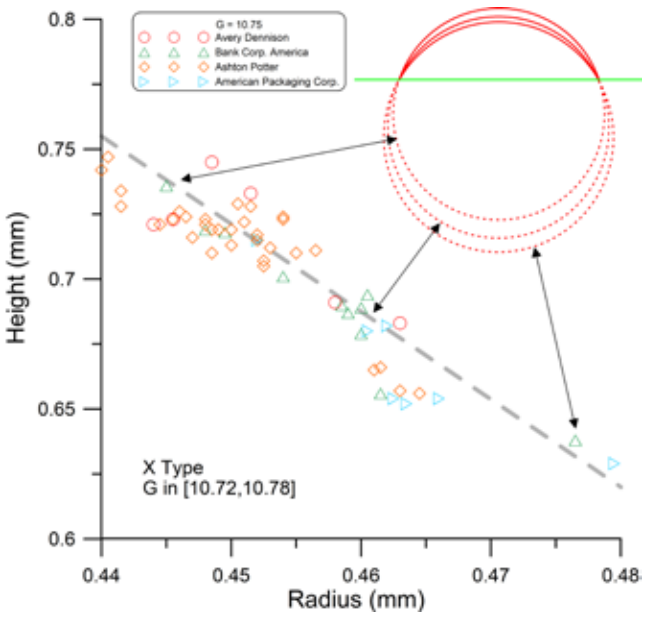


If the appearance of a die cut edge is peculiar, this level of generic characterization and comparison with other die cuts' features would be advisable. Because of the small amount of variation observed in the production of a stamp issue, examples seen in Table 1, seemingly small differences might be significant. It would be important to gather reference examples of the same issue that have been used or handled similarly for comparison.

The characterization approach described in this paper could become increasingly useful if printing methods for counterfeit self-adhesive stamps continue to improve. A recent example is the counterfeit of the 2014 Flag and Fireworks coil stamps produced by offset lithography (Snee, 2017). While they can be still be distinguished by small differences in the printing, the die cuts closely mimic those of the genuine stamp, differing by about 0.2 gauge units, but this is the only familiar comparison method. An effort by the counterfeiter to match the die mats used in the production of the genuine stamps is likely to be very difficult given the precision with which the methods presented in this

***Figure 11.*** A plot of height vs. radius for X-type die cuts having gauge values in the range of 10.72 to 10.78. A line drawn through the data highlights the linearity of this data. Profiles from different locations along this line reveal a tradeoff between larger radius and reduced height with arcs confined to this small gauge range. This is illustrated in the upper right where arcs of different radius are constrained to the same gauge length along the green centerline through the die cut. This trade-off likely explains some of the linear relationships in Figure 10.

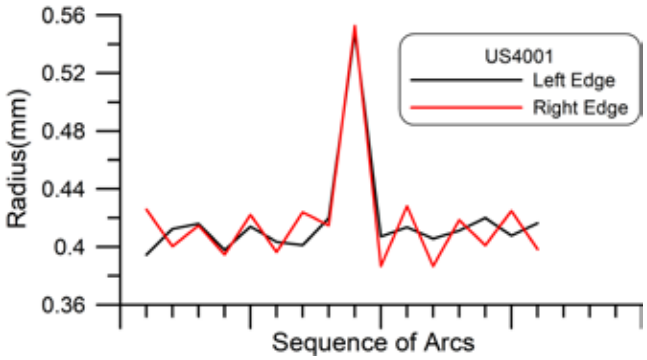


***Figure 12.*** Alignment of the sequences of radii for the right and left edges of the 24c Common Buckeye stamp shown in Figure 5. A computer correlation of sequences of radii for different die cuts matches these together.

study can characterize a die cut.

A more detailed level of fingerprinting can also be pursued along the same lines as that using the sequential pattern of perforation features (Mustacich, 2014). The sequence of peak and valley measurements is used to fingerprint the die cut, for example, the sequence of radii can be used to fingerprint the first example of atypical edges in Figure 5.

The radius is plotted in Figure 12 according to the sequence of the arc fits for the left and right stamp edges, top to bottom. The large radius in the center position results in a larger value in the middle of the sequence. The separate fingerprints for the two edges show nearly perfectly large deviation in radius overlays in both position and size. These fingerprints could readily match using a simple computer program to align and match sequences, done by testing the range of possible sequence alignments to find alignments with minimum differences.

While the typical variations of features in die cut stamps are small, these are possibly large enough to carry out pattern matching related to position on a sheet of die cut stamps, especially if there are a few anomalous features large enough to create a useful fingerprint. Table I reveals that die cut stamps can have standard variations a bit larger than the measurement variation of about ±0.003-0.005mm. It may be possible to use fingerprinting sequences of radii or other features that differ sufficiently to match to specific positions on a die cut sheet. This is an open question for future research.

## Summary

My study demonstrates the ability of computer-based analysis of scanned images to characterize the shape of die cuts by finding the best size and positioning of a circular arc to fit each peak and valley of the die cut profile along the edge of a stamp. This method has the flexibility to fit circular arcs to the full range of die cuts in the survey, allows for irregularity of the peaks and valleys (including relatively triangular ones), and avoids limiting the peak and valley analysis to a single periodic waveform that is simply fit to the edge of the stamp.

Letting the individual analysis of each peak and valley "float" independently still results in gauge measurement precision of about ± 0.001 gauge unit. Measurements of arc radii for peaks and valleys, arc offsets from center line, and heights all have standard deviations in the micron range. Once a die cut image has been scanned and cropped, the computer-based analysis requires less than a second.

A survey of 1,280 die cuts, with respect to production year, revealed the general characteristics used by different producers and how these have evolved over time. Within the sampling limits of this survey, there was a general trend toward fewer contract producers using their preferred gauges and die cut profiles. Data clusters around certain parameter choices, and this provides reference values expected for different producers at different times. These reference values can provide a basis for forensic examination of die cuts, and, in the case of well-made counterfeits, the precision of this characterization method may be very difficult to defeat regarding comparison with genuine die cuts.

## Appendix

The specific U.S. stamps used for this study are listed in order of Scott Catalogue number as follows (duplicates noted parenthetically): 2915C, 2915D, 2920, 2920D, 2921, 3018, 3031, 3031A, 3049A, 3050, 3050A, 3052, 3052D, 3122, 3125, 3133, 3137, 3176, 3177, 3204, 3207, 3208, 3228, 3230, 3244, 3263, 3266, 3268, 3271, 3276, 3278, 3279, 3280, 3282, 3283, 3315, 3331, 3438, 3447, 3450, 3451, 3452, 3464, 3468A, 3470, 3475, 3477, 3482, 3484, 3485, 3496, 3497, 3498, 3499, 3501, 3522, 3526, 3534, 3548, 3549B, 3550, 3557, 3558, 3559, 3560, 3613, 3614, 3647, 3648, 3660, 3669, 3672, 3695, 3749A, 3750, 3754, 3755, 3756, 3756A, 3757, 3770, 3773, 3774, 3781, 3782, 3783, 3803, 3804, 3812, 3813, 3820, 3829, 3829A, 3830, 3832, 3833, 3835, 3836, 3838, 3839, 3854, 3862, 3863, 3869, 3870, 3871, 3872, 3874, 3875, 3876, 3877, 3879,3880, 3881, 3882, 3896, 3897, 3898, 3904, 3905, 3906, 3911, 3925, 3930, 3936, 3938, 3943, 3966, 3968, 3969, 3970, 3974 (2), 3975, 3978, 3980, 3982, 3983, 3985, 3995, 3996, 3998, 4001, 4001A, 4002, 4020, 4029, 4030, 4031, 4032, 4073, 4077, 4078, 4079, 4100, 4117, 4118, 4119, 4120, 4121, 4122, 4124, 4125, 4126, 4127, 4128, 4130, 4133 (2), 4134, 4135, 4136, 4138 (2), 4139, 4140, 4141, 4142, 4147, 4151, 4158, 4164, 4165, 4186, 4187, 4189, 4190, 4191, 4191, 4196, 4197, 4199, 4200, 4201, 4202, 4205, 4206, 4208, 4210, 4219, 4220, 4221, 4222, 4223, 4226, 4227 (2), 4259, 4263, 4265, 4266, 4267, 4270 4271, 4334, 4335, 4341, 4346, 4347, 4349, 4350, 4351, 4358, 4359, 4372, 4373, 4374, 4375, 4376, 4377, 4387, 4389, 4390, 4393, 4395, 4396,4397, 4406,4407, 4408, 4415, 4416, 4421, 4424, 4433, 4434, 4435, 4436, 4437, 4445, 4450, 4471, 4473, 4474, 4472, 4473, 4475, 4476, 4477, 4484, 4492, 4493, 4494, 4495, 4496, 4502, 4503, 4504, 4512, 4520, 4525, 4526, 4529, 4530, 4545, 4547,4552, 4558, 4565, 4570, 4583, 4584, 4587, 4590, 4591, 4603, 4623, 4624, 4625, 4626, 4627, 4628, 4653, 4666, 4667, 4672, 4702, 4703, 4704, 4705, 4711 (2), 4721, 4726, 4741, 4742, 4749, 4764, 4782, 4786, 4789, 4790, 4800, 4803, 4804, 4805, 4806, 4807, 4815, 4816, 4821, 4824, 4845, 4846, 4847, 4854, 4855, 4856, 4857,

4860, 4869, 4870 (2), 4880, 4892, 4907, 4916, 4921, 4945, 4952,4957, 4962, 5035, 5036, 5037, 5038, 5039, 5040, 5052, 5053, 5054, 5055, 5056, 5057, 5059, 5060, 5061, 5064, 5091, 5092, 5100, 5105, 5130, 5131, 5201, B1, B2, B3

## References


Blanks, R. 2005a. Current Recognized Varieties of the Sea Coast Coil. *The United States Specialist* May 2005: 223–28.

Blanks, R. 2005b. A Sea Coast Die Cut Variety Surfaces. *The United States Specialist* Sept 2005: 423–25.

Blanks, R. 2005c. New "Rounded Shoulder" Bring Atlas Statue Coil Die Cut Types to Four. *The United States Specialist* Oct 2005: 466-68.

Blanks, R. 2010. Third Generation ATM Die Cutting Arrives. *The United States Specialist* Oct 2010: 445–50.

Linder, L., and D. A. Dromberg. 1983. *The Serpentine Rouletted Stamps of Finland Issues of 1860 and 1866. Translation from The Handbook of Finnish Stamps*. The Scandinavian Philatelic Foundation, Thousand Oaks, CA.

*Linn's Yearly Stamp Yearbook, 1995–2016*. Amos Media Publishing, Sidney, OH.

Mustacich, R. 2014. Freak or Fake? A New Fingerprinting Method for Distinguishing between Original and Fraudulent Extra Perforation of 19th Century Revenue Stamps. *The American Revenuer* 67 (1): 2–19.

Mustacich, Robert V. 2016. Measurements of Stamp Separation Features by Digital Image Analysis. In: Barwis, J. H. and T. Lera, editors. *Proceedings of the Second International Symposium on Analytical Methods in Philately.* Akron, Ohio: The Institute of Analytical Philately, pp. 73–85.

Nazar, R. 2013. Die Cut Production Varieties of the 32c Flag over Porch Self-Adhesive Stamp Produced by the BEP in Coils of 100. *The United States Specialist* Nov 2013: 510–24.

Nazar, R. 2019. *Die Cut Types, Incision Styles, and Shoulder Cuts.* http://www.usastamps.com/references/PNC_Catalog/Numbering_System/Extended.htm#Die_Cuts. Nazar Publication, NJ.

Scott Publishing Company. 2016. *Scott Specialized Catalogue of United States Stamps and Covers.* Sidney, Ohio: Amos Media Co.

Snee, C. 2017. Counterfeit United States 2014 Flag and Fireworks Coil Stamps Have Surfaced. *Linn's Stamp News*, Feb 27, 2017. Amos Media Publishing, Sidney, OH. https://www.linns.com/news/us-stamps-postal-history/2017/february/counterfeit-united-states-flag-and-fireworks-coil-stamps.html

Smithsonian, 2019. Smithsonian National Postal Museum website. *Regular Definitive Issues, Flora & Fauna Issues, 33-cent Blackberries*. https://arago.si.edu/category_2040820.html

Wista, 2019. So far self-adhesive stamps have only been cut (kiss-cut, die-cut). Wista GmbH, Schwaigern, Germany. https://wista.com/eng/postagestamps.php?type=selfadhesive

# A Quantitative Color Analysis of the US 3¢ 1861 Issue

*Jan Hofmeyr*

## Abstract

In this paper I argue that reflectance technology should be used to formalize the classification of stamp shades. The US 1861 3¢ serves well for this purpose because of the range of shades and their values. My analysis draws attention to two fundamental problems with traditional methods, which I call 'Reference Copy' and 'Cluster Algorithm' problems. I test a range of spectrographic sampling methods and suggest a formal protocol for future measurement. The paper concludes by suggesting the use of CIE 1976 Lab coordinates for some of the key shades of the stamp.

## Introduction

This research is based on 33 used examples of the 1861 3¢ stamp of the USA. The stamps range in color from pink to brown. Twenty-seven have been expertized by various agencies like the Philatelic Foundation or Professional Stamp Experts. Nine have been expertized by two agencies. In five of the nine instances, experts have come to different conclusions about color.

It is not surprising agencies sometimes disagree about color. People differ in their ability to discriminate between shades; agencies use different shade reference copies. Advanced technological measurement should help to narrow down these variations.

When it comes to stamp shades, most of the advanced work has focused on three questions: what are the spectrographic characteristics of a stamp; what are the elements in the ink; and how do the two relate? My purpose in this paper is to focus on spectrographic analysis. The USA 1861 3¢ stamp is a good subject because of the range of its shades and their range in value. My analysis should help both to build the case for spectrographic measurement; and to formalize the identification of the 1861 3¢ shades.

## Shades of the US 1861 3¢ postage stamp

The *Scott Specialized Catalogue of United States Stamps and Covers* recognizes four classic shades of the 1861 3¢ stamp: pink, pigeon blood pink, rose-pink, and rose. Within 'rose,' it lists a further seven: bright rose, dull rose, rose red, brown red, pale brown red, dull brown red, and deep pinkish rose, making 11 different colors. The shades differ significantly in market value. A good used 'bright rose' shouldn't cost more than $150. A good used 'pink' could cost as much as $5,000. The two shades can quite easily be mistaken for each other. Being right about color is therefore important.

Like many stamps, the catalogued shades of the 1861 3¢ are a small subset of the range that can be distinguished by the naked eye. In a study of some 6,000 3¢ stamps on envelopes, Michael McClung claims to have seen over a hundred shades (McClung 1993). He settled on 54, ranging from the pinks of 1861 to the red and brown colors of the mid-1860s. For the *Scott Specialized Color Guides for United States Stamps* (2005), he reduced the number of shades to 48, and gave them approximate dates by looking at when they were cancelled. He then suggested 12 main groups of shades. Nine of the 12 are identical to nine of the 11 listed in the *Scott Specialized Catalogue*. Both schemes can be traced to the work of Perry and Ashbrook (see Herzog 1981).

McClung used the incidence of each shade in his vast inventory to attach to them a 9-point rarity scale. Classic rose = 1 (very common). Pigeon blood pink = 9 (very rare). Original pink (an expensive stamp in good condition) = 7. McClung rated three additional shades at '7': bright brown red, crimson rose, and brown. He listed three at '8': claret, carmine lake, and brick red. Despite their rarity, none of the later shades are catalogued.

### *Notes about the Philatelic Analysis of Color*

In an important article published in the London Philatelist in 2011, Herendeen, Allen, and Lera set out a method

for color discrimination using reflectance technology. For validation purposes, they tested 68 examples of a red stamp from Slovenia. Experts recognize nine shades of the stamp, but the test was limited to four. An expert sorted the stamps into the four shades. The stamps' 1976 CIE Lab (Lab) characteristics were then independently established using the Foster + Freeman Video Spectral comparator 6000 (VSC).

The main purpose of the experiment conducted by the three authors was to see whether the VSC measurement had any value for philatelic color measurement. The test was successful but raised two important questions. First, there were stamps that had been expert-sorted into a shade that fell almost precisely between two shades when measured by the VSC – what should one do about those? And second, would a purely machine-led mathematical process lead to the same clusters as the expert classification. Let's look at why these are important questions.

The existence of VSC borderline stamps is not surprising. It confirms there can be stamps about which experts might legitimately disagree. However, a thought experiment makes it clear this is potentially a serious problem. Imagine two experts, each of whom has an expertized reference collection. And, suppose their sets of reference stamps are as depicted in Figure 1 i.e. slightly different from each other.

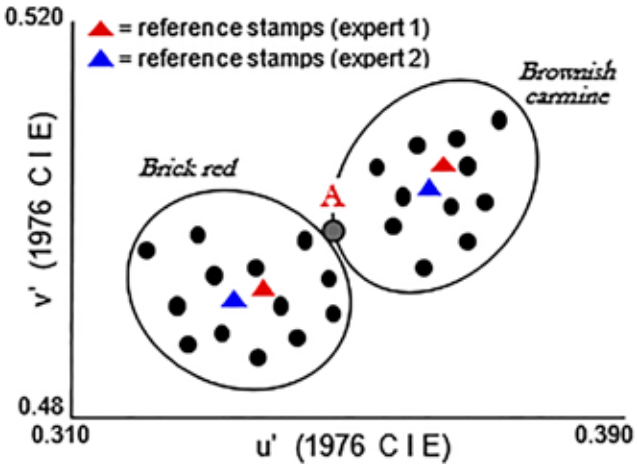


***Figure 1.*** The Reference Copy problem. Stamp 1 lies at the VSC border between two shades. It is closer to Expert 1's 'brick red' reference stamps, but closer to Expert 2's 'brownish carmine' reference stamps.

Imagine each expert is asked to assign a borderline stamp ('A' in Figure 1) to a shade. Because of their reference stamps, Expert 1 is more likely to assign 'A' to 'brick red'; but Expert 2 is more likely to assign it to 'brownish carmine'. This difference would arise, not because they see the stamps differently, but because of marginal differences between their reference copies. I refer to this as 'the Reference Copy' problem. It is serious if the two shades differ significantly in value. Some experts mitigate this by being cautious when expressing an opinion about borderline stamps.

The second problem runs deeper. Herendeen et al introduced a number of key terms in their paper including 'convex hull' (CH), and 'MacAdam ellipse' (MA). A CH is a polygon drawn around the CIE color coordinates produced by a group of stamps' VSC measures. The coordinates will have a center that can be mathematically determined. If you create a region whose periphery is ΔE76 <= 2.3 from the center (that is, the Euclidean distance at which a difference in color becomes 'just noticeable'), then you have an MA. The MA is a region around the center within which the average human sees only one color when compared with the center. CHs appear bigger than MA's because the average human eye typically sees many more shades than are recognized in catalogues.

Their validation showed that the CHs of the stamps in each expert-sorted shade, formed relatively distinct clusters of VSC coordinates (Herendeen et al 2011, 114). But the CHs were created a priori by a human expert. What would have happened if mathematical algorithms had been used to determine the stamps' cluster centers? Would they have agreed with the experts'?

In current expert practice, reference copies and a practiced eye are used to determine stamp shades. In effect, this involves non-mathematical clustering that uses reference copies as if they are cluster centers. But clustering algorithms applied to VSC measures might create mathematically determined cluster centers that do not match experts' traditional reference copies. What then? I call this 'the Cluster Algorithm' problem. It is a known problem applied to both human and machine expertizing. It is a problem to which I'll return later in the paper.

The Institute of Analytical Philately has held three symposia since 2011. The analysis of inks and colors was a substantial part of each agenda. Analytic methods included X-ray diffraction (XRD); X-ray fluorescence (XRF); attenuated total reflectance (ART); Fourier transform infrared (FTIR); spectrographic reflectance; and 300/600 dpi scans combined with color analysis using Adobe Photoshop (for an overview of most of these methods, see Lera, Giaccai, and Little 2012). The studies have shown the value of such methods. Examples include:

- Distinguishing different printings of a stamp (Brittain 2013)
- Linking ink constituents to shades (Barwis and Brittain 2016; Charles 2017)
- Assisting with expertizing (Lyons 2017)

These methods have not led to simple forensic solutions to the challenge of shade classification. Cibulskis's work helps to explain why (Cibulskis 2016, 2017). Using relatively inexpensive equipment (Canon LiDE 120 color scanner), he scanned and analyzed 2,499 examples of the German 'Crown and Eagle' 3pf stamp. He then used a clustering algorithm and the ΔE76 = 2.3 (the 'just noticeable difference'), to establish how many visibly different shades there were. There were 63 – far more than are ever likely to be recognized in any catalogue. By increasing ΔE76 to 4.5 and using an anti-clique clustering method, he reduced the number to 18, still more than double the 8 shades recog-

nized in a catalogue. He suggests a ΔE76 <= 5.8 would deliver the number of shades one typically finds in catalogues (Cibulskis 2016, 39). But it's important to recognize that at such a distance, the average human eye would easily see differences between stamps assigned to the same shade.

From this discussion we see that advanced technology has highlighted three core questions in shade classification:

a. By what *formal criteria* does one reduce the number of shades the human eye can see (or that reflectance technology produces), to a manageable number?
b. How does one reconcile the fact small differences in expert reference copies can lead to big differences in the shades to which stamps get assigned (the Reference Copy problem)? It is why experts, for a long time, have understood the importance of having an extensive reference library.
c. What should one do if the cluster centers produced by reflectance technology do not coincide with the coordinates of experts' traditional reference stamps (the Cluster Algorithm problem)? Physiological differences between the ways in which humans see colors, exacerbate this problem.

### *The forensic analysis of the USA 1861 3¢ stamp*

The 1861 3¢ is an engraved stamp (see Figure 2). Its printed area measures about 20mm x 25mm. Its inked surface is characterized by lines and small patches of color. None of the patches measures much more than 0.5mm across. The National Bank Note company printed more than 2 billion of the stamps between 1861 and 1867.

Nobody has spent more time writing about the shades of this stamp than Michael McClung. He did not believe reflectance technology could help. To quote:

> I found that the toning of paper has such a significant effect on light wave sensors that they were of no help... Maybe someday we will have an electronic device that can focus on a tiny speck of ink... but we are not there yet (McClung 2012, 229).


***Figure 2.*** The 1861 3¢ stamp. The biggest blocks of color are around the '3's and the 'U' and 'S.'

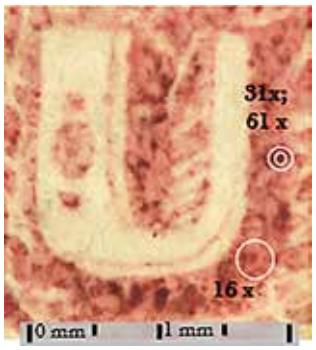


***Figure 3.*** Magnification at 61x. The image illustrates patches selected for 16, 31, and 61x.

Perhaps McClung did not know how accurate VSC instruments are. The VSC 6000 is capable of zeroing in on an area no bigger than 61 microns in diameter. As we will see, it quite easily isolates patches of ink that are small and dense enough to be free of paper toning.

As far as I'm aware, the only forensic analysis of 1861 3¢ shades, is an article written by Edward Liston for the *Collectors' Club Philatelist* (July-August 2016). Using what he called 'difference spectra,' he showed the VSC 6000 could be used to distinguish between pink, pigeon blood pink, and rose pink. It is a slim paper based on just a few stamps. Although it is light on methodological precision (there is no information on how Liston sampled specks of ink for measurement) his results are encouraging.

## VSC measurement: methodological challenges

### *Basics of the approach*

For this study I used the Foster + Freeman VSC 6000 at the Smithsonian Postal Museum. I measured the spectrographic characteristics of 33 stamps and kept the VSC settings constant at the following values: light source = flood; background = 0%; long-pass filter = VIS; color sharpness = 8; digital magnification = 1; brightness = 60; auto-exposure integration = 400 mS. I varied the analogue magnification by 8, 16, 31, 61, and used a white marble chip to reset the machine when the software indicated it was required.

I made 151 observations in total, an average of 4.6 per stamp, but varied the number of observations from stamp to stamp for experimental purposes. Twenty-four of the stamps were sampled three or more times.

I used the CIE 76 Lab coordinates to record the color of each sample, then the ΔE76 to measure the distances between samples = 11,325 distances. A complete record of the Lab coordinates and ΔE76 distances can be found in Appendix A (the table is too big to be printed—see the Institute website to download a copy at HTTP://WWW.ANALYTICALPHILATELY.ORG/DOCUMENTS/HOFMEYR_APPENDIX_1.XLSX.

Figure 3 shows the resolution one can achieve with VSC magnification. At 61x, it is easy to isolate specks to satisfy McClung. But the figure also shows at 16x magnification (for instance), a stamp's ink density can vary quite significantly within what appears to the naked eye, to be small patches of solid ink.

For this research, I began measurement at 16x magnification, focused on relatively dense patches of ink around '3,' 'U,' and 'S,' and selected areas that appeared, under magnification, to be free of cancelling ink. But 16x can encompass a patch that is internally quite variable. It quickly became apparent using a 'clean and inked' verbal protocol at 16x magnification could result in Lab coordinates that exceeded a ΔE76 of 5.8. I therefore concluded it was important to test systematic variations in sampling.

**Table I**

**Mean Δ76 distances between samples within the 15 stamps**

| No. of samples | 6 | 7 | 9 |
|---|---|---|---|
| ΔE76 observations | 15 | 21 | 36 |
| Stamp number 1 | 8.3 | 11.6 | 7.6 |
| 2 | 6.6 | 6.6 | 15.1 |
| 3 | 8.1 | 8.0 | 17.0 |
| 4 | 13.4 | 11.0 | |
| 5 | 9.6 | 9.9 | |
| 6 | 9.4 | | |
| 7 | 9.3 | | |
| Mean ΔE76 | 9.2 | 9.4 | 13.2 |

*Understanding Table I. The first column shows the results for the 7 stamps sampled 6 times. The second, for 5 stamps sampled 7 times; the third, for 3 stamps sampled 9 times. Sampling a stamp six times created 15 pair-wise ΔE76 distances between its samples; seven times, 21; nine times 36. The table's cells show the mean ΔE76 distance within each stamp. For example, the distance between the samples of the first stamp sampled six times = 8.3, and so on. If this is still confusing, I am open to your suggestions.*

### *Shade variation within a stamp as a function of the patch selected for sampling*

Consider a stamp that has been sampled five times, and assume all samples conform to the verbal protocol 'clean and inked.' The result would be five Lab coordinates and (5 x 4)/2 = 10 ΔE76 distances between them. A stamp sampled six times, would produce (6 x 5)/2 = 15 distances; and so on. These distances would tell how much shade variation was within a stamp as a function of the sampled patches.

Table I shows the within-stamp sample distances for 15 stamps sampled six or more times. As can be seen, the mean ΔE76 distances between within-stamp samples was 10.1 – more than four times a 'just noticeable difference' of 2.3.

It is important to remember these were not carelessly selected samples. All conformed to the verbal standard 'clean and inked at >= 16x magnification'. Given these distances, how can we be sure a different researcher, working to the same verbal protocol and level of magnification, would replicate the results. Clearly, when it comes to sample selection for spectrographic measurement, we need to develop something more than a strict verbal protocol.

### *Shade variation as a function of magnification*

The most effective way to ensure a sample consists of clean, dense ink, is to zero in on a speck dense and small enough. This requires magnification which, in turn, raises a question about whether varying degrees of magnification might lead to differing Lab outcomes. Therefore, four stamps of very different shades were selected to test the effects of varying magnification, while keeping the sampled patch constant (see Figure 4). The patches were selected to be of a similar ink density, whether 8x or 61x magnified. Table II shows the resulting Lab coordinates and the ΔE76 distances between them.

***Figure 4a.*** The four stamps selected for sampling. The White 'X' marks the area sampled.

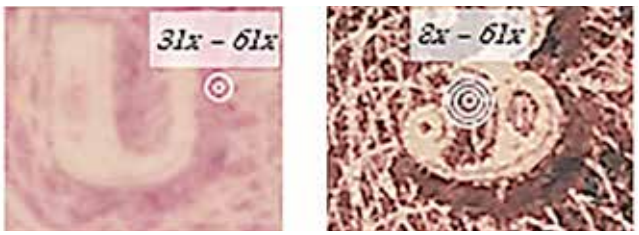


***Figure 4b.*** The sampling process. The pink samples came from a dense patch in the 'U'. Two samples were taken at 31x and 61x respectively. The carmine lake samples came from a dense patch in the left '3' and formed a set of diminishing circles from 8x to 61x magnification.

As the table shows:

1. Magnification at 8x is highly problematic. None of the 8x within-stamp samples meets the <= 5.8 criterion suggested by Cibulskis. In fact, the 8x sample for the carmine-lake stamp, is closer to the samples for the brown red stamp, than any of the other carmine-lake samples!
2. All the within-stamp samples >= 16x produce coordinates that satisfy the ΔE76 <= 5.8 criterion. Though higher levels of magnification sometimes lead to measures visibly different (i.e. ΔE76 > 2.3), they do so within a narrow range.

From this analysis we can conclude magnification > 16x within a sample patch, once the patch has been selected, does not lead to visibly different shades. It is important to bear in mind these results pertain to the 1861 3¢. They suggest the unreliability of magnification <= 8x, but the reliability of magnification >=16x.

### *The effect of variations in ink density*

The most effective way to achieve a clean inked sample by VSC is to zero in on a small speck of ink. What the human eye sees in a stamp, howeveer, is a blend of all visible hues. This includes toned paper and less dense patches of ink. This means the two processes are fundamentally different.

**Table II**

**A test of the effect of magnification on Lab coordinates for the 1861 3c**

| | CIE Lab | | | ΔE76 distances between samples | | | | | | | | | |
|---|---|---|---|---|---|---|---|---|---|---|---|---|---|
| | L | a | b | P 31 | P 61 | B16 | B31 | C8 | C16 | C31 | C61 | L8 | L16 | L31 |
| Pink: 31 | 64.2 | 27.3 | 5.2 | | | | | | | | | | | |
| Pink: 61 | 62.8 | 29.5 | 7.8 | 3.7 | | | | | | | | | | |
| B Red:16 | 54.6 | 26.5 | 8.7 | 10.2 | 8.8 | | | | | | | | | |
| B Red: 31 | 51.2 | 29.7 | 6.5 | 13.3 | 11.7 | 5.2 | | | | | | | | |
| C Lake: 8 | 52.9 | 25.2 | 8.3 | 11.9 | 10.8 | 2.2 | 5.1 | | | | | | | |
| C Lake: 16 | 47.0 | 26.2 | 5.2 | 16.3 | 16.3 | 8.4 | 5.6 | 6.7 | | | | | | |
| C Lake: 31 | 46.0 | 27.4 | 2.4 | 18.4 | 17.8 | 10.7 | 7.0 | 9.3 | 3.2 | | | | | |
| C Lake: 61 | 45.9 | 27.0 | 2.9 | 18.4 | 17.8 | 10.5 | 7.0 | 9.0 | 2.7 | 0.6 | | | | |
| L Brown: 8 | 53.4 | 13.4 | 6.7 | 17.7 | 18.7 | 13.3 | 16.4 | 11.9 | 14.4 | 16.4 | 16.0 | | | |
| L Brown: 16 | 43.2 | 13.9 | 5.1 | 24.9 | 25.2 | 17.4 | 17.8 | 15.2 | 12.9 | 14.0 | 13.6 | 10.3 | | |
| L Brown: 31 | 46.7 | 14.6 | 0.7 | 22.1 | 23.1 | 16.4 | 16.8 | 14.4 | 12.4 | 12.9 | 12.6 | 9.1 | 5.7 | |
| L Brown: 61 | 43.7 | 12.9 | 3.1 | 25.1 | 23.5 | 18.3 | 18.7 | 16.2 | 14.7 | 14.7 | 14.3 | 10.4 | 2.3 | 4.2 |

*The level of magnification is after the shade name on the left, for example, the first stamp is Pink and the level of magnification, 31x. The resulting Lab coordinates are in columns 2-4. The rest of the table is the matrix of ΔE76 distances between the stamps. Big distances have been greyed out to make them easier to distinguish from stamps close in shade. Distances that meet a ΔE76 <= 5.8 standard are in red. Within stamp shade distances that don't satisfy the criterion are in mauve.*

Experts try to deal with these effects by relatively simple means such as selecting what looks like a representative patch, masking it to exclude surrounding influences, then comparing it with reference shades. Within the selected patch, they apply what can best be described as subjective cognitive adjustments in an attempt to strip out residual non-ink influences like toned paper.

Their resulting classifications are a blended view based on what they feel is just the ink. Unlike machines, they are unable to zero in on small, consistent, densely-inked patches at very high magnification.

The main advantage of the expert process is it will tend to render judgments closer to what ordinary people see. The problem, however, is subjective. People differ both in their ability to discriminate, and in the way they might try to correct for non-ink influences. Machines, by contrast, simply measure. A machine approach which eliminates non-ink factors by magnification, however, gives up the attempt to replicate the kind of 'blended' view that results from experts' bigger patches.

This leads to the question: how, if at all, would the Lab coordinates, based on a magnified sample, differ from Lab coordinates that explicitly measure the kind of blended patch an expert might select?

To test for this, I chose a subset of 12 stamps and designed a set of sample pairs called 'typical' and 'dense.' Typical' samples looked like the stamp as a whole and were an attempt to replicate a sample an expert might select. 'Dense' samples used VSC magnification to zero in on a speck small and dense enough to exclude non-ink influences (Figure 5 illustrates the difference between the two types of samples).

The results in Table III show:

1. The mean ΔE76 distance between each 'typical' and 'dense' sample pair = 13.4 i.e. five times a 'just noticeable difference'. Only one sample-pair met a ΔE76 <= 5.8 criterion.
2. There was a highly consistent pattern to the direction in which the coordinates shifted: 'L' decreased, 'a' increased, 'b' decreased.


***Figure 5.*** The White 'X' marks the areas from which the samples were taken. 'T' (typical) and 'D' (dense) show the areas ('O') under magnification.

**Table III**

**An analysis of "Typical" and "Dense" ink patches in 16 stamps**

| Expert | Author | Type | L | a | b | ΔE76 |
|---|---|---|---|---|---|---|
| Pink | Pink | T | 73.5 | 19.7 | 8.3 | |
| | | D | 64.4 | 27.9 | 7.2 | 12.3 |
| P Blood Pink | P Blood Pink | T | 63.7 | 23.1 | 13.8 | |
| | | D | 52.8 | 24.6 | 9.9 | 11.7 |
| Bright Rose | Bright Rose | T | 73.5 | 20.2 | 15.1 | |
| | | D | 58.6 | 32.5 | 9.2 | 20.2 |
| Bright Rose | Bright Rose | T | 69.2 | 19.4 | 17.3 | |
| | | D | 59.9 | 28.9 | 5.4 | 17.8 |
| Rose/BR Red | BR Red | T | 62.9 | 22.6 | 18.2 | |
| | | D | 50.3 | 28.6 | 14.6 | 14.4 |
| Rose | Rose | T | 71.8 | 22.0 | 14.8 | |
| | | D | 59.3 | 29.3 | 8.1 | 16.0 |
| Rose | Rose | T | 66.1 | 21.9 | 18.6 | |
| | | D | 60.1 | 23.7 | 16.8 | 6.5 |
| Rose | Rose | T | 66.0 | 22.8 | 12.7 | |
| | | D | 57.8 | 27.6 | 8.4 | 10.4 |
| N A | Brown Red | T | 63.6 | 25.0 | 12.8 | |
| | | D | 54.6 | 26.5 | 8.7 | 10.0 |
| N A | Brown Red | T | 58.0 | 22.5 | 22.8 | |
| | | D | 52.3 | 21.9 | 18.5 | 7.2 |
| Brown Red | Brown Red | T | 67.0 | 21.8 | 12.5 | |
| | | D | 50.7 | 32.9 | 5.6 | 20.9 |
| Pale B Red | Dull Red (N) | T | 72.6 | 12.4 | 23.4 | |
| | | D | 57.3 | 25.5 | 14.8 | 21.9 |
| Pale B Red | Pale B Red | T | 66.3 | 18.2 | 27.2 | |
| | | D | 58.3 | 23.1 | 20.0 | 11.8 |
| Deep B Red | Deep B Red | T | 53.7 | 22.3 | 13.7 | |
| | | D | 43.1 | 20.2 | 4.9 | 13.9 |
| Deep B Red | Brick Red | T | 53.8 | 24.5 | 29.9 | |
| | | D | 51.4 | 25.0 | 28.6 | 2.8 |
| Deep B Red | C'mine Lake | T | 60.2 | 22.7 | 12.6 | |
| | | D | 46.6 | 27.5 | 4.8 | 16.4 |
| | | Means | 10.3 | -5.3 | 5.5 | 13.4 |

Stamp shades are on the left. The sample type ('Typical' or 'Dense') is indicated by the rows 'T' and 'D,' followed by the Lab coordinates (L a b) columns. The last column is the ΔE76 distance between 'Typical and Dense'.

In summary, the 'typical' (i.e. expert) samples result in shades different in hue from 'dense' samples, but the shift has an encouraging consistency. 'Dense' samples are darker ('L' decreases), redder ('a' increases), and less yellow ('b' decreases). This was true for 22 of the 24 'a/b' coordinates for a range of shades from pink to deep brown red.

The test also revealed some important differences between the shades. The 12 stamps included two 'bright rose' and two 'pale brown red'. Although the 'typical-dense' sample pairs for the two shades produced ΔE76 distances > 5.8; the 'typical-to-typical' and 'dense-to-dense' distances, satisfied an ΔE76 <= 5.8 criterion. This means the stamps classified as 'bright rose' or 'pale brown red,' were close to each other in shade, whether based on 'typical' or 'dense' samples. When it comes to these two shades, expert and machine processes would have produced identical classifications.

By contrast, the 'rose' and 'deep brown red' stamps were far apart (6.9 and 15.9 respectively). This points to important historical weaknesses in the approach to 1861 3¢ shade classification.

The problem with 'rose' is it is a catch-all for anything that isn't one of the three early, valuable shades (i.e. pink, rose pink, pigeon blood pink). As such, it covers a great many shades that are visibly different. Although the addition of seven shades within 'rose' (bright rose, brown red, pale brown red, etc.) has led to less variation, it still leaves 'rose' as a shade with too much internal variation to be useful. It is not surprising the VSC measurement of 'rose' produces Lab coordinates that are far apart by ΔE76.

The problem with 'deep brown red' is very different. In spite of the fact the later, dark brown red shades are very distinctive, they aren't even catalogued. Early philatelists seem to have been mesmerized by the early pinks. As a result, 'deep brown red' has become a catch-all for a great number of shades that haven't been properly studied.

Now to the actual shades themselves.

## VSC characteristics of 1861 3¢ shades

### *Approach*

Appendix A (see Institute website) reports 151 Lab coordinates for 33 stamps which includes a matrix of the 11,325 ΔE76 distances between them. Table IV (next page spread) is the resulting Lab and ΔE76 summary report. It

shows (with ΔE76 <= 5.8 highlighted in bold red):

- The conventional color name for each stamp (from the earlier to the later colors)
- The number ID that I gave each stamp (n)
- The number of samples measured for each stamp ($y_1$)
- The number of samples used to calculate the Lab mean for each stamp ($y_2$)
- The Lab mean for each stamp; and (at the bottom), the mean of Lab means
- A matrix of the ΔE76 distances between the mean Lab of each stamp
- And in the bottom row: the mean ΔE76 of each stamp from all the others

Colors were assigned on the basis of expert certificates. Where two experts disagreed, I selected the one with which I agreed. Unexpertized stamps were assigned to colors by me, based on the *Scott Specialized Color Guide*.

The selection of sub-samples for the calculation of means, was based on the following criteria (see Appendix A to verify):

- Except for those which began with fewer than 3 observations, a minimum of 3 observations for each stamp was retained.
- Where there were enough observations, I omitted outliers and all 8x magnification measures. These are highlighted in gray.

I defined a stamp's sample as an 'outlier' if its ΔE76 > 11.6 from its ΔE76 mean. This is twice the ΔE76 <= 5.8 criterion for a shade.

In the analysis that follows, I report on both the machine results and whether or not they make visual sense to my expert eye. It is important to remember two stamps will appear identical to the average human eye as long as ΔE76 <= 2.3, but the criterion used to highlight potential groups was more than twice that (i.e. ΔE76 5.8).

The following discussion is detailed, difficult to follow, and based on the data presented in Table IV. The table itself is at the end of the paper because of its size.

### *The Lab coordinates of shades*

**Pink**

Stamps 1, 2, and 14 of the 33 stamps are expertized 'pink.' Visually, stamp 1 is what McClung would have called a 'carmine pink'. Stamps 2 and 14 are more lavender. All three are both visually and ΔE76 different from their historical close cousins, the rose and pigeon blood pinks (stamps 3, 17, 12, and 13). Based on the ΔE76 <= 5.8 criterion, three additional stamps had to be included in the discussion: 16 (expertized 'bright rose'), 20 (expertized 'rose'), and 23 (unexpertized but assigned to 'brown red' by me).

The easiest stamps to discuss are 2 and 14, as they belong together both visually and by ΔE76. They have a lavender tint that makes them look similar to the 'pigeon bloods,' and, by ΔE76, they are actually closer to the pigeon bloods than to the carmine pink.

The carmine pink (stamp 1) is unique. It's mean distance from all stamps = 16.6. This is much higher than all the other stamps in the pinkish range. The only stamp that comes close by ΔE76, is stamp 20 ('rose'). Visually however, the latter stamp is yellower and darker – it is a classic example of the early rose shades that came close to pink. Stamp 1, by contrast, is a true pink. Its definitive Lab characteristic is that it is the closest of all 33 stamps, to 'b' = neutral.

Stamp 16 (expertized as 'bright rose'), is a wonderful example of how quantitative measurement can improve the classification of stamps into shades. It is closer to the lavender pink stamps both visually and by ΔE76; and by ΔE76, it is far from the two other stamps expertized as 'bright rose'. I believe the experts made a mistake with this stamp and it should be reclassified as 'lavender pink'.

Stamp 23 is an anomaly, as it hasn't been expertized. Visually it looks close to brown red, but by ΔE76 it is also close to a number of stamps in the pigeon blood pink to deep rose range. Because it is closer to the latter stamps than to pink, I suggest it be set aside in the discussion of the pinks.

Summary: the results argue for two well-defined sets of pink Lab coordinates. Stamp 1 = carmine pink = 60.8, 30.0, 1.9. Stamps 2, 14, and 16 = Lavender pink = 64.8, 25.8, 7.2.

**Pigeon blood pink and Rose pink**

Three of these stamps were only measured once, the fourth three times, including once when I first began assessing the experiment. These results should therefore not be used for quantitative classification because there isn't enough data to provide confidence.

**Bright Rose**

Three stamps (5, 15, 16) have been expertized as 'bright rose'. Based on both a visual inspection and the ΔE76 distances, I've argued stamp 16 is lavender pink. This leaves stamps 5 and 15, which are visually indistinguishable, as this is confirmed by their ΔE76 = 2.0. As can be seen from Table 4, they are far from all other stamps, therefore a distinctive shade whose Lab coordinates can be used to define 'bright rose'.

Summary: Stamps 5 and 15 = Bright Rose = 65.3, 25.0, 14.6.

**Pale Brown Red**

Based on their mean ΔE76 distances from all other stamps (24.1 and 26.8 respectively), the two most unique stamps in this study are stamps 9 and 10 (expertized as 'pale brown red'). What sets them apart are their high 'L' and low 'a' values. The ΔE76 between them = 6.6 which fails to satisfy the <= 5.8 criterion, but their closeness to each other and distance from all other stamps puts them in a distinctive color space. My suggestion is their Lab coordinates be considered for 'pale brown red'.

Stamp 11 is anomalous. It has been expertized as both 'brown red' and 'pale brown red,' but visually and by ΔE76 it is neither. It looks too red to be 'pale brown red,' and too pale to be a true 'brown red'. I believe it may be a good example of 'dull red,' but the results are too anomalous to assign it to any shade with confidence.

**Table IV**

## Stamps' Lab coordinates and a matrix of the distances between them

ΔE76 distances between the stamps

| | ID | CIE Coordinate | | | | | Pink | | | PB Pink | | R Pink | | Bright Rose | | | Rose | | | |
|---|---|---|---|---|---|---|---|---|---|---|---|---|---|---|---|---|---|---|---|---|
| Shade | n | $Y_1$ | $Y_2$ | L | a | b | 1 | 2 | 14 | 12 | 13 | 3 | 17 | 5 | 15 | 16 | 4 | 18 | 19 | 20 |
| Pink | 1 | 7 | 5 | 60,8 | 30,0 | 1,9 | | | | | | | | | | | | | | |
| | 2 | 7 | 7 | 63,9 | 26,2 | 8,0 | 7,8 | | | | | | | | | | | | | |
| | 14 | 6 | 5 | 66,6 | 25,8 | 7,5 | 9,1 | 2,8 | | | | | | | | | | | | |
| Pigeon Blood | 12 | 3 | 3 | 58,3 | 23,9 | 11,9 | 11,9 | 7,2 | 9,7 | | | | | | | | | | | |
| | 13 | 1 | 1 | 60,9 | 29,9 | 12,7 | 10,8 | 6,7 | 8,8 | 6,7 | | | | | | | | | | |
| Rose Pink | 3 | 1 | 1 | 59,7 | 32,1 | 14,6 | 12,9 | 9,8 | 11,8 | 8,8 | 3,1 | | | | | | | | | |
| | 17 | 1 | 1 | 60,1 | 22,4 | 24,6 | 23,9 | 17,4 | 18,7 | 13,0 | 14,1 | 13,9 | | | | | | | | |
| Bright Rose | 5 | 3 | 3 | 66,2 | 25,2 | 14,2 | 14,2 | 6,7 | 6,8 | 8,4 | 7,2 | 9,5 | 12,4 | | | | | | | |
| | 15 | 3 | 3 | 64,4 | 24,9 | 15,0 | 14,5 | 7,1 | 7,9 | 7,0 | 6,5 | 8,6 | 10,8 | 2,0 | | | | | | |
| | 16 | 5 | 4 | 64,0 | 26,1 | 6,0 | 6,4 | 2,1 | 3,0 | 8,6 | 8,3 | 11,4 | 19,4 | 8,6 | 9,2 | | | | | |
| Rose | 4 | 4 | 4 | 66,8 | 19,5 | 16,5 | 18,9 | 11,2 | 11,0 | 10,7 | 12,6 | 14,6 | 10,9 | 6,2 | 6,1 | 12,8 | | | | |
| | 18 | 3 | 3 | 62,6 | 25,1 | 21,2 | 20,0 | 13,3 | 14,4 | 10,4 | 10,0 | 10,1 | 5,0 | 7,9 | 6,5 | 15,4 | 8,5 | | | |
| | 19 | 2 | 2 | 61,9 | 20,1 | 31,3 | 31,0 | 24,2 | 25,0 | 20,2 | 21,1 | 20,7 | 7,3 | 18,4 | 17,2 | 26,1 | 15,6 | 11,3 | | |
| | 20 | 6 | 5 | 57,6 | 29,4 | 5,8 | 5,1 | 7,5 | 9,9 | 8,3 | 7,7 | 9,5 | 20,3 | 12,8 | 12,4 | 7,3 | 17,3 | 16,8 | 27,5 | |
| Bright Rose Red | 6 | 7 | 5 | 54,9 | 26,7 | 14,9 | 14,6 | 11,3 | 13,9 | 5,3 | 7,1 | 7,2 | 11,8 | 11,4 | 9,7 | 12,8 | 14,0 | 10,1 | 19,0 | 9,9 |
| | 7 | 6 | 4 | 54,6 | 31,4 | 8,8 | 9,4 | 10,7 | 13,4 | 9,0 | 7,6 | 7,8 | 19,1 | 14,2 | 13,4 | 11,2 | 18,8 | 16,1 | 26,3 | 4,7 |
| Deep Rose | 8 | 9 | 7 | 59,3 | 28,0 | 12,8 | 11,2 | 6,9 | 9,3 | 4,3 | 2,5 | 4,5 | 13,1 | 7,6 | 6,4 | 8,5 | 11,9 | 9,5 | 20,3 | 7,3 |
| Pale Brown Red | 9 | 4 | 4 | 76,7 | 14,0 | 16,9 | 27,1 | 19,8 | 18,2 | 21,5 | 22,8 | 25,0 | 20,1 | 15,6 | 16,6 | 20,7 | 11,3 | 18,4 | 21,5 | 27,0 |
| | 10 | 9 | 6 | 75,3 | 10,8 | 22,5 | 31,6 | 24,0 | 22,9 | 23,9 | 25,8 | 27,5 | 19,2 | 18,9 | 19,3 | 25,2 | 13,5 | 19,1 | 18,5 | 30,7 |
| | 11 | 6 | 5 | 57,5 | 23,8 | 16,4 | 16,1 | 10,8 | 12,9 | 4,6 | 7,9 | 8,8 | 8,7 | 9,0 | 7,1 | 12,5 | 10,2 | 7,1 | 16,0 | 12,0 |
| Brown Red | 21 | 1 | 1 | 56,0 | 22,3 | 21,8 | 21,8 | 16,4 | 18,2 | 10,3 | 12,8 | 12,7 | 5,0 | 13,0 | 11,1 | 18,2 | 12,4 | 7,2 | 11,4 | 17,6 |
| | 22 | 2 | 2 | 56,5 | 28,3 | 10,8 | 10,0 | 8,2 | 11,0 | 4,9 | 5,1 | 6,3 | 15,5 | 10,8 | 9,6 | 9,2 | 14,8 | 12,6 | 22,8 | 5,2 |
| | 23 | 2 | 2 | 59,1 | 25,8 | 10,8 | 9,9 | 5,6 | 8,2 | 2,4 | 4,9 | 7,5 | 14,3 | 7,9 | 6,9 | 6,9 | 11,5 | 11,1 | 21,5 | 6,4 |
| | 24 | 2 | 2 | 55,2 | 22,2 | 20,7 | 21,1 | 15,9 | 17,9 | 9,5 | 12,5 | 12,5 | 6,3 | 13,1 | 11,2 | 17,6 | 12,7 | 8,0 | 12,8 | 16,7 |
| | 25 | 2 | 2 | 51,4 | 27,2 | 25,5 | 25,5 | 21,5 | 23,7 | 15,6 | 16,2 | 14,6 | 10,0 | 18,7 | 16,9 | 23,3 | 19,4 | 12,2 | 13,9 | 20,8 |
| | 26 | 4 | 4 | 58,8 | 25,6 | 16,2 | 15,1 | 9,7 | 11,7 | 4,7 | 6,0 | 6,8 | 9,0 | 7,7 | 5,8 | 11,5 | 10,0 | 6,3 | 16,3 | 11,2 |
| Deep Brown | 27 | 9 | 5 | 47,2 | 28,6 | 14,5 | 18,6 | 18,1 | 20,9 | 12,3 | 13,9 | 13,0 | 17,5 | 19,3 | 17,7 | 19,1 | 21,8 | 17,2 | 23,9 | 13,6 |
| Red | 29 | 6 | 4 | 50,5 | 25,0 | 7,2 | 12,6 | 13,5 | 16,2 | 9,2 | 12,8 | 13,8 | 20,1 | 17,2 | 16,0 | 13,7 | 19,6 | 18,6 | 27,2 | 8,5 |
| | 32 | 4 | 4 | 48,0 | 21,4 | 18,1 | 22,4 | 19,5 | 22,0 | 12,3 | 16,4 | 16,3 | 13,8 | 19,1 | 17,1 | 20,7 | 19,0 | 15,4 | 19,2 | 17,6 |
| | 28 | 7 | 4 | 46,4 | 27,0 | 3,8 | 14,9 | 18,1 | 20,6 | 14,7 | 17,3 | 17,9 | 25,3 | 22,4 | 21,4 | 17,8 | 25,2 | 23,9 | 32,3 | 11,6 |
| Carmine Lake | 33 | 6 | 4 | 47,3 | 30,1 | 5,5 | 14,0 | 17,2 | 19,9 | 14,1 | 15,4 | 15,5 | 24,3 | 21,4 | 20,3 | 17,2 | 24,8 | 22,5 | 31,3 | 10,3 |
| Lake Brown | 30 | 6 | 4 | 45,4 | 13,9 | 4,8 | 22,5 | 22,5 | 24,5 | 17,7 | 23,6 | 25,1 | 26,1 | 25,5 | 24,3 | 22,3 | 25,0 | 26,3 | 31,8 | 19,7 |
| Brown | 31 | 7 | 4 | 41,6 | 14,0 | 6,9 | 25,5 | 25,4 | 27,7 | 19,9 | 25,6 | 26,7 | 26,9 | 28,0 | 26,6 | 25,5 | 27,5 | 27,7 | 32,3 | 22,2 |
| Meanx | | 151 | 120 | 58,0 | 24,4 | 13,6 | 16,6 | 13,1 | 14,7 | 10,8 | 11,9 | 12,9 | 15,4 | 13,2 | 12,3 | 14,1 | 15,0 | 13,7 | 21,4 | 13,6 |

Summary: Stamps 9 and 10 = Pale Brown Red = 76.0, 12.4, 19.7.

**Brown Red**

Going by the ΔE76 distances, the 'brown reds' fall into two distinct groups: one, stamps 21 and 24; the other, stamps 22 and 23. Although stamp 26 satisfies the ΔE76 <= 5.8 criterion and could be grouped with stamps 22 and 23, it is closer to other stamps that are more 'rose' or 'pale/dull,' and should not be considered in the definition of 'brown red'. Stamp 25 (the Ashbrook certified 'brown red'), fails the ΔE76 <= 5.8 criterion with respect to all stamps, but it is single digit away from stamps 21 and 24 (ΔE76 = 7.6 and 7.9 respectively), and double digits away from all others. I propose it should be grouped with stamps 21 and 24, and the three of them be considered for the quantitative definition of brown red. What sets these stamps apart is their mean 'L' = 54.2 is quite dark, but with a unique set of 'a' and 'b' coordinates far along the red and yellow spectrums (22.9 and 22.7 respectively).

| B Rose | | | P Br Red | | | Brown Red | | | | | | Deep Brown Red | | | | CL | LB | |
|---|---|---|---|---|---|---|---|---|---|---|---|---|---|---|---|---|---|---|
| 6 | 7 | 8 | 9 | 10 | 11 | 21 | 22 | 23 | 24 | 25 | 26 | 27 | 29 | 32 | 28 | 33 | 30 | |
| | | | | | | | | | | | | | | | | | | |
| | | | | | | | | | | | | | | | | | | |
| | | | | | | | | | | | | | | | | | | |
| | | | | | | | | | | | | | | | | | | |
| | | | | | | | | | | | | | | | | | | |
| 7,8 | | | | | | | | | | | | | | | | | | |
| 5,0 | 7,0 | | | | | | | | | | | | | | | | | |
| 25,3 | 29,3 | 22,7 | | | | | | | | | | | | | | | | |
| 26,9 | 32,3 | 25,4 | 6,6 | | | | | | | | | | | | | | | |
| 4,2 | 11,2 | 5,8 | 21,5 | 22,8 | | | | | | | | | | | | | | |
| 8,3 | 16,0 | 11,2 | 22,8 | 22,4 | 5,8 | | | | | | | | | | | | | |
| 4,7 | 4,2 | 3,5 | 25,5 | 28,2 | 7,3 | 12,6 | | | | | | | | | | | | |
| 6,0 | 7,5 | 3,0 | 22,1 | 25,0 | 6,2 | 12,0 | 3,6 | | | | | | | | | | | |
| 7,3 | 15,1 | 10,6 | 23,4 | 23,2 | 5,1 | 1,4 | 11,7 | 11,2 | | | | | | | | | | |
| 11,2 | 17,6 | 15,0 | 29,8 | 29,1 | 11,5 | 7,6 | 15,6 | 16,7 | 7,9 | | | | | | | | | |
| 4,3 | 10,4 | 4,2 | 21,3 | 23,0 | 2,2 | 7,0 | 6,6 | 5,5 | 6,7 | 12,0 | | | | | | | | |
| 8,0 | 9,8 | 12,2 | 33,0 | 34,2 | 11,6 | 13,1 | 10,0 | 12,8 | 11,9 | 11,9 | 12,2 | | | | | | | |
| 9,1 | 7,8 | 10,9 | 30,1 | 32,4 | 11,7 | 15,9 | 7,7 | 9,4 | 14,6 | 18,5 | 12,3 | 8,8 | | | | | | |
| 9,3 | 15,3 | 14,1 | 29,7 | 29,6 | 10,0 | 8,9 | 13,2 | 14,1 | 7,7 | 10,0 | 11,8 | 8,1 | 11,8 | | | | | |
| 14,0 | 10,5 | 15,8 | 35,5 | 38,0 | 17,1 | 20,9 | 12,3 | 14,5 | 19,6 | 22,3 | 17,6 | 10,8 | 5,7 | 15,4 | | | | |
| 12,6 | 8,1 | 14,2 | 35,4 | 38,0 | 16,2 | 20,1 | 10,7 | 13,6 | 18,8 | 20,7 | 16,4 | 9,2 | 6,2 | 15,4 | 3,6 | | | |
| 18,9 | 20,2 | 21,4 | 33,6 | 34,9 | 19,4 | 21,7 | 19,1 | 19,1 | 20,4 | 25,3 | 21,1 | 17,7 | 12,4 | 15,5 | 13,2 | 16,4 | | |
| 20,0 | 21,8 | 23,3 | 36,5 | 37,2 | 20,9 | 22,3 | 20,9 | 21,4 | 20,9 | 24,8 | 22,7 | 17,3 | 14,1 | 14,8 | 14,2 | 17,2 | 4,3 | |
| 14,3 | 16,3 | 10,9 | 24,1 | 26,8 | 11,4 | 14,1 | 11,7 | 11,2 | 13,7 | 18,1 | 11,3 | 16,1 | 14,8 | 15,3 | 18,9 | 18,1 | 22,3 | 23,9 |

Stamps 22 and 23 form a tight group (ΔE76 = 3.6) and are also close to stamp 8 (classified as 'deep rose'). Although they are within a ΔE76 <= 5.8 range of a number of the other stamps, the three are much closer to each other (mean ΔE76 = 3.4) than to any other stamps. They can therefore be considered a group with mean Lab = 58.3, 27.4, 11.5.

Summary: Stamps 21, 24, and 25 = Brown Red = 54.2, 22.9, 22.7. Stamps 22, 23, and 8 = Deep Rose = 58.3, 27.4, 11.5.

**Rose**

Stamps 4, 18, 19, and 20 were expertized as 'rose.' As Table 4 shows, however, by ΔE76 distances, each of these stamps is far from the other. Visually, they are also easily distinguished. Stamps 18 and 20 are quite pink, Stamps 4 and 19 are both visually and ΔE76 unique. These four stamps exemplify the problems of a 'catch-all' shade too wide to be useful. Absent more research, it is best to simply note their characteristics.

**The Deep Brown Reds and Browns**

These seven stamps are 27 to 33. Historically, this is a somewhat disgracefully neglected range of shades. It is a difficult space in the spectrum, both because of the way in which environmental factors can affect the ink, and because of the eye's acuity in the space. My experimental results lead to two distinctive groups: stamps 28 and 33 (ΔE76 = 3.6); and stamps 30 and 31 (ΔE76 <= 4.3). Visual examination confirms these groupings.

Stamp 28 has been expertized as 'deep dark brown'. Visually and by ΔE76 however, it is closer to stamp 33 (expertized as 'carmine lake'), than to any of the deep dark browns. Precisely because this is a very difficult shade and these are very distinctive stamps, this set makes a good candidate for the quantitative definition of 'carmine lake'. Carmine lake therefore = 46.9, 28.6, 4.6. Its Lab characteristics are very unique: dark and far out on the 'a' (red) spectrum, but close to neutral on the 'b' (blue-yellow) spectrum. It is a beautiful shade. I believe expertization of stamp 28 as 'deep dark brown' is simply wrong.

Stamps 30 and 31 join Stamp 9 in being the most unlike any other stamps but are both visually and quantitatively very like each other. Neither has been expertized, and a lay person would probably describe them as dark brown. They therefore form the basis for a tentative quantitative definition of 'dark brown' = 43.5, 14.0, 5.8.

Summary: None of the expertized 'deep brown red' stamps are close to each other. But stamp 28 is a very distinctive and rich shade close to Stamp 33 = carmine lake. Therefore: stamps 28 and 33 = carmine lake = 46.9, 28.6, 4.6. Stamps 30 and 31 = Dark Brown = 43.5, 14.0, 5.8.

The remaining three stamps in this group are neither close to each other, nor to anything else. They exemplify the problem with these later shades in that they have not been sufficiently studied.

**Bright Rose Red**

There are only Stamps 6 and 7 expertized as 'bright rose red'. They are quite far apart from each other, both visually and by ΔE76 (7.8). Their Lab coordinates locate them quite close to other stamps that have been difficult to classify (11, 20, 26; 8, and 22). One could argue they fall loosely into what I've called the 'deep rose' group, more research is needed.

## Conclusions

### *The challenge of the science of shade classification*

The subjective difficulties associated with correctly identifying the shade of a stamp have been long known and written about. They include factors such as shade changes due to environmental effects, and the effect of paper tone and lighting on the appearance of a shade. Over time, to mitigate the many problems, experts have built substantial libraries of reference copies, compared notes, and subjected themselves to round-robin and comparative testing. Far from resolving these challenges, bringing reflectance technology to the problem has only served to highlight the fact there are deeper, more scientific challenges. The three I have highlighted are:

1. The challenge of developing formal (non-subjective) criteria for reducing the number of shades the eye can see, to a number useful for cataloguing.
2. The 'Reference Copy' problem: reflectance technology shows small differences between experts' reference copies, can lead to serious inconsistencies when experts assign a shade to a stamp.
3. The 'Cluster Algorithm' problem of different grouping methods, leads to different clusters which, in turn, lead to different cluster centers. Experts need to think about how to develop a common standard.

Paradoxically, the fundamental problem is the acuity of the average human eye. We need to create groups that reduce the great number of shades we can see, to a manageable number, but that will result in groups with varying centers and fuzzy edges. Machine measurement will not eliminate these problems but should help to eliminate the intractable subjectivity (and resulting inconsistency) that accompanies human expertizing.

### *Methodological challenges of sampling for shade measurement*

I tested three variations in spectrographic sampling:

1. Sample according to the following verbal protocol: under magnification, identify clean and solidly inked patches. Take at least five samples
2. Compare patches typical of an expert approach, with patches that leverage the ability of machines to zero in on dense ink at high levels of magnification
3. Choose a clean, inked patch. Start at 8x magnification then increase the magnification through 16x to 61x

The results of the first experiment suggest the verbal protocol is too informal. It leads to Lab coordinates so far apart that different researchers could produce different mean Lab outcomes. We need a stricter protocol that specifies three things: a) a minimum level of magnification; b) a minimum number of samples; and c) a precise standard for the consistency of the ink within a select sample patch, completely free of extraneous influences, and with an ink density that neither varies, nor is so thin as to be translucent. We need to record every sample location and store the locations as part of the sample information.

The need for the second experiment (a comparison of 'typical' versus 'dense' samples), arises because the traditional expert approach uses what I call 'typical' samples, but dense samples are needed for machine reliability. The results show the two kinds of sample lead to different conclusions as to hue, but that the differences might not matter as long as a shade is visually narrow in scope. Shades that are a 'catch-all' for a visually wide range, or have been poorly studied, will be problematic. The results strengthen the

**Table V**

**Suggested Lab coordinates for shades of the 1861 3c stamp**

| | | CIE Coordinates | | | ΔE76 distances | | | | | | |
|---|---|---|---|---|---|---|---|---|---|---|---|
| Shades | Stamp IDs | L | a | b | CP | LP | BR | PBR | BR | DR | CL |
| Carmine Pink | 1 | 60,8 | 30,0 | 1,9 | | | | | | | |
| Lavender Pink | 2, 14, 16 | 64,8 | 25,8 | 7,2 | 7,9 | | | | | | |
| Bright Rose | 5, 15 | 65,3 | 25,0 | 14,6 | 14,4 | 7,4 | | | | | |
| Pale Brown Red | 9, 10 | 76,0 | 12,4 | 19,7 | 29,3 | 16,8 | 17,3 | | | | |
| Brown Red | 21, 24, 25 | 54,2 | 22,9 | 22,7 | 22,9 | 18,8 | 13,9 | 24,4 | | | |
| Deep Rose | 8, 22, 23 | 58,3 | 27,4 | 11,5 | 10,3 | 7,8 | 8,0 | 24,6 | 12,7 | | |
| Carmine Lake | 28, 33 | 36,9 | 28,6 | 4,6 | 24,1 | 28,0 | 30,3 | 44,9 | 25,7 | 22,5 | |
| Dark Brown | 30, 31 | 43,5 | 14,0 | 5,8 | 23,9 | 21,3 | 26,0 | 35,4 | 21,9 | 20,8 | 16,1 |

*The Lab coordinates in this table are a quantitative definition of the centroid in the 1976 CIE color space, for the named shade. They are derived from the mean coordinates for the relevant stamps in Table IV. The data in Table IV prove the distance of each stamp from others, and its closeness to its shade's centroid.*

case for machine measurement because the ability to zero in on small patches at high magnification more likely will lead to reliable measurement.

The third experiment suggested 8x magnification is unreliable, but 16x or greater magnification produces consistent results, as long as one is zeroing in on the same inked patch.

### *The Lab coordinates of shades of the 1861 3¢ stamp*

Table V is a summary of proposed Lab coordinates for shades of the 1861 3¢ stamp. They are provisional, and more measurement and analysis is needed but they constitute well-defined and distinctive regions within the 1976 CIE color space. As the table shows, they are far from each other. As seen in Table 4 and the ensuing discussion shows, the stamps that make up each shade are both close to each other and to the shade center shown in this table.

More work should be done to attempt to replicate these results. I am relatively confident they would prove to be stable, as long as my measurement protocols are followed.

## Acknowledgements

I would like to thank John Barwis, Jim Allen, and Tom Lera for their many comments and answers to questions; and for their guidance when designing the research and interpreting the results. A special word of thanks to Susan Smith at the Smithsonian for letting me into her lab space, showing me how to use the machine, consistently helpful comments on measurement; and for making a valiant effort to get the X-ray machine working. I hope that I wasn't too burdensome as a guest. For myself, I had a wonderful five days.

## References

Barwis, John H. and Harry G. Brittain. 2016. Ink Composition of the US 3¢ Stamps 1870–1883. In: Barwis, J. H. and T. Lera, editors. *Proceedings of the Second International Symposium on Analytical Methods in Philately.* Akron, Ohio: The Institute of Analytical Philately, pp. 49–56.

Brittain, Harry G. 2013. Infrared Spectroscopic and X-ray Diffraction Studies of the Typograph Confederate 5c Stamps. In: Lera, T., J. H. Barwis, and D. L. Herendeen, editors. *Proceedings of the First International Symposium on Analytical Methods in Philately.* Washington, DC: Smithsonian Institution Scholarly Press, pp. 47–56.

Charles, Harry K. 2017. Exploring Color Mysteries in the United States Large and Small Numeral Postage Due Stamps Using X-ray Fluorescence Spectrometry. In: Smith, Susan and J. H. Barwis, editors. *Proceedings of the Third Symposium on Analytical Methods in Philately.* Akron, Ohio: The Institute of Analytical Philately, pp. 97–126.

Cibulskis, John. 2016. Towards a Stamp-oriented Color Guide: Objectifying Classification by Color. In: Barwis, J. H. and T. Lera, editors. *Proceedings of the Second International Symposium on Analytical Methods in Philately.* Akron, Ohio: The Institute of Analytical Philately, pp. 31–40.

———. 2017. The Colors of the Germany crown and Eagle Series. In: Smith, Susan and J. H. Barwis, editors. *Proceedings of the Third Symposium on Analytical Methods in Philately.* Akron, Ohio: The Institute of Analytical Philately, pp. 35–50.

Herendeen, David L., James A. Allen and Thomas Lera. 2011. Philatelic Shade Discrimination Based on Measured Color. *The London Philatelist* 1384, Vol. 20 (April).

Herzog, William K. 1981. 3¢ "near pink" and Ashbrook's "pinkish rose." *The Chronicle* 111, Vol 33:3 (August).

Lera, Thomas, Jennifer Giacci and Nicole Little. 2013. A Scientific Analysis of the First Issue of Chile, 1853-1862, London Printing. In: Lera, T., J. H. Barwis, and D. L. Herendeen, editors. *Proceedings of the First International Symposium on Analytical Methods in Philately.* Washington, DC: Smithsonian Institution Scholarly Press, pp. 19–34.

Liston, Edward. 2016. A New Technique for Analyzing the Optical Spectrum of Stamp Inks. *Collectors Club Philatelist,* Vol. 95:4 ( July-August).

Lyons, Larry. 2017. Using the Bruker XRF to Distinguish the Six Different Printings of the U.S. Newspaper Stamp Designs N4 and N5. In: Smith, Susan and J. H. Barwis, editors. *Proceedings of the Third Symposium on Analytical Methods in Philately.* Akron, Ohio: The Institute of Analytical Philately, pp. 127–134.

McClung, Michael. 1993. Shades of the 1861 3¢. *The Chronicle* 159, Vol. 45:3 (August).

———. 2012. Colors in Print. *The Chronicle* 235, Vol. 64:3 (August).

Soctt Publishing Company. 2005. *Specialized Color Guides for United States Stamps.* Sidney, Ohio: Amos Media Co.

Scott Publishing Company. 2015. *Scott Specialized Catalogue of United States Stamps and Covers, 94th edition.* Sidney, Ohio: Amos Media Co.

# Philatelic Applications of Wavelength Resolved Fluorescence

*Richard Judge*

## Abstract

This paper begins with a brief introduction to the photophysics behind luminescence, then looks at the profiles of three commercial mercury (Hg) UV sources. The traditional use of Hg lamps and the qualitative description of fluorescence have been augmented by much more powerful, narrow wavelength diode lasers and a quantitative look at fluorescence. Because of the enhanced fluorescence from the lasers, wavelength separation of the emitted light is possible (wavelength resolved fluorescence).

The visual emission of a pair of face identical contemporary Canadian stamps with different taggants is interpreted from the resolved fluorescence. The fluorescence signal induced by the diode laser is sufficiently strong to see the emission from the stamp paper itself. Through a principle component analysis, the partitioning of the resolved fluorescence from the 2¢ Admiral issue was found to parallel the two major shades.

## Introduction

Fluorescent and phosphorescent tagging of postage stamps is a well known and understood aspect of present day philately. Multiple research articles have appeared in philatelic literature. A review published by the United States Stamp Society as a reprint (Paquette, 2015), summarizes the fluorescence seen in US stamps. The tagging in Canadian stamps is well documented in the Unitrade Specialized Catalogue of Canadian Stamps (Harris, 2019). A listing of "Fluorescence in Canadian Stamps" by E.R. Crain is found in *The Canadian Philatelist* (Crain, 1976:9). For a comprehensive understanding, the reader is directed to the book by Wayne Youngblood (Youngblood, 1989).

For the most part, in the above texts, luminescent compounds have been added to (or coated on) the stamp to aid in the sorting and cancellation of mail. This study focuses on the fluorescence properties of the ink and paper and not on intentionally added luminescent compounds. My goal is to use resolved fluorescence, where the emitted light (fluorescence or phosphorescence) is separated into its component wavelengths, as a spectroscopic tool to identify and catalog stamps, specifically turn of the 20th century Canadian stamps.

In my previous paper on the Canadian 2¢ red Admiral ( Judge, 2019), changes were observed in the chemical makeup of the ink with time. This paper will show the same is true with the resolved fluorescence and, like the other spectroscopies used, a correlation to shade is shown for the Admiral issue.

## Luminescence Overview

Figure 1 is a simplified diagram of the processes occurring when molecules absorb radiation. The top figure shows a typical absorption spectrum of an ink pigment on the surface of a stamp. The 'bumps' or bands are the colors (wavelengths) strongly absorbed by the pigment when a continuum (light containing all frequencies) impinges on the surface. The two arrows show the narrow frequencies of light from UV sources inducing absorption in specific color regions by the ink pigments.

The middle figure shows the emission spectrum results when the molecule absorbs these narrow frequencies. Note the emission spectrum is almost a mirror image of the higher energy portion of the absorption spectrum but is shifted to longer wavelengths. The molecule has absorbed light in the blue region of the spectrum but has emitted in the red region.

The bottom figure shows why. Process A (Absorption): Electrons in molecules can transition from stable (ground) states to unstable (excited) states by the absorption of light of sufficient energy. Within the ground and excited states are substates indicated by dashed, solid and thin horizontal lines respectively. For simplicity, only transitions from the lowest level of the ground state to various excited state

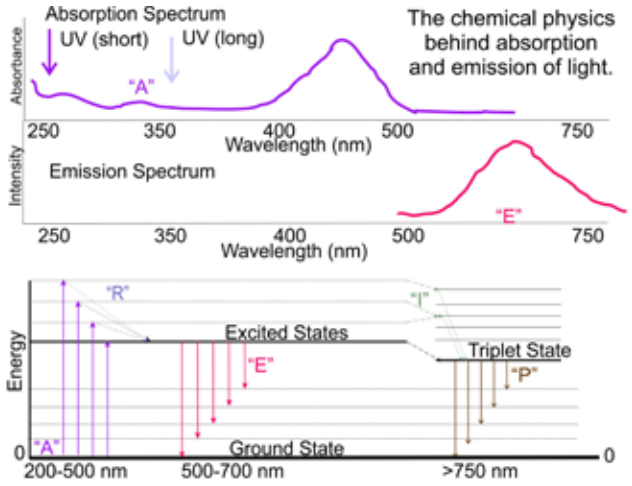


***Figure 1.*** The upper trace shows the absorption spectrum of a dye. In the middle trace, the dye is exited with UV light. The resultant emission is red shifted as indicated by the red spectrum line. In the lower graph, a molecular explanation is shown. The absorption (A) is the result of transitions to excited states. The emission (E) is the result of transitions from the lowest level of the excited state to various ground state levels. Phosphorescence (P) is the result of emission from a lower energy triplet state crossed into from the excited state.

levels are shown. The length of the vertical transition lines is proportional to the frequency of light absorbed and gives rise to the upper absorption spectrum. The longer the arrow, the more the transition frequency is towards the blue.

Process R (Relaxation): Once the molecule is in the excited state, it will lose the excess energy as it quickly moves to the lowest level in the excited state.

Process E (Emission): From there, the molecule can directly return to the sublevels in the ground state as indicated by the downward pointing arrows. Loss of this energy as light emission is called fluorescence. Again, the length of the arrows in the diagram is proportional to the frequency of light emitted. The shorter the arrow the greater the light is shifted to the red.

Process I (Intersystem Crossing): A less probable occurrence is the crossing of the molecule from the excited state to a second, lower energy excited state.

Process P (Phosphorescence): From this state the molecule can emit light of a frequency that has moved even further to the red.

Compounds in the stamp make transition to excited states by interacting with light from an external source. Most philatelists are familiar with mercury (Hg) lamps which supply light with a very narrow range of frequencies (single colors). Typically, this is achieved by filtering

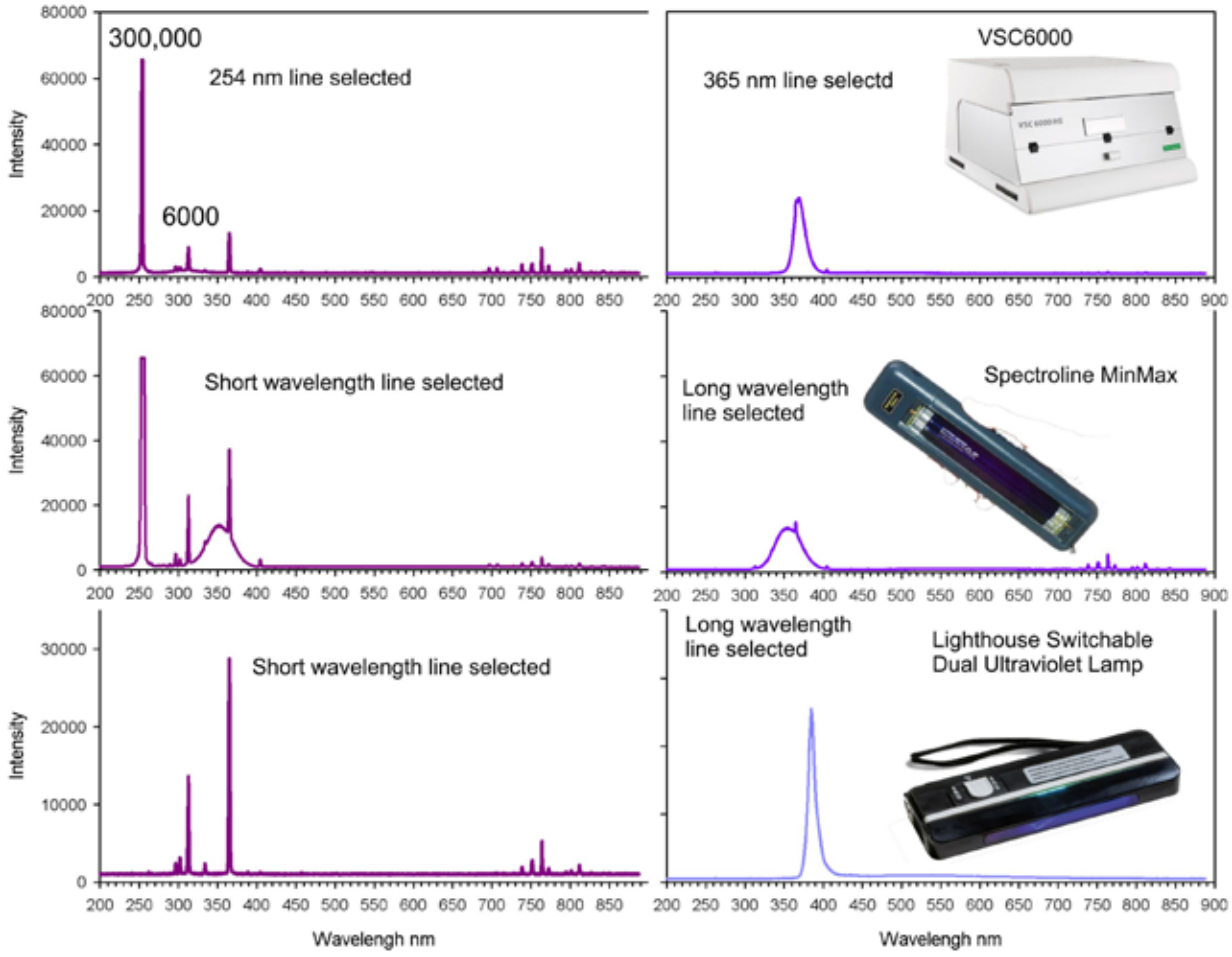


***Figure 2.*** Comparison of three commercially available UVA and UVC light sources.

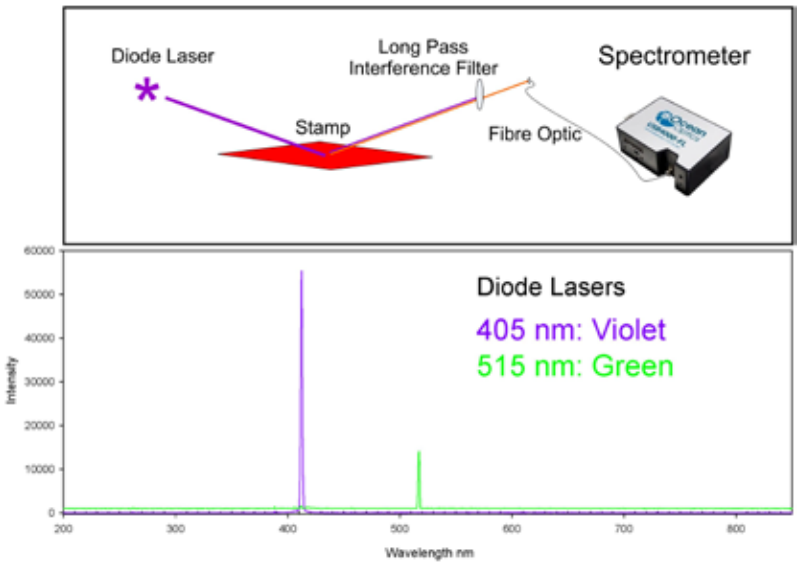


***Figure 3.*** The lower part of figure 3 illustrates the single frequency narrow wavelength laser light of the 405nm and 515 nm diode lasers. The upper portion shows the use of an interference filter placed between the stamp and the detector to eliminate the strong scattered exciting laser line but allowing the weak fluorescence wavelengths greater than 450 and 550 to reach the detector.

the emission from the Hg lamp with filters so either 254nm light (Far UV, UVC, or short wavelength UV) or 365nm light (near UV, UVA or long wavelength UV) is selected. Recently, inexpensive diode lasers became available across the full visible spectrum and can be used in fluorescence experiments to vary the excitation wavelength.

In practice, the commercially available Hg excitation sources have different emission spectra. Figure 2 shows the emission spectra of three commercially available Hg UV sources. The 254nm source (UVC) from two manufactures have 365nm as an additional emission line, although the 254nm line is greatly enhanced. This is not the case for the Lighthouse lamp tested for this study as UVC line is missing and the weaker 313nm line (UVB) of Hg is used and is stronger. The long wavelength selection mode successfully filters the 365nm (UVA) from various sources. Note the Lighthouse unit is not a Hg line and is shifted by about 20 nm to the red. It is a 380nm light emitting diode.

Philatelists should take into consideration the fluorescence hue detected by the eye may depend on the lamp used. Contrast this with the diode lasers shown in lower part of Figure 3. The emission lines are very sharp and intense with a linewidth typically around 6nm. Because of the superior performance of the diode lasers, the commercial sources were only used to confirm the resolved diode laser spectra tracked the commercial 365 sources, which was the case.

## Experimental Conditions

The diode emission spectra were recorded using an Ocean Optics USB4000 spectrometer with a resolution of 2nm. The emission was collected by a UV grade fiber optical cable after the fluorescence was passed though a long pass interference filter to eliminate most of the exciting light as illustrated in the upper part of Figure 3.

Two custom built diode lasers supplied the excitation source. A violet 405nm 150mw diode laser, coupled with a 450nm long-pass interference filter, was used for all stamps studied. A green 515nm 10mw diode laser, couple with a 550nm long-pass interference filter, was used for additional testing.

A VSC6000 supplied the Hg excitation lines at 254nm (8w, total power dissipation) and 365nm (9w, total power dissipation). The spectrometer in the VSC6000 had a resolution of 10nm. Since the Hg emission is considerably weaker than from the diode lasers, the resolved emission from the VSC6000 was noisy and suffered from an artifact from the spectrometer, giving apparent distinct sharp peaks. These were shown to not be present with the diode lasers and the Ocean Optics spectrometer. However, the integrated maxima and overall shape of the VSC6000 curves agreed with both the violet and green laser spectra from the USB4000.

The emission spectra from the stamps are broad with minor variations in profile. The differences among the spectra are best seen using a second derivative of the intensity. A Savitsky-Golay (Savitsky, 1964:1627) reduction initially computes the smoothed spectrum, followed by a first and second derivative calculation. The second derivative will de-convolute a broad spectrum with a complex profile into a spectrum with negative going peaks at the same wavelength location as the maximum and shoulders.

## Results

### *Luminescence in Current Era Postage Stamps*

The choice of exciting wavelength has a significant effect on which compounds in the stamp will absorb the light and move molecules to an excited state. By selecting the proper light source one can selectively excite specific compounds in the stamp. As an example, consider the tagging compounds needed for the proper operation of modern mail cancellation machines. A good example can be seen in two Canadian stamps. Although face identical, they have different types of taggant where a chemical was added to either the paper or ink to give luminescence.

In Figure 4(a), the resolved fluorescence for Scott 1696a (booklet stamp) is shown when excited by Hg 254nm frequency light. The narrow band centered at 525nm is responsible for the green glow of these stamps. However, when the stamp is irradiated with 365nm light, the peak at 525nm disappears and a very shallow, broad band appears near 500nm, Figure 4(b).

Contrast this with the irradiation of Scott 1697 (coil stamp) with 254nm light, shown in Figure 4(c). Only the

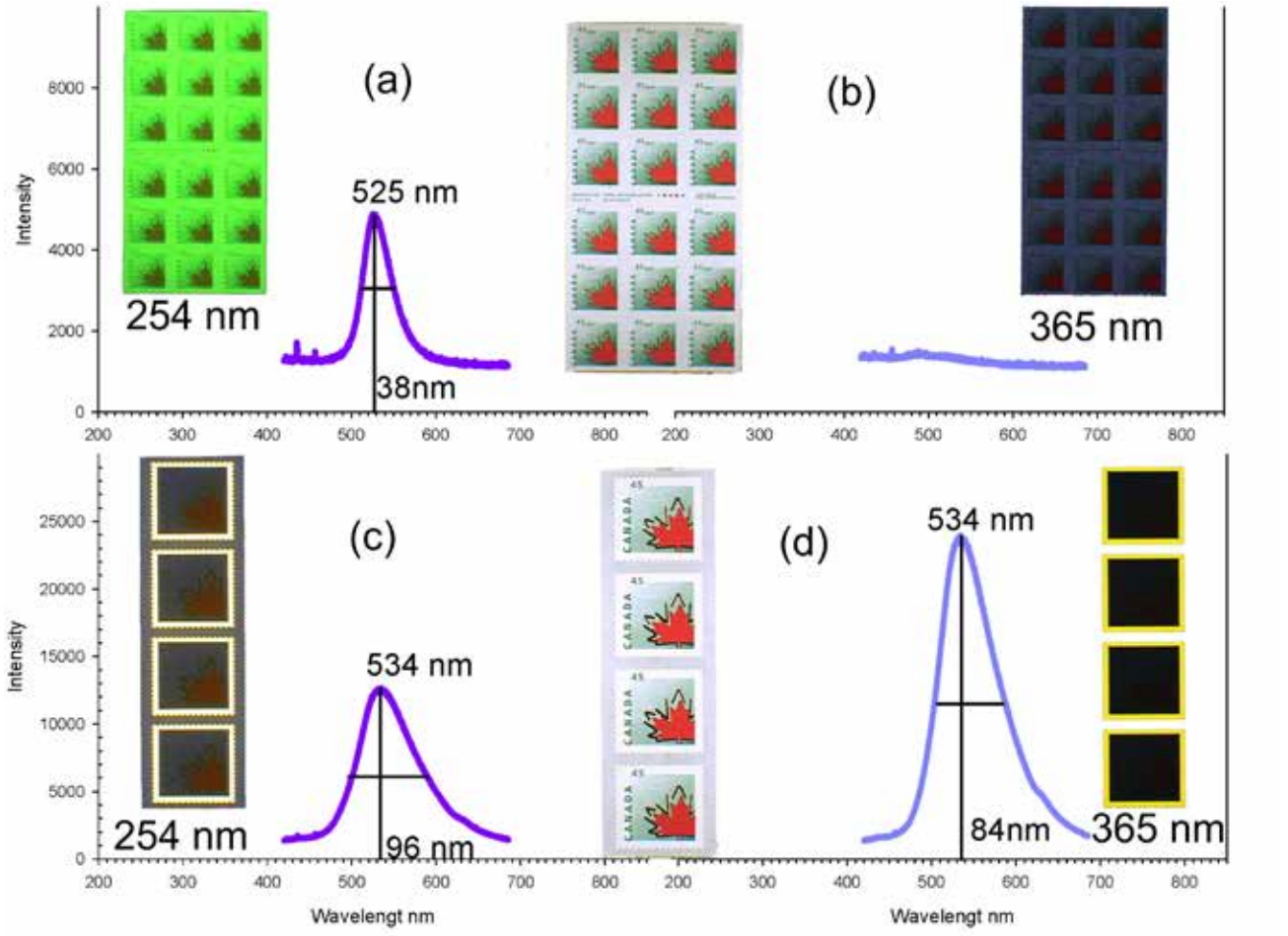


***Figure 4.*** Upper traces (a) and (b) show the response of a booklet pane to UV 254 and UV 365 light. The coil stamp shown in traces (c) and (d) use a different taggant in the selvage area only.

selvage area of the stamp is fluorescent and the peak is shifted and broadened. To the naked eye, a white border has appeared around the stamps. When the same stamp is irradiated with 365nm light as shown in Figure 4(d), the band remains at 534nm but with a smaller half-width. The band has a different asymmetry with intensity shifted to the red and results in a yellow hue.

A whitening agent was added to the paper resulting in a white border since the fluorescence appears on the gum side of the stamp and retains its white color under both 254 and 365nm light. The absorption spectrum of a modern whitening molecule (a triazine-stilbene derivative) has absorption maxima at 220 and 330nm (Guo, 2017:45536) which explains the fluorescence under both lines.

However, the yellow glow from the border face of the stamp must be from a different added taggant not responding to 254nm light. The XRF spectrum of the booklet stamps contains a high level of zinc. Thus, a doped zinc silicate molecule with emission at 520 nm is likely responsible for the fluorescence of the booklet stamp (Sohn, 1999:2780). The XRF spectrum of the coil stamps contains a high level of calcium, the yellow fluorescence is likely due to a doped calcium silicate.

### *Luminescence from the Paper*

Although the paper in contemporary stamps commonly has brightener compounds, turn of the twentieth century papers were free of added whiteners, with no need for taggants. However, the paper does still fluoresce weakly. Consider the irradiation of the selvage area of an Admiral 2¢ carmine stamp shown in Figure 5 (upper) with the violet diode laser. The signal from the selvage is greatly enhanced by the 405nm 150mW (violet) diode laser excitation source and, to a lesser extent, by the 515nm 10mW (green) diode laser. The fluorescence peaks at 494nm.

Scientific literature has noted this emission maximum (Olmstead, 1993:61) between 430–490nm, with the longer wavelength due to light exposure of commercial modern paper pulp. The authors point out the source for the emission is not clear. Regardless of the source, there is no doubt the emission is from the stamp paper and not from any added chemicals in the paper given the close resemblance between Whatman Filter paper (an cellulose medium used as filter paper in chemistry laboratories) and the selvage area of the stamps. This is shown in lower half of Figure 5 using the second derivative to highlight the peak positions (negative going peaks in the 2nd derivative plot) and the general match of the plots.

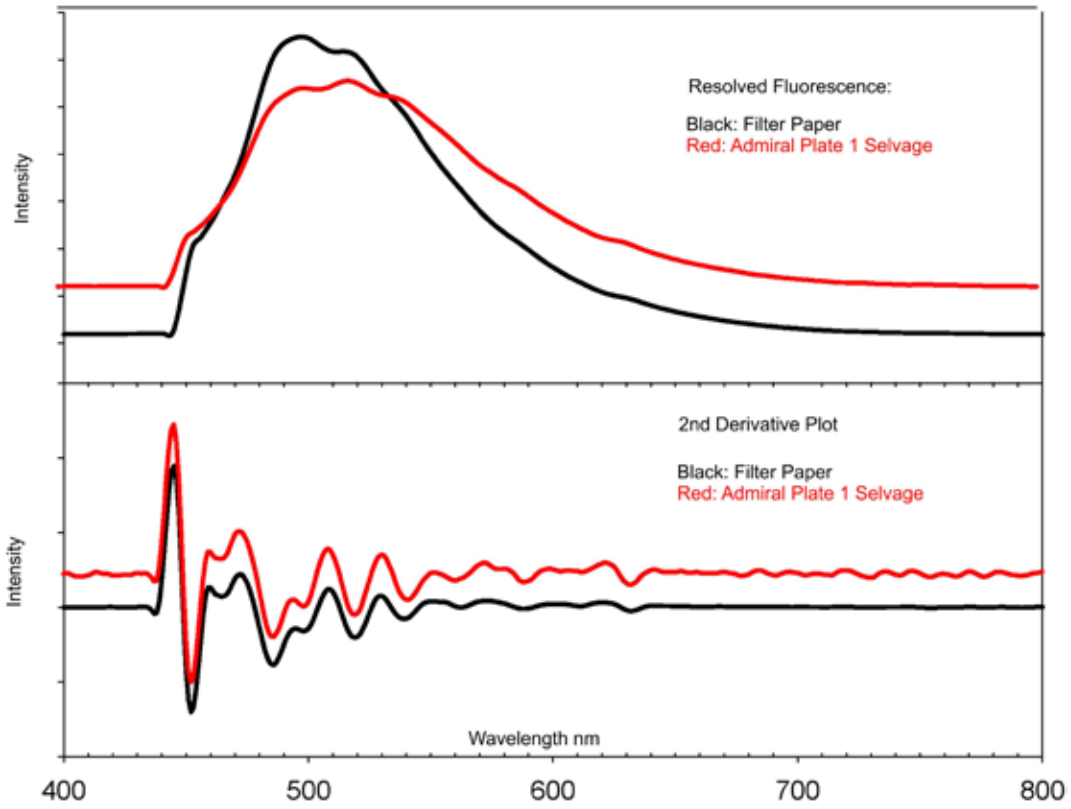


***Figure 5.*** Comparison of the resolved fluorescence from cellulose (filter paper) and the selvage area of Scott 106 Admiral Plate 1. The maximum intensities have been scaled to be similar. The bottom plot shows the second derivative of both curves and the near perfect correspondence by wavelength. The negative peaks of the second derivative correspond to the peaks and shoulders of the upper trace.

As an addendum to the above discussion, Olmstead et al (Olmstead, 1993) have noted irradiation of the paper with short wavelength light can cause noticeable yellowing of the paper. Cellulose absorbs in the ultraviolet and tails weakly into the violet/blue visible region. Prolonged irradiation can cause the absorption curve to change and moves the paper absorption profile farther into the visible. The effect on the reflectance spectrum of engraved stamps and the perceived shade of a stamp will consequently shift with time.

### *Ink Fluorescence: The 2¢ Carmine Admiral Issue*

An engraved stamp will have a significant surface area not covered by ink. As a consequence the emission spectra of the ink portion of the stamp will show the paper emission. The variation of the emission spectrum of the Admiral issue is studied in this section.

All spectra from plate blocks 1 though 160 show the same contribution due to the paper. This study did not attempt to quantify the emission from plate to plate but rather note, the maxima and general profile.

The most striking change in the resolved fluorescence is between stamps from the early (1–60) and the later plates (100–160). The two major shades have been variously described by philatelists as rose carmine or deep rose red for the early printing, and carmine or dark carmine for the latter printing.

Figure 6 shows the two major types of resolved fluorescence from the first and last plates of this issue. The contribution by the paper is the same in both, as indicated by the green tracer lines. It is clear the fluorescence confirms the visual distinction. Also, the later ink has a much greater fluorescence than the paper or earlier inks. Nonetheless, the second derivative clearly shows the paper's contribution.

This study had 105 plate blocks which presents a problem of partitioning the spectra in groups. I attempted to group like spectra as type 1 , 1a, 1b, ... type 2, 2a. ... based on major and minor peak locations. In all, about 9 types were found. But the differences ranged from small within sub-groups to significant between the major groups, 1 and 2. Spectra within each subgroup generally overlapped nicely. For example, 15 spectra within type 1 and 1a were near perfect matches. Nonetheless, I feel the classification scheme is arbitrary. A method based on statistics was used instead, which yielded only two distinct groups.

A principle component analysis (PCA) can be performed on this data set. PCA is a statistical method used to confirm the partitioning of a group of samples sharing common features or, in this case, a common pigment chemistry. PCA takes a system with a large number of variables and reduce it to a handful of significant variables.

For the Admiral plate blocks, the second derivative emission profiles range from wavelengths 415 to 800nm, some 386 points or variables for each plate block. The PCA will reduce this to a few variables accounting for most of the observed properties. As a rule, the number of variables ranges from one to four, but for ease of visualization, usually only the first two are chosen. This two-dimensional plot is a 'score plot' where the most significant variable ('A') is plotted against the second most important ('B'). This is shown in the upper part of Figure 7 where the partitioning of the plate blocks into two distinct groups is clearly seen. The two variables account for 71 % of the variability in the spectrum.

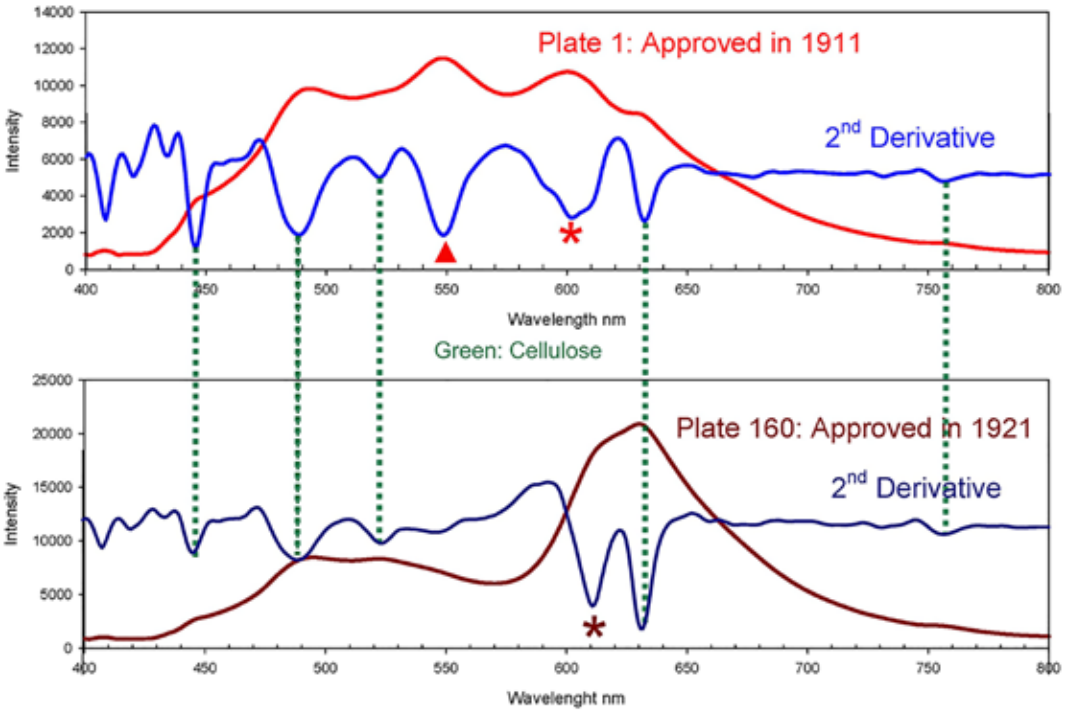


***Figure 6.*** Resolved emission of plate 1 (red trace) and plate 160 (dark red trace). The second derivatives are blue and dark blue respectively. The fluorescence due to the paper is common in both and is shown with the green tie lines. Note the small shift in frequency between 600 and 620 nm peaks of the second derivative noted by the asterisk. This accounts for the shift in shades of the two plate blocks.

The lower half of Figure 7 shows the variation of the "A" score with time. Here, the "A" score is plotted against the approval date of the plate expressed as the number of days since December 12, 1911. Around day 1328 (August 5, 1915), the value of "A" oscillates from negative to positive for a short period as shown by the green and cyan points of Figure 7. The points then remain constantly positive.

The primary reason of this PCA study is to show the most likely reason for the change in fluorescence and the plots of Figure 6 and 7 is the difference in the pigments used in the stamp ink. Based on other evidence (Judge, 2019) these pigments started with synthetic dyes.

The resolved fluorescence has shown that only two major types of dyes are in use. Closer examination of the resolved fluorescence shows small shifts in profiles within the two major classes. Spectra from plates 1 though 14 (11 in all) are remarkably similar while small changes start to occur near plate 17 as illustrated in Figure 8. Here a small shift in frequency of the maximum emission gives a small change in hue. A mix of the two types continues until plate 67 where a third small change occurs. Stronger shifts are found around plate 81, the region of noticeable ink bleed-through to the back of the paper. The emissions from the carmine region from plates 99 onward are remarkably the same.

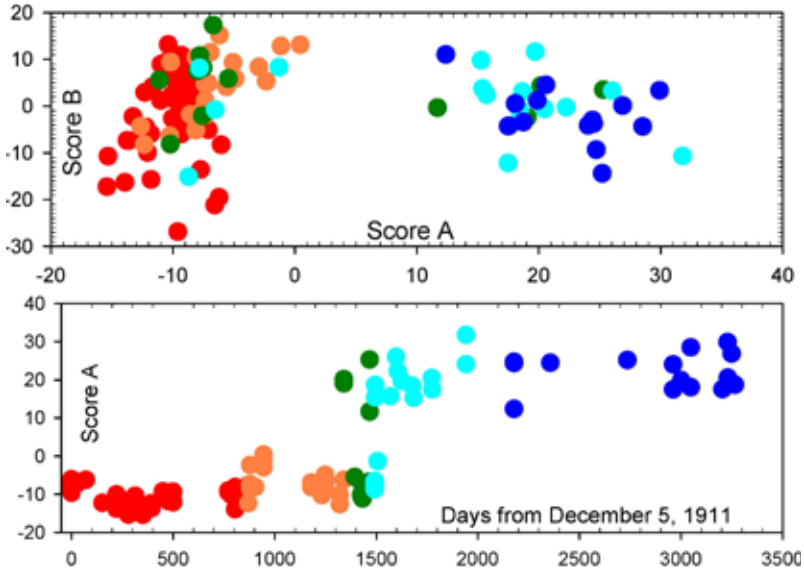


***Figure 7.*** The upper plot shows the principle component analysis (PCA) of the 2nd derivative spectrum of the resolved fluorescence of 105 Admiral plate blocks. A clear partitioning into two groups is seen. The bottom plot shows the partitioning is time dependent with an area or crossover of the dyes used around day 1400 or August 1915.

Within the stamps up to plate 99, small changes in the molecular structure of the dye could account for the wavelength shifts.

## Conclusion

This paper has given a brief introduction to the role of luminescence in philately. The traditional use of Hg lamps and the qualitative description of fluorescence have been augmented using much more powerful and narrow wavelength diode lasers. Because of the enhanced fluorescence from the lasers, resolved fluorescence using fiber optic spectrometers is possible. This has opened up the study of these stamps. The near constant profile of the resolved fluorescence of ink-free stamp paper is an unexpected observation.

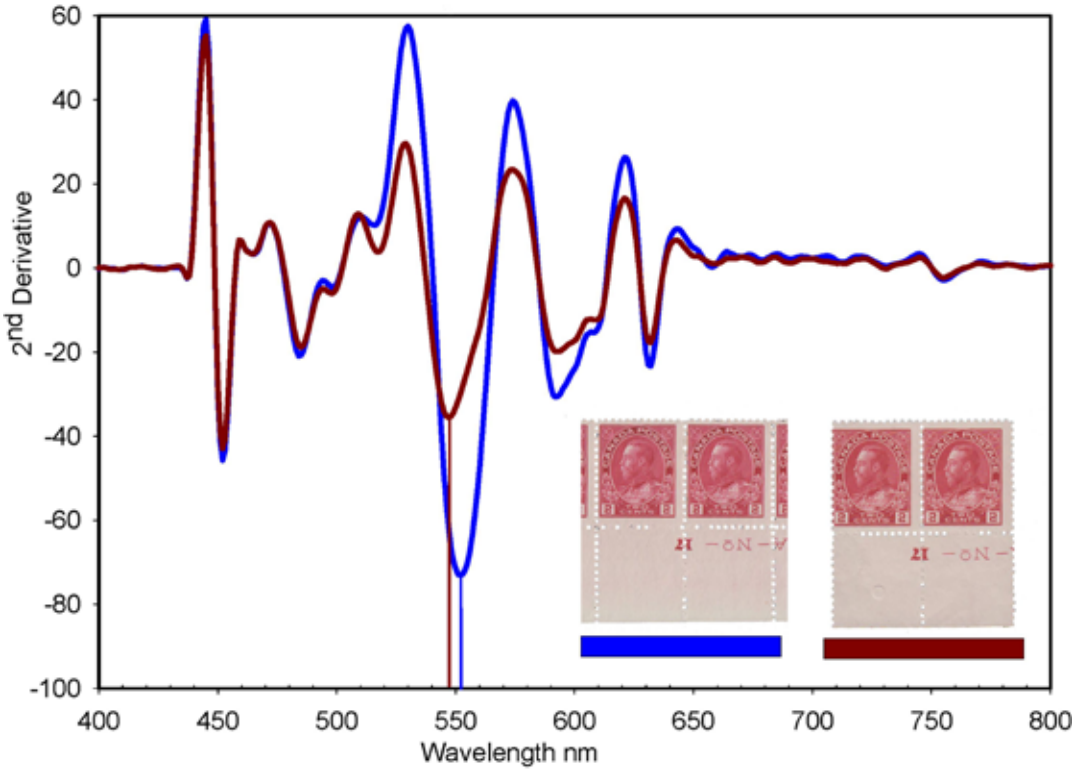


***Figure 8.*** A small change in the maximum of the main emission band at ~550 nm gives a small shift in hue. Note color reproduction in the processing of this figure may not give an accurate representation of the shade differences.

The paper fluorescence is remarkably similar over the papers studied from the 1910s to the 1920s. Through a PCA, the partitioning of the fluorescence from the red 2¢ Admiral issue was found to parallel the two major shades. Furthermore, the stamps issued around 1915 were found to belong to both groups, suggesting experimentation with ink chemistry during a short time period.

## References

Crain, E.R. 1976. Fluorescent Ink on Canadian Stamps. *The Canadian Philatelist,* 27(1), pp 9–15.

Guo, Mingyuan, Guanghua Zhang, Lun Du, Hua Zheng and Guojun Liu. 2017. Water-soluble, anti-yellowing polymeric fluorescence brighteners. *Journal of Applied Polymer Science,* app 45536.

Harris, D. Robin editor. 2019. *2019 Unitrade Specialized Catalogue of Canadian Stamps.* Unitrade Press, Toronto, Ont.

Judge, Richard H. 2020. Chemistry of Aniline Inks, 2-cent Admiral Issues of Canada. In: Smith, Susan and J. H. Barwis, editors. *Proceedings of the Third Symposium on Analytical Methods in Philately.* Akron, Ohio: The Institute of Analytical Philately.

Olmstead, Jennifer A. and Derek G. Gray. 1993. Fluorescence emission from mechanical pulp sheets. *Journal of Photochemistry and Photobiology A: Chemistry,* 73. pp. 59–65.

Paquette, Gene and Ken Lawrence. 2015. Luminescent Tagging On United States Stamps: A Series of Articles Reprinted From The United States Specialist. *United States Stamp Society, Reprint #4.*

Plotner, Jurgen and Andreas Dreuw. 2006. Solid State Fluorescence of Pigment Yellow 101 and Derivatives: a conserved property of the individual molecules. *Physical Chemistry Chemical Physics,* 8, pp. 1197–1204.

Savitzky, Abraham and M. J. E. Golay. 1964. Smoothing and Differentiation of Data by Simplified Least Squares Procedures. *Analytical Chemistry,* 36(8) pp. 1627–1639.

Sohn, Kee-Sun, Bonghyun Cho, and Hee Dong Park. Photoluminescence 1999. Behavior of Manganese-Doped Zinc Silicate Phosphors. *Journal of the American Ceramic Society,* 82 (10). pp. 2779–84.

Youngblood, Wayne. 1989. Stamps that Glow. *Linn's Stamp News,* December 1.

# 1894 and 1895 Series First Bureau Postage Due Stamps: Questions of Color, Fluorescence, and Early Use: Part I

*Harry K. Charles, Jr.**

## Abstract

This paper examines the production and early use of the First Bureau postage due stamps in some detail. The printing and first issuance to postmasters of these First Bureau dues occurred between 1894–1897. These stamps were perforation 12 and initially printed in sheets of 200 (two 100-stamp panes, side by side) on unwatermarked paper (1894 Series). Within about a year the paper was switched to a double-line, watermarked variety for most of the postage due denominations. High values of 30¢ and 50¢ were in low demand, so the reprinting and switch to double-line, watermarked paper for these values did not occur until the 1896-1897 period. The 1895 Series double-line, watermarked printings in sheets of 200 stamps continued until replacement in 1910, when the Bureau of Engraving and Printing (BEP) introduced new 400 subject sheet layouts and changed the paper to a single-line watermark variety.

The 1894 and 1895 Series postage due stamps exist in a variety of colors and shades, and both are fluorescent and non-fluorescent under ultraviolet light. Using data collected by X-ray fluorescence spectrometry and observations of fluorescence under ultra-violet light, this paper explores many of the aspects of First Bureau postage due stamp colors. This paper focuses on the ink composition and fluorescence of the essays and proofs associated with the development of the First Bureau postage due stamps. The data shows all but one of the claret colored essays fluoresce and have ink compositions similar to the vermilion postage due stamps. The die proofs are mostly non-fluorescent (except for a few 2¢ denominations) with ink spectra like those of the non-fluorescent claret First Bureau postage due stamps. X-ray fluorescence ink spectra are used to compare stamps and proofs with visual color differences.

## Introduction

The 1¢ to 50¢ First Bureau postage due stamps issued from 1894 to 1897 encompass 16 major *Scott Catalogue* numbers [1] based on stamp denomination, watermark, and, to some degree, color as listed in Table I. These stamps cover the range of Scott nos. from J29 to J44 with color descriptions ranging from vermilion to shades of carmine and claret. The J29 through J37 stamps were perforation 12, printed on unwatermarked paper, and were referred to in the literature as the 1894 Series of First Bureau postage due stamps, although some denominations did not issue to postmasters until 1895. See Table I.

The J38 through J44 postage due stamps were also perforation 12, but the paper was double-line watermarked. These seven stamps are often referred to as the 1895 Series of First Bureau postage dues, although again certain denominations were not issued until 1896, and in one case, 1897 (30¢, J43). For simplicity, the stamps printed on unwatermarked paper studied in this paper will be the 1894 Series (Scott nos. J29 to J37). Similarly, the 1895 Series will refer to the stamps printed on double-line watermarked paper (Scott nos. J38 to J44).

Figure 1 illustrates three 2¢ values from the 1894 and 1895 Series postage dues. The 2¢ vermilion J30 (1894 Series) is on the left, the 2¢ J32 claret (1894 Series) is in the middle, and the 2¢ J39 (1895 Series) is on the right, again in

* Laurel, MD 20723

**Table I.**

**1894 and 1895 Series Postage Due stamps by Denomination, Scott No., Color, Watermark, and Issue Date to postmasters as Listed in the *Scott Catalogue***

| Value | 1894 Series Unwatermarked | | | 1895 Series Watermarked Double Line | | |
|---|---|---|---|---|---|---|
| | Scott No. | Color(s) | Issue Date [a] | Scott No. | Color(s) | Issue Date [a] |
| 1¢ | J29<br>J31 | Vermilion, pale vermilion<br>Deep claret, claret, lake | [b]<br>08/14/1894 | J38 | Deep claret, claret, carmine, lake | 08/29/1895 |
| 2¢ | J30<br>J32 | Vermilion, deep vermilion<br>Deep claret, claret, carmine, lake | [c]<br>07/20/1894 | J39 | Deep claret, claret, carmine, lake | 09/14/1895 |
| 3¢ | J33 | Deep claret, lake | 04/27/1895 | J40 | Deep claret, claret, rose red, carmine | 10/30/1895 |
| 5¢ | J34 | Deep claret, claret | 04/27/1895 | J41 | Deep claret, claret, carmine rose | 10/15/1895 |
| 10¢ | J35 | Deep claret | 09/24/1894 | J42 | Deep claret, claret, carmine, lake | 09/14/1895 |
| 30¢ | J36 | Deep claret, claret, carmine[d], pale rose [e] | 04/27/1895 | J43 | Deep claret, claret | 04/21/1897 |
| 50¢ | J37 | Deep claret, pale rose [f] | 04/27/1895 | J44 | Deep claret, claret | 03/17/1896 |

a. The date issued to postmasters

b. The data and arguments in this paper are inconclusive as to whether the vermilion or the claret shades were issued first.

c. The data and arguments in this paper strongly support the fact the vermilion shades were printed and issued first; therefore the issue date listed in the *Scott Catalogue* should be associated with J30 rather than J32. In fact, the earliest known appearance of tied 2¢ stamps in the claret shade (on cover) postdate the vermilion 2¢ stamps by several months.

d. Listed in the *Scott Catalogue* as J36a

e. Listed in the *Scott Catalogue* as J36b

f. Listed in the *Scott Catalogue* as J37a


***Figure 1.*** Examples of the 1894 and 1895 Series 2¢ perforation 12 unwatermarked postage due stamps. The J30 vermilion 1894 Series is on the left, the J32 claret 1894 Series is in the middle, and the double line watermarked J39 claret 1895 Series is on the right.




***Figure 2.*** First Bureau 2¢ postage due stamps in a deep claret shade. The unwatermarked J32 deep claret 1894 Series is on the left, the double-line watermarked J39 deep claret 1895 Series is on the right.

a claret color. J32 and J39 also exist in a dark or deep claret color as shown in Figure 2. Given below are more insights into the colors of the 1894 and 1895 Series First Bureau postage dues.

## Analytical Method

Analysis for the First Bureau postage due stamps (mint and used on covers), proofs, and essays consisted of ultraviolet fluorescence observations and the collection of elemental ink spectra using X-ray fluorescence spectrometry. Using a hand-held Bruker Tracer III-SD X-ray fluorescence spectrometer, the author collected ink spectra from a variety of First Bureau postage due stamps, essays, and proofs. A support stand for the hand-held X-ray source and detector assembly gave the unit needed stability to make repeatable measurements. Spectra collection parameters included a 40-kilo electron volt (keV) source voltage and a 60-second collection time. Sixty seconds was selected in a 2017 study (Charles 2017) based on the need for relatively rapid analysis and for compatibility with prior measurements. At 60 seconds or above, the X-ray count for a given

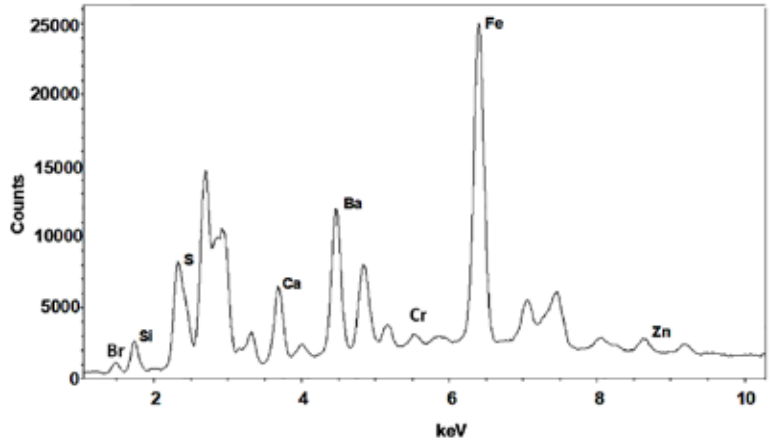


***Figure 3.*** A typical X-ray Fluorescence Spectrum of a J30 Vermilion postage due Stamp with eight of the 10 selected elemental peaks labeled. The peaks associated with the remaining two elements, Pb and Hg, have energies outside the energy range shown.

element is a linear function of time with a correlation coefficient of almost one. Charles, in the same study, concluded a single measurement of the X-ray spectrum was sufficient to collect a representative data set for a given sample. Such a data set allows comparison with another single spectrum result from a similar sample, having the same design and analyzing the same sub-region on both stamps. Figure 3 is a typical ink spectrum of a small numeral postage due stamp (J30).

While full spectra are interesting and necessary to explore the nuances of all the elements in the ink, comparing them for multiple samples is somewhat difficult due to the overlap of critical peaks and some limitations in the analysis software. To simplify data presentation and allow side-by-side comparisons, bar charts of the elemental X-ray counts for selected peaks are used. The 10-count peaks selected for this study are barium (Ba*), bromine (Br), calcium (Ca), chromium (Cr), iron (Fe), mercury (Hg*), lead (Pb*), sulfur (S), silicon (Si), and zinc (Zn).

The left side of Figure 4 is a bar chart for the original spectrum presented in Figure 3. At the right is a bar chart for the average peak values of fifteen J30 stamps, including the one illustrated in Figure 1. Table II gives the mean, standard deviation, and coefficient of variation for each of the ten selected peaks in the 15-stamp sample lot. All bar charts used throughout the study involve the same ten peaks. Peaks for elements denoted by an asterisk (*) represent the intensity of X-ray emissions from the L1 energy levels of these elements only. The other peaks are typically from K-shell emissions. Note, while peak heights (counts) are proportional to the concentration of a given element, estimating the concentrations of different elements just by comparing the relative peak heights is not possible due to different fluorescent yields from each given element [2]. The peak heights do provide an indication of what elements are present and which have a strong response. More importantly, they are useful for easily comparing the ink composition of one stamp to another as shown below.

## 1894–1895 Series Postage Dues: Quantity Issued

The Bureau of Engraving and Printing (BEP) printed the First Bureau postage dues in sheets of 200, containing two 100-stamp panes, side by side. In fact, it was not until 1910 that a 400-subject plate was introduced for the postage due stamps. From July 1, 1894, through June 30, 1910, over 421 million postage due stamps, encompassing all seven stamp denominations, were produced from 200-subject plates. The bulk of the 421 million First Bureau Postage Due stamps (over 83%) were the 1¢ and 2¢ denominations, 110 and 240 million, respectively. Charles gave a breakdown of stamp production, by denomination and fiscal year, for each of the seven First Bureau postage due stamps (1¢ to 50¢), in Table II, Appendix O, of his book (Charles 2013).

By looking at the issue dates in Table I, it is clear the 1894 Series had a very limited, exclusive existence, except the 30¢ and 50¢, and was replaced by the 1895 Series during the late summer and early fall of 1895. Hence, the 1¢ 1894 Series stamps had a little over a year exclusive existence window, the 2¢ about a year and two months, the 3¢ and 5¢ approximately six month windows, and for the 10¢ almost a year. The 50¢ window was about 11 months long but stretched into calendar year 1896. The 30¢ remained in service until 1897, giving it an approximate two year window. Considering the very short period of exclusive use, the question arises as to how many 1894 Series stamps were actually issued.

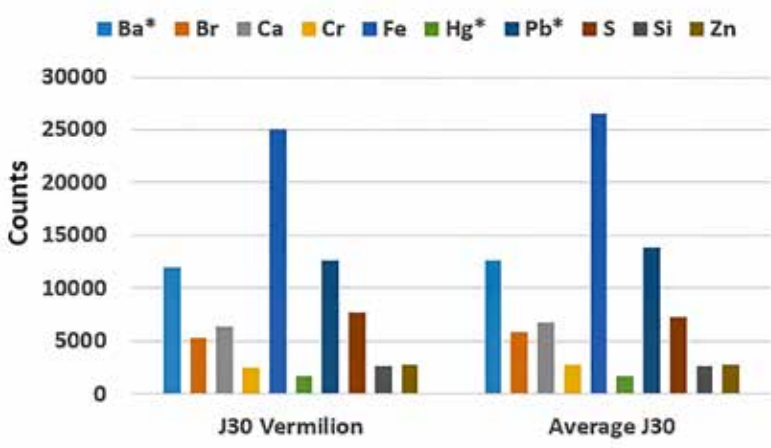


***Figure 4.*** On the left. an X-ray spectrum-derived bar chart for the 10 selected peaks from the spectrum of the two-cent J30 vermilion stamp shown in Figure 1. On the right is a bar chart of the average peak values for a reference lot containing fifteen J30 stamps.

**Table II**

**J30 Reference Lot: Mean (μ), Standard Deviation (σ), and Coefficient of Variation (σ/μ)**

| Elemental Peak | Peak Count Average, μ | Standard Deviation, σ | Coefficient of Variation (CV), σ/μ | CV Corrected for small sample size |
|---|---|---|---|---|
| Ba* | 12,652 | 874 | 0.0691 | 0.0702 |
| Br | 5,926 | 770 | 0.1299 | 0.1321 |
| Ca | 6,763 | 256 | 0.0378 | 0.0385 |
| Cr | 2,768 | 139 | 0.0502 | 0.0511 |
| Fe | 26,506 | 776 | 0.0293 | 0.0298 |
| Hg* | 1,654 | 107 | 0.0647 | 0.0658 |
| Pb* | 13,929 | 698 | 0.0501 | 0.0510 |
| S | 7,346 | 275 | 0.0374 | 0.0381 |
| Si | 2,689 | 219 | 0.0814 | 0.0828 |
| Zn | 2,761 | 96 | 0.0348 | 0.0354 |

The mean (μ), standard deviation (σ), and coefficient of variation (σ/μ) for each of the ten selected peaks for the J30 reference lot of 15. Even with the small sample or lot size correction, the coefficients of variations are small (< 0.1 or 10% for 9 out of the 10 count peaks).

*Peaks for elements denoted by an asterisk (*) represent the intensity of X-ray emissions from the L1 energy levels of these elements only. The other peaks are typically from K-shell emissions.

Clearly the overwhelming majority of the postage due stamps issued from FY 1895 to FY 1910 (some 421 million) were the 1895 Series. The actual number of 1894 Series stamps issued is somewhat shrouded in mystery since printing records of the time failed to distinguish the paper type. McIntire made an estimate of the number of 1894 Series stamps of 19,126,000 total stamps; however the source or basis for his estimates were not provided in his paper (McIntire 1969).

Based on the issue dates in Table I, it is clear all the postage due stamps issued in from July 1, 1894, to June 30, 1895, were printed on unwatermarked paper. John Luff stated "...the minimum number of 1894 Series postage dues is the fiscal year 1895 baseline number of 16,810,387 stamps" (Luff 1902). To determine the final numbers of 1894 Series due stamps issued, one must add to this baseline a prorated portion of subsequent fiscal year(s) issued numbers up until the time of the introduction of the 1895 Series stamps. Assuming a linear proration based on days of 1894 Series use prior to the introduction of the 1895 Series, the author has produced an estimate of 20,500,00 stamps inclusive of all seven denominations, which is about 7% larger than the McIntire number. Thus, of the approximate 421 million 1894 and 1895 Series postage due stamps issued, at least 400 million, or over 95%, were the 1895 Series.

## 1894–1895 Series Postage Dues: Plate Numbers

Table III presents plate numbers and imprint types for the 1894 and 1895 Series postage due stamps. For 17 years (1894-1910), the BEP printed the First Bureau postage due stamp designs from 200-subject plates. In fact, both the 30¢ and 50¢ denominations used the same plate for the entire period. First Bureau postage due plates were laid out with 20 subjects horizontally and 10 subjects vertically. Cutting between the 10th and 11th vertical columns separated the 200-subject sheet into two panes of 100. Each pane had plate numbers at the top and bottom above stamp 7 and below stamp 97, respectively, as counted from the upper left on the right pane and the upper right on the left plane. The BEP imprints were above stamps 5 and 6 and below stamps 95 and 96 on each pane. There are no side imprints or plate numbers. Certain plates (plate no. 57 bottom right) have the numbers displaced by one position (McIntire 1969). Plates also have arrows in the margins and gutter guidelines. Plates numbered 159 and below had top, bottom, and side arrows (bisected by a line) but no gutter guidelines (photographs of the approved plate proofs at the National Postal Museum are shown below). Plates numbered 246 and higher had both horizontal and vertical guidelines in the central gutters as well as arrows in the margin. According to Cleland (1987), most of the early plates had gutter guidelines added in November 1895, but he was unsure about whether it included plates 60, 147, and 159. Earlier plates, numbers 34 and 57, have no guidelines due to their cancellation prior to November 1895.

## 1894–1895 Series Postage Dues: Color

### *Basic Color(s)*

Color selection for the First Bureau postage due stamps was done quickly because of the need to produce the 2¢ postage due stamps. There were only enough large numeral dues on hand for two or three days (Dickey 1984). Figure 5 at the left illustrates a BEP proof of the 2¢ large numeral postage due design (Arfken 1991) pulled from the ABNCo die, recently transferred to the BEP. This proof is deep claret, darker than the bright claret of the last large numeral postage dues (J22 to J28) and bears the wording "O.K. for Color" and the date "July 12" (1894). It also has "No. 1" in pencil, probably indicating the first postage due proof pulled at the Bureau. According to philatelic literature, this unique proof is the approved color sample for the First Bureau dues [3].

Figure 5 also shows ink spectra bar charts on the right for the color proof described above, as well as a J32 1894 Series postage due stamp in claret. The bar graphs are similar, displaying very strong calcium peaks with the proof containing more lead than the corresponding stamp. Neither the proof nor the stamp fluoresces under UV light. Thus, when the ink formulations are correct, the non-fluorescent 1894 Series postage due stamp color matches, or is very similar to, the approved color proof.

**Table III**

**Plate Numbers and BEP Imprint Markings[a] for the 200-subject Plates (1894 and 1895 Series Postage Due stamps)**

| Scott No. | Value | Imprint No. | | | |
|---|---|---|---|---|---|
| | | I | II | IV | V |
| **1894 Series** [b] | | | | | |
| J29 | 1¢ | 57 | | | |
| J30 | 2¢ | 34 | | | |
| J31 | 1¢ | 57 | 147 | | |
| J32 | 2¢ | 60, 159 | | | |
| J33 | 3¢ | 70 | | | |
| J34 | 5¢ | 71 | | | |
| J35 | 10¢ | 72 | | | |
| J36 | 30¢ | 73 | | | |
| J37 | 50¢ | | 74 | | |
| **1895 Series** [c] | | | | | |
| J38 | 1¢ | 57 | 147 | 246 | 1632, 1777, 1778, 1779, 1780 |
| J39 | 2¢ | 60, 159 | | 247, 268 | 1099, 1242, 1243, 1244, 1245, 1783, 1784, 1785, 1786 |
| J40 | 3¢ | 70 | | 254 | 1631, 1787 |
| J41 | 5¢ | 71 | | | 255, 1642, 1792 |
| J42 | 10¢ | 72 | | 256 | 1633, 1781, 1782 |
| J43 | 30¢ | 73 | | | |
| J44 | 50¢ | | 74 | | |

a. The Durland. Catalog describes the BEP marginal imprint markings I, II, IV, and V (Cleland, 2012)

b. Unwatermarked, perforation 12 postage due stamps issued to postmasters in the 1894-95 period.

c. Double-line watermarked, perforation 12 postage due stamps issued to postmasters in the 1895-97 period.


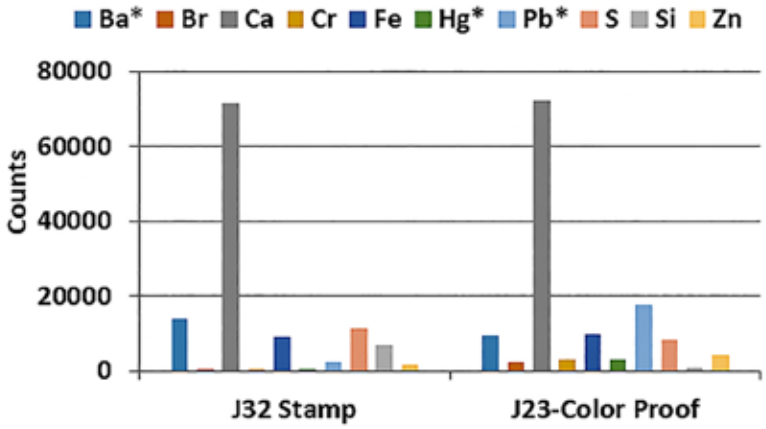


***Figure 5.*** Below, on the left is the J23P1 printed at the BEP as the color sample for the 1894 Series First Bureau dues. The proof printed on India paper is die sunk on card. The die sinkage of this proof measures 47.0 mm x 58.9 mm, and the backing card measures 52.1 mm wide by 66.0 mm high. The proof has a vertical tear through the middle. On the right is X-ray peak bar chart comparisons for the 2¢ J32 stamp shown in Figure 1 with the J23 color model for the First Bureau postage due stamps. The spectra are very similar with color proofs having more lead. A very strong calcium peak dominates both spectra.

As mentioned above, the 1894 Series postage due stamps (J29 to J37) are all perforation 12 and printed on unwatermarked paper. These stamps cover a wide range of colors from bright almost scarlet appearance to a deep dark shade of claret or lake [4] (as shown in Table I). Many are very similar to the approved color proof shown in Figure 5. A search of the philatelic literature adds at least another ten colors to the 1894 and 1895 Series picture, such as lilac, violet rose, crimson, etc. It is possible, with an established stamp reference collection, color gauges, and books such as White and Bower (1986), to distinguish between the various colors of the First Bureau dues.

There are two vermilion, unwatermarked, perforated 12 postage due stamps issued in the 1894 Series: the 1¢ (J29) and 2¢ (J30). Since there are no perforation or watermark differences between these stamps and the other 1894 Series dues, early collectors had difficulty in identifying the vermilion dues. If mint stamps are available, however, there are now known gum differences between the vermilion and claret dues. The gum on mint J29 and J30 stamps is lighter, smoother, and thinner than on the clarets, sometimes slightly crackly or even "spotted." The 2¢ J30 stamps appear most often with the spotted gum and is the same type found on the very early printings of the First Bureau regular issue stamps.

Bower (1971) reported the use of ultraviolet light (UV) to distinguish the J29 and J30 vermilion stamps from the other 1¢ and 2¢ First Bureau dues. The vermilion dues fluoresced "orange" under long wavelength UV light. This indicated the ink contained the aniline dyes as used by ABN-Co. on the bright claret large numeral postage due stamps (J22 to J28), which also fluoresced (Charles, 2017). While Bower, at the time, thought the other 1¢ and 2¢ 1894 Series dues (J31 and J32, respectively) did not fluoresce, we now know other colors of the 1894 and 1895 Series dues (deep clarets for example) exist in both fluorescent and non-fluorescent varieties (Cleland, *et. al.*, 2009). It is clear fluorescence alone is not a unique distinguisher of the rare vermilion dues. Fluorescence coupled with gum differences now allows experts to identify the vermilion dues, assuming the stamps are mint and with gum.

### *Color Variations*

Why did the colors very so much? Most philatelic historians point to poor and variable quality in the pigments and lack of standards in the ink mixing processes. While

***Figure 6.*** 1894 Series postage due large die proofs (LDP). The non-fluorescent 1¢ LDP (Scott J31P1) is on the left and the fluorescent 2¢ LDP (Scott J32P1) is on the right. Each proof appears quite similar in color, yet their ink spectra are very different, as shown in Figure 7.

indeed these things may have been true, there were also two other elements at work at the BEP from the latter half of 1894 into 1895. These elements resulted from the hectic pace and tremendous pressure BEP personnel were under to design and rapidly deliver large quantities of postage stamps and the facilities in which they worked, especially those mixing ink in the "cellar."

The cellar was dark, improperly illuminated for color determination, lacked ventilation and was without temperature or humidity control. It was also subject to dust, moisture, and temperature variations, all of which could affect ink viscosity. To compensate, the ink mixers would add more or less solvent (water) to produce an ink suitable for printing, which also produced subtle color variations in the process. The ink was, by necessity, mixed in small batches because they did not have facilities for storing bulk loads of pigments. Thus, each time a batch of a specific color ink was prepared for the same stamp, it used a different pigment lot typically procured at a different time. This batch phenomenon may have been the single biggest issue in color variations in the First Bureau dues, especially during the early days of stamp production at the Bureau.

In the summer of 1894, there was a shortage of red ink at the BEP based on correspondence from the BEP head to an ink pigment vendor. One letter called for a vendor to ship immediately. The pigment vendor engaged to supply the emergency red ink to the BEP was the same one who had supplied the bright claret ink for the 1891 Series of large numeral postage dues. Given the time urgency placed on the shipment by the BEP, this ink could have been the same, or a slight variant of, the ink used to print the bright claret postage dues. It is quite likely this ink fluoresced like the bright claret large numeral dues (Charles, 2017). This could explain the fluorescent behavior seen in the early First Bureau postage due stamps, proofs, and essays.

Considering many factors, including hectic schedules, poor facilities, pigment quality and availability, and lack of personnel familiar with the stamp making process, it is reasonable to expect the wide range of color variations as reported over the years in the First Bureau postage dues. Thomas F. Morris II (1962), reporting on his father's notes and records, said his father "refers casually to the new design for the seven values of the 1894 Postage Due Series being concerned mainly with the inconsistency of the deep claret color specified; vermilions, carmines, lakes, and roses appear in this issue."

### *Early Proofs & Essays*

To further explore the First Bureau postage due stamps, it is necessary to consider the early essays, proofs, and, of course, the early stamps themselves (J29, J30, J31, and J32). The early essays of interest consisted of the claret J31E-1. J31E-2, J32E-1 (very dark brownish claret), J33E-3, J36E-1, and J37E-2 as described in the book by Charles

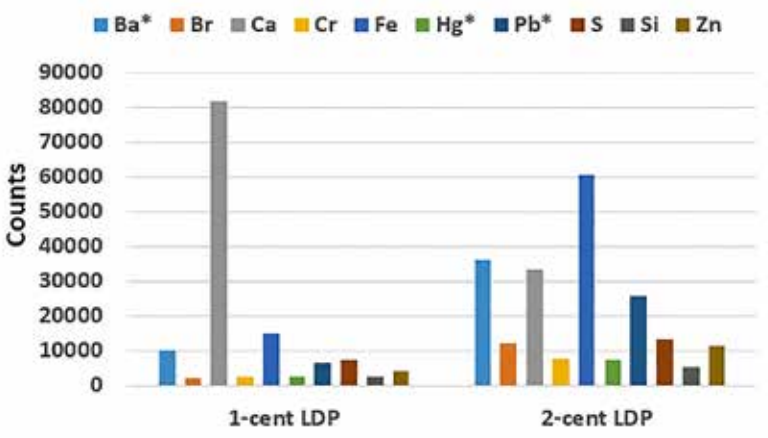


***Figure 7.*** X-ray bar charts for the J31P1 (1¢) and the J32P1 (2¢) LDPs. The 1¢ proof does not fluoresce, and its spectra are similar to the approved color sample as shown in Figure 5. The 2¢ proof is fluorescent with a bar chart similar to a vermilion fluorescent stamp, although it appears darker in color.

(Charles, 2013). All these claret essays fluoresced. Charles illustrated the 2¢ J32E-1 essay in a previous article (Charles, 2017), along with the associated X-ray spectra derived bar chart [5]. The chart, while having strong Fe, Hg, and Pb peaks, did not match the bar graph for the J30 vermilion stamp. The bar graph did, however, match one of the dark brownish claret trial color proofs (J31TC1) described below.

Early proofs consist of the J31P1 to J37P1 large die proofs, J32TC1 trial colors, the J31P5 imperforate plate proof printed on stamp paper in a claret color, the J32P4 imperforate plate proof printed on card in a claret color, as well as the approved plate proofs for the these early issues residing in the Smithsonian. Examples of J31P1 (1¢) and J32P1 (2¢) large die proofs are shown in Figure 6. The 1¢ large die proof does not fluoresce, but the 2¢ large die proof does. Figure 7 illustrates X-ray spectra-derived bar charts for these proofs. The non-fluorescent 1¢ large die proof has a chart similar to the approved color sample shown in Figure 5, while the 2¢ large die proof's spectral response is similar to that of a J30 vermilion stamp (Figure 4) with a slightly enhanced lead peak – probably accounting for the darker color. Of the more than 40 remaining First Bureau large die proofs in the author's collection, only a pre-crack proof [6] of J33P1 fluoresced under long wavelength UV light.

The two known J32TC1 trial color proofs fluoresce. Illustrated by Charles (2017) with their respective bar charts, the trial color proof bar charts both had strong Fe, Hg, and Pb peaks. One of the trial color proofs bar charts matched identically with the bar chart of the J32E-1 essay. The closeness of the match indicated this trial color proof was made soon after the essay was printed and quite possibly with the same batch of ink. The BEP, in the summer of 1894, made minor corrections to dies, such as the addition of detail in the corner ornaments, very rapidly due to the pressure to meet stamp shortages.


***Figure 8.*** Roosevelt album page (circa 1903) containing Scott Nos. J31P2 to J36P2 (1894 Series) on a semi-circular arc about the 50¢ Scott No. J37P2. The page measures approximately 173mm high by 277mm wide. As only 85 Roosevelt Albums were produced, intact pages are quite scarce.

The J31P5 and the J34P4 imperforate plate proofs fluoresce orange under long wavelength UV light. The previous paper by Charles (2017) illustrated these plate proofs along with their X-ray bar charts. As reported, both spectra had strong Ba, Fe, and Pb peaks, but there were significant differences in the spectra between the 1¢ J31P5 claret fluorescent proof, a 1¢ J29 vermilion fluorescent stamp, and a 1¢ non-fluorescent claret stamp. For J34P4, the X-ray spectra-derived bar chart is different from the bar chart of a J30 vermilion stamp. Both plate proof spectra were significantly different when compared to a non-fluorescent J32 stamp whose spectrum was dominated by a very strong Ca peak.

The approved plate proofs at the Smithsonian National Postal Museum also fluoresce as discussed in the separate section below.

### *Later Proofs*

One particularly interesting set of proofs is the circa 1903 small die proofs of the 1894-1895 Series postage due stamps mounted in a Roosevelt Album. Figure 8 illustrates the First Bureau postage due page from a typical Roosevelt presentation album [7]. These proofs, displayed in a semi-circular fashion on the page, appear to be claret in color. Figure 9 presents on the left an example of a 3¢ J33P2 proof cut from a Roosevelt Album page. An unmounted J33P2 is next to the proof excised from the Roosevelt page. Due to the visual difference in color between the unmounted proof and the proof cut from the Roosevelt page, it was possible that the unmounted proofs were from a different printing which used a lighter and brighter ink (perhaps more scarlet) than the ink used for the original mounted proof.

Because the 100 original 3¢ Roosevelt proofs were all printed February 13, 1903, it is unlikely to expect major variations in ink composition. Figure 9, normalized to the calcium peak, presents X-ray spectra-derived bar charts for both proofs. Clearly, both charts are almost identical, with the excised Roosevelt proof containing slightly more lead than its un-mounted counterpart, which might explain its slightly darker color. Based on the similarity of the spectra, it would be difficult to make the case for the unmounted proofs coming from a different printing. Perhaps two slightly different batches of ink were mixed on the same day, or more likely, the color shade differences are due to the different history of the two proofs, including glue mounting, more exposure to light, and various atmospheric elements.

### *Fluorescence*

The author made a trip to the Smithsonian National Postal Museum to check the approved plate proofs of the First Bureau postage dues (1894-1895 Series) for fluorescence. Table IV below presents the results of this inspection. Of the 11 proof sheets inspected, two exhibited strong


***Figure 9.*** On the far left is a J33P2 small die proof excised from a Roosevelt album page (See Figure 8). Next to the excised proof is an unmounted J33P2 small die proof, which visually appears brighter and lighter than the excised proof. On the below left are the bar charts, normalized to the calcium peak of the excised proof for both the mounted and unmounted proofs. The charts were nearly identical except the excised proof had slightly more lead and sulfur than the unmounted proof.

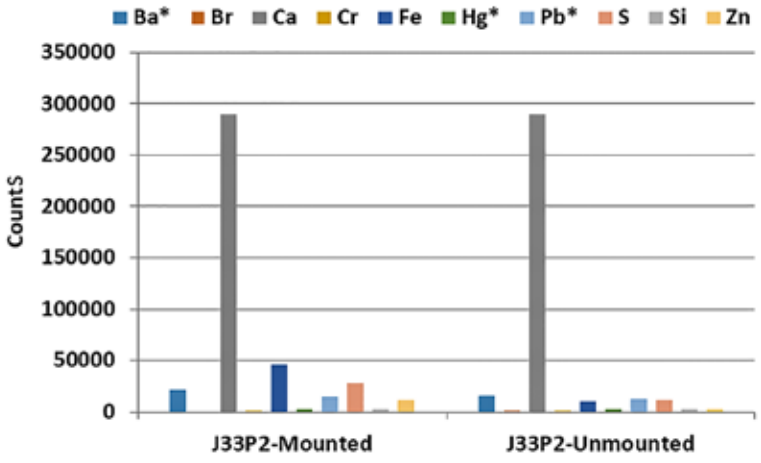


fluorescent behavior and one had a slight hint of a response. Plate no. 57 for the 1¢ postage due value had a strong fluorescent response, while the approved plate proof from plate no. 147 did not. Under room light, the proof from plate no. 57 was claret and appeared bright with sharply defined lines. The proof sheet from plate no. 147 was much darker and, as a result, the stamp images did not appear as bright as those on the no. 57 plate, yet they had similar sharply defined lines. Figure 10 is a composite image of the two plates under ultraviolet (UV) light (312 nm wavelength). Clearly, the two proofs responded differently under the UV illumination.

The proof sheet for the 2¢ value (plate no. 34) also displayed strong fluorescent behavior


***Figure 10.*** Comparison of the fluorescent response (under 312nm wavelength UV illumination) of the approved First Bureau postage due plate proof number 57 (top) with the fluorescent response of approved plate proof number 147 (bottom). Plate proof number 57 glowed bright under the UV illumination.

**Table IV**

**Fluorescence Behavior of the 1894 Series Postage Due Plate Proofs at the Smithsonian National Postal Museum**

| Denomination | Plate # | Approval Date | Color | Fluorescence |
|---|---|---|---|---|
| 1¢ | 57 | 08/11/1894 | Claret | YES[a] |
| | 147 | 02/14/1895 | Dark Claret | NO |
| 2¢ | 34 | 07/14/1894 | Claret | YES[a] |
| | 60 | 08/27/1894 | Dark Claret | NO |
| | 159 | 03/22/1895 | Dark Claret | NO |
| 3¢ | 70 | 09/11/1894 | Dark Claret | NO |
| 5¢ | 71 | 09/11/1894 | Dark Claret | NO |
| | | Unsigned | Dark Claret | NO |
| 10¢ | 72 | 09/11/1894 | Dark Claret | NO |
| 30¢ | 73 | 09/12/1894 | Dark Claret | NO |
| 50¢ | 74 | 10/04/1894 | Dark Claret | [b] |
| | 74 | Unsigned | Brownish Claret | NO |

a. Strong fluorescence under 312 nm wavelength ultraviolet (UV) light

b. There was a hint of fluorescence at 312 nm wavelength; probably needs to be re-examined.

under long wavelength UV radiation, while the second approved proof sheet in the 2¢ series (plate no. 60) did not. The approved 2¢ proof sheet from plate no. 159 also did not fluoresce. Under room light, the proof from plate no. 34 appeared bright with sharply defined lines and was claret in color. The proof sheets from plate nos. 60 and 159 were much darker in color and did not appear as bright, but again they possessed sharply defined lines. Figure 11 shows scanned images of the proof sheets for plate nos. 34 and 60. It is clear from Figure 11 there are visible color differences between the two approved proof sheets. Figure 12 is a composite image of plate nos. 34 and 60 under UV light at 312 nm wavelength. Again, just like the 1¢ proof sheets (Figure 10), there is clearly a difference in the response of the two proofs under UV illumination.

The approved proof sheets for the 3¢ to 30¢ denominations did not fluoresce and were all in the deeper claret color. Both 50¢ proof sheets were in the darker color, but only one had approval signatures. The signed 50¢ proof had a hint of fluorescence and warrants further examination under different wavelengths of UV light.

The fluorescent versus non-fluorescent statistics for the 1894 and 1895 series postage dues were compiled by Cleland *et. al.* (2009). From Cleland's results and this author's observations, one can draw the following conclusions:

1. There is very little, if any, fluorescence in the unwatermarked dues (1894 Series, J29 to J37) outside of the 1¢ and 2¢ denominations ( J29 to J32). In fact, the Cleland study noted only one 3¢ and one 5¢ fluorescent stamp. The author does not have a fluorescent 3¢ or 5¢ claret ( J33 or J34, respectively) in his collection,
2. The discovery of the fluorescent Philippines 50¢ denomination as reported by Charles (2017) and Charles, *et al.* (2016) confirms previously unknown fluorescent J44 stamps exist and this, coupled with the hint of fluorescence in the approved 50¢ plate proof (Table IV), suggests fluorescent J37 (plate no. 74) stamps might also exist.
3. In the double-line watermarked dues (1895 Series, J38 to J44), fluorescence appears in most denominations and plate numbers below 300 on a frequent basis - nominally in the range of 30 to 50%.

## Summary

This article explored some aspects of the color and fluorescence in both 1894 and 1895 Series postage due stamps and their essays and proofs. It is clear the printing of the 1894 and 1895 Series of postage due stamps used both fluorescent and non-fluorescent ink. It appears fluorescence in the 1894 Series was confined to the lower stamp denominations, namely the 1¢ and 2¢, although Cleland *et al.* (2009) reported a single 3¢ J33 and a single 5¢ J34 that fluoresced. Also, all the claret colored essays of the First Bureau dues fluoresced. The approved plate proofs at the Smithsonian National Postal Museum for plate no. 34 (the first 2¢ plate) and plate no. 57 (the first 1¢ plate) strongly fluoresce under UV illumination. Historically, fluorescence in these 1¢ and 2¢ 1894 Series postage due stamps was associated with the vermilion color (*i.e.,* J29 and 30).

A wide range of colors can exist in these stamps, from the so-called vermilions to dark claret and dark brown shades, including the First Bureau essays and trial color proofs (Charles 2017). There are marked differences in ink composition between the fluorescent and non-fluorescent stamps, with most non-fluorescent stamps having a very similar ink composition or spectra (see Figures 5, 7, and 9). The composition spectra for the fluorescent stamp ink, while having the same overall appearance (which is markedly different from the non-fluorescent spectra), are not as uniform with respect to the different elemental peak ratios. These differences in peak ratios may explain the color range encountered in the fluorescent inks, ranging from pale vermilion to deep brown-claret shades. It appears a strong iron peak exists in the deep brown-claret shades, while in most claret shades (non-fluorescent) the spectra are dominated by a very strong calcium peak. Part II of this article will use X-ray fluorescence spectrometry to determine the identity of stamps on cover and to establish a timeline for the introduction of various colors.

## Acknowledgements

The author wants to thank Thomas Lera, then at the Smithsonian National Postal Museum (NPM), for help in collecting the initial X-ray spectra for some of

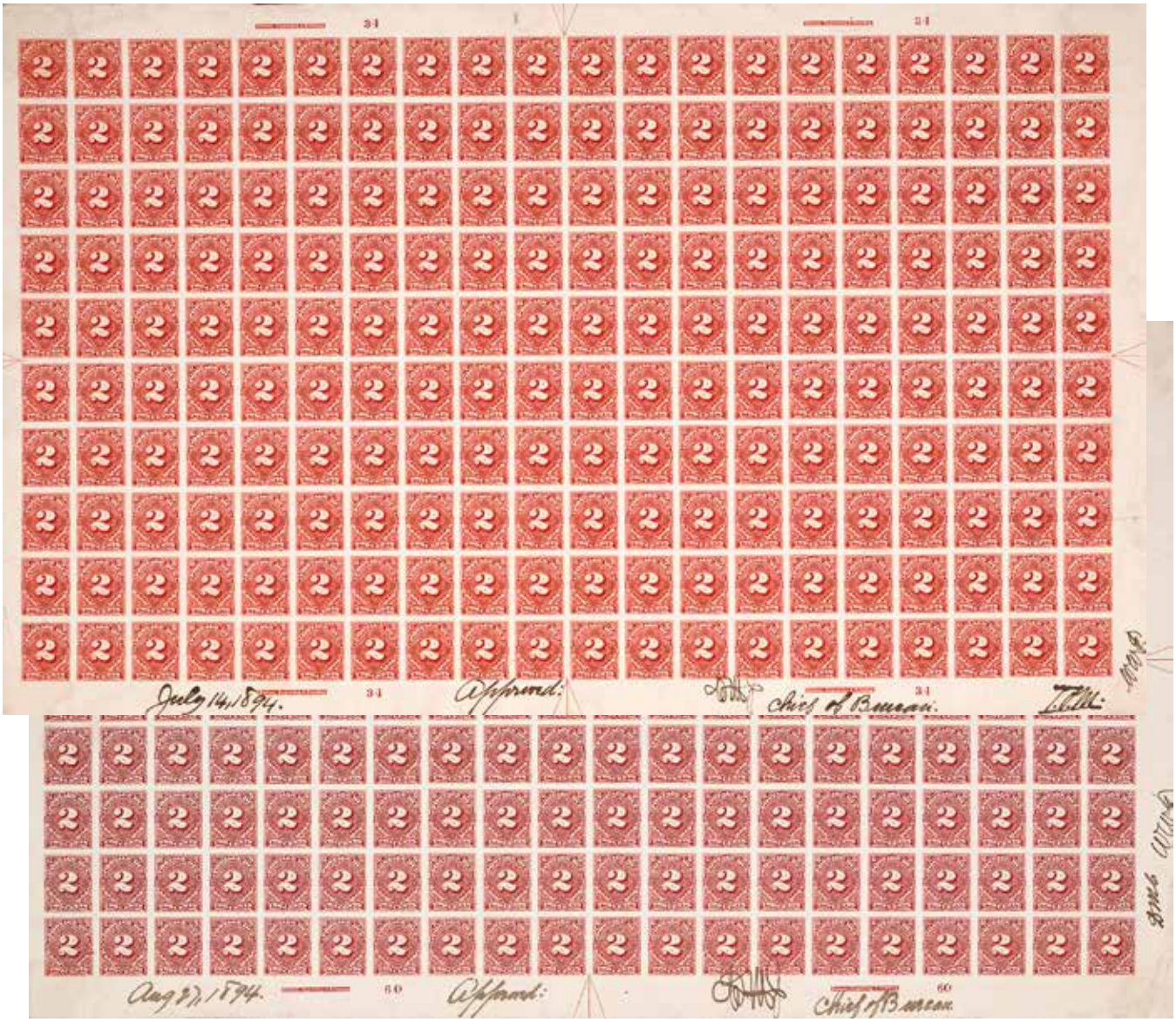


***Figure 11.*** Scans of the approved 2¢ First Bureau postage due proof sheets for plate nos. 34 (upper left) and 60 (lower right). The proof sheet for plate no. 34 is brighter and lighter than the proof sheet for plate no. 60. The proof sheet for plate no. 34 fluoresces while the proof sheet for plate 60 does not. (Images courtesy of the National Postal Museum.)

the samples used in this study, Jim O'Donnell (NPM) for his help in finding the proof sheets, and Susan Smith (NPM) facilitated the collection of additional spectra from both the original and subsequent samples.

## End Notes

[1] The Scott Publishing Company, 911 Vandemark Road, Sidney, Ohio 45365-0828 publishes the *Scott Standard Postage Stamp Catalogue*. Scott Numbers are a Scott Publishing Company trademark. add correct citation.

[2 In stable atoms electrons occupy discrete energy levels (shells or orbitals) with a specific binding energy. The innermost shell is the K-shell containing 2 electrons, the next is the L-shell with 3 subshells and containing 8 electrons total, next is the M-shell with 5 subshells and 18 electrons, and so forth. X-ray fluorescence spectrometers can generate source X-rays with sufficient photon ionization energy to eject an inner shell electron from its orbit or shell (*i. e.*, overcome its binding energy). An outer shell electron, to maintain atomic stability, fills this electron "vacancy" created in the inner shell, primarily K- and L-shells. Fluorescence can occur when an X-ray photon is emitted (release of energy) as the outer shell electron moves into the lower energy inner shell. The fluorescent X-ray energy peaks identify the element, and the peak intensity is proportional to its concentration.

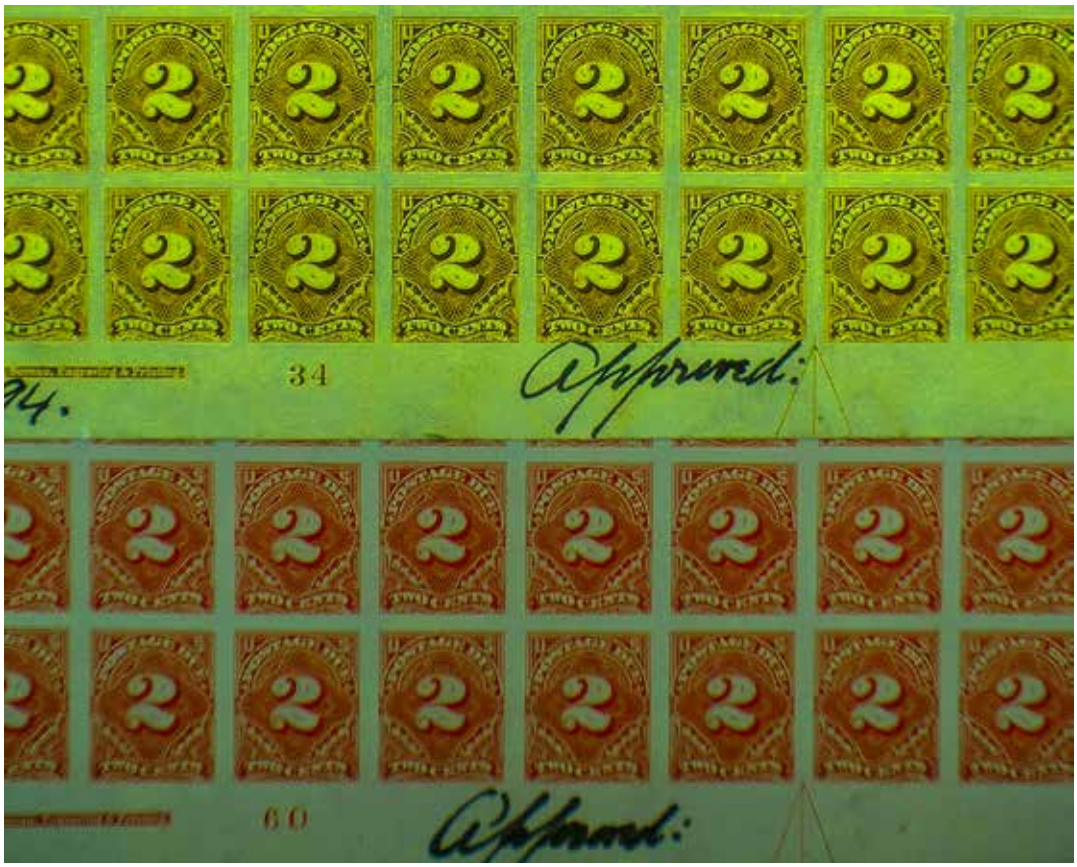


***Figure 12.*** Comparison of the fluorescent response under 312 nm wavelength ultraviolet light of the approved First Bureau postage due plate proof no. 34 (top) with fluorescent response of approved plate proof no, 60 (bottom). Plate proof no. 34 glowed bright under the UV illumination. (Images courtesy of the National Postal Museum.)

Binding energies and/or energy levels in every element are different and are characteristic of the particular element. As mentioned above, as the electron separates from the inner shell of the atom and an electron from a higher energy shell falls into the hole in the lower shell, it releases energy equivalent to the difference between the energy levels involved. The released energy can be in the form of an X-ray or transferred to other shell electrons (Auger effect). The probability of an X-ray resulting from this event is called the fluorescent yield "γ" and depends on the element's atomic number and the shell in which the hole or vacancy occurred. The value of γ is very low for the light elements (e.g. $10^{-4}$ for boron) and almost reaches a value of 1 for the K-shell X-rays of heavier elements such as uranium.

[3] This proof was from the Earl of Crawford collection. James Ludovic Lindsay (1847–1913) was the 26th Earl of Crawford and a world recognized philatelist. He built several outstanding collections of Great Britain and the United States. Crawford's philatelic library was the largest and most complete of his time. His United States collection contained unmatched holdings of essays, proofs and engraver's models and designs from banknote company and U.S. Government archives. It included the unique set of full sheets of plate proofs of United States stamps from 1857 to 1893.

[4] Lakes are generally purplish red pigments prepared from lac or cochineal. Lac is a resinous substance usually secreted by scale insects and chiefly used in the form of shellac. Cochineal is a red dye consisting of the dried bodies of female cochineal insects used typically as a biological stain and/or indicator. The traditional use of the term "lake" to describe certain deep purplish red shades of the postage due stamps seems somewhat warranted, although the true meaning of the term as a color is uncertain. In the dye and pigment industry, a lake refers to any of a wide range of bright, translucent organic pigments composed of a soluble dye absorbed or combined with an inorganic carrier. Lakes can have many hues from red to blue and even yellow.

[5] The Charles (2017) article in the *Proceedings of the Third International Symposium on Analytical Methods in Philately* illustrates the essays and proofs and their X-ray spectra-derived bar charts described in this section. If the reader refers to that article, they can find the 2¢ J32E-1 essay pictured in Figure 19 on page 102. Its bar chart appears in Figures 20 and 21 on page 103. The 2¢ J32TC1 trial color proofs also appear in Figure 19 (page 102) with bar charts given in Figures 20 and 21 (page 103). The plate proofs J31P5 and J34P4 appear in Figure 24 on page 105, while the respective bar charts appear in Figure 26 (page 106).

[6] The 3¢ die was hardened on August 18, 1894. During the hardening, the original 3¢ die cracked, probably due to a flaw in the metal or an improper heat-treating and quenching cycle. Regardless of the cause, this crack in the die would have produced a noticeable line in the finished stamp, causing rejection by the Post Office Department. To prevent the complete loss of time and associated cost of the failed 3¢ die, they clamped the

cracked 3¢ die to close the crack, then used it to make a transfer roll. The crack appeared as a raised line on the transfer roll, which allowed removal with a graver and the tool marks burnished away. The repaired transfer roll was then hardened and used to make a new die for preparation of the 3¢ stamp printing plates. Walter McIntire gives the complete story in his article "United States Postage Due Stamps: The Broken 3¢ Die-Series of 1894," *The Bureau Specialist*, Vol. 36, No. 4 (April 1965), pp. 124-126.

[7] Roosevelt albums (circa 1903) are presentation albums containing small die proofs of all current and prior United States stamps (including the postage dues). High-ranking Post Office Department officials and members of Congress received these albums as gifts. The BEP produced eighty-five Roosevelt albums, so named because of their issuance during the presidency of Theodore Roosevelt. A picture of an intact Roosevelt album is in Charles (2013, 151).

## References


Arfken, George B. 1991. *Postage Due: The United States Large Numeral Postage Due Stamps 1879–1894*, Chicago: Collectors Club of Chicago, Chapter 2.

Bower, Warren R. 1971. Ultraviolet Identification of U. S. Postage Due Stamps and Proofs, *Essay-Proof Journal*, Vol. 28, pp. 99–100.

———. 1986. Update on the Vermilion Bureau Postage Dues, *The United States Specialist*, Vol. 57, No. 11, November , pp. 532–533.

Charles, Jr., Harry K. 2013. *United States Postage Due Stamp Essays, Proofs, and Specimens,* The Collectors Club of Chicago, 289 pages.

———. 2020. Exploring Color Mysteries in the United States Large and Small Numeral Postage Due stamps using X-ray Fluorescence Spectrometry. In: Smith, Susan and J. H. Barwis, editors. *Proceedings of the Third Symposium on Analytical Methods in Philately.* Akron, Ohio: The Institute of Analytical Philately, pp. 87–116..

Charles, Jr., Harry K. and Clarke Yarbrough. 2016. United States Possession Postage Due Stamps: Philippines Part II, *The United States Specialist*, Vol. 87, No. 3, March, pp. 210–235.

Cleland, W. Wallace. editor, *2012 Durland Standard Plate Number Catalog*, United States Stamp Society, Katy, TX, pp. A21–A22.

Cleland, W. Wallace. 1987. Printing History of the Early Postage Due Plates, *The United States Specialist*, Vol. 58, No. 8, August, pp. 339–347.

———. 1987. Printing History of the Early Postage Due Plates – 2," *The United States Specialist*, Vol. 58, No. 10, October, pp. 437–445.

Cleland, W. Wallace, Clarke Yarbrough, and William Schuman. 2009. Early Postage Dues with Fluorescent Ink, *The United States Specialist*, Volume 80, No. 7, July, pp. 293–296.

Dickey,Budd. 1984. Beginnings of Postage Stamp Production by the Bureau of Engraving and Printing, *The United States Specialist*, Vol. 55, No. 11 (November), pp. 487–493.

Luff, John N. 1902. *The Postage Stamps of the United States*, New York: Scott Stamp and Coin Company, pp. 245–252.

McIntire, Walter A. 1969. The 1894 and 1895 Bureau Printed Postage Dues, *The United States Specialist*, Vol. 38, No. 5 (May) pp. 204–210.

Morris II, Thomas F. 1962. The Life and Work of Thomas F. Morris (1852–1899)—Designer of Bank Notes and Stamps, *The Essay-Proof Journal*, Vol. No. 97, pp. 9–16.

White, R. H. and W. R. Bower. 1986. *Encyclopedia of the Colors of United States Postage Stamps: Volume V: The Postage Due Issues 1879–1916*, Philatelic Research Ltd. Germantown, MD, pp. 10–12, 47–56.

# 1894 and 1895 Series First Bureau Postage Due Stamps: Questions of Color, Fluorescence, and Early Use: Part II

*Harry K. Charles, Jr.**

## Abstract

This paper examines the early use of the 1894 and 1895 Series First Bureau postage due stamps on cover. It is the continuation of Part I in which the distinction in elemental content between fluorescent and non-fluorescent ink on essays, proofs, and stamps was made using X-ray fluorescence spectrometry combined with ultraviolet fluorescence. In Part II, working with dated First Bureau postage due stamps on cover, the study results led to the development of a timeline for the introduction of certain stamp colors or varieties. For example, the data showed the 2¢ vermilion First Bureau postage due stamp went into circulation before the 2¢ claret postage due stamp, which was the government approved color for the issue. The limited data to date is unclear as to whether the 1¢ postage due stamp in vermilion appeared before the 1¢ claret variety, but it is likely.

## Introduction: Recap of Part I

Part I ((Charles, 2020b)) presented a detailed study of elemental ink composition of the 1894 and 1895 Series First Bureau postage due essays, proofs, and stamps, using X-ray fluorescence spectrometry combined with simple X-ray fluorescence. It also described the basic instrumentation and analysis techniques used to develop the X-ray fluorescence spectra-derived bar charts. These charts are the primary method used for stamp and color comparisons. The results indicated the ink composition for fluorescent and non-fluorescent stamps were quite different with the non-fluorescent essays, proofs, and stamps displaying a consistently strong calcium peak in relationship to the other constituent elements measured (Part I, Figures 5, 7, and 9). The fluorescent stamp spectra were much different, consistently displaying strong barium, lead and mercury peaks along with calcium (See below and Part I, Figures 4 and 7). Given the strong consistency of the results with essays, proofs, and stamps, it was then applied to stamps on cover to determine the particular stamp color and, coupled with the postal markings, determine when it was used.

*Laurel, MD 20723

### *1894–1895 Series Postage Dues on Cover*

As mentioned in Part I ((Charles, 2020b)) and the article by Charles (2020), the dating of 1894 and 1895 Series postage due stamps on cover is extremely difficult due to the small population of properly tied stamps. The 2¢ vermilion postage due printing, J30, occurred over a two-month period before plate no. 60 replaced the un-hardened plate no. 34. The earliest documented cover (EDC) recorded for the J30 vermilion fluorescent postage due stamp is August 10, 1894, about 27 days after the plate went to press. This cover, previously illustrated by Charles (2020a), was a post card mailed from Germany July 31, 1894. The receiving post office applied the J30 postage due stamp on August 10, 1894. The EDC for the 1¢ J29 vermilion is November 14, 1894, as shown in Table 1. An illustration of this cover appeared in Charles (2017). Bower (1986) also reported a 1¢ J29 vermilion cover with a November 15, 1894, date. Figures 1 and 2 illustrate early use covers for J29 (November 19, 1894) and J30 (August 30, 1894), respectively, in the author's collection. Bower (1986) also reported an early use cover for J30, August 22, 1894. Both the J29 and J30 stamps on these early use covers fluoresced orange under long wavelength UV light.

**Table I**

**Earliest Documented Cover (EDC) of the 1894 Series Postage Dues (Scott Nos. J29–J37)**

| Denom. | Scott No. | Plate No. | Plate Approval Date | Issue Date to Postmasters | Color[a] | Earliest Documented Use on Cover | Comments |
|---|---|---|---|---|---|---|---|
| 1¢ | J29 | 57 | 8/11/1894 | 8/14/1894 | Vermilion | 11/14/1894<br>11/19/1894 | Pre-cancel<br>Figure 1, Pre-cancel |
| | J31 | 57 | 8/11/1894 | ? | Deep Claret | 10/06/1894[b] | Figure 4 |
| | | 147 | 2/14/1895 | ? | Deep Claret | | |
| 2¢ | J30 | 34 | 7/14/1894 | 7/20/1894 | Vermilion | 8/10/1894<br>8/30/1894 | <br>Figure 3, Stamp Tied |
| | J32 | 60 | 8/27/1894 | ? | Deep Claret | 10/31/1894[c] | Figure 5 |
| | | 159 | 3/22/1895 | ? | Deep Claret | | |
| 3¢ | J33 | 70 | 9/11/1894 | 4/27/1895 | Deep Claret | | |
| 5¢ | J34 | 71 | 9/11/1894 | 4/27/1895 | Deep Claret | 7/17/1895[d] | Figure 6 |
| 10¢ | J35 | 72 | 9/11/1894 | 9/24/1894 | Deep Claret | 6/08/1895[e] | Figure 8 |
| 30¢ | J36 | 73 | 9/12/1894 | 4/27/1895 | Deep Claret | | |
| 50¢ | J37 | 74 | 10/14/1894 | 4/27/1895 | Deep Claret | | |

a. The general color listed in Scott for the First Bureau Dues (J29–J37). The shades of claret range from very dark/deep to light almost rose. The vermilions have a similar situation ranging from pale to deep vermilion.

b. APEX Certificate No. 190455 (March 5, 2010) states "United States, Scott No. J23 and J31, used on cover from Great Britain, back stamped 10/6/1894 NY and 10/8/1894 Appleton Rec'd, EDU for J31 as of certificate date, genuine, 1¢ stamps defective." See Figure 4.

c. APEX Certificate No. 192551 (August 6, 2010) states "United States, Scott No. J32, used on stationery entire (crease), 10/31/1894, EDU [as] of certificate date, Brockton, Mass., back stamped Boston same date, genuine in all respects." See Figure 5.

d. Earliest in author's collection. See Figure 6.

e. Earliest in the author's collection with spectral data. See Figure 8. The author has a single J35 tied to a cover from England dated October 22, 1894, which is less than 30 days after the issue date.

Because the watermarks on these perforation 12 stamps cannot be reliably determined while the stamps are attached to the covers, the question arises, is it possible to tell whether the J29 and J30 stamps on cover are actually J29 and J30 or just a fluorescent version of the J31 or J32 clarets? Since the dates on all the covers described above all fall well before the dates of issue for the J38 and J39 double line watermark 1895 Series postage dues, clearly these stamps must be from the 1894 Series postage dues. Figure 1 presents X-ray spectra-derived charts for the J29 vermilion stamp and the J29 stamp on the cover. In looking at the charts, the J29 vermilion stamp and the stamp on the cover appear almost identical, further indicating this is a J29 on cover.

Since the date on this early use cover was 43 days later than the earliest recorded date for a non-fluorescent J31, one must consider whether this early use of a J29 fluorescent stamp might simply be a use of a fluorescent J31 claret. Figure 2 compares the J29 spectra-derived charts with a chart formed from the spectrum of a claret 1¢ fluorescent J31 Postage Due stamp. According to Cleland (Cleland *et. al.*, 2009), about 25% of the stamps from plate no. 57 (first plate for the 1¢, perforation 12, un-watermarked dues) fluoresce. As seen in Figure 2, the chart for the J31 fluorescent stamp is similar to those of the J29 samples, with a slight reversal in the relative heights of the calcium and barium peaks suggesting a different formulation in ink; to make such a distinction with confidence requires the study of many more samples.

Figure 3 illustrates the X-ray spectra-derived charts for the J30 vermilion stamp and an early use J30 stamp on the cover (August 30, 1894), along with the cover image. In comparing the charts of the J30 vermilion stamp and the stamp on the cover, the appearance is almost identical, indicating this is very likely a J30 on cover. As listed in Table 1, the earliest known use date for the J32 claret stamp is October 31, 1894, which is more than 80 days after the reported EDC for the J30 vermilion of August 10, 1894. Given the early use date, the color, the fluorescence under UV light, and the fact that Cleland (Cleland *et. al.*, 2009) reported no fluorescent claret 2¢ postage dues in the 1894 Series (J32), the stamp on the cover in Figure 3 is a vermilion J30. The author does not have any fluorescent 2¢ claret unwatermarked postage dues in his collection.

Since we have explored the early use of the 1¢ and 2¢ vermilions, what about early uses for the non-fluorescent

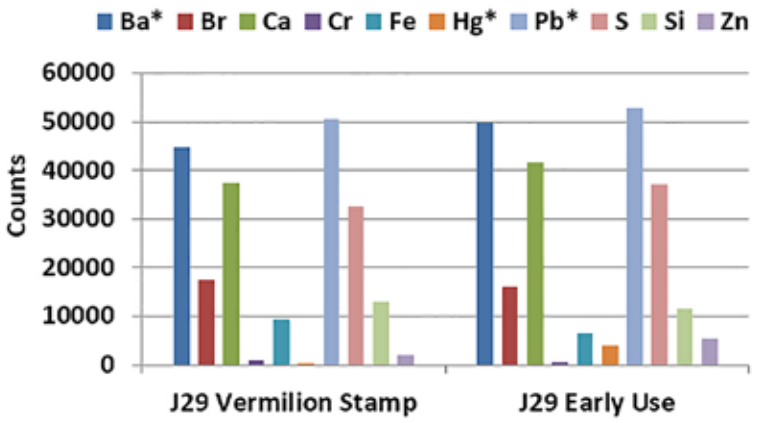


***Figure 1.*** Above is an early use cover for the J29 fluorescent deep vermilion postage due stamp. Cover postmarked on November 19, 1894, just five days after the EDC (see Table 1). On the left are the charts for the J29 vermilion stamp and the J29 stamp on the early use cover. The charts are very similar, indicating this stamp on the cover is a J29 vermilion.

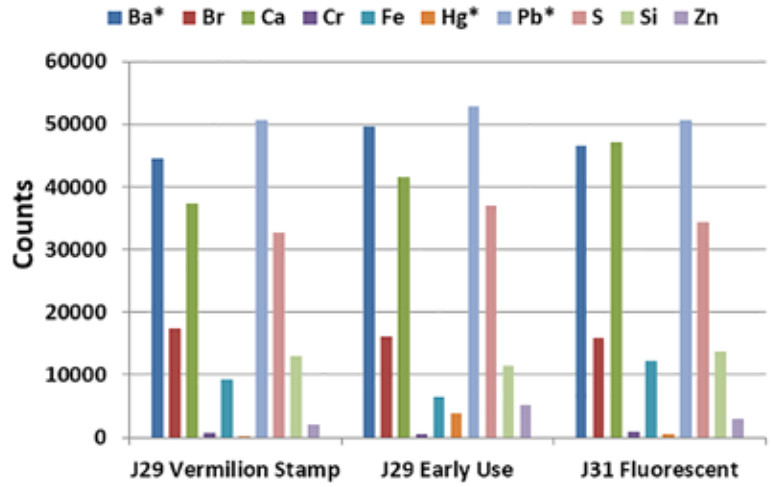


***Figure 2.*** On the left, charts for a J29 vermilion stamp, J29 vermilion stamp on the early use cover at center, and a fluorescent J31 stamp on right. The chart for the J31 fluorescent stamp is similar to those of the J29 samples, with a slight reversal in the relative heights of the calcium and barium peaks

"claret" stamps? Figure 4 illustrates an October 6, 1894, cover from Great Britain that contains four 1¢ (J31) claret postage due stamps in addition to three J23 large bank note dues [1]. This cover was the EDC as of the March 5, 2010 certificate date (APEX No. 190455). Figure 4 also illustrates the X-ray derived chart for this stamp, along with the chart for a non-fluorescent J31 stamp. Each bar chart contains a very strong calcium peak consistent with all non-florescent 1894 and 1895 Series postage dues.

Figure 5 illustrates a postal stationery cover mailed from Brockton to Boston, Massachusetts, on October 30, 1894. It was overweight, and the postmaster used a 2¢ claret 1894 Series postage due J32 stamp as receipt for payment. According to the certificate accompanying this cover, it was the EDC for the 2¢ claret as of August 6, 2010 (APEX No. 192551).

Figures 6 and 8 show additional 1894 Series covers. Figure 6 illustrates a pair of 5¢ claret J34 postage due stamps used on July 17, 1895. Since the 5¢ 1894 Series postage due stamps issue date to postmasters was April 27, 1895, this makes it a relatively early use of J34. In addition, since the 1895 Series 5¢ postage due stamps (J41) were not issued


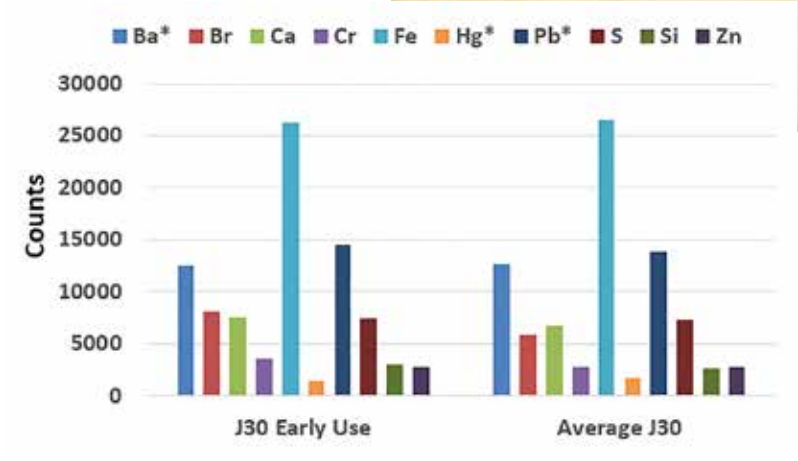


***Figure 3.*** An early use cover for the J30 fluorescent deep vermilion postage due stamp, mailed August 30, 1894, above. August 30, 1894, is just 20 days after the EDC (See Table I). A double oval Philadelphia hand stamp ties the 2¢ J30 postage due stamp. On the left are the charts for the average J30 vermilion stamp and the J30 stamp on the early use cover. The charts are very similar, indicating this stamp on the cover is a J30 vermilion.


***Figure 4.*** On left is the October 6, 1894, EDC for the 1¢ claret J31 postage due stamp (as of March 5, 2010). The cover has four 1¢ claret postage due stamps as well as three 2¢ large numeral postage dues paying the 10¢ postage due fee (5¢ international rate plus the UPU doubling penalty). Below are charts for the J31 claret stamp and the J31 stamp on the early use cover to Appleton, Wisconsin. The charts are very similar, indicating the 1¢ stamps on the cover are a J31 clarets.

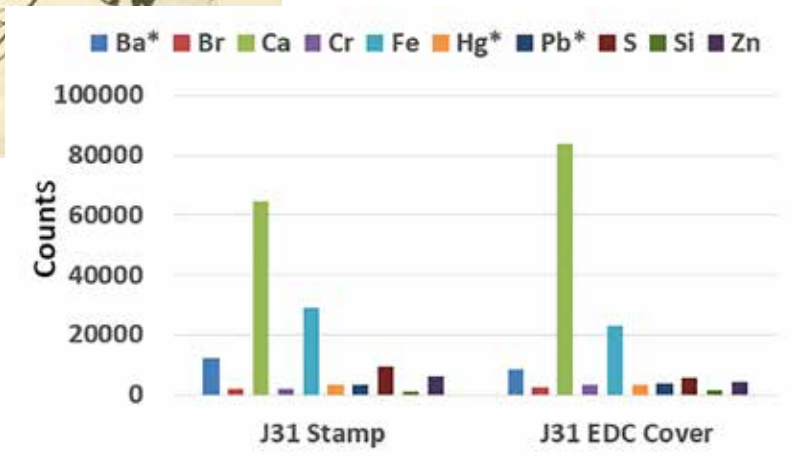


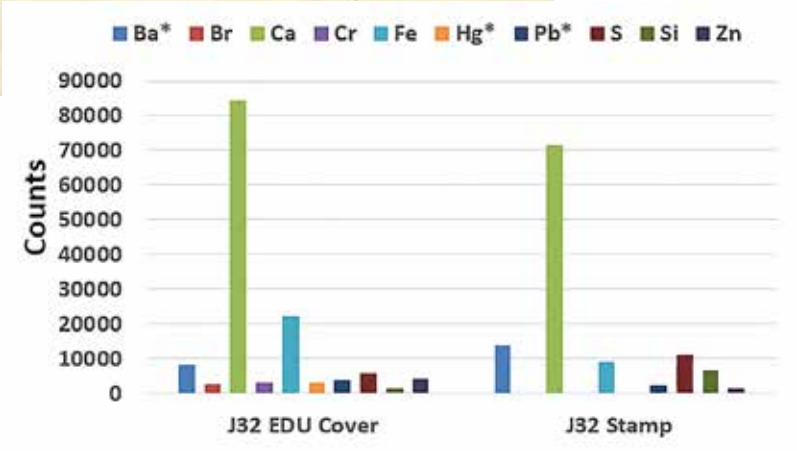


***Figure 5.*** On left is EDC for the 2¢ claret J32 postage due stamp (as of August 6, 2010). Cover mailed from Brockton, Massachusetts on October 30, 1894, to Boston. It was assessed 2¢ postage due (probably for being overweight). The payment was receipted by a 2¢ 1894 Series (J32) postage due stamp. The charts are on the right are for the stamp on the early use cover and a non-fluorescing J32 reference stamp.

until October 15, 1895, it makes the identification relatively straightforward. Figure 7 shows an X-ray spectrum-derived chart for these stamps. Individual J34 stamps have not been analyzed to date, but it is expected their spectra charts will be similar to those of the stamps shown on cover in Figure 6, which is similar to the non-fluorescent varieties of both the 1894 and 1895 Series First Bureau postage dues.

Figure 8 shows a pair of 10¢ claret J35 postage due stamps used on June 8, 1895, a little less than six months after their issue date on September 24, 1894, and before the September 14, 1895, issue date of J42 in the 1895 Series. Figure 7 also contains the chart for these stamps. The chart shows the typical strong calcium peak of the non-fluorescent stamps of the 1894 and 1895 Series First Bureau postage dues.

The author has not been able to find 1894 Series 3¢, 30¢, and 50¢ postage dues used on cover between their issue dates and the subsequent issue dates of the corresponding stamps in the 1895 Series. Recent correspondence with the American Philatelic Research Library indicated they were not able to find early use dates for J33 through J37. The 3¢ 1894 Series J33 ap-


***Figure 6.*** This cover mailed from England to Bar Harbor, Maine, was assessed 10¢ postage due when it entered the United States mail stream in New York on July 7, 1895. The payment of the 10¢ postage due was receipted with a vertical pair of 1894 Series 5¢ postage due stamps (J34) when the letter arrived in Bar Harbor.

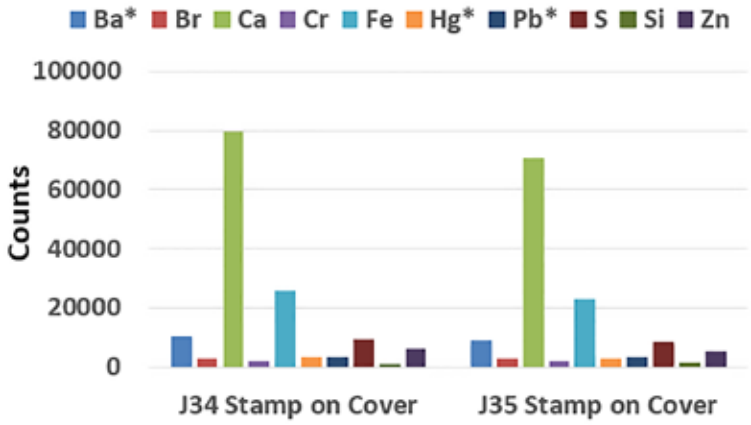


***Figure 7.*** X-ray spectra derived charts for the 1894 Series 5¢ J34 pair and the 10¢ J35 pair of postage due stamps on cover (Figures 6 and 8). Each spectra is dominated by a strong calcium peak which is consistent with the other non-fluorescent 1894 and 1895 Series postage dues.


***Figure 8.*** Packet boat cover mailed without postage, addressed to New Bedford, Massachusetts. It was assessed 20¢ postage due, and the June 8, 1895, payment was receipted in New Bedford with a pair of 1894 Series 10¢ postage due stamps (J35).

pears to be extremely difficult to find on cover due to the lack of a 3¢ rate. Thus, it would only appear in making up higher rates or if the cover was underpaid by 3¢. The issued quantity of the J33 unwatermarked dues was about 170,000.

The 1895 Series 3¢ is also scarce on cover, especially ones used during the 1895-1897 timeframe. The earliest dated copy of an 1895 Series 3¢ Postage Due J40 on cover in the author's collection is dated March 30, 1899 (See Figure 9). It is a pair used to pay a 6¢ postage due assessment. The author invites readers to send images of early use covers for the 1894 Series of postage due stamps especially for the 3¢, 5¢, and 10¢ denominations. Please alert me to any identified use of either 1894 or 1895 Series 30¢ and 50¢ denominations on cover. I have in my possession a 1907 use of the 30¢ and 50¢ Postage Due stamps from the 1895 Series as shown in Figure 10.

As a final illustration, consider the cover in Figure 11. Mailed from England on June 19, 1896, the cover was double weight and hence charged 8¢ postage due, which included the penalty. One 5¢ J25 Large Numeral postage due stamp and two First Bureau postage due stamps receipted the payment. According to the Philatelic Foundation Certificate #0181737, the 1¢ stamp is J31 (non-fluorescent) and the 2¢ was identified as a J30 vermilion stamp. The 2¢ stamp does indeed fluoresce, and the color is distinctly different from the other two stamps, so it was determined to be vermilion. EDC's for the 2¢ vermilion are in the summer of 1894, almost two years prior. Given the limited time in which plate no. 34 vermilion stamps were printed, one wonders if this is truly a stamp from plate no. 34 or simply a lighter version of J32 printed with fluorescent ink. Note the 1¢ First Bureau stamp and the claret ABNCo. Large Numeral due appear similar in color, although the closeness of the engraved lines on the 1¢ stamp makes it appear somewhat darker.

An X-ray spectrum derived bar chart for this 2¢ stamp is also shown in Figure 11, along with the spectrum of the average values for a J30 vermilion stamp reference lot. It is clear the bar charts are very similar with almost identical iron and barium peaks. The 2¢ First Bureau cover stamp from England contains a little more lead than the reference stamp lot. Given the closeness of the spectra, the fluorescence and the general appearance of the stamp, it is indeed a J30 vermilion and not a fluorescent J32, despite the late date of use.


***Figure 9.*** Left, 3¢ Pair of the 1895 Series postage dues (J40) on cover.

***Figure 10.*** (Below) Piece of a package wrapper containing two 50¢ J44 postage dues as well as one each 30¢ (J43), 10¢ (J42), and 2¢ (J39) postage due stamps. The package, containing printed matter, was mailed from England to the United States in June 1907. Upon arrival, the package was inspected and found to contain a letter class of mail. This caused the post office clerk to reclassify the wrapper to the letter rate and charge the difference ($1.42) between the prepaid printed matter rate and the letter rate. The package arrived at the Dead Letter Office on June 6, 1907. The Farnham, England July 4 CDS suggests the U. S. Dead Letter Office returned the package to the original sender.


## Discussion

From the above information and that contained in Part I ((Charles, 2020b)), the reader should have gained an appreciation for the difficulty in the identification of particular 1894 Series, and to some extent, the 1895 Series postage due stamps. Color, fluorescence, watermarks and even gum type all play a role in the positive identification of a particular stamp. A lot of the major questions center on the distinction between the vermilion J29 and J30 postage due stamps and their J31 and J32 claret counterparts. Bower (1971) had thought fluorescence was the key, but we now know shades of claret also fluoresce in both the 1894 and 1895 Series. In addition, the century-old controversy of whether vermilion or claret stamps surfaced first appears from time to time in the literature.

Given the data presented above, it is clear the vermilion 2¢ postage due stamps (J30) went to press first:

1. Plate no. 34 printed the J30 postage due stamps
2). Plate no. 34 was only used between July 14 and September 10, 1894


***Figure 11.*** On the left is a double weight cover from England (July 18, 1896). Rated 8¢ postage due, the postage due payment was receipted with one 5¢ (J25), one 2¢ (J30), and one 1¢ (J31). Both the 5¢ ABNCo. Large Numeral postage due and the 2¢ First Bureau due fluoresce. On the right is the bar chart for the J30 postage due stamp on the cover showing a comparison with the chart for the J30 reference average.

3. All known stamps and proofs from plate no. 34 fluoresce
4. Colors of stamps from plate no. 34 are clearly different than those of later printings, being brighter and lighter as is the approved plate proof in the National Postal Museum
5. The listed EDC for J30 is August 10, 1894, just 20 days after the issuance of the new postage due stamps to postmasters.
6. Since the First Bureau design stamp was not tied on the EDC, some may argue it was added later or replaced another stamp, but the early use cover dated August 20, 1894, in Figure 3 clearly has the 2¢ vermilion tied.
7. The EDC, as of August 6, 2010, for the 2¢ claret is October 30, 1894.

From the statements above, it can be determined the light, bright shade J30 vermilion of the fluorescent 2¢ First Bureau dues appeared first.

The question of whether the 1¢ J29 vermilion came before the darker more claret 1¢ First Bureau postage due (J31) stamps is not clear, and there are several factors which lead to this uncertainty. These include:

1. The first plate for the 1¢ First Bureau postage due stamp was plate no. 57. The approved proof sheet, at the National Postal Museum, bears the date August 11, 1894. The stamps on this proof sheet both fluoresce and are lighter and brighter in color than those on the subsequent proof sheet plate no. 147, which does not fluoresce (Figure 10 of Part I (Charles, 2020b)).
2. The plate proof on stamp paper J31P5 fluoresces, although is a deeper color shade than the J29 vermilion (Charles, 2020a).
3. The earliest EDC for the J29 vermilion is November 14, 1894, which is three months after the August 14, 1894, issue date of the new 1¢ stamps to postmasters. This has caused some authors to consider vermilion was not the color of the 1¢ first printing. However, there was at least a two-month supply of ABNCo large numeral postage dues in the hands of postmasters (Charles, 2013), which needed to be used up before the newly issued First Bureau dues would be placed in service.
4. A second, early use 1¢ fluorescent vermilion cover is shown in Figure 1. This cover is dated November 19, 1894.

5. The EDC (as of March 5, 2010) for the non-fluorescent 1¢ claret is October 6, 1894 (Figure 4), which precedes the EDC for the J29 vermilion by about a month and is consistent with the two-month supply of 1¢ Large Numeral dues available to postmasters.

Thus, based on these limited examples and the fact plate no. 57 was in use until sometime in 1896, it is very difficult to conclude definitively which came first. The EDC and the cover in Figure 4 might suggest that the J31 1¢ non-fluorescent claret may have been issued first, and the vermilions shortly thereafter as a color variant. Contrary to this, there are several logical or common-sense factors suggesting the J29 vermilion came before the J31 claret.

Vermilion inks were used in the summer of 1894 for the 2¢ J30 stamp; thus, it makes sense the same ink formulations would be used for the 1¢ postage due stamps produced essentially during the same timeframe. After printing, stamps were stored awaiting distribution and, typically, the stored stock was not rotated before distribution; hence, newer stock would be on top and shipped to postmasters while the older stock remained in storage. Since there was a least a two-month supply of the former 1¢ Large Numeral postage dues at the BEP, it is likely that remaining Large Numeral dues were shipped to postmasters before any of the new designs. With the limited number of early uses J29 and J31 stamps on cover, and with the current EDU covers appearing within one month of each other, common sense suggests the 1¢ vermilion came first. To support the conclusion fully will require the analysis of many more J29 and J31 covers.

Putting the question of which stamp came first aside, the bigger questions involve color and fluorescence (or lack thereof). Several factors determine a stamp's color including ink composition, homogeneity, pattern density of the design (to some extent), ink-paper interactions, environment, and, of course, perceptions of the human eye. Two stamps of the First Bureau postage dues that started out as the same color in 1894 (over 120 years ago) could look very different in color today due to effects of the environment, storage method, and the exposure to light. Thus, color is not enough to distinguish whether a particular stamp came from a certain printing or not.

Bower (Bower, 1971) thought fluorescence was the answer. If First Bureau 1894 Series dues fluoresced, they were either the 1¢ J29 or 2¢ J30 vermilions. If they did not fluoresce, then they were claret (J31 and J32). This seemed reasonable until the discovery of fluorescence in certain 1¢ values that were claret or deep claret in color. Cleland (Cleland *et. al.*, 2009) reported about 25% of the claret stamps associated with plate no. 57 fluoresced. All examined 2¢ stamps from plate no. 34 appeared to be vermilion and lighter and brighter when compared to their so-called claret counterparts, and they fluoresced, so there was little issue [2].

The question is what to do about the 1¢ values that fluoresce? Should we call them vermilion even if they are distinctly different in color? Clearly, when the inks fluoresce, they have a widely different ink composition as shown in the X-ray spectra in Figures 1, 2, 3, and 11 of this article and Figures 7 and 9 of Part I. This suggests a sorting of the stamps by fluorescence and their ink composition rather than color alone.

The information and discussion above lead to the statement "all vermilion stamps fluoresce but all stamps that fluoresce are not vermilion." I hope readers can align with this statement and move onto the bigger issue of how the fluorescent and non-fluorescent 1894 and 1895 Series postage due stamps should be listed in future Scott catalogues. The author suggests the following.

1894 Series

1. For the J29 and J30 "vermilion" issues: leave the listings the same but add a note stating the vermilion color postage due stamps fluoresce.
2. For the J31 through J37 "claret" issues: leave the listings the same except add a note stating, "some of the claret colored, perforation 12, unwatermarked First Bureau postage due stamps exist in both fluorescent and non-fluorescent varieties."

1895 Series

1. For the J38 through J44 "claret" issues: - leave the listings the same but add a note stating, "almost all of the claret colored, perforation 12, double-line watermarked First Bureau postage due stamps exist in both fluorescent and non-fluorescent varieties." According to current information, a fluorescent variety of the 30¢ J43 is the only one unknown.

While these statements are not as strong as some First Bureau postage due stamp experts would like, they represent a first step in recognizing that fluorescent varieties exist, and color links to fluorescence through constituent elements of the ink. Ink composition, as we know, was variable in the early days of the BEP stamp production, so variability in stamp color is to be expected. Analysis of fluorescence and ink composition together have shed some light on this variability.

## Summary

This article explored some aspects of the color and fluorescence in both 1894 and 1895 Series postage due stamps on cover. Coupled with the results of the companion article (Part I), it is definitively clear that the printing of the 1894 and 1895 Series of postage due stamps used both fluorescent and non-fluorescent ink. It appears fluorescence in the 1894 Series was confined to the lower stamp denominations, namely the 1¢ and 2¢, although Cleland *et. al.* reported a single 3¢ J33 and a single 5¢ J34 that fluoresced. The approved plate proofs at the Smithsonian National Postal Museum for plate no. 34 (the first 2¢ plate) and plate no. 57 (the first 1¢ plate) strongly fluoresce under UV illumination. Historically, fluorescence in these 1¢ and 2¢ 1894 Series postage due stamps was associated with the vermilion J29 and 30.

A wide range of colors can exist in these stamps from the so-called vermilions to dark claret and dark brown shades (for example, the First Bureau essays and trial color

proofs ((Charles, 2020b))). There are marked differences in ink composition between the fluorescent and non-fluorescent stamps, with most non-fluorescent stamps having a very similar ink composition or spectra (Figures 4, 5, and 7). The composition spectra for the fluorescent stamp ink, while having the same overall appearance which is markedly different from the non-fluorescent spectra, are not as uniform with respect to the different elemental peak ratios. These differences in peak ratios may explain the color range encountered in the fluorescent inks ranging from pale vermilion to deep brown-claret shades.

It appears a strong iron peak exists in the deep brown-claret shades, while in most non-fluorescent claret shades the spectra are dominated by a very strong calcium peak. Identification of specific stamps on cover has been performed by comparing the X-ray fluorescence spectra derived bar charts for the cover stamps with the charts of known individual stamps. By this technique, along with recorded dates and postal markings, it is shown the J30 2¢ vermilion postage due stamp was issued first, before its claret counterpart. The case for the J29 1¢ vermilion postage due stamp is not as compelling, although logic suggests it was initially printed prior to the 1¢ non-fluorescent claret stamp.

## End Notes

1. Until 1894, private banknote companies produced the United States postage stamps. The American Bank Note Company held the U.S. government's stamp contract at the time of the introduction of the postage due stamps in 1879. The first U.S. postage due stamps were of classic design and featured a large central numeral signifying the amount of postage due; hence they were the referenced as the large numeral dues. All subsequent postage due stamp designs have smaller numerals. Since they were designed and printed by a bank note company rather than the Bureau of Engraving and Printing, which designed and printed all subsequent postage due stamps, they have also become known as the Bank Note Dues.
2. In *The United States Specialist,* the Cleland article (Cleland, *et. al*., 2009), there is a major error in reporting fluorescence versus non-fluorescence. On page 294, Figure 1 caption, Cleland states, "The proof on thin cardboard of plate 34 (above) has non-fluorescent ink…" This is clearly an error. While the ink may be slightly darker than the recognized vermilion, the ink glows bright orange under long wavelength ultra-violet light. Several copies of these thin cardboard proofs reside in the author's collection and all fluoresce brightly. The same is true for the 1¢ imperforate stamp proofs printed on gummed stamp paper. All of the stamp paper proofs fluoresce orange under long wavelength UV light.

## References

Bower, Warren R. 1971. Ultraviolet Identification of U. S. Postage Due Stamps and Proofs, *Essay-Proof Journal*, Vol. 28, pp. 99–100.

———. 1986. Update on the Vermilion Bureau Postage Dues, *The United States Specialist*, Vol. 57, No. 11, November, pp. 532-533.

Charles, Jr., Harry K. 2013. *United States Postage Due Stamp Essays, Proofs, and Specimens,* The Collectors Club of Chicago, 289 pages.

———. 2020a. Exploring Color Mysteries in the United States Large and Small Numeral Postage Due stamps using X-ray Fluorescence Spectrometry. In: Smith, Susan and J. H. Barwis, editors. *Proceedings of the Third Symposium on Analytical Methods in Philately.* Akron, Ohio: The Institute of Analytical Philately, pp. 87–116.

———. 2020b.1894 and 1895 Series First Bureau Postage Due Stamps: Questions Color, Fluorescence, and Early Use: Part I. In: Lera, T. and J. H. Barwis, editors. *Proceeding of the Fourth International Symposium on Analytical Methods in Philately.* Akron, Ohio: The Institute of Analytical Philately, pp. 79–91.

Cleland, Wallace, C. Yarbrough, and W. Schuman. 2009. Early Postage Dues with Fluorescent Ink, *The United States Specialist*, Volume 80, No. 7, pp. 293–296.

Scott Publishing Company. 2019. *Scott Specialized Catalogue of United States Stamps and Covers.* Sidney, Ohio: Amos Media Co.

# Support the IAP

**Institute for Analytical Philately, Inc.**
**PMB 31, 1668 Merriman Road**
**Akron, OH 44313**

| Level | Annual Amount | My Payment |
|---|---|---|
| Patron* | $100 | $ _____ |
| Sponsor* | $100 | _____ |
| Supporting | $100 | _____ |
| Sustaining | $ 50 | _____ |
| Institutional | $250 | _____ |
| Additional donation | | _____ |
| Total | | $ _____ |

You may donate through PayPal (knilsestuen@analyticalphilately.org) or be sending a check payable to the "Institute for Analytical Philately, Inc." to the address above.

Your donation may be tax deductible since the Institute is a tax-exempt organization under Section 501 (c) (3) of the Internal Revenue Code. We will provide a receipt to you.

Thank you again for your support.

**Patron and Sponsor levels require $5,000 and $2,000 initial pledges and $100 annual contribution.*

Name _____

Address _____

City _____

State / Province and Post Code _____

Country _____

Email _____ @ _____

Phone number _____

# Editors and Authors Contact Information


| | |
|---|---|
| Thomas Lera | frontier2@starpower.net |
| John Barwis | jbarwis@charter.net |
| Harry G. Brittan, PhD, FAAPS, FRSC | hgbrittain@gmail.com |
| Aaron N. Shugar | shugaran@buffalostate.edu |
| Daniel W. Brinkley, III | danwb3@bellsouth.net |
| Robert Hisey, PhD | bobhisey@comcast.net |
| Lin Yangchen | linyangchen@gmail.com |
| Robert V. Mustacich | bob@mustacich.com |
| Jan Hofmeyr, PhD | hofmeyr1953@gmail.com |
| Richard Judge | ch2se@sbcglobal.net |
| Harry K. Charles, Jr., PhD | harry.charles@jhuapl.edu |
| James Allen | stampmole@charter.net |
| Susan Smith | SmithSu@si.edu |

# Institute for Analytical Philately, Inc.

## Preliminary Application for an IAP Research Grant

Please complete the following form describing yourself and your proposed research effort. This informa- tion will be used to evaluate the merits of the proposed work and its relationship to the mission of the Institute. This is only a first step. If there is interest in your proposed work, you will be contacted by one of the Institute Directors with further instructions on preparing a formal proposal. The greatest weight is given to projects that develop new methodologies promising to be of lasting significance to philately.

Please print legibly and answer all questions. This form may also be completed at: WWW.ANALYTICALPHILATELY.ORG.

| | | |
|---|---|---|
| Name: | | |
| Address: | | |
| City: | State/Country: | Postal Code: |
| E-mail Address: | | Telephone: |
| Name of Project | | |
| Brief Description: | | |
| | | |
| | | |
| Do you have, or do you think you might get, additional funding from another philatelic organization? | | |
| If yes, please indicate the organization or the program manager and provide contact information. | | |
| | | |
| What level of funding are you requesting? | | |
| How long will your effort take to complete? | | |
| Describe other related research you have performed, if any. | | |
| | | |
| | | |
| Describe your professional and philatelic experience as it relates to the proposed effort. | | |
| | | |
| | | |
| | | |
| Describe the importance of the proposed effort to philately. | | |
| | | |
| | | |
| | | |
| | | |
| | | |
| Do you have an idea of where to publish the results of your work? | | |
| | | |
| | | |

Return the completed form to: The Institute for Analytical Philately, Inc., PMB 31, Akron, OH 44313. If you have questions or need help, please call +1.616.399.9299 between 8AM and 6PM Eastern Time.